ProQuest LLC.
789 East Eisenhower Parkway
P.O. Box 1346
Ann Arbor, MI 48106 – 1346

BULGE FORMING OF TUBULAR COMPONENTS

by

Mark Ian Hutchinson BSc.

A Thesis submitted to the
COUNCIL FOR NATIONAL ACADEMIC AWARDS
in partial fulfilment for the degree of
DOCTOR OF PHILOSOPHY.

Sponsoring Establishment : Department of Mechanical
and Production Engineering,
Sheffield City Polytechnic,
Sheffield.

Collaborating Establishment : I.M.I. Yorkshire Fittings Ltd.,
P.O. Box 166,
Leeds.

JUNE 1988

ACKNOWLEDGEMENTS

The author wishes to express his sincere gratitude to Dr R.Crampton, Dr S.Ali and Prof M.S.J.Hashmi for their encouragement and helpful supervision during the course of this project.

The technical assistance offered by Mr R.Teasdale and his staff was much appreciated and in particular the author wishes to thank Messrs R.Sidebottom, A.Fletcher, D.Woodhead, L.Evans, R.Wilkinson and J.Taylor.

The author would also like to express his gratitude to Mr W.Rushton of I.M.I. Yorkshire Fittings Ltd. for providing financial support and materials towards this research, and also for his encouragement.

Finally, a very sincere thanks goes to my mother for her understanding and encouragement during the whole course of this research.

DECLARATION

The author declares that no part of this work has been submitted in support of another degree or qualification to this or any other establishment. The author further declares that he has not been a registered candidate or enrolled student for another award of the CNAA or other academic or professional institution during the course of the research programme.

M.I.HUTCHINSON

ABSTRACT

BULGE FORMING OF TUBULAR COMPONENTS

M. I. HUTCHINSON

The bulge forming process is a method for shaping tubular components using an internal hydrostatic pressure combined with a compressive axial load. Initial investigations involved carrying out an extensive literature survey to determine the components which could be formed and the effects of using lubricants and different tube materials. Die-blocks were designed to produce tee pieces, cross joints and off-set joints, and electronic on-line instrumentation was incorporated so that the forming pressures and loads could be accurately monitored.

A series of tests were carried out in the forming of:

(1) tee pieces, cross joints and off-set joints from copper tubes of two different wall thicknesses,
(2) tee pieces using different types of plungers,
(3) tee pieces using die-blocks coated with various lubricants,
(4) tee pieces from aluminium, copper and steel tubes,
(5) tee pieces using die-blocks with various branch radii.

From the resulting components, formed with various combinations of internal pressure and compressive axial load, the limits for a successful forming operation were established. Further analysis of these components was then undertaken to evaluate the effects of the internal pressure and axial load on the bulge height and the wall thickness in the deformation zone. From these results, which have been illustrated graphically, the greatest effect on the resulting bulge can be seen to be the compressive axial load.

Theoretical analyses are presented, which predict the wall thickness distribution around the bulge zone and also the axial loads required in the forming process. Comparison of these predictions with the experimental results shows fairly good agreement.

CONTENTS

LIST OF FIGURES, PLATES AND TABLES

Plate No.

Table No.

NOMENCLATURE

a	semi-length of unsupported tube in the die cavity.
dx_1	initial semi-axial deformation causing thickening of the cap wall.
dx_2	secondary semi-axial deformation causing a tubular branch to form.
f	apparent strain factor.
h_1	initial height of an element prior to forming.
h_2	height of an element after forming.
h_*	height of an element on an expanded spherical cap from the junction of the spherical cap and the tubular branch.
H_1	initial height of the cap prior to forming.
H_2	height of the cap after forming.
H_S	height of a formed spherical cap.
L_f	final length of the tube.
L	length of the tubular branch.
L_D	length of the tubular branch formed from the axial deformation.
L_o	length of the tubular branch formed from the expansion of the spherical cap.
m	ratio between the meridional and circumferential strain.
P	internal pressure.
r_o	original radius of the tube.
r_B	branch radius.
t_o	original wall thickness of the tube.
t_L	wall thickness at the junction of the spherical cap and the tubular branch.
t'	wall thickness of an element on an expanded spherical cap.
t	wall thickness at any point.

x_0, x_1, x_2	meridional position of an element.
X	length of the tube.
X_0	original length of the tube.
y	height of an element up the side branch from the root.
y_1, y_2	diameter of the circle, of which the cap is an arc of, minus the height of the cap.
ℓ_c	radius of curvature of the cap in the circumferential direction.
ℓ_L	radius of curvature of the cap in the meridional direction.
ℓ_S	radius or curvature of the spherical cap.
σ	stress.
σ_y	yield stress.
ϵ	logarithmic strain.
μ	Coulomb friction coefficient
F	axial load.
h	height of an element.

1. INTRODUCTION

1.1) The Bulge Forming Process

The bulge forming process is a method where by tubular metal components can be shaped without the use of cutting tools. Instead, internal hydrostatic pressure is transmitted via a medium such as a liquid (e.g. hydraulic fluid or water), an elastomer (e.g. rubber or polyurethane), or a soft-metal (e.g. lead or a lead alloy). This internal pressure is applied to a tubular blank whilst it is contained in a die bearing the shape of the component to be formed. Where the tube wall is unrestrained, expansion occurs until the required shape is formed.

Bulge forming occurring as a result of pure internal pressure has a major limitation of producing excessive thinning of the tube wall, which leads to rupture of the tube for only moderate expansions. However, if a compressive axial load is applied to the ends of the tube, metal can be fed into the deformation zone during forming. Provided that this axial load is large enough to cause axial deformation of the tube blank i.e a reduction in length, a much greater expansion can be obtained with less tube wall thinning occurring.

The bulge forming process has been described in numerous articles and patents. A patent by **Grey et al.(1)** in 1939 described a process used for the manufacture of seamless metal fittings having branches e.g. tees and

crosses. This was achieved by subjecting a tubular blank to forces causing it to upset by plastic deformation to a blank of approximately tee shape. It entailed the control of the forces such that rupture of the blank was avoided, and which, in the course of the upsetting operation, employed both endwise mechanical pressure applied to both ends of the tubular blank and co-ordinated internal hydraulic pressure within the tubular blank. The hydraulic pressure was carefully controlled so that it did not exceed certain limiting values at various stages of the upsetting operation.

In the course of the upsetting operation on the tubular blank, there was a substantial flow of metal from certain regions of the blank to certain other regions, thereby increasing the thickness and therefore the strength of these latter regions.

No specially formed blanks were required, because the machine was adapted to use tubular blanks made from standard and commercial copper tubing, and required no special treatment or pre-forming except the cutting of the blanks from long lengths of the tubing.

The process involved putting a tube blank in between two die halves which were clamped together. A compressive axial load was then applied to the ends of the tube via plungers which entered the ends of the die block. The internal pressure was transmitted by a liquid through a drilled passage in one of the plungers, using a pump to provide the pressure, and a check valve to maintain the pressure at a given level

during forming. The tube blank was filled with fluid from a tank in which the die block was immersed. The actual forming process involved increasing the internal pressure to an initial value of between 3000 psi.(21 MPa) and 6000 psi.(42 MPa) after the plungers had sealed the ends of the tube blank. Hydraulic rams were then used to advance the plungers and axial deformation occurred causing an increase in the internal pressure. The maximum value of this pressure was controlled by a preset pressure relief valve, set to a value of between 6000 psi.(42 MPa) and 10,000 psi.(69 MPa), depending on the diameter and wall thickness of the tube used. This combination of axial load and internal pressure pushed the tube wall into the recesses of the die, so forming the tee piece. The formed tee piece exhibited thickening of the wall opposite the side branch and at the side branch junction, but this was deemed advantageous as it provided added strength and reinforcement to the parts subjected to the greater stress when the tee piece was in service. The manufacture of the component was completed with the cutting-off of the cap of the formed branch followed by the machining of the ends to equal lengths.

Although the basic process was by no means new, it was the first time that the deforming pressures (applied by the plungers to the tube ends, and internally by the hydraulic pump) were related in such a manner that a satisfactory tee was produced.

An article by **Crawford(2)** described a factory owned by the 'Empire Brass Manufacturing Company' which produced seamless copper pipe installations, which were used for heating and water supply services, from 0.5" (12.5 mm) to 3" (75 mm) including elbows, tee's, couplings and return bends.

The tube blanks were cut to length and then filled with a soft-metal (a bismuth-lead-tin alloy with a melting point of 280 ^{o}F) which was poured in for most of the tube's length. Endwise pressure was applied to both the filler metal and tubing whilst they were restrained in a die. The dies varied in size from 0.5" (12.5 mm) to 2" (50.0 mm). After the process was completed the metal filler was removed by heating the components in an oil bath.

The soft-metal filler process produced well shaped components, but had the disadvantage of requiring the filler metal to be added before, and removed after the process, which was much more time consuming than with a liquid medium. In a patent presented by **Stalter(3)**, a new method was introduced in an attempt to perfect the soft-metal filler approach. A comparison had been carried out by Stalter between a solid filler rod, and filler cast into the tube. It was found that the casting technique had the advantage of giving a better fit between the slug and the inner wall of the blank, but did require expensive, complex and bulky equipment. The equipment also had high maintenance expenses and involved a high direct labour

cost. Even though the cast filler slug gave a better fit than the rod insert technique, the cast slug exhibited substantial shrinkage when it solidified and cooled, preventing the tube from being completely filled because of the shrinkage cavities created.

On the other hand, the technique of using a rod type insert slug eliminated the undesirable casting process and enabled the rods to be cut to fairly close tolerance lengths for filler volume control. This had disadvantages, in that it required the molten metal to be firstly cast into billets which were cumbersome to handle, then extruded into long rods and then cut into the desired length slugs. This required a time consuming process and a costly sawing operation. Furthermore, the casting of the rods had a high scrap rate, and in the sawing of the rods, there was a substantial loss of the filler material through chips and dust.

Another disadvantage possessed by both of the aforementioned techniques was the difficulty in carrying out the production operations automatically, and because of this, there were high expenses incurred in the manual part of the process.

The patent detailed a method of forming a branch type fitting from a tubular blank of a pre-determined diameter and length by measuring out a specific amount of pellets of filler material capable of compaction into a unitary body. The compacted pellets were in the form of a rod corresponding in

internal diameter to that of the tubular blank. When pressure was applied to the ends of the blank whilst it was contained in a die, it deformed into a predetermined shape.

As the rod started off as small pellets, it was easy to introduce it into the tubular blank, and thus the process was much easier to automate.

1.2) Bulge Formed Components

The bulge forming process, when applied to open ended tube blanks, has been catagorised into two main types. These are:

(1) Axisymmetrical Components.

(2) Asymmetrical Components.

1.2.1) Axisymmetrical Components

Axisymmetrical components are ones which have a uniform expansion over their whole circumference. That is, they exhibit symmetry around their axis. Components which come under this category are ones such as: shouldered hollow shafts and expansion/reduction pipe joints (formed by halving bulge formed components centrally to give two joints) - see Figure 1. In the forming of these components there is a critical relationship between the axial load and the internal pressure. When an expansion has started to occur, there is a tendency for the axial load to become too large for the strength of the tube wall to withstand, and the tube buckles.

1.2.2) Asymmetrical Components

Asymmetrical components are those which have a localised or sectional expansion, such as tee or cross pieces. The bulge forming method of manufacture for a component such as a tee piece is much cheaper than the alternative methods which are: machining from a casting or a welded design. There is a large variation of asymmetrical components which have different diameters,

branch angles, and alignments to the main branch (Figure 2)

1.2.3) Commercially Manufactured Components

Although much of the published work on bulge forming is of a theoretical or experimental nature, there are numerous examples of the process being used in industry. In particular, the process, when applied to the manufacture of pipe fittings, either for the gas or water related industries, has drastically reduced the cost of components. As stated previously, the only alternative method of production is either by casting and machining, or welding. These methods incur high manual costs, and are usually multi-staged processes.

As well as copper components, the process has also been successfully used with mild steel, brass and aluminium.

An article which appeared in **Metallurgia(4)** described a hydrostatic cold forming multi-ram-press of 1000/850/850 tons (clamping and two axial rams) capacity which was used by 'Wellman Enefco Ltd.' to produce tee pieces within the range of 1.5" (38 mm) to 8" (203 mm) diameter, and wall thicknesses of between 2.00 mm and 8.00 mm. The tube blanks needed no special preparartion, being simply pieces of standard quality steel tube cut to length with reasonably square ends. The top ram consisted of a compound of concentric rams (the outer one for opening, closing and clamping the dies). The inner ram was used to control the formation

of the branch. The movements of the side ram and branch forming ram were controlled during the forming operation, although the internal pressure could not be independantly changed.

A bulge forming process is also used by I.M.I. Yorkshire Fittings Ltd.' to produce pipe fittings, and by 'Raleigh' in the manufacture of bicycle frame brackets. However the main exponents of the process are the Japanese, who use bulge forming for a variety of components. In addition to the types of asymmetrical components produced for pipe fittings, they have also produced stepped hollow shafts for use in electric motors, wheel hubs for bicycles, rear axle casings for cars and lorries, and large-sized structure parts.

1.2.4)Associated Applications

Apart from axisymmetrical and asymmetrical components such as those described previously, the bulge forming process has also been used to manufacture other types of components.

An article by **Smith(5)** noted the design of a machine which could produce components using a hydrostatic bulge forming technique which allowed for component expansions over 100%. The system was very similar to that patented by **Grey et al.(1)** except that the pressurising medium was water. The main use for the process was in the manufacture of brass kitchen tap spouts. These were made from lengths of tube bent into a 'v' shape. The bent tube was placed into an appropriately shaped die, filled with water and

pressurised. Load was then applied to the ends of the tube to push them in, thus forming the tube into the shape of the die.

Patents(6 and 7) taken out for a Dutch organisation described a device which bent pipes and formed elbow fittings. The device consisted of two die blocks that could slide across one another, perpendicular to the tube blank that was placed through them both. The tube contained in the dies was filled with a substantial incompressible medium in the form of oil, rubber, or a similar material and then pressurised at each end by a pressure transmitting plunger. The two die halves were so shaped that, when the tube was loaded to such an extent that plastic deformation occurred, one half was forced to slide across the other due to the forces on the tube. Using this process, two 'square' elbows (small corner radius) were obtained from one tube blank. If, however, slightly differently shaped dies were used and forced to slide across one another using an external force during the process, it was possible to obtain curved elbows. The advantage of this method of bending tubes was that it was possible to obtain a very small radiused bend and nearly constant wall thickness at the point of bending. Previously this had been extremely difficult, or even impossible to do, and in cases where a small radius was achieved, the outer wall thickness was very thin with respect to the rest of the tube.

A similar process to the above was used by

Remmerswaal et al.(8), who used an elastic medium to transmit the internal pressure. The tubes were filled with the elastic medium and then bent into two 90^{o} bends by placing them into two die halves which slid perpendicular to one another. When pressure was applied to the tube ends and the elastic medium, an angular 'Z' shaped product was formed. The relationship between the bend radii and wall thicknesses also agreed with the above.

Boyd et al.(9) did similar work with dies sliding perpendicular to one another. Initially tests were carried out using water as a medium and a 3" (75 mm) outside diameter tube in a 3.5" (87.5 mm) diameter die, but when the internal pressure caused bulging, ovality occurred, stopping the two die halves from closing properly. When 2.7" (67.5 mm) outside diameter tubes were used in the same die, but with an infeed compressive load supplied to the die ends, severe buckling occurred. The internal fluid was then changed to oil that could be pressurised independantly, but buckling still occurred during bending. This, however, was removed by increasing the internal pressure once the die-halves had closed. The resulting components had less change in the wall thickness than conventional methods.

Powell et al.(10) used the slide die process to bend aluminium tubes of 1" (25 mm) outside diameter. The machine used an air/hydraulic intensifier which was capable of producing up to 69 MN/m^2. It was found that

by applying a restraining force to the sliding die half, the thickness of the tube wall could be increased.

Theory was provided equating the external force supplied to the power dissipation due to internal shear (obtained from an Upper Bound solution), frictional power losses (between the tube and the die), and the restraint loss (the force exerted to restrain the die-half from sliding). The final equation could be used to calculate the internal pressure from the flow stress, the relative wall thickness, and the geometry given by the bend angle. The correlation between the theoretical and practical results was relatively close.

Woo(11) detailed the use and operation of a machine that had been developed to form aluminium and pewter vessels from circular blanks. Using one rig, the blank was deep drawn through a 'Tractix' die, passed through an ironing die, and finally filled with oil and bulged into the required shape using internal pressure and axial load.

With the exception of some car axle housings made in Japan, most bulge formed components are small in size. However, **Yoshitomi et al.(12)** described hydraulic bulge forming equipment which could be applied to large size structure parts as well as small ones. The machine was a three ram type similar in all but size to the ones described previously. A variety of components were formed with the design of pipe truss structures in mind. The components were used as joints between main

and branch pipes in order to achieve weight reduction and also reduce the stress concentrations which were normally generated by welding. The tube blanks were 1100 mm in length, 430 mm outside diameter, and had a wall thickness of 14 mm.

1.3) Failures Of The Process

There are two main modes of failure, and one secondary type. The two main modes result in total destruction of the component, whereas the secondary type results in the component failing to achieve a satisfactory surface finish or shape.

The first mode of failure is that caused by fracture during expansion. The fracture is caused by excessive thinning of the tube wall in the area of maximum expansion (normally the centre of the domed area). The reasons for this are two fold; either the internal pressure is too high, or an inadequate axial load is used when trying to obtain a large expansion. Theoretically, it is possible to expand indefinitely, if metal is continually being fed into the deformation zone (assuming that the coefficient of friction is zero), and the internal pressure is closely regulated. However, without this regulation, the wall thickness decreases until rupture.

The second mode of failure is that of buckling. This is caused by insufficient internal pressure compared to the compressive axial load. In mild cases the problem can be seen as wrinkles on the main branch, but in severe cases the whole tube buckles and the branch becomes mis-shapen. Components also become buckled if, after fracture, the axial load is still applied. This is because the internal pressure cannot be maintained once there is a 'leak' in the system. In most cases, the imbalance between the pressure and the

axial load occurs midway through the process, but there are two occasions where this is not so. Firstly, when the plungers are advancing on the tube to seal the ends, if the sealing load is too high, there is slight crumpling of the walls. Although this is often very difficult to detect visually, these faults can cause buckling during the forming process, even if the internal pressure and compressive axial load are perfectly balanced. Secondly, if excessive fluid remains on the die block surfaces prior to a tube blank being introduced, when the die halves are clamped together, entrapment of this fluid can also cause slight crumpling of the sample. As in the above case, these small defects can result in severe buckling.

The main reason that components are rejected after being fully formed is that of shrinkage. This occurs around the radius of the die and refers to the situation where the wall of the component is not in contact with that of the die. It can be caused by the branch radius being too small, or by insufficient internal pressure (but not so low as to cause buckling). The problem is overcome by modifying the die shape, or by better regulation of the internal pressure, or by a combination of the two.

In the forming of satisfactory components, it is essential to use the correct relationship between the axial load and the internal pressure.

Examples of the modes of failure are shown in Plate 1.

1.4) Previous Investigations

1.4.1) Axisymmetrical Bulge Forming

There have been numerous investigations into axisymmetrical bulge forming, and the following are representative extracts. **Al-Qureshi(13)** presented experimental evidence showing the difference between the bulging of thin-walled tubes using the rubber forming technique with polyurethane and the hydraulic forming process. It was found that greater circumferential expansions of thin-walled tubes, up to 50% and greater for some materials, was obtainable using the rubber forming technique and was well worth considering as a simple alternative to other forming processes, such as electro-hydraulic forming. Also, simultaneous operations e.g. piercing, forming and shearing could be easily achieved.

The rubber insert, however, created greater frictional forces than hydraulic fluid, and this led to greater circumferential and longitudinal strains. It was concluded that the highly-developed hydraulic forming machines gave better results than rubber forming machines.

Limb et al.(14) used a bulge forming rig consisting of a vertical hydraulic ram for clamping the die together and two horizontal rams, each with a 300 kN capacity. Forming was carried out using 1.5" (36 mm) outside diameter seamless tubes of commercially pure aluminium, aluminium alloy (HV9 - Al/Mag/Si alloy), copper, 70/30 brass, and low carbon steel, in varying

wall thicknesses - 0.048" (1.22 mm) to 0.080" (2.03 mm).

The most satisfactory method of producing thin-walled tubes was found to be by increasing the internal pressure incrementally in steps during the ram movement. A large increase in the wall thickness occurred in the main branch during the process. The formed tee had a very pronounced dome if there was no lubricant between the tube and the die. The best lubricant was found to be P.T.F.E. film, followed by collodial graphite and Rocal. With lubricants the dome of the tee was much flatter, and the length of the branch increased by as much as 20%. The wall thickness of the branch was also found to have increased.

In a later paper **Limb et al.(15)** used the same machine (except with a higher oil pressure capability). Three different shapes of axisymmetric components were formed, all in the same die. The die had a large central cavity, and inserts were used to give two different sized unsupported regions on either side of the insert. The same sized tubes and materials were used as in the previous investigation. The bursting pressure of the tube was first found with no axial load, and then two-thirds of this value was used as the initial internal pressure. The rams were advanced and the pressure increased until failure, and thus the forming limits were established. Each type of tube was formed by the maximum amount, without bursting or buckling, sectioned, and strain measurements taken. In

all expanded regions, thinning of the wall occurred, but thickness distributions varied considerably according to the geometry. When failure occurred, brass and steel tended to fail by buckling due to the inability of the machine to provide a sufficiently high internal pressure.

In addition to the above, tees were also formed. The softer materials were formed with little or no thinning of the branch wall, whereas the stronger materials showed considerable reductions in wall thickness in the branch.

Finally, lubrication was investigated using eight different lubricants, by measuring the maximum length of the branch formed. The P.T.F.E. film was again found to give the largest bulge height, if rather expensive, and the next best, and cheaper, was P.T.F.E. spray. Tellus 27 was found to be the worst.

Woo(16) and **Woo et al.(17)** derived a theory which used the relationship between the cicumferential strain and the thickness strain. The circumferential strain was obtained from a numerical solution, taking the end conditions into account (using a computer package), whilst the thickness strain was obtained by considering the volume consistency of the material. In order to satisfy the end conditions, the effect of anisotropy was introduced using relevant parameters.

Two stress-strain curves were used to calculate the theoretical strains, one being determined from tensile tests, the other obtained from

measurements taken during bulging. It was suggested that the stress-strain relationships should be determined from the actual tube bulging process, which could also cover a strain range larger than that possible in a tensile test.

A theory predicting the limiting bead height (a bead being a small radiused circumferential bulge on the tube surface), the total applied load, and the total ram movement required to form circumferential cylindrical beads was presented by **Al-Qureshi(18)**. As with the author's previous work, an elastomer rod technique was used to produce bulge forming. Dies were used with either single, or multiple corrugations of width 6.4 mm. Lanolin was used as a lubricant between the die tools and the outer surface of the workpiece, and the elastomer rod was dusted with French chalk to prevent undue adhesion to the internal surface of the workpiece.

The theory was found to be in remarkably close agreement with the experimental results obtained using tubes made from different materials.

Banerjee(19) carried out experiments on a rig which clamped the ends of thin-walled (0.225 mm) aluminium tubes, and bulged them with internal oil pressure. The length of the tubes was kept constant throughout the bulging process, which was carried out slowly until rupture. Theory was provided to find the pressure at instability (from the stress and strain at instability), taking strain-hardening into

consideration. Graphs were produced for both experimental and measured results of the diameter/length ratio against pressure and bulge height. There was good agreement in the pressure results, but there were discrepancies for the bulge height values.

Kandil(20) conducted work into the effect of the radius of draw on bulge forming. Axisymmetrical components were formed from tube blanks of sizes 12.7 mm to 38.1 mm diameter and 1 mm thickness. The radius of draw (the radius at the root of the branch) varied from 4 mm to 8 mm. The tube materials used were brass 63, copper and aluminium, all of which were annealed before forming.

During forming, the oil inside the tube was compressed by the plunger, but there was no load applied to the tube. The maximum expansions were 63.7% with brass, 33% with copper, and 14.4% with aluminium.

From the results, an empirical relationship was obtained which predicted that the hydrostatic bulging load was directly proportional to the deforming-resistance and the tube diameter, and was inversely proportional to the drawing speed.

A rubber insert was used as the internal pressurising medium in the bulge forming process used by **Badran et al.(21)**. No axial loads were directly applied during bulging, although friction between the rubber and the tube blank did apply some axial load which fed the tube into the die.

The theory presented gave equations for the internal pressure required for various increments in the deformation angle, assuming that the free part of the tube (the bulged part), formed the arc of a circle. An expression for the thickness of the bulged wall at any deformation angle was also derived. The equation for pressure was then modified to include work-hardening using the value of the current yield stress, determined from a stress-strain curve.

The equations were used to produce graphs to predict the various values of pressure required for any deformation angle, neglecting and including work-hardening.

Saver et al.(22) conducted work on the theory of failure of bulge formed tubes due to buckling and fracture. This was applied to the forming of parts with very pronounced bulges such as rear axle housings. A numerical solution was used to compute values of axial load and internal pressure, from increments in the diameter of the bulge. The algorithm was based on five principles: strain-displacement relations; incompressibility; effective stresses and strains (plasticity theory); equations of equilibrium; and boundary conditions.

The rig used applied axial load and internal pressure at a finely adjustable ratio, in order to apply various constant stress ratios.

Tubular blanks of 1.5" (38 mm) outside diameter with a wall thickness of 0.050" (1.27 mm) were

slowly bulged until failure; measurements being taken in between load increments. Experimental forces used compared favourably with predicted values, although the actual fracture strains were slightly higher than those predicted.

Fuchizawa et al.(23) conducted experimental work on thin-walled cylinders of finite length. Experimental results such as strain distribution, relationships between the internal pressure and the tube radius, bursting pressure, critical expanding radius (radius at the centre of the cylinder when it bursts), were obtained. These results were compared with analytical ones calculated by a strain incremental and logarithmic total strain theories. In general, the experimental results agreed with the analytical ones by the strain incremental theory except in the case of critical expanding radius of short cylinders.

Manabe et al.(24) described the development of an automatic testing system for tubular materials under bi-axial stresses by the use of a micro-computer. The system was used to study bulge forming of thin-walled tubes under internal pressure and axial load. Experimental analysis was carried out in order to examine deformation behaviour and limit the expansion of aluminium tubes for linear and non-linear loading paths. In the linear path, it was found that the limit expansion of a tube increased as the stress ratio (meridional stress/circumferential stress) approached zero.

1.4.2) Asymmetric Bulge Forming

There has not been the same amount of papers published on asymmetric bulge forming as on axisymmetric bulge forming, but the relevant papers are detailed below.

A hydraulic system very similar to that used by **Grey(1)** was described in a patent submitted by the **'Agency of Industrial Science and Technology'(25).** Again a hydraulic medium and synchronised piston movement were used. Production of tees , crosses and other branched components was possible. However, the machine was different to the ones stated previously as it had a movement limiting device, located inside the die cavity, to prevent rupture of the bulged portion of the tube. The device featured a hydraulic operated rod which could move transversely to the main machine axis in the die cavity to allow the bursting pressure limit to be increased.

Ogura et al.(26 and 27) wrote two papers which investigated the bulge forming process and in particular the work that had been done in Japan. Tee pieces varying in size from 0.5" (12.7 mm) to 12" (305 mm) outside diameter were produced and examples of the working pressures for different diameters used were: a 4" (102 mm) outside diameter tee piece was produced using a press with a 4000 kN clamping force to hold the die halves together, and two 2500 kN side rams for applying the compressive axial load. These components were produced in multi-capacity

dies and the cycle times ranged from 30 to 60 seconds. The larger tees were formed singularly on a machine with a 13 MN clamping ram, and two 7000 kN side rams, with a cycle time of 50 to 120 seconds.

Components were also formed with two axially aligned but staggered side branches. These formed similarly to tees , but it was found that the tube blank had to be deformed twice as much to produce the same height(s) of branch. The same was also found to be true of the forming of components with two circumferentially aligned branches, except for the case where the angle between the two was 180^{o}. In that case, the forming process was slightly different, as the metal build-up that occured opposite a non-aligned branch was used to help form the branch. Also, because of the symmetrical manner of plastic flow, there were fewer variations in the deformation resistance and therefore less compressive axial force was required.

With components consisting of four branches, two of which were large, circumferentially aligned and very close to one another, problems were encountered. The recesses in the die which produced the large branches were found to allow the tube wall to fracture at a relatively small pressure, because there was not enough support for the tube. The problem was overcome by controlling the rate of expansion of the two large branches during the forming process, preventing rapid bulging and thinning of the tube wall. This was achieved using similar movement limiting devices to those patented in (25) except

that the rods were now controlled by a cam connected to the horizontal plungers.

For the range of components that were formed, internal pressures of between 100 MPa to 300 MPa were used, depending on the diameter of the tube being formed. As this internal pressure had to be sealed inside the tube using end plungers, it was necessary to obtain a good seal, and thus the ends of the plungers, which butted up against the ends of the tube blank, were ground to a 'v' around the ring in contact, resulting in a high pressure acting on a small seating area.

Considerable friction forces between the tube and the die were created by the high pressure required for the forming process, and this resulted in rapid die wear. Molybdenium Disulphide was found to be a good lubricant for reducing the wear of the die, especially if permeated through bonderite treated surfaces.

Lukanov et al.(28) described a method of forming tee components so as to minimise the amount of wall thickening that occurred in the main branch. The method involved forming two staggered tees from a single blank tube, with branches on opposite sides of the tube.

In the formed tees the increase in wall thickness was reduced to 15%, and a greater branch height was obtained. This reduction allowed the initial tube blank to be reduced in length by 4%, compared with the forming of one tee.

1.5) Aim Of The Current Investigation

The investigation carried out initially involved a literature survey in order to assess the previous work carried out into the bulge forming of tubular components. This survey also highlighted the various components that were formable using a bulge forming process, and the machines and the forces required for their production.

As an introduction to the actual process, tests were carried out on the bulge forming rig designed and commissioned by **Barlow(29)**. These tests were on a tee piece and showed the limitations of the machine.

With this information, the aims of the investigation were formulated;

1) Re-design certain parts of the bulge forming rig in order to allow on-line instrumentation to be fitted,

2) Design a range of axisymmetrical and asymmetrical dies to be used in conjunction with the bulge forming rig,

3) Carry out tests with the rig, varying the dies, tube blank dimensions, materials and lubricants,

4) Analyse the formed components to show the effect of various combinations of internal pressure and compressive axial load on the bulge height and the wall thickness around the deformation zone,

5) Compare the geometry of the formed components with theoretical predictions.

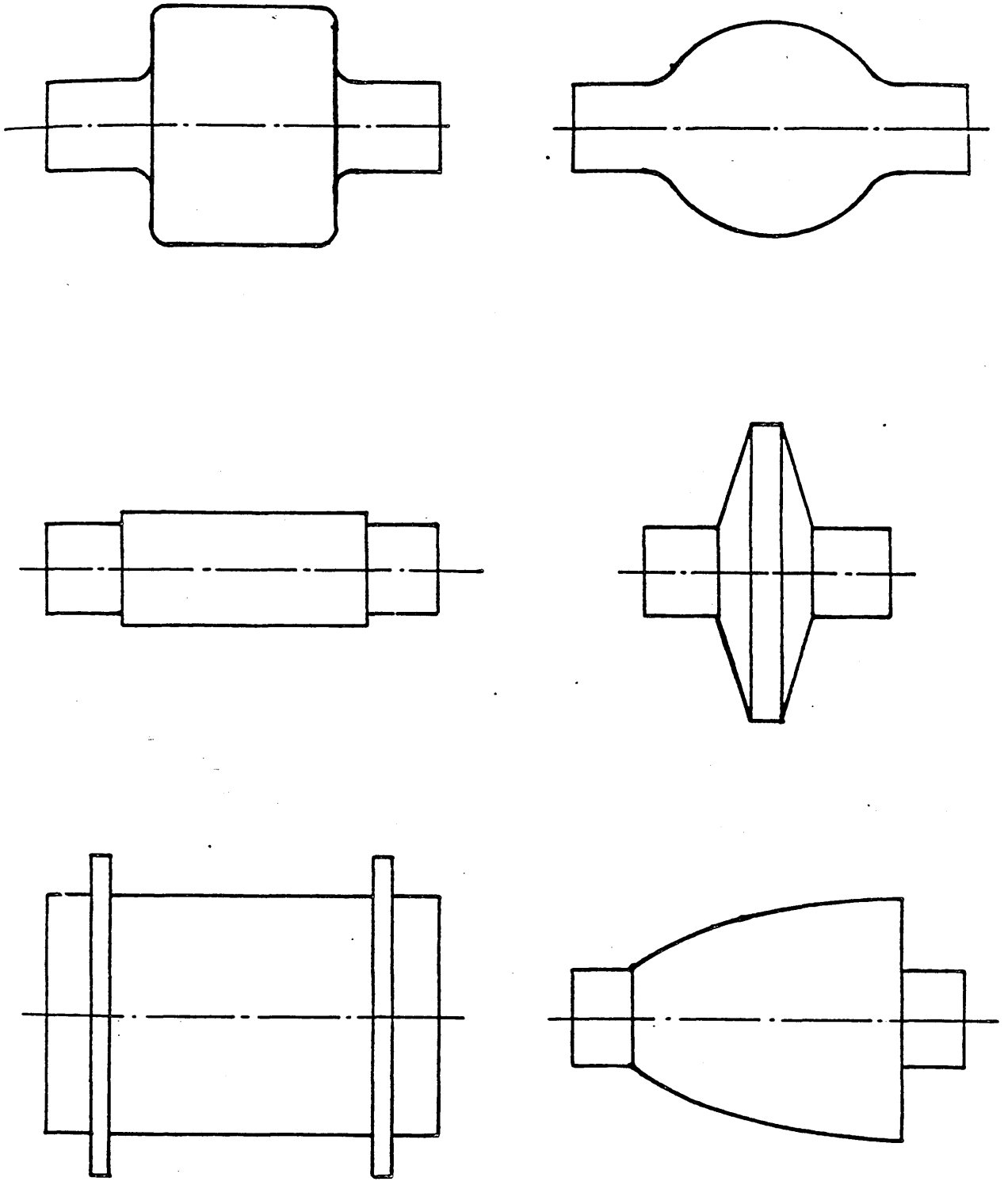

FIGURE 1

Schematic Diagram Of Typical Axisymmetrical Components.

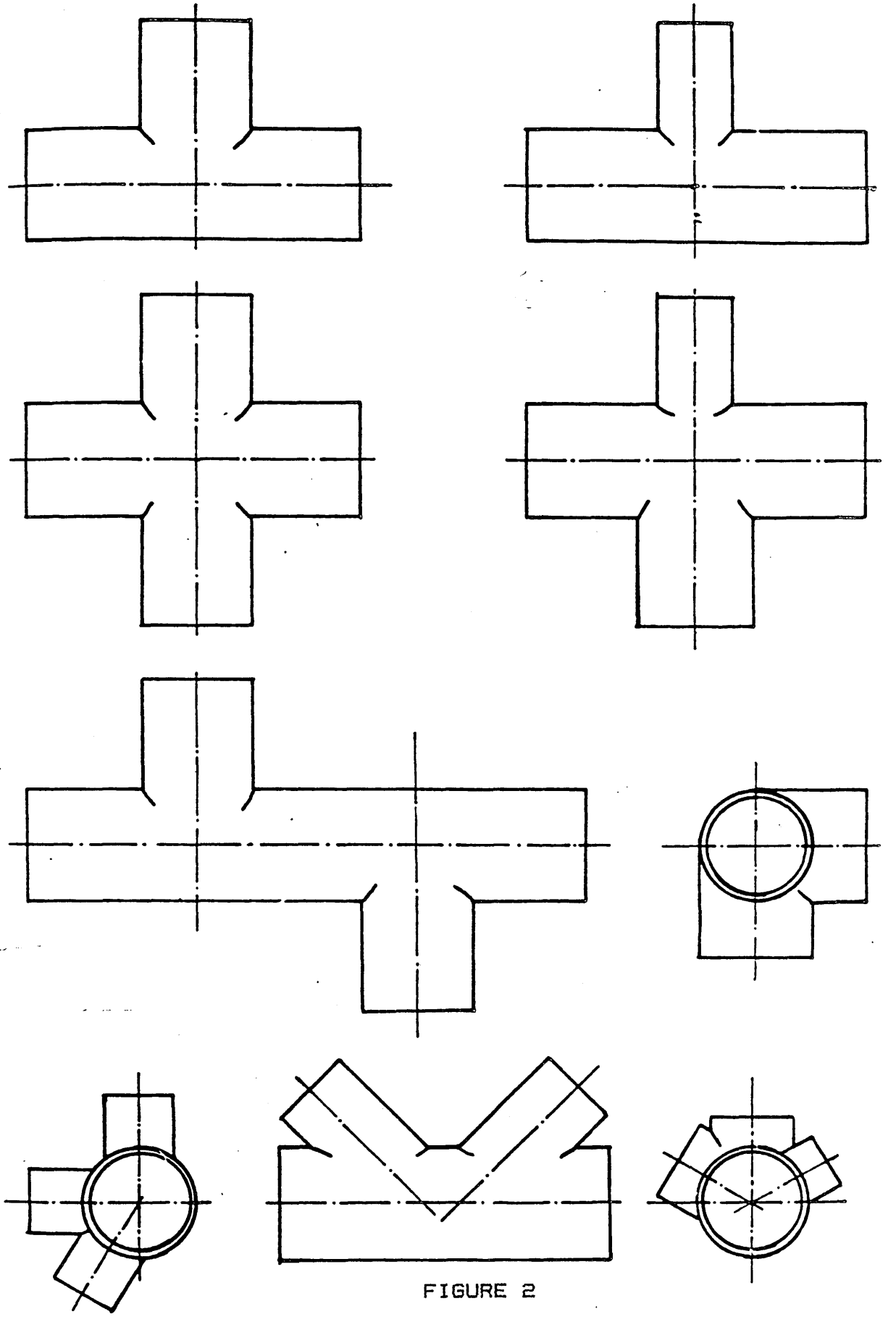

FIGURE 2

Schematic Diagram Of Typical Asymmetrical Components.

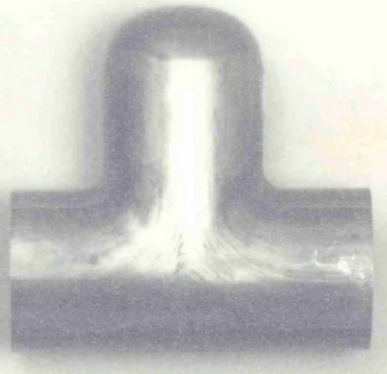

PERFECT COMPONENT

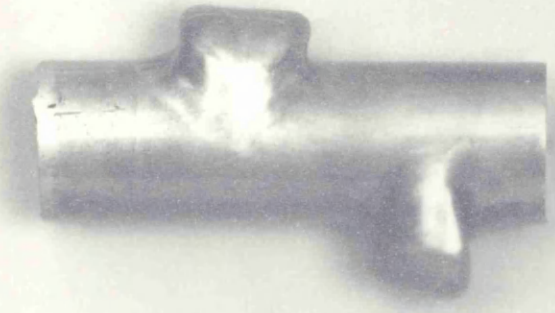

BUCKLING

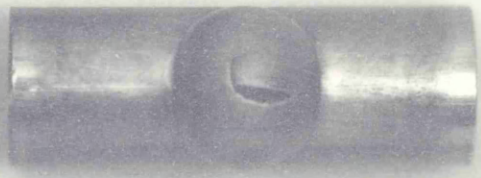

RUPTURE

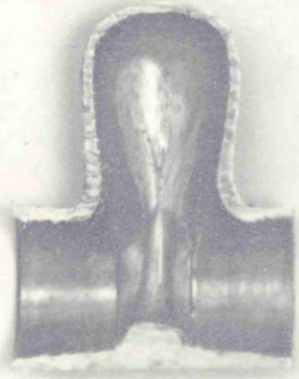

FLUID ENTRAPMENT

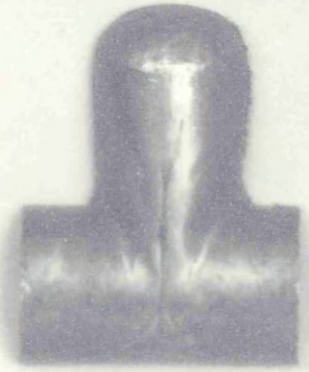

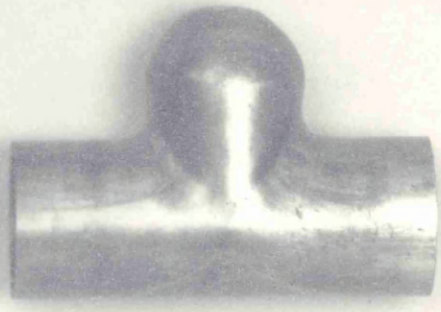

SHRINKAGE

PLATE 1

TYPES OF FAILURE IN TUBULAR COMPONENTS

2. THE BULGE FORMING MACHINE DESIGN

2.1) The Bulge Forming Machine Specifications

The specifications that follow are of the bulge forming machine (Plate 2) prior to the alterations necessary for the testing carried out in this work. The design and commissioning of the machine was conducted by **Barlow(29)**.

2.1.1) The Hydraulic Components

2.1.1.1) Hydraulic Supply Pressure

A maximum internal pressure of 69 N/mm^2 is available for the forming process, being obtained by using a main circuit pressure of 17.5 N/mm^2 which is increased to the necessary forming pressure through a 6.5:1 pressure intensifier.

2.1.1.2) The Hydraulic Cylinders Applying Axial Load

In order to provide axial deformation of the tube during forming, two hydraulic cylinders, each with a diameter of 125 mm and a stroke of 100 mm are used. The stroke is suitable for the insertion of a 150 mm tube blank into the die-blocks with the plungers withdrawn and to provide sufficient axial deformation of it during forming. It also allows the use of longer tube blanks which may be required for more complicated component shapes.

2.1.1.3) The Hydraulic Pump and Electric Motor

The power source for the hydraulic system is a variable displacement piston pump driven by a 7.5 kW electric motor. This pump is capable of operating at

pressures of up to 21 N/mm^2, but is set at an operating pressure of 17.5 N/mm^2.

The maximum theoretical forces that can be applied by the hydraulic cylinders are 215 kN for the cylinders applying the compressive axial load, and 352 kN for the clamping cylinders.

The maximum flow rate of the hydraulic pump is 32 litres/minute according to the manufacturers specifications, but less than this is obtained when operating at 17.5 N/mm^2 and using only a 7.5 kW motor. Thus the maximum theoretical flow rate is 25.7 litres/minute.

The actual delivery flow rate is in fact a little less than this due to the volumetric efficiency of the pump being less than 100%, and due to losses in the circuit between the pump and the cylinders. The maximum velocity during the outward stroke (closing the two die halves) is therefore, 21 mm/s, hence a full stroke of 150 mm is completed in just over 7 seconds. For the return stroke (opening the die), the velocity is faster, 31 mm/s due to the smaller piston area around the piston rod. This gives a return stroke time of under 5 seconds. For the cylinders applying the compressive axial load, the outward velocity is 17 mm/s, and for the return stroke, 25 mm/s. This gives an outward stroke time of under 6 seconds and a return stroke time of 4 seconds to complete the 100 mm stroke of both cylinders.

2.1.2) The Hydraulic Circuit

The hydraulic circuit performs three functions i.e. to connect the power unit and control the supply to:

1) the hydraulic cylinder clamping the two die halves together,

2) the two hydraulic cylinders providing the compressive axial load,

3) the internal pressurised region of the tube blank.

These are controlled independently and each has different control requirements.

2.1.2.1) The Clamping Hydraulic Cylinder

The function of the hydraulic circuit providing the clamping force is simply one of extending and retracting the cylinder rod. The basic component of this part of the hydraulic circuit is thus simply a directional control valve with three positions - one position to extend the ram (to close the two die halves and when together to provide the clamping force), one to stop it, and one to withdraw it (to open the die).

2.1.2.2) The Hydraulic Cylinders Applying Axial Load

The two cylinders providing the compressive axial load move relative to one another, in order to produce equal deformation of each end of the tube and so form the bulge centrally on the tube. This is achieved by the use of a flow divider in the circuit between the pump and the hydraulic cylinders. This divides the flow from the pump into equal parts

regardless of the load on each cylinder, and so synchronises the movement of the two cylinders. A pressure reducing valve is also used to control the force being applied to the ends of the tube. A directional control valve controls the extending and withdrawing of the cylinders.

2.1.2.3) **The Internal Pressurised Region of the Tube Blank**

As mentioned previously, a maximum pressure of 69 N/mm^2 is required for the forming of components. This is achieved from the supply pressure by the use of a pressure intensifier between the pump and the high pressure circuit. Again, a pressure reducing valve is also used, but this time its functions are:

1) to by-pass the pressure intensifier (in order to fill the tube blank, prior to forming, quickly at the lower supply pressure),

2) to stop the supply, and,

3) to supply the pressure intensifer, and thus generate a high forming pressure.

Also on this high pressure circuit is a valve connected to the opposite end of the tube in order to bleed air while filling the tube with oil. The air would not have much effect on the formed component, but in the event of a rupture in the hydraulic system, the highly compressed air would prove very dangerous.

The complete circuit used on the machine is illustrated in Figure 3.

All of the solenoids operate on a 24 Volt D.C.

supply and are manually controlled by switches. The switch arrangement is illustrated in Figure 4. Although all of the testing carried out for this thesis was performed using the manual switches, a micro-processor system is being developed to replace these and to automate the system.

2.1.3) The Structural Design of the Machine

The two cylinders applying the compressive axial load are located on opposite sides of the die-blocks, acting in line and inwards towards each other. The die-block is split axially in relation to the tube blank, so the clamping cylinder is mounted perpendicular to the other two cylinders. To facilitate the arrangement of the cylinders, the clamping cylinder is mounted vertically and acts downwards onto the die-block, with the other two cylinders mounted horizontally, on either side of the die-block, acting inwards. This is illustrated in Figure 5, along with the general mounting arrangements.

2.1.3.1) Assembly

With respect to the present work, the most important parts of the machine are the die-block assembly, and the plungers. Figures 6, 7 and 8 show the tee piece, cross joint, and off-set joint die-blocks, whilst Figure 9 shows how the die-block is constructed i.e. a central removable die-block contained in a larger holder.

The plungers, Figures 10 and 11, are connected to the cylinder rods by means of a collar which fits

over the plungers and then bolts to the mount. This allows for a floating connection, which ensures that the plungers always locate correctly in the die when transmitting the axial load to the ends of the tube. The ends of the plungers are stepped so that they locate into the end of the tubes. This end section is tapered to help in sealing the end of the tube when the inside is pressurised with oil. To allow the oil in, and the air out, both plungers are drilled through, one being connected to a flexible hydraulic hose, and the other to a bleed valve.

2.2) Alterations to the Bulge Forming Machine

2.2.1) The Die-Blocks

The die-blocks used in the machine consist of a holder and an insert. The die-block referred to as the 'holder' is attached to the 'Desoutter' die set by two sets of clamps (one set of four for the bottom half, one set of four for the top). The holders are positioned with dowels which pass through them and into holes drilled in the die-set. When the holders are aligned, they are clamped in place and require no further adjustment.

The inserts were designed so that they were easily interchangable (the holders take a considerable time to position due to the necessity for the machine to be partially dismantled - the plungers infringe about 15 mm at either end of the bottom die-block holder, as can be seen in Plate 3). As stated previously, when the holders are correctly positioned, they can remain unaltered for any of the inserts used. The inserts are made of hardened steel (EN21) so that they are more resilient to knocks and wear. They are 120 mm long, 100 mm wide, and 50 mm deep - Figure 6. Each insert is held in place by four Allen screws which pass through it and locate in holes drilled in the holder (the screws do not pass into the die-set). Two of the holes (diametrically opposite) in each of the inserts are threaded so that screws can be used to dislodge them if they become jammed (a seal is often created by the hydraulic fluid caught between the

holder and insert). Although the inserts can often be dislodged by pulling on the screws, by making the drilled holes in the inserts larger than in the holder, it is possible to 'push' the inserts out by screwing down the bolts. The range of insert shapes can be seen in Figures 6, 7 and 8.

2.2.1.1) **Variation to the Inserts Branch Radius**

When the original inserts were made, the corners where the central passage connected to the branch were rounded off without any degree of accuracy (one corner had a radius of 2.5 mm, the other 3.5 mm). However, from the initial tests it was clear that the radius of the corner at this intersection was critical in the formation of components. Therefore, the corners of the inserts used in the testing were all of a given radius (2 mm, 3 mm, 4 mm, or 5 mm). Not only was the radius a given size at the face of the inserts, but the corners were also blended all the way around the intersection.

2.2.2) **Instrumentation**

The initial machine design lacked any accurate method of recording the hydraulic fluid pressure and the plunger loads. There was only one permanent gauge in the hydraulic circuit and that measured the system pressure. In addition, there were also some temporary point gauges which recorded the value of the low-pressure circuit pressure, the piston pressure, and the sealing pressure, but these were inaccurate (the readings were subjects to a +/- 10% error). In order

to obtain accurate results for use with the wall thickness analyses, it was necessary to incorporate electronic on-line instrumentation in the bulge forming machine.

2.2.2.1) **Compressive Axial Load**

The axial load is applied by two plungers which simultaneously advance on the tubular blank. The movement of the plungers is controlled by hydraulic fluid which is split equally between the cylinder rods by means of a flow divider. As long as the flow divider is kept clean, it can be assumed that the flow to the two cylinders is equal (if it becomes dirty, the components formed have bulges which are no longer central). Thus, only one load reading was felt to be necessary, and this meant that only one of the plungers needed altering to accept the instrumentation.

The cylinder rods/plungers were designed so that they were not connected to each other, but so that the plungers were free-floating in a sleeve attached to the cylinder rod.

It was decided that the best method of recording the axial load would be to use a load-washer. It was necessary to use a specific load-washer, as it was found that although several types were suitable, with regard to range, only one in the 'Kistler' range was small enough to fit into the system, and still be able to record the necessary values, without major alterations. The washer used was a 'Kistler 200' (maximum load 200 kN).

To make a suitable position for the washer, the plunger was removed from the machine and an inset cut into it to locate the washer. The inset surface was ground smooth, and a polished ring used on the other side of the washer to ensure an even load distribution. The assembly was then aligned and connected, and the load washer cable fed out from the sleeve through the hole used to connect the bleed valve - see Figure 12.

2.2.2.2) **Internal Pressure**

The choice of device needed to record the internal pressure depended on the positioning of it, and the accuracy required. It was decided that a piezo-electric pressure transducer should be used, since that would give a higher degree of accuracy than a strain gauge device, and would be easily connected to any electrical monitoring equipment. The most important criterion was the position of the transducer, because it could go in either the high or low pressure circuit. However, with it in the low pressure circuit, it would be necessary to multiply the reading by the intensifying factor when the machine was operating in the high pressure mode (during deformation). Therefore, the transducer was placed in the circuit near to the inlet plunger.

The maximum internal pressure was known from the machine specifications, and a transducer with the required range picked (a 'Kistler 601H' - maximum pressure 104 N/mm^2). There was no place where a hole could be drilled and tapped to mount the transducer in

the original circuit, so a metal seating-block was designed and connected in the circuit between the fluid pipe and plunger. The transducer screwed into this block so that its bottom surface lay flush with the passage along which the fluid passes - see Plate 4.

2.2.2.3) **Axial Plunger Displacement**

Although the internal pressure and axial load readings were of the greatest significance, it was still necessary to be able to relate the increase of the above to the advancement of the plungers. This could be achieved by recording the movement of the plungers with respect to time. In order to do this, a linear displacement transducer, with a 100 mm range was used (a 'Kistler D2/1000 A'). This was attached to the side of the lower die-block and was positioned such that it lay parallel to the plungers, and started reading the plunger's progress just prior to the sealing of the blank (only one plunger was monitored, for the same reason as for the axial load).

Unfortunately, there was no smooth even surface for the transducer tip to push against, so a metal plate had to be attached to the bleed valve to fulfil this role - see Plate 5.

2.2.2.4) **Recording Equipment**

The transducer and load-washer readings were fed to scaling amplifiers where they were calibrated. The pressure transducer gave an output of 15 pico-coulomb/bar, but this was calibrated to give 20.70 $N/mm^2/cm$ on a recorder and oscilloscope.

Likewise, the load-washer gave 2.17 pC/N, but this was calibrated to give 20 kN/cm. The displacement transducer, however, gave a value in cm's, and it was not necessary to do any calibration.

The values from the amplifier were fed into an oscilloscope, ultra-violet seven line recorder, and digital voltmeters. The oscilloscope gave an instant visual record, whereas the recorder gave a hard copy. This incorporated a time-base grid which allowed the period of formation to be calculated.

The digital voltmeters were used to set the values of the axial load and internal pressures, because they were more accurate than the gauges on the valves. However, the values used for the calculations were obtained from the ultra-violet trace.

2.2.3) Other Alterations

Although most of the alterations carried out were on the die-blocks or for the instrumentation, some work was done on the machine in order to rectify long standing problems.

2.2.3.1) Removal of the Plunger Guides

Attached to either side of the lower die-block holders, there were guides to align the plungers with the die-block (Figure 9). However, the design of the guides was such that the upper die-block had to pass in between them every time a test was carried out. Unfortunately, one of the guides became loose and on lowering the upper die-block, came into contact with the guide. This caused damage to the die-block holder

and the guide, and the machine could not be used until the surface of the holder had been ground flat again.

On studying the machine set-up, it appeared that the guides were unnecessary, because the plungers always infringed on the lower die-block, and were not advanced until the upper die-block was clamped in place. Therefore, the guides were removed and a variety of tests which had been carried out with the guides in place, redone. There was no apparent difference and hence the guides were never replaced.

In addition to the advantage of having no possibility of die-block damage, because the guides were absent, the plungers could be dismantled very quickly, without the need to unfasten the die-block holder.

2.2.3.2)Plunger Tapers

The plungers were designed with tapered ends, so that a precise fit was achieved with the tube blank. This angle of taper was increased from 0.5^{o} to 3.0^{o} after the initial tests, to analyse the effect of the friction created by the contact between the plungers, tube, and die-blocks. The reason for this alteration is dealt with in the next chapter ('Test Procedure').

2.2.3.3)Alterations Carried Out For I.M.I. Fittings Ltd.

In order to carry out tests on different diameter tubes, the machine was altered to accept die-blocks used by ' I.M.I. Fittings Ltd. The main area of alteration was that of the cylinder-rods/plungers. A coupling was designed which allowed the smaller

diameter plungers to be connected to the cylinder rods, and also to encompass the load-washer and the pressure transducer. A variety of plungers were used with this configuration, and are displayed in Plate 6.

The die-blocks supplied were ones capable of producing two components at the same time, but this facility was never used because there was insufficient room for the necessary couplings. The die-blocks were clamped to the 'Desoutter' die-set in the same way as the ones used in the rest of the tests.

2.3) Rectification Of Manufacturing Faults

The majority of the problems associated with the machine were caused by the design of the die-blocks. The method of production of the die-blocks was to part machine them whilst bolted in the holders. This proved successful in the production of components, but created problems when the die blocks were made differently. Although the die-blocks which were made in conjunction with the holders operated in the machine, they were out of tolerance (up to 0.5 mm difference between the two ends of a die-block). When new die-blocks were made, the machinist found that the dies would not fit in the holders. The holders were checked and also found to be out of tolerance.

The holders were re-machined and brought back into tolerance, and the new die-blocks, when inserted, were checked and found to have a flatness tolerance within 0.025 mm over their surfaces. In order to bring the holders back into tolerance, it was necessary to enlarge the holes where the inserts fitted. This meant that the holders were no longer able to act as locators for the inserts, and hence to rectify this, and to ensure a perfect matching of the two halves, alterations were made. Firstly, the die-block holders had their surfaces machined so that the die-blocks stood proud, and the load bearing surfaces were those between the inserts. To ensure the plungers entered the die-blocks correctly, and were not mis-aligned by the passage in the holders (this occurred with the old set

of dies, and led to extensive damage to the die-blocks, holders and plungers), the passage was enlarged to 26 mm. However, by enlarging the passage, a step was created between the holders and the blocks. The die-blocks were therefore modified so that where the junction of the two passages occurred, there was a tapered zone.

To align the two die-blocks, two of the holes for bolting the inserts in place on each half were drilled out and dowelled. These ensured the matching of the halves with respect to each other, but not the holders or plungers. This was achieved by fitting two locating screws in the side of the lower die-block holder. These forced the lower die-block against one of the inside walls of the holder (which had been machined so that it was an exact distance from the centre-line of the passage), and so, when the assembly was bolted together, there was accuracy in all three planes.

At the same time as the above alterations, the changes to the tapers of the plungers were made. When the machine came to be tested, it proved nearly impossible to form a component without it suffering from folds over its surface (Plate 1). For all combinations of internal pressure and compressive axial load, the folds occurred. They were very similar to those created by buckling (when there is not sufficient internal pressure for a given axial load), and at first it was felt that the initial sealing load was too great. However, this was reduced, and there was still

no improvement in the process.

Eventually, after much cross-checking, the fault was shown to be that of fluid entrapment. This occurs when hydraulic oil is left on the surface of the dies prior to the insertion of a tube. When the die-blocks were closed, the clamping force compressed the tube against the die walls, and the fluid was unable to escape. The effect of this was to slightly buckle the tube walls (if a tube was removed at this stage, prior to the forming process, the buckling was hardly noticeable), and so when the axial load was applied, there was insufficient axial strength. The tube, therefore, folded at the point of buckling and then continued to form normally. In some cases, the fold appeared as little more than a line on the component surface, but inside, there was a fold of material standing 5 mm proud of the wall and running the whole length of the branch.

The reason the problem occurred with the new dies was that, because all of the surfaces were perfectly flat, the oil would not drain away (in the old dies, the oil tended to drain away because there was a 0.5 mm variation in flatness across the die-block surface), and merely settled in pools on the dies.

The problem was overcome by scribing several interconnecting lines on the die-block surfaces (Plate 7). These allowed the oil to be forced away from the area under the tube when the clamping force was applied. Another problem associated with this occurred

when the scribed lines became blocked with copper and dirt, and the folds reappeared. The problem was overcome by cleaning the dies, and then rounding the edges of the scribed lines to prevent them from becoming blocked through shearing material from the tube surfaces.

The only other operating fault that occurred was that of a lack of internal pressure. At one stage the maximum internal pressure the system would provide was 41.40 N/mm^2 (and not the 69 N/mm^2 the pump was set to deliver). The problem was found to be a leaking gauge, which, when replaced, allowed the system to be operated at the maximum pressure.

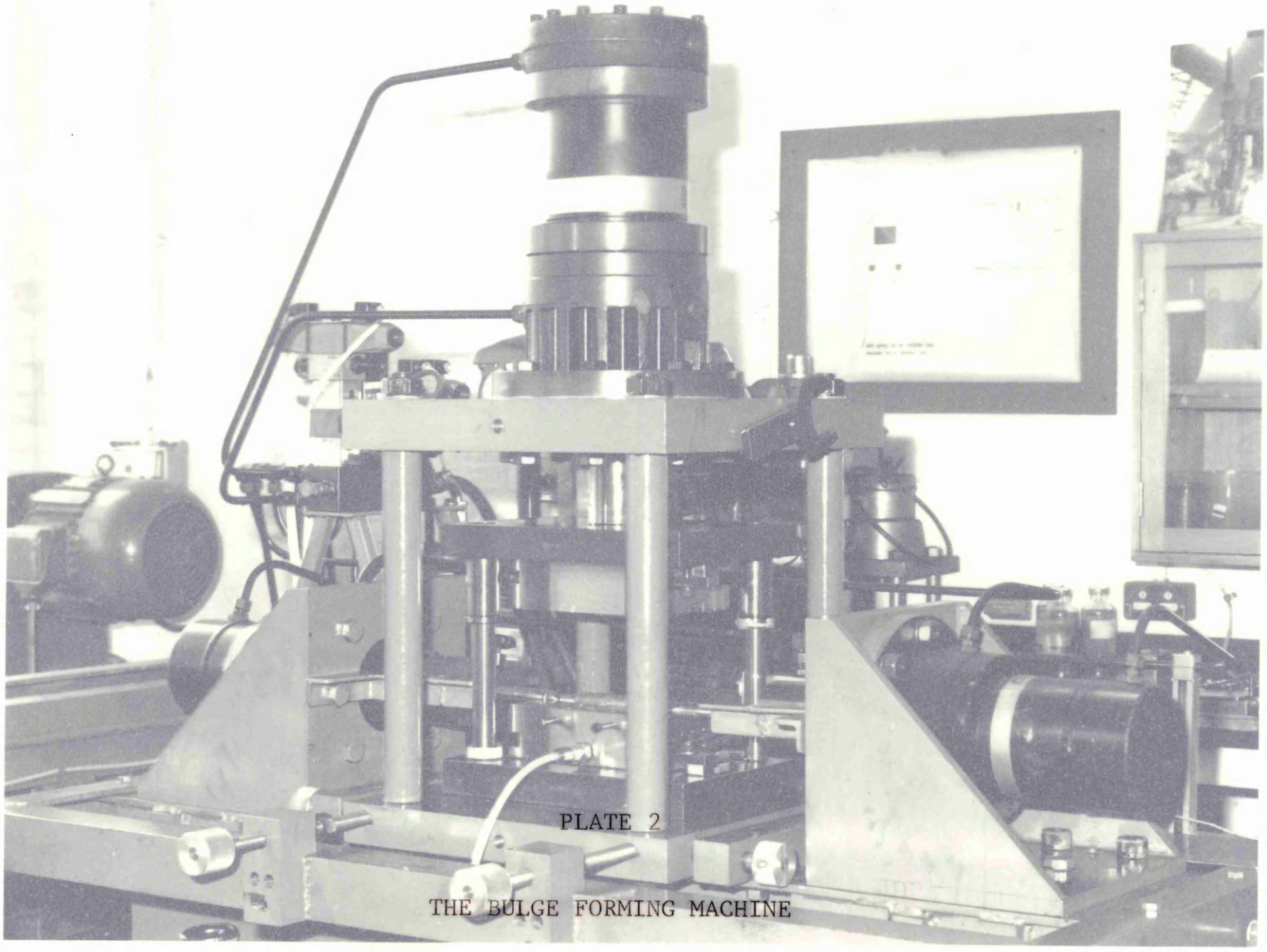

PLATE 2

THE BULGE FORMING MACHINE

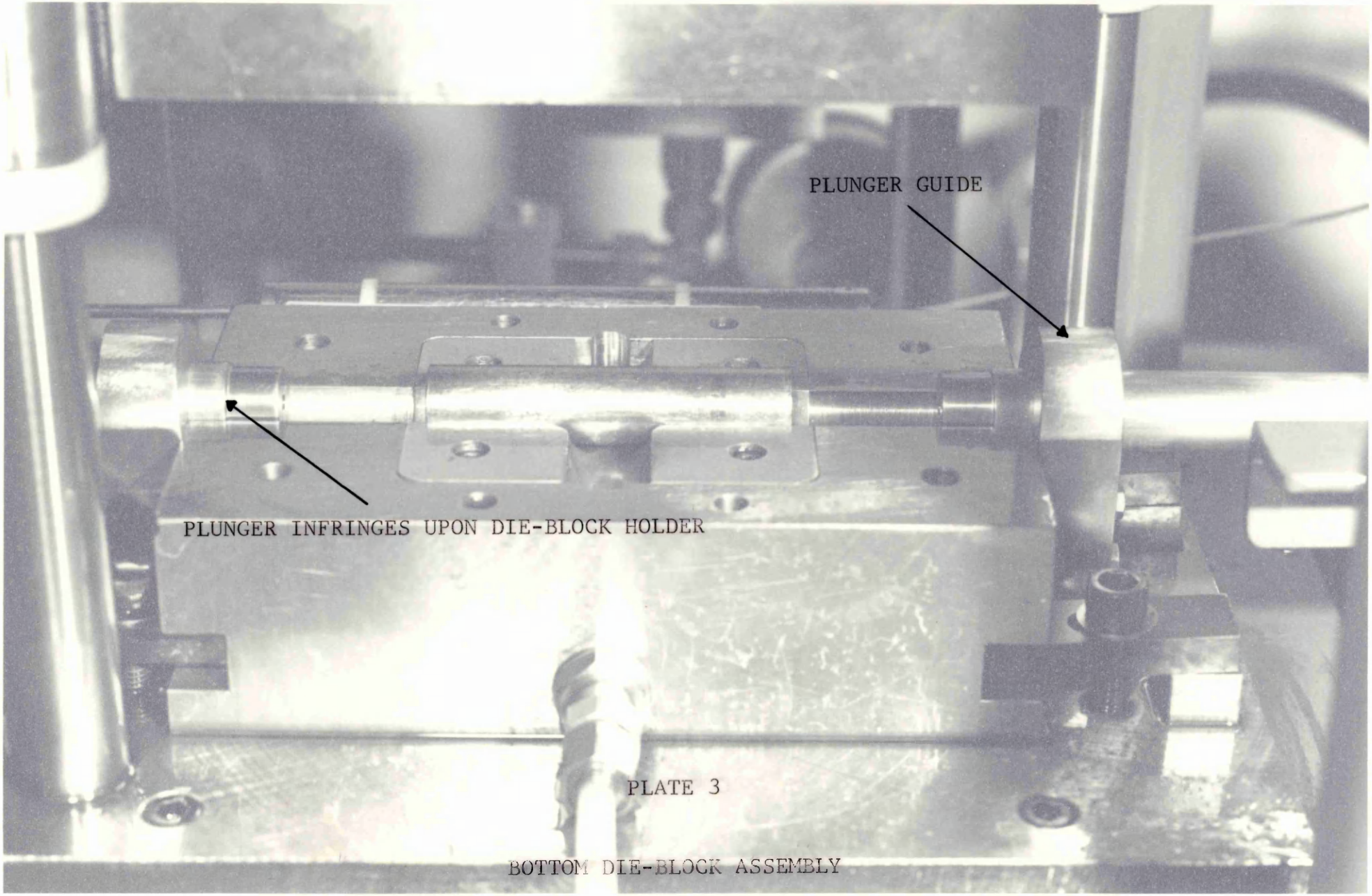

PLATE 3

BOTTOM DIE-BLOCK ASSEMBLY

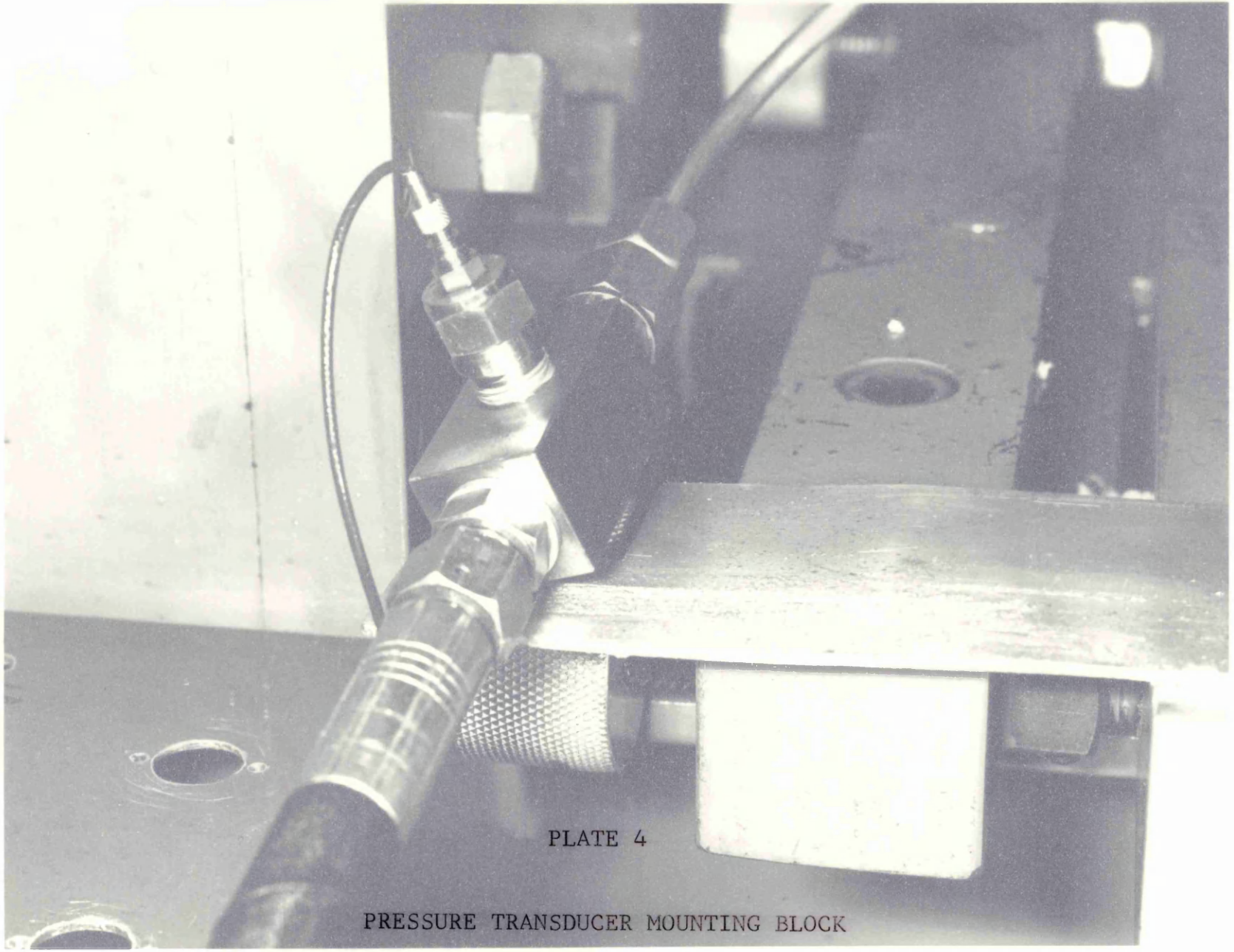

PLATE 4

PRESSURE TRANSDUCER MOUNTING BLOCK

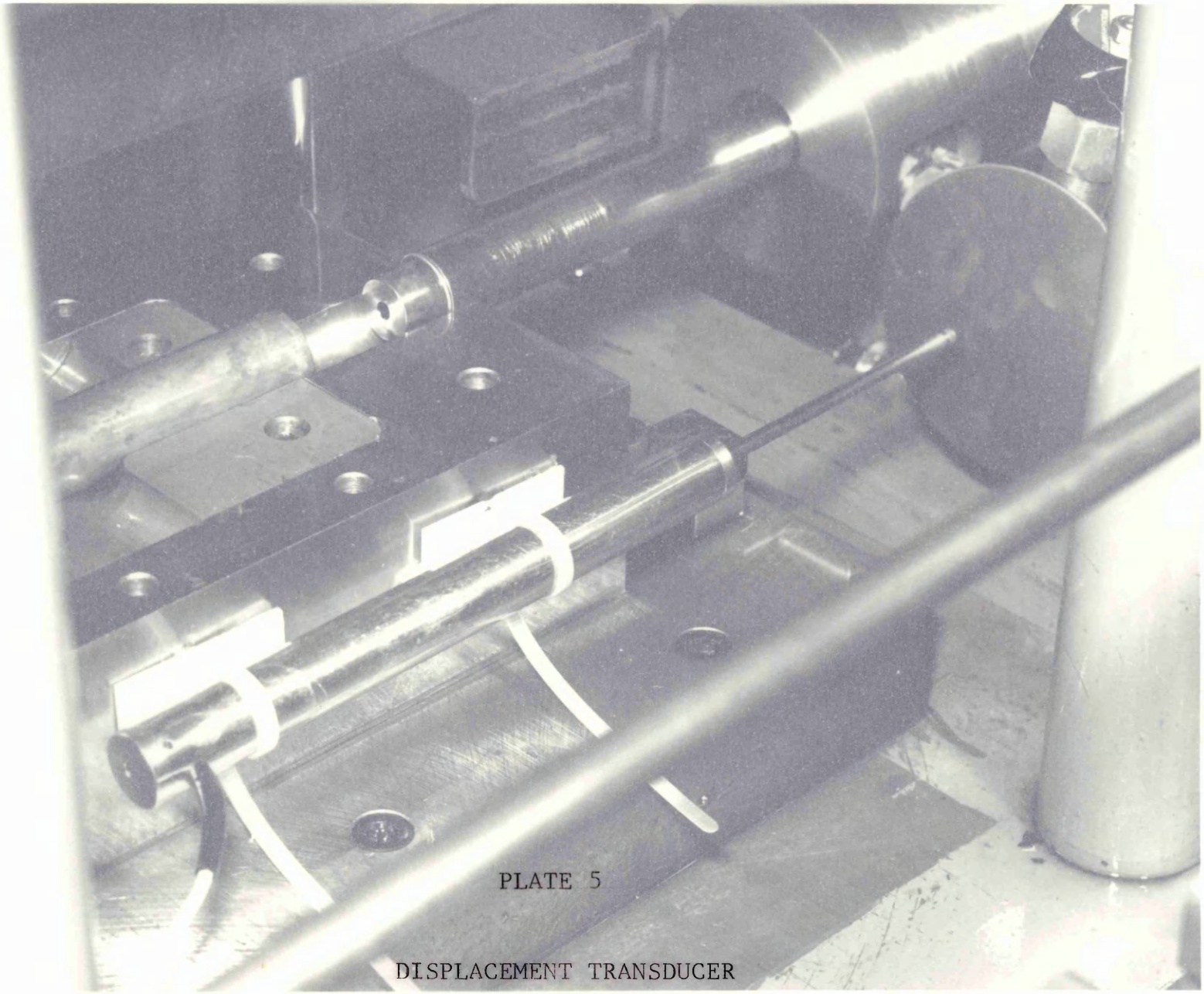

PLATE 5

DISPLACEMENT TRANSDUCER

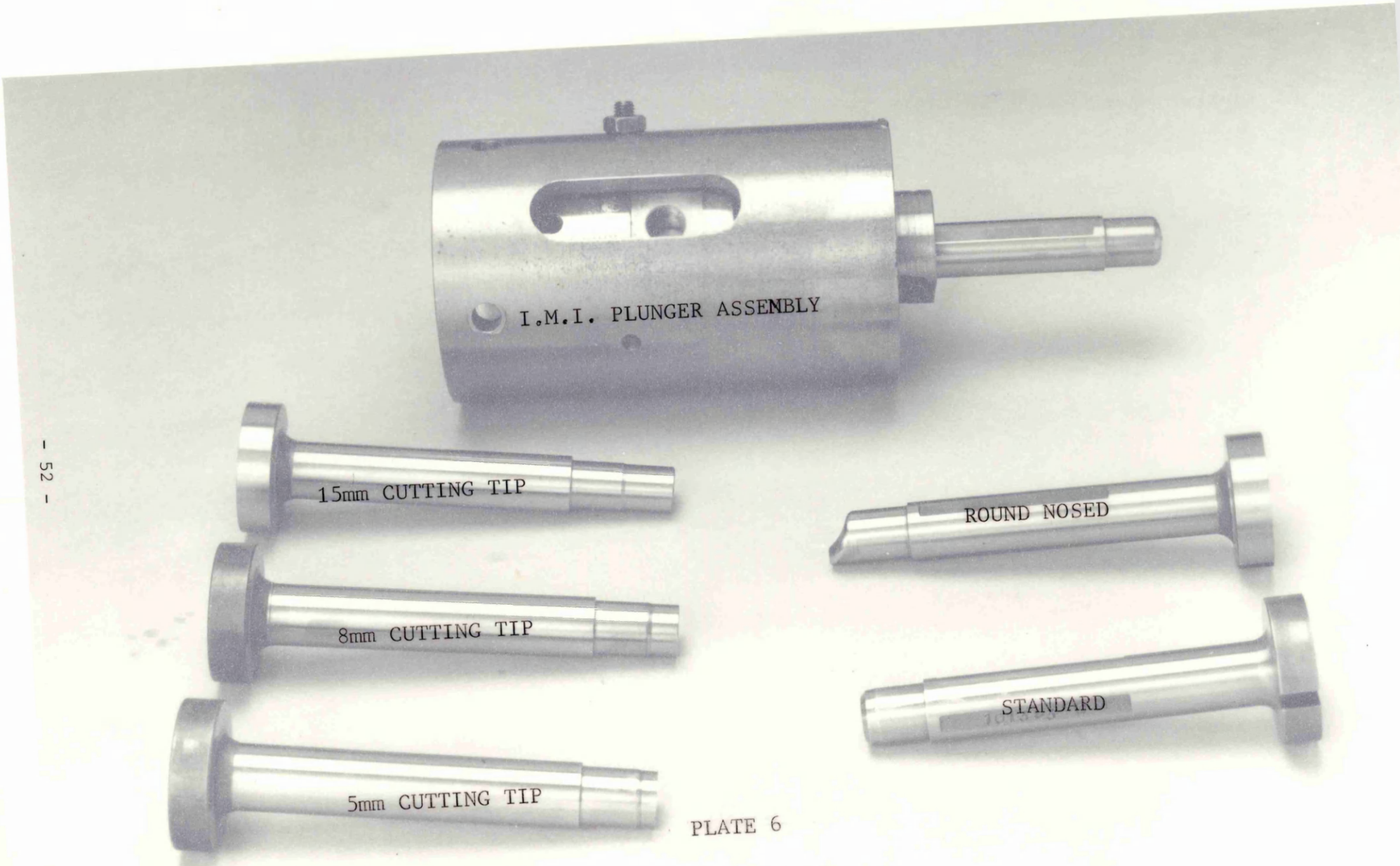

PLATE 6

PLUNGER VARIATIONS

PLATE 7

DIE-BLOCKS WITH SCRIBE LINES

DIE-BLOCKS WITH SCRIBE LINES

PLATE V

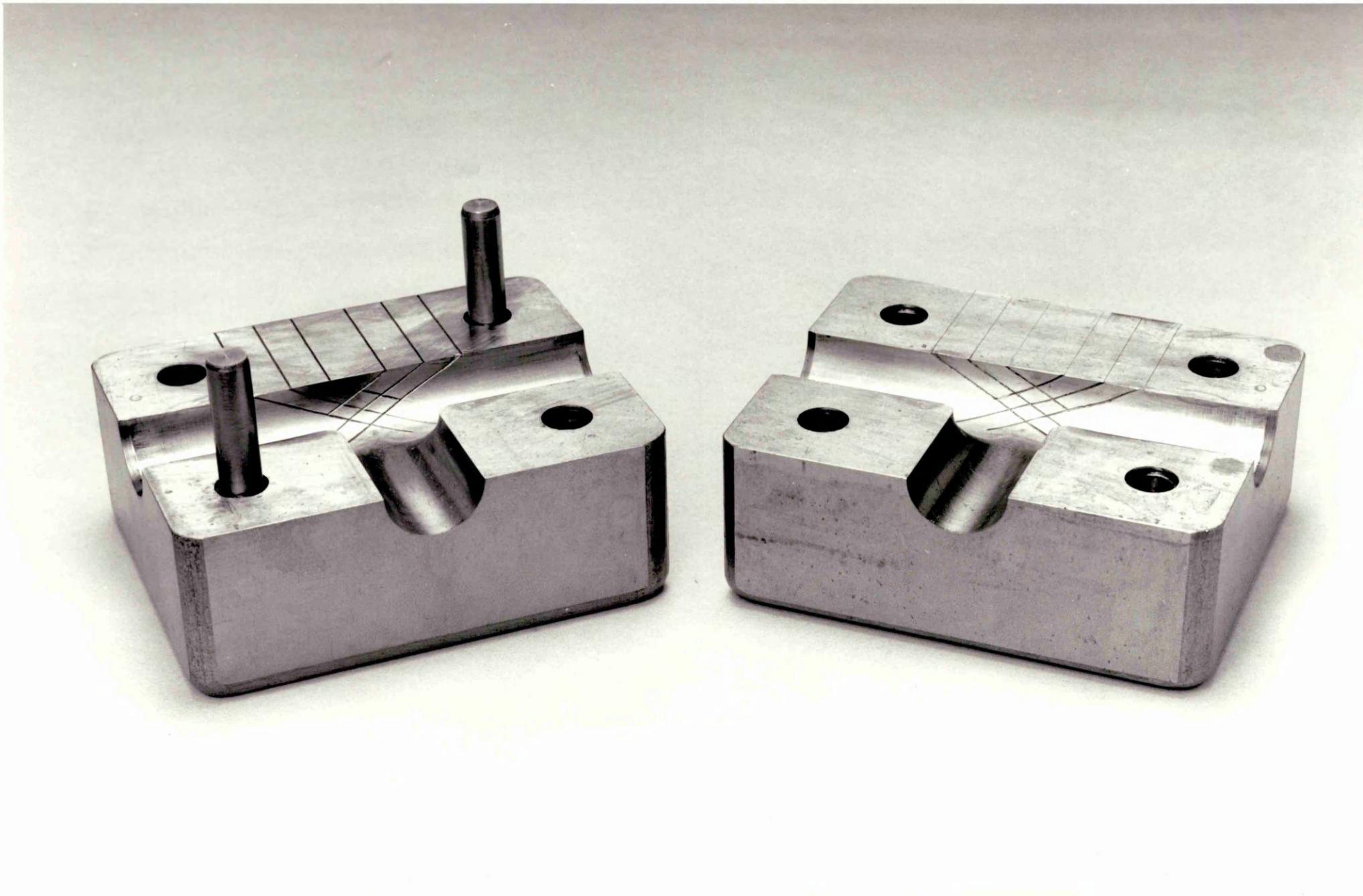

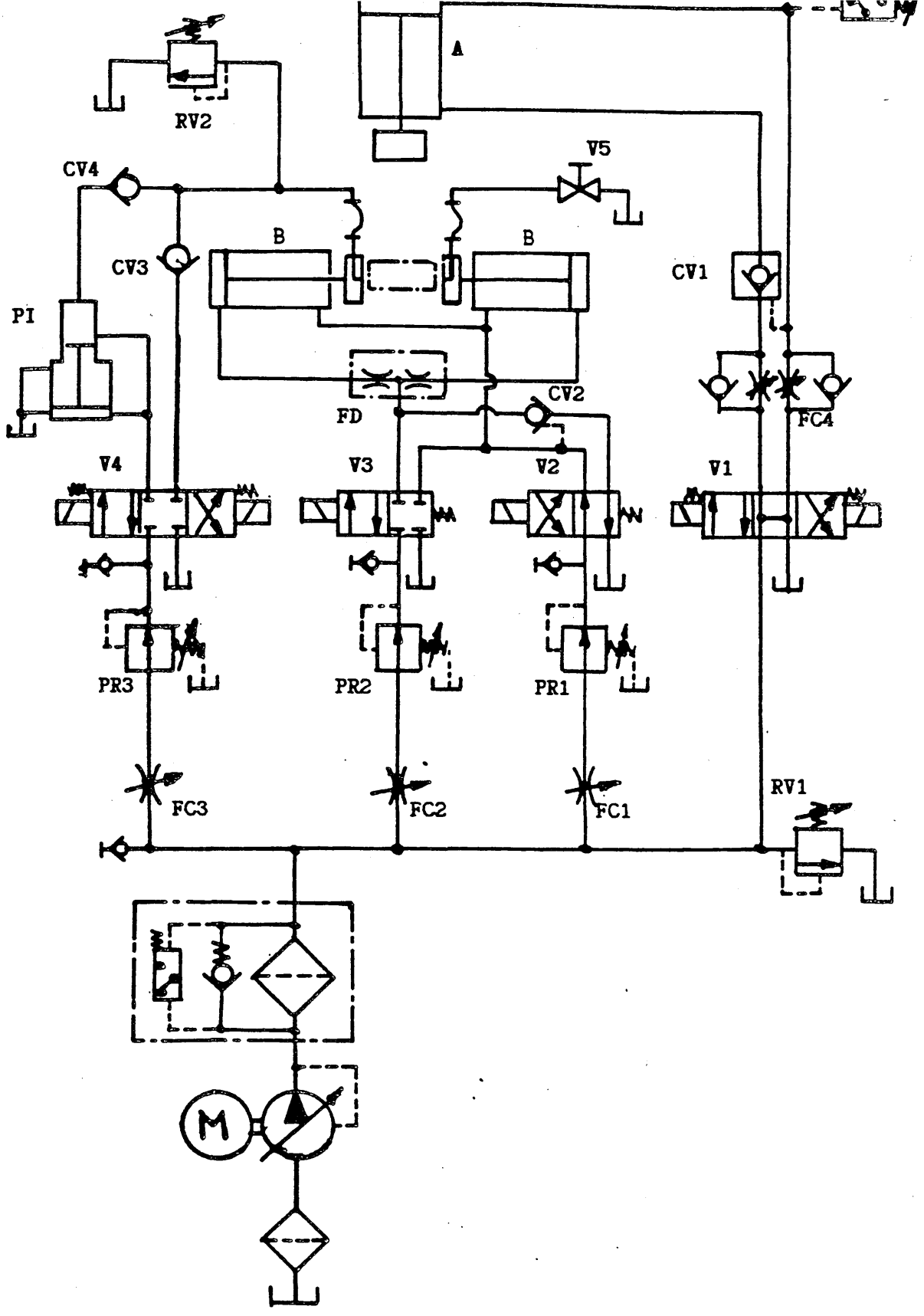

FIGURE 3

The Design Of The Hydraulic Circuit.

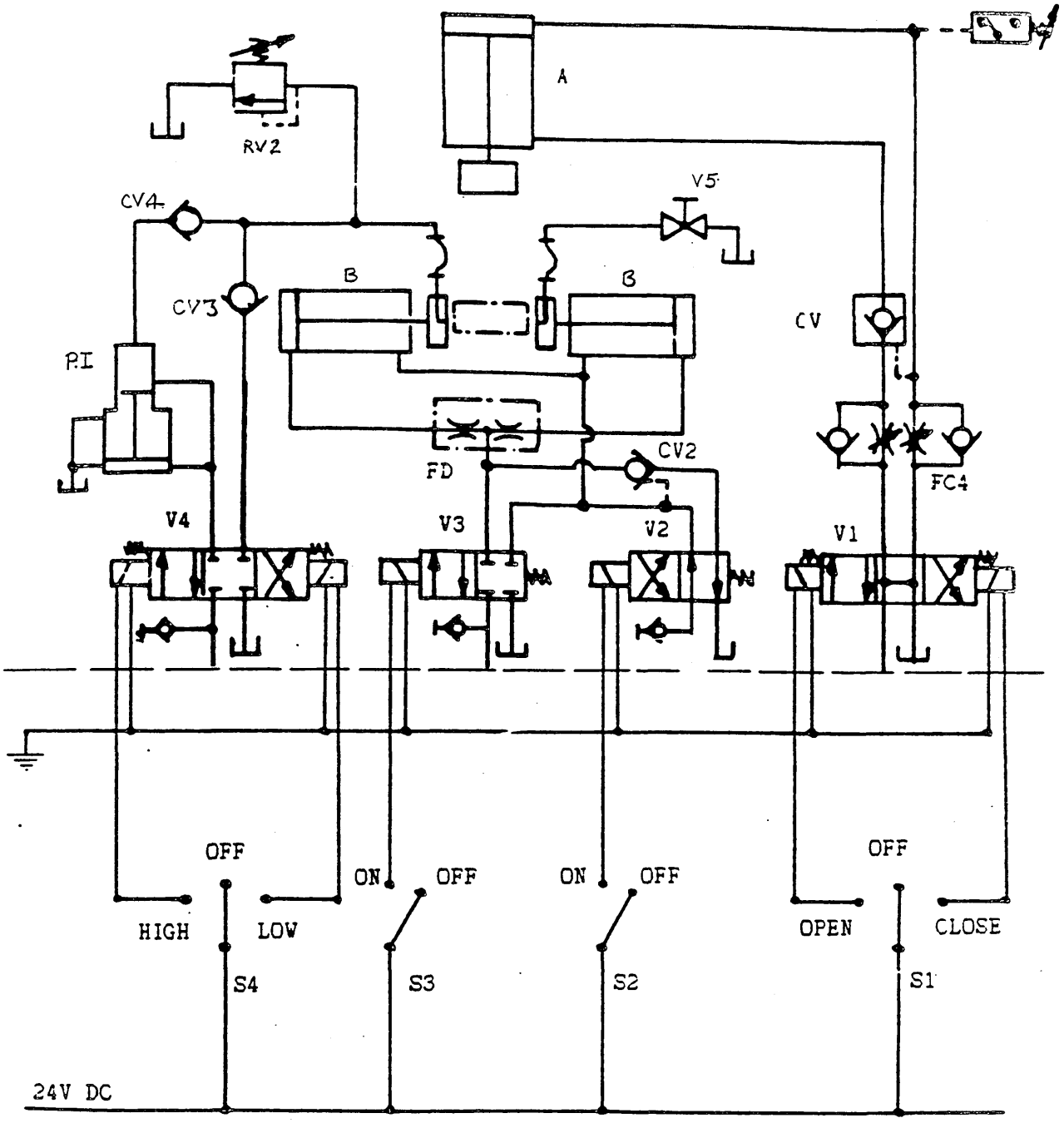

S4		S3		S2		S1	
POSITION	ACTION	POSITION	ACTION	POSITION	ACTION	POSITION	ACTION
HIGH	Supply fluid to the pressure intensifier.	ON	Extend plungers using a large axial compressive force to cause deformation.	ON	Extend plungers using a small force for initial sealing.	OPEN	Open the die block to allow access to the forming area.
OFF	No flow.					OFF	Standby state.
LOW	Bypass the Pressure intensifier for initial filling.	OFF	No flow.	OFF	Retract plungers to allow release of the formed component.	CLOSE	Close and clamp the die halves together.

FIGURE 4

The Switch Arrangement For The Solenoid Valves.

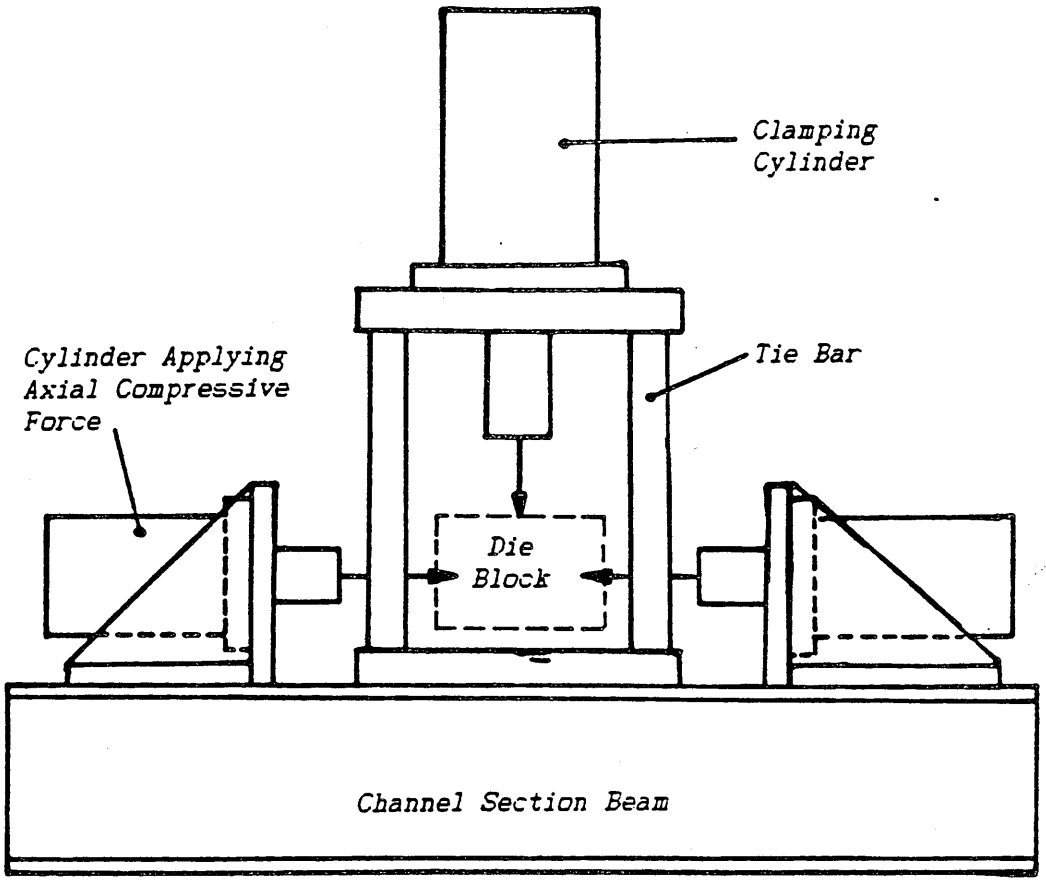

FIGURE 5

The Arrangement Of The Hydraulic Cylinders.

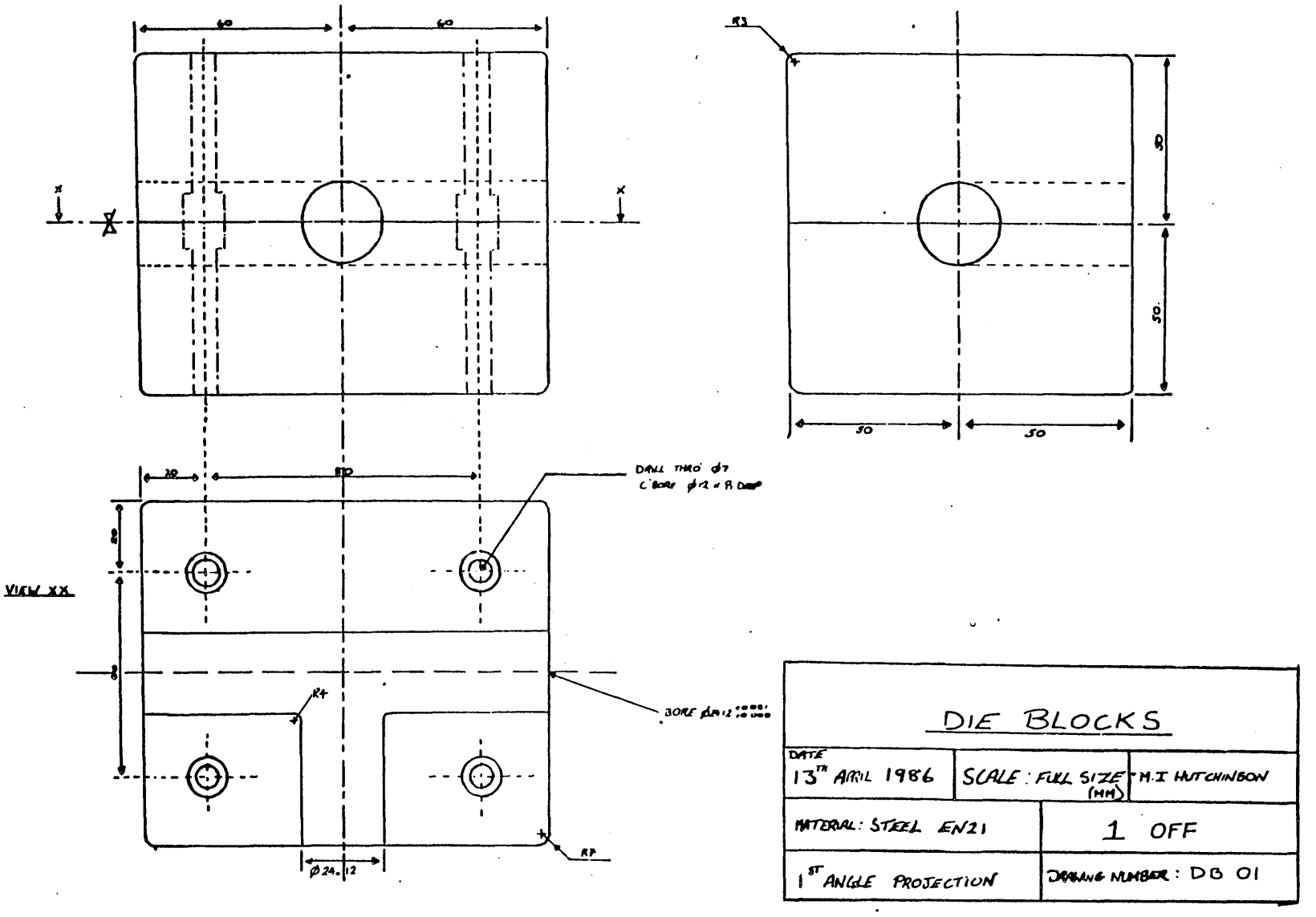

FIGURE 6 : The Tee Piece Die-Blocks.

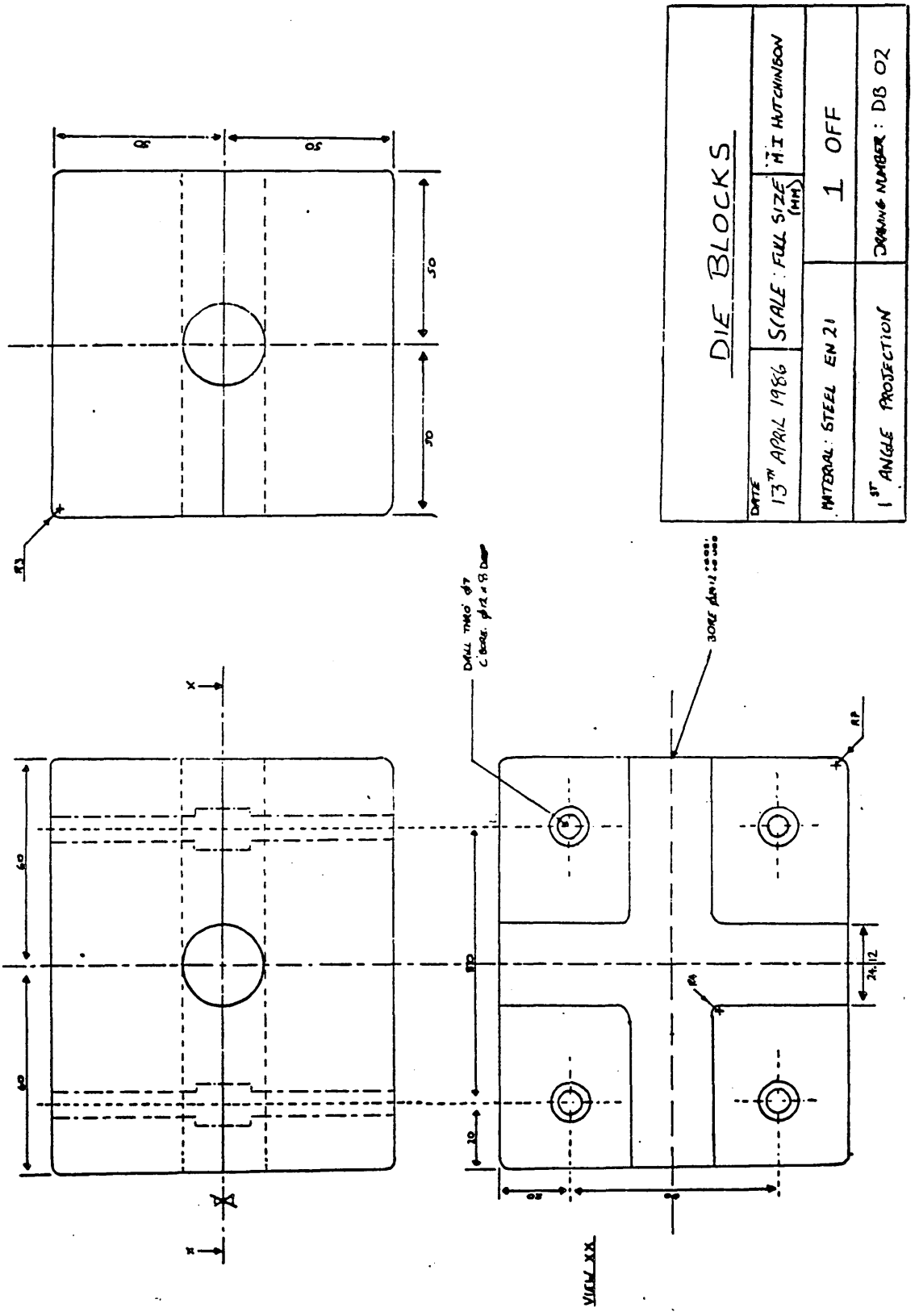

FIGURE 7 : The Cross Joint Die-Blocks.

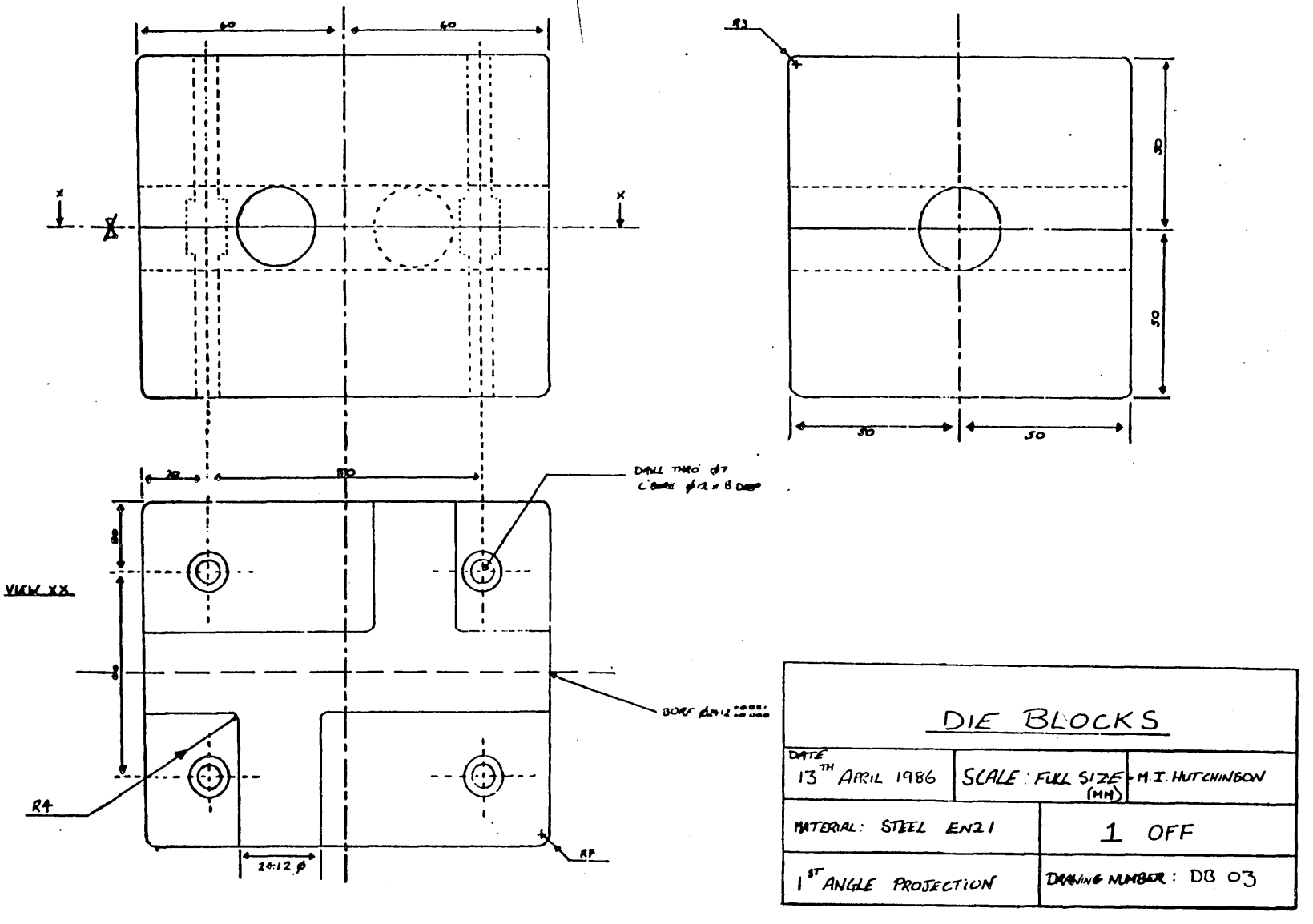

FIGURE 8 : The Off-Set Joint Die-Blocks.

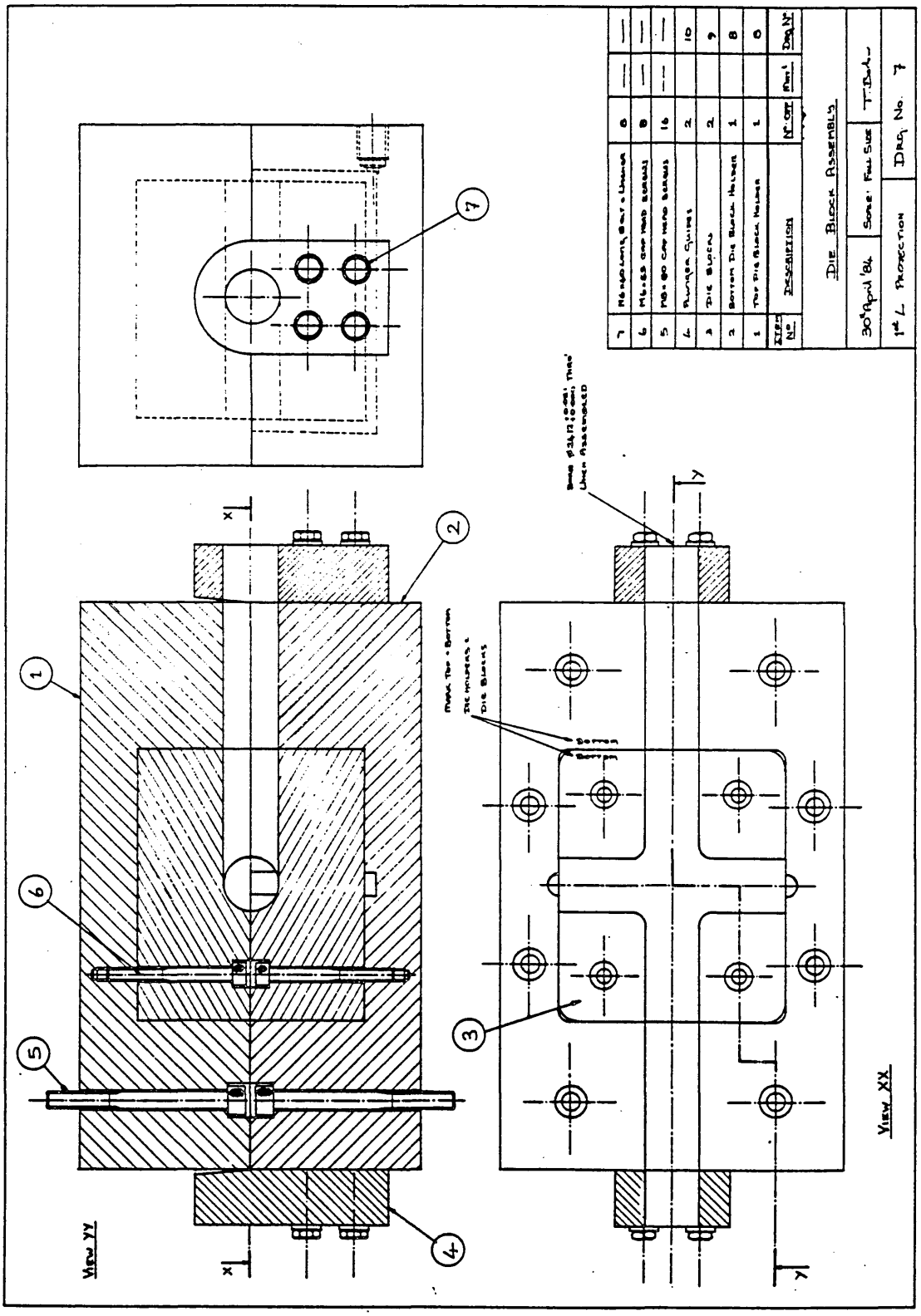

FIGURE 9 : The Die-Block Assembly.

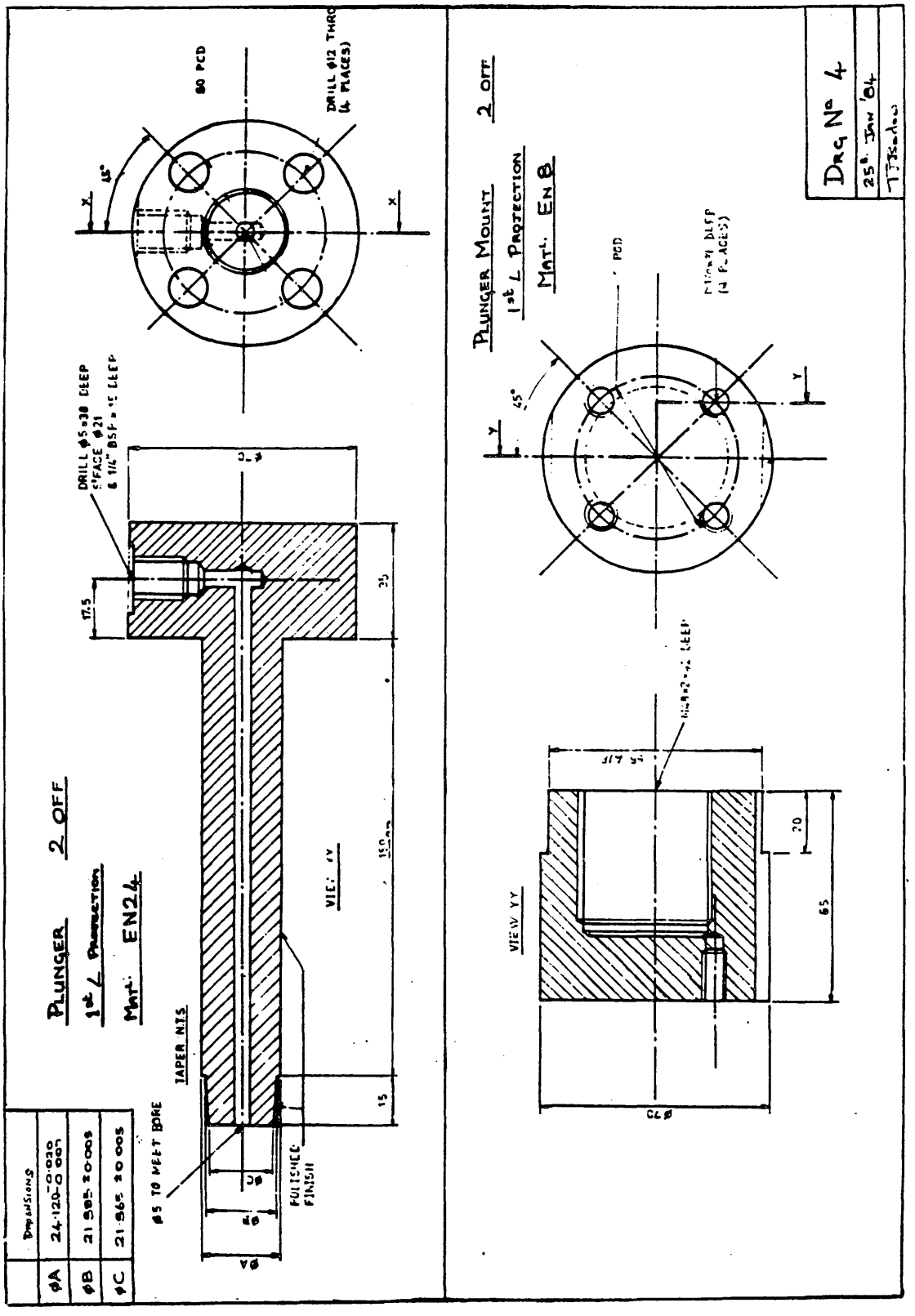

FIGURE 10 : The Plunger And Plunger Mounts.

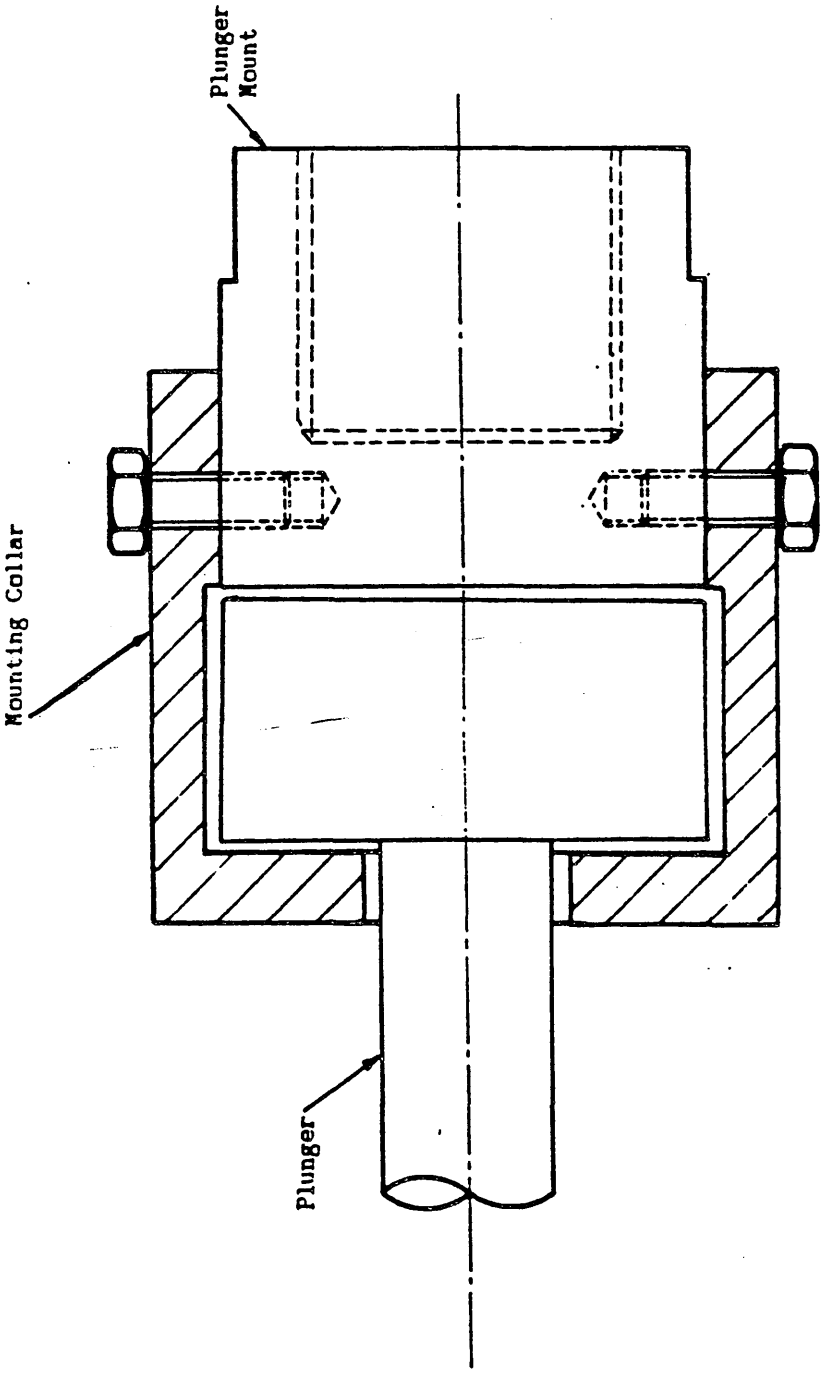

FIGURE 11 : The Plunger Mounting Collar.

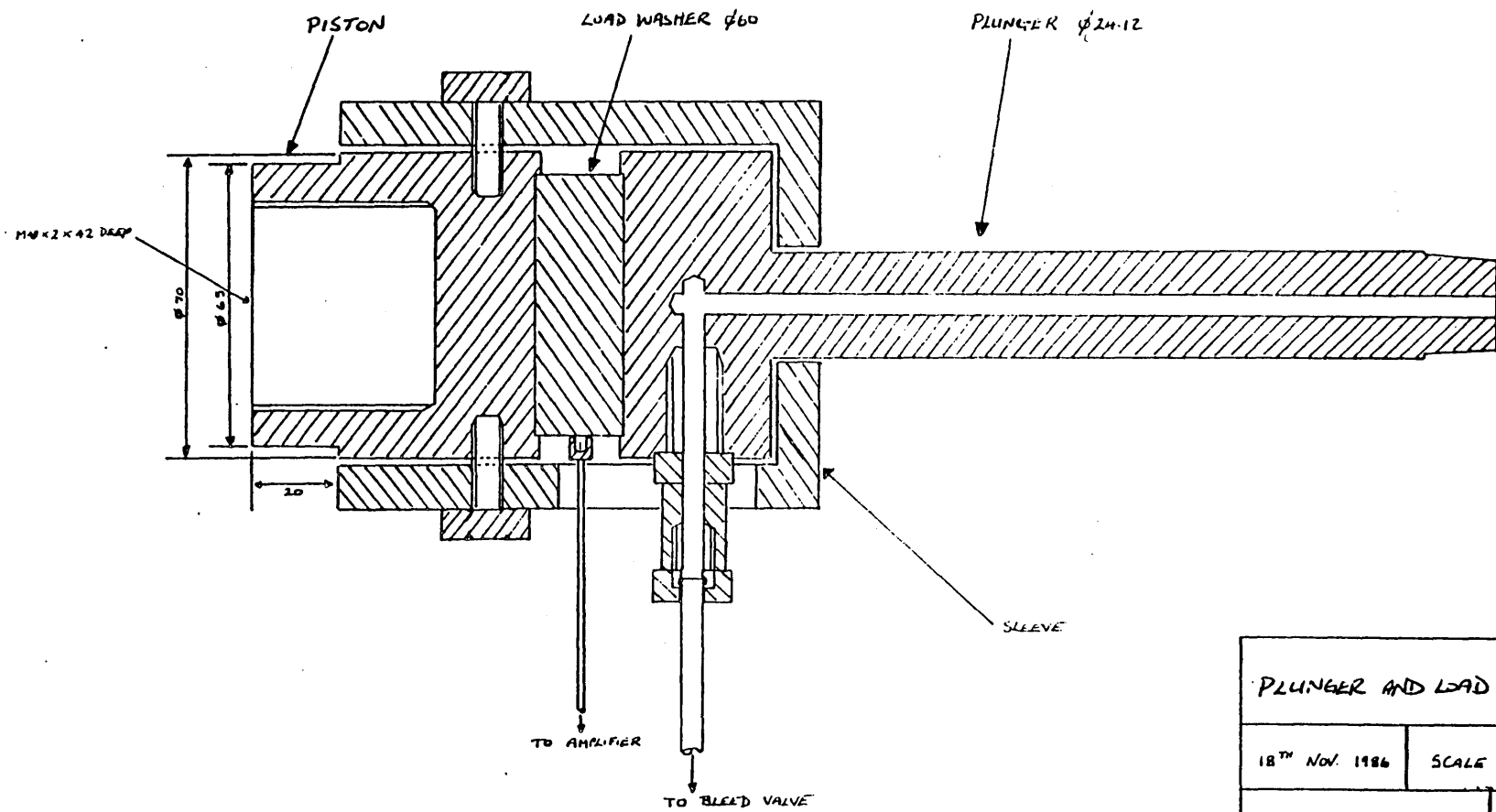

PLUNGER AND LOAD WASHER ASSEMBLY.		
18TH NOV. 1986	SCALE 1:1	
MAT'L : STEEL EN 27	ALL DIMENSIONS IN MM	
LEFT SIDE ASSEMBLY.	DRAWING NO FIG. 2.	

FIGURE 12 : The Plunger And Load Washer Assembly

3. TEST PROCEDURE AND RESULTS

3.1) Test Material

The initial stages of the design of the bulge forming rig involved estimating the size of the tube blank to be used in the forming operation. This was so that the forces involved could be allowed for in the rest of the design. For design considerations, a nominal value of 25 mm diameter and 150 mm length was chosen. The actual tube blank used for the tests was decided on at a later time, before the final dimensioning of the dies and plungers. The original tubes used were of copper and had an outer diameter of 24.12 mm, a wall thickness of 1.37 mm, and came in lengths of 107 mm.

The first set of comparison tests involved the use of copper tubing of a different wall thickness to that stated previously. Since all of the copper tubes used in the investigation were supplied by M.I. Yorkshire Fittings Ltd., it was necessary to accept a size of tube from their production lines. The tubes used in the comparison had an outside diameter of 24.12 mm, a wall thickness of 1.03 mm, and were 147 mm in length.

To compare the effect of tube materials on the bulge forming process, copper, mild steel and commercially pure aluminium were used. The blanks had outside diameters of 24.12 mm, wall thicknesses of 1.37 mm and were 107 mm in length.

The testing of the lubricants was performed on

copper tubes of dimensions: 16.86 mm outside diameter, 94.14 mm length and 0.95 mm wall thickness. These blanks were also obtained from Yorkshire I.M.I. in an annealed condition.

3.2) Operating Procedure

The operation of the machine requires the clamping of a tube blank in the die-blocks, with the subsequent application of internal pressure and axial load. However, the combination and the order in which the internal pressure and axial load are applied determines the final shape of the component.

The design of the machine is such that these forces can be varied to form components at different stages of expansion and various procedures can be used relating to the internal pressure used. The high pressure part of the hydraulic circuit is equipped with a pressure reducing valve to control the internal pressure. In the forming of components there is a decrease in the volume inside the tube due to the axial deformation (except in the case of forming due to pure internal pressure only), which generates a high pressure. Thus, the pressure reducing valve can be used to set the initial internal pressure which can be allowed to increase to any value, as long as that is less than the value at which the pressure relief valve is set (nominally 69 N/mm^2). Alternatively, the relief valve can be used to set a maximum system pressure, which limits the forming process.

Application of compressive axial load, if great enough, results in the axial deformation of the tube, i.e. the tube gets shorter. As would be expected, the greater the axial load, the more deformation that occurs. Therefore, to take the control of the internal

pressure a stage further during the process, the axial deformation can be carried out in stages. During each stage the internal pressure is set to a constant value, and at the end of each stage, when the deformation has stopped, both the internal pressure and the compressive axial load are increased.

The test procedures for these different processes follow a common initial stage, which is as follows (the hydraulic components and switches refer to Figures 3 and 4 respectively).

1) Connect the control board operating the solenoid valves to a 24 V D.C. supply and turn on the isolator to the electric motor and start it.

2) Open the die by moving switch S1 to the OPEN position (during periods of rest, when the motor is still running, the switch should be returned to the central - STANDBY - position to prevent excess heat from being generated in the main relief valve).

3) Place a tube blank centrally on the bottom die; the length, diameter and wall thickness of which have already been noted.

4) Close the die-block by moving switch S1 to the CLOSE position.

5) Move switch S2 to extend the horizontal hydraulic cylinders, and so bring the plungers into contact with the tube blank. The forces acting on the tube are controlled by the pressure reducing valve PR1 which should be set to provide sufficient force to seal the ends of the tube without causing any axial

deformation.

6) Having sealed the ends of the tube, it can then be filled with oil by moving switch S4 to the LOW pressure position, causing the pressure intensifier to be by-passed to fill the tube quickly at low pressure. At the same time the valve V5 should be opened to allow the air to escape from the tube. Once clear oil starts to flow out, this valve can then be shut off to allow internal pressure to be generated.

The rest of the procedure depends on the mode of operation required, and this will be dealt with separately for the three different variations.

3.2.1) Fixed Internal Pressure During Bulging

For this mode of operation, the high pressure relief valve RV2 is set at a predetermined value, and then during the forming process, the internal pressure increases until it reaches the set value and is then relieved. After operations 1 - 6 have been completed, the procedure is as follows:

7) Move switch S4 from the LOW pressure position to the HIGH pressure, which causes the pressure intensifier to be activated, generating a high pressure inside the tube blank. This pressure is controlled by the adjustment of the relief valve RV2, with the pressure reducing valve PR3 adjusted to provide a pressure just greater than that required.

8) Once the tube is subjected to an internal pressure, the compressive axial load should be applied (the duration between the application of the internal

pressure and the compressive axial load should be very small, and preferably simultaneous). This is achieved by moving switch S3. The forces acting on the ends of the tube are controlled by the pressure reducing valve PR2 which should be set sufficiently high as to cause axial deformation.

9) On completion of the forming process, when the forming plungers stop moving, or the tube bursts, switches S2, S3 and S4 are moved to the off position. This causes the plungers to be retracted, and stops the internal pressure supply. This pressure is released as soon as the plungers move apart. To open the dies to gain access to the formed component, switch S1 is moved to the OPEN position.

Having removed the formed component, the machine is then ready for another blank to be placed in the dies for the next forming operation. As an alternative to the above process, step 8 can be omitted, causing the tube to be formed due to internal pressure alone. In this case, the axial load is only used to seal the tube and not to deform it.

3.2.2) Increasing Internal Pressure During Bulging

For this process the initial pressure is set by the pressure reducing valve PR3, and increases during the process to a value determined by the relief valve RV2. Ideally the relief valve RV2 should be set before hand, either at the end of a previous test or by subjecting a blank to the required pressure. Again this procedure follows on after operations 1 - 6 have been

completed.

7) Move switch S4 from the LOW to the HIGH pressure position. The pressure inside the tube blank is controlled by the pressure reducing valve PR3 which should be varied to produce the required initial internal pressure.

8) Once the tube is subjected to the internal pressure, the compressive axial load should be applied by moving switch S3 to the ON position. The force acting on the ends of the tube is controlled by the pressure reducing valve PR2. During forming, the internal pressure will increase, due to the decrease in internal volume, until it reaches the value set by the relief valve RV2. A constant pressure will be maintained once this pressure is reached,and until the completion of the forming process, after which it will drop due to leakages.

9) After completion of the forming process, switches S2, S3 and S4 should be moved to the OFF position, and the dies opened by moving switch S1 to the OPEN position.

3.2.3) Increasing Internal Pressure In Stages

This process is similar to forming a component with a fixed internal pressure, but at the end of the deformation the internal pressure and axial load are increased to produce another deformation. The first axial load applied to the end of the tubes should thus be fairly small, to allow it to be later increased to produce a further deformation. Again steps 1 - 6 should

be followed.

7) Move switch S4 from the LOW to the HIGH pressure position, which causes the pressure intensifier to be activated, generating a high pressure inside the tube blank. This pressure is controlled by the adjustment of the relief valve RV2, with the pressure reducing valve PR3 adjusted to provide a pressure just greater than that required.

8) Once the tube is subjected to an internal pressure, the compressive axial load should be applied. This is achieved by moving switch S3. The forces acting on the ends of the tube are controlled by the pressure reducing valve PR2 which should be set to a suitable value for the initial deformation.

9) When the deformation has stopped i.e. the plungers have stopped moving, the internal pressure can be increased by adjustment of the relief valve RV2 (the pressure reducing valve PR3 may also require adjustment so that a sufficient pressure is being produced from the pressure intensifer).

10) After increasing the internal pressure, the axial deformation can be continued by adjusting the pressure reducing valve PR2, so as to increase the axial load acting on the ends of the tube.

11) When the deformation has stopped, steps 9 and 10 can be repeated, increasing the internal pressure and axial load again, or the component can be removed from the machine by moving switches S2, S3 and S4 to the OFF position, and moving switch S1 to the

3.3) Analysis of the Formed Component

After the bulge forming process was complete, the components were taken from the die-blocks and their final lengths and bulge heights measured with a digital Vernier calliper (initially the readings were taken with a rule, but the Vernier improved accuracy and speeded up the process). The components were then cut in half through the centre of the bulge (the original tee piece and cross joint components were cut lengthwise, but this tended to damage the domes of the bulges. However, these 'halves' were better for presentation, as can be seen in Plates 8, 9 and 10. A 0 mm to 25 mm round-nosed (1 mm radius) micrometer was used to take wall thickness measurements at selected 'x' and 'y' co-ordinates, starting at a point on the tube wall just before the bulge, and finishing at the centre of the dome. The position of the measurement points can be seen in Figure 13a.

All of the components were marked with their given test numbers in both ink and by scribing, and then stored for future cross-checking.

The results of the tests carried out using the hydraulic bulge forming machine can be divided into two types. Firstly, there are those which deal with the feasibility of the process, and concentrate on the formation of a tee piece, cross joint and a non-symmetrical component. Secondly, there are those which show the effect of using different forming materials, lubricants, plunger variations and die-block

geometries. Whereas the initial tests show the forming limits of different components, the latter ones deal with comparisons between different parameters on a given shape.

3.4) Tee Piece

A die-block with branch radius of 3 mm (Figure 13b) was used to form the tee pieces. Two thicknesses of copper tubing were used: 1.37 mm and 1.03 mm.

The method of testing was that the axial deformation load would be set at a value, and then the internal pressure incremented in steps of 3.45 N/mm^2 from a value which was just sufficient to seal the tube blank (3.45 N/mm^2), to one where the tube burst. The value of the internal pressure was regulated by the pressure relief valve (RV3).

From the results obtained from the tests, three types of graphical representation were selected:

1) the ratio of the wall thicknesses at any point on the formed bulge compared to the original tube blank (t/t_0) were plotted against the 'y' co-ordinate where the thickness measurement was taken;

2) the ratio of the bulge height to the original radius of the blank (H/r_0) was plotted against the internal pressure required to give that amount of deformation, and;

3) the ratio of the final length of the tube blank compared to the original length (L_f/L_0) was plotted against the compressive axial load.

The trends shown by these graghs enabled diagrams to be drawn which show the forming zones of the various components.

3.4.1) Tee Piece - 1.37 mm Wall Thickness

The tee pieces were formed using three values of compressive axial load: 43 kN, 85 kN and 128 kN. For each of these loads, a value of internal pressure was selected which caused a small bulge to form (20.70 N/mm^2). Test were then taken in increments of 3.45 N/mm^2 until the tube burst, and at that stage the next load would be selected. Figures 14 to 17 show graphical representations of the results.

The components formed with the 43 kN compressive axial load developed only small bulges (the bulges were not 'branches' but merely domed surfaces on the wall of the cylindrical tubes), and burst at a pressure of 48.30 N/mm^2. There was no sign of buckling with an internal pressure of 20.70 N/mm^2 and the percentage of original wall thickness did not drop below 70%. The maximum bulge height was 4.38 mm. See Figure 14.

With an axial load of 85 kN, the components formed consisted of a branch with a domed top. There was some buckling with an internal pressure of 20.70 N/mm^2, and as previously, the tube burst at 48.30 N/mm^2. Again, the percentage of original wall thickness did not drop below 70%, but the increase in axial load tripled the bulge height to a value of 12.00 mm. However, in the tests carried out at 43 kN and 85 kN, the bulge heights were not sufficient to deem the components 'fully-formed' (a fully-formed component being one where all three 'branches' are of

approximately the same length). See Figure 15.

The tests carried out with an axial load of 128 kN produced the greatest bulge heights. All of the components formed with an internal pressure of under 37.95 N/mm^2 suffered from buckling, but those above that were fully-formed. The upper forming pressure was 55.20 N/mm^2, and the lowest value of the percentage of original wall thickness recorded was 65%. For this reduction in wall thickness, a bulge height of 21.58 mm was obtained. See Figure 16.

Graphical representations of selected tests for the previous three axial loads are shown in Figure 17.

Although the above are the results obtained for the forming range of a tee piece, it was found that it was possible to improve upon the values by using a two stage process. If a tube blank was initially formed at, say, an internal pressure of 34.50 N/mm^2, and then the pressure relief valve (V3) opened up so that the pressure rose to 55.20 N/mm^2, the component would have an increased bulge height, but not the same amount of reduction in wall thickness as if it had been formed initially at 55.20 N/mm^2 (in cases where the tube burst at 48.30 N/mm^2 with a one stage deformation, it was possible to exceed 58.65 N/mm^2 if a two stage process was used.

Figure 18 shows the relationship between the axial deformation load and the internal pressure, and is split up into four areas. Failure of the forming

process will occur if the forming conditions fall into areas C or D. Area C indicates that the axial deformation load is too high, or the internal pressure is too low, resulting in buckling of the tube occurring. Fracture of the tube will occur in area D. This was found to occur in the dome formed by the internal pressure. Fracture will also occur if the initial conditions fall into area B. In order to form a perfect component, the conditions have to fall into area A. However, after the deformation has been partly completed, the forming conditions may move into area B.

3.4.2) Tee Piece - 1.03 mm Wall Thickness

The thinner walled tee pieces were formed using compressive axial loads of 43 kN, 85 kN and 106 kN. Loads in excess of 106 kN caused buckling for all values of internal pressure. Figures 19 to 22 are the graphical representations of the results, and Figure 23 shows the forming zone. As in the previous tests, the 43 kN load was insufficient to create a branch and a dome was formed on the side of the tube. The maximum value of internal pressure the tube could withstand was 31.05 N/mm^2, and this created a bulge height of 5.0 mm, with a corresponding reduction in wall thickness ratio of 63% at the dome centre. See Figure 19.

The tests carried out using an 85 kN load produced a tee piece which was fully-formed, but which would only withstand 31.05 N/mm^2 pressure. At this value, a bulge height of 19.1 mm was achieved for a

reduction to 71% of the original wall thickness. See Figure 20.

With a load of 106 kN, it was possible to operate the machine with internal pressures up to 34.50 N/mm^2. At this maximum value, a bulge height of 28.5 mm was recorded with a corresponding minimum wall thickness ratio of 58%. See Figure 21.

The two stage deformation process was tried again, and similar results obtained to those for the thicker material. All other trends were the same as for the thicker material.

The tests showed that it was possible to form tee pieces from various thicknesses of material. The thinner the wall of the tube, the more limited the range of compressive axial loads and internal pressures that could be used (buckling and rupture occurred at values of load and pressure in thinner walled tubes that thicker ones would withstand). However, both thicknesses produced perfectly acceptable tee pieces.

In the formation of a tee piece, material is forced into the deformation zone to form the branch. However, because the tube is uniformly compressed and there is only one branch formed, there is a considerable build-up of material on the opposite side to the branch (percentage of original wall thickness in the order of 250%). This build-up is a major problem for manufacturers and is discussed later.

The minimum value of the percentage of the original wall thickness is always recorded at the

centre of the dome and tubes always burst around this area. Although in the manufacturing process the domes are sheared-off to create the third branch, the value recorded at the dome is still the most relevant point.

Figures 24 to 29 compare the variations in the two types of tube blank.

3.5) Cross Joint

Tests were again carried out using two sizes of tube blank (1.03 mm and 1.37 mm wall thicknesses). The testing and analysis were the same as those used for the tee piece.

3.5.1) Cross Joint - 1.37 mm Wall Thickness

The cross joints were formed using compressive axial loads of 43 kN, 85 kN, 106 kN, 128 kN and 149 kN. The mimimum internal pressure used was 27.60 N/mm^2 and the increment was 3.45 N/mm^2 per test. All of the above tests were one stage formations, although several two-stage ones were performed in order to verify the results obtained from the tee piece. Graphical representations of the results are shown in Figures 30 to 33.

The components formed with the compressive axial 'sealing' load (43 kN) were only partially bulged, and with an internal pressure of 48.30 N/mm^2, the bulge heights were only 4.5 mm (there was no visual difference between the bulges [except in the case where a burst occurred], and therefore only one set of values were recorded and no graphical representation made). With this pressure, the minimum wall thickness ratio was 67%. Burst components were noted with an internal pressure of 51.75 N/mm^2 and above.

With an axial load of 85 kN, the components were not fully-formed. The bursting pressure was 55.20 N/mm^2, and the highest forming pressure was 51.75 N/mm^2. This value gave a bulge height of 12.0 mm

which consisted of a branch and dome, unlike the lower axial load. The minimum wall thickness ratio was 85%. See Figure 30.

When the axial load was increased to 106 kN, buckling was observed for internal pressures up to and including 34.50 N/mm^2. Above this value, the components were deemed fully formed. At 44.85 N/mm^2, there was a bulge height of 18.0 mm and a minimum wall thickness ratio of 80%.

Using an axial load of 128 kN gave the best results over the widest range of pressures. Although some buckling occurred for the low pressures, the rest had a good shape and it was only at pressures of around 55.20 N/mm^2 that over-forming or bursting occurred (over-forming was deemed to have occurred when the lengths of the remaining branches were in the order of half that of the bulge height. The components were not flawed in anyway, but the length of the branches made them unusable as fittings). For an internal pressure of 51.75 N/mm^2, a bulge height of 19.5 mm was achieved with a minimum wall thickness ratio of 82%. See Figure 31.

To give an example of how the cross joint was deemed to be fully formed, it is necessary to check the final length of the component. For the above, the final length was 60.5 mm, and the diameter of the tube 24.12 mm. Therefore each of the branches is (60.5-24.12)/2, which is 18.19 mm - this compares with a bulge height of 19.5 mm. An over developed component

might have a final length of 50.0 mm, which would give branch lengths of 13 mm, compared to a bulge height of 25.0 mm.

The tests carried out with an axial load of 149 kN proved unsuccessful, because all of the components were either buckled or over-deformed. The only specimen produced without flaws was produced with an internal pressure of 48.30 N/mm^2. This gave a bulge height of 28.0 mm and a minimum wall thickness ratio of 88%. The branches were only 7.0 mm in length, which is 25% of the bulge height. See Figures 32 and 33

The results from tests on components formed with a two-stage process were similar to those from the tee piece. An increase was seen in the bulge heights and wall thicknesses, and the value of internal pressure before a component burst was increased.

When comparing the formation of a tee piece and cross joint from the same wall thickness, there were comparable bulge heights for the same values of axial loads and internal pressures. However, the tee piece had a minimum wall thickness ratio which was up to 15% less than the comparable cross joint value. Although the tee piece could be analysed as half a cross joint, the fact that there is a build up of material opposite the branch in a tee piece affects the wall thickness. Some material does flow from the lower half of the tee piece, but most of it remains in the lower section of the branch. However, in the cross joint there is an equal distribution of the material

and this means that there is a greater volume of metal in the bulge, which, given a similar bulge height, means that the walls are thicker. The bulge height is dictated by the axial load, internal pressure and the material properties, and as they were constant for any two relevant tests, the bulge heights were similar.

3.5.2) **Cross Joint - 1.03 mm Wall Thickness**

The results obtained for the cross joint formed with the thinner material showed the same trends as with the thicker material, but formation took place at lower compressive axial loads and internal pressures. The axial loads were 43 kN, 64 kN and 85 kN, with internal pressures starting at 20.70 N/mm^2 and incrementing in 3.45 N/mm^2 steps. Graphical representations of the results are shown in Figures 34 to 39.

With an axial load of 43 kN, there was only partial deformation for internal pressures of 20.70 N/mm^2 and 24.15 N/mm^2, and the highest value achieved without bursting was 27.60 N/mm^2. At this pressure, the bulge height was 4.0 mm, and the minimum wall thickness ratio was 89%. See Figure 34.

The most successful axial load was found to be 64 kN and although the components could only be formed over the same range of internal pressure as the 43 kN load, with an internal pressure of 27.60 N/mm^2, a bulge height of 12.0 mm was achieved and a minimum wall thickness ratio of 80%. See Figure 35.

The 85 kN load produced components, but at the

lower values of internal pressure (up to 24.15 N/mm^2), the specimens were buckled. At a value of 31.05 N/mm^2, the bulge height was 26.0 mm, and the minimum wall thickness ratio 80%. See Figures 36 and 37

Although cross joints could be formed from the thinner material, the values of internal pressure and compressive axial load capable of producing a component were limited - perhaps only one internal pressure for any given axial load. Generally speaking, for both the tee piece and cross joint, it seemed that the diameters of the tube blank and branch compared to the wall thicknesses were the important ratios when determining the range over which a component could be properly formed. See Figures 38 and 39

3.6) Off-Set Joint

As stated previously, it was felt that the build-up of material on the opposite surface to the branch affected the wall thickness ratio. In order to analyse this, and the formation of a non-symmetrical component, a die was designed which had branches at 180^{o} to each other, but not on the same axis (Figure 8). The reason for the selection of this shape was that if it proved successful, it could be used to form two tee pieces from the same tube, the component being divided after the formation process. The thinner walled tubes (1.03 mm) were selected, since they allowed larger deformations for any given pressure/load combination.

In the tests carried out, no combinations of axial load or internal pressure created a perfectly shaped component. All the bulges were lop-sided, with the sides of the branches nearest to the tube ends being longer than the inner ones (Figure 13c). The compressive axial loads used were 43 kN, 64 kN, 85 kN and 106 kN. With a load of 43 kN, the tubes withstood the highest pressure, 31.05 N/mm^2, resulting in bulge heights of 5.0 mm, with a minimum wall thickness ratio of 65%. The other three values of axial load could only withstand a pressure of 20.70 N/mm^2, and for this value; the 64 kN test produced bulge heights of 7.0 mm with a minimum wall thickness ratio of 67%, the 85 kN test produced bulge heights of 10.0 mm with a minimum wall thickness ratio of 75%, and the 106 kN test had

bulge heights of 17.0 mm with a minimum wall thickness ratio of 77%.

Figures 40 to 49 show how the percentage of original wall thickness varies against 'y' for the off-set joint, tee piece, and cross joint components formed from tubes of 1.03 mm wall thickness. There is the least reduction for the cross joint, followed by the tee piece, and then the off-set joint component. However, the cross joint and tee piece are correctly shaped, whereas the off-set joints are not. The bulge heights obtained for any combination of compressive axial load and internal pressure are similar for all three shapes - the value obtained for the off-set joint being a maximum and not at the centre of the dome, as with the tee piece and the cross joint.

3.7) Tee Pieces Formed From Aluminium, Copper and Steel

Tests were carried out on three different materials - copper, steel and commercially pure aluminium. All of the tube blanks were of the same dimensions: 107 mm in length, 24.12 mm outside diameter and 1.37 mm wall thickness. The materials were annealed prior to testing and the tube surfaces were of a similar surface finish.

Testing was performed over a range of internal pressures and compressive axial loads. The steel and copper components were formed over the same range: 27.60 N/mm^2 to 62.10 N/mm^2 internal pressure and 85 kN to 149 kN compressive axial load. The aluminium, however, would not form in these ranges and was tested between 6.90 N/m^2 and 20.70 N/mm^2 internal pressure and 43 kN and 106 kN compressive axial load.

The results obtained from the tests were not analysed in the same manner as for the previous components. In those cases, the results were used to obtain all the variations over which deformation took place, in order to ascertain in what ranges a component was best formed. However, for these tests a comparison was sought between the various materials when used to form a tee piece. Unlike the tests carried out on one material, here the forming ranges differed and this meant that it was impossible to graphically represent the trends without adjusting the axes.

Graphs were plotted of:

1) the ratio of the bulge height to the

original tube radius compared to the internal pressure (Figure 50),

2) the percentage of the original tube length compared to the compressive axial load (Figure 51) and,

3) the percentage of the original wall thickness at varying 'y' co-ordinates on the branch (Figures 52 to 59).

However, where previously the graphs were for fixed axial loads and internal pressures, here that was inapplicable. Instead, the results were analysed and three similar sets of results (one for each material) were plotted and their forming ranges shown.

Table 1 (page 209) shows the maximum forming values for the tests.

3.7.1) Aluminium

The aluminium tubes were formed using four compressive axial loads: 43 kN, 64 kN, 85 kN and 106 kN and internal pressures starting at 6.90 N/mm^2 and incremented in 3.45 N/mm^2 steps until failure.

The components had a very poor surface finish with the material flow lines in the deformation zone being very noticeable.

3.7.2) Copper

The copper was tested with compressive axial loads of 85 kN, 106 kN, 128 kN and 149 kN. The internal pressures used varied from 27.60 N/mm^2 to 55.20 N/mm^2 and the results obtained at the maximum forming pressures are shown in Table 1.

The trends for these tests were the same as

the previous tests on copper. The surface finish of the components was satisfactory, although the flow paths of the material in the deformation zone could be seen.

3.7.3) Steel

As might have been expected, the steel required the highest values of compressive axial load and internal pressure to produce a formed component. Even at the maximum forming limits of the machine, the steel had not achieved a branch height which could have deemed the component fully-formed.

For the full range of internal pressures and axial loads used, there were no cases where the components were buckled or burst. The surface finish of the steel components appeared polished even after major deformations.

3.7.4) Compression Tests on the Tube Material

Compression tests were carried out on the three materials to obtain stress-strain relationships. Tubes of the material were machined, and several rings of 5 mm length of each material obtained. These were coated with lubricants and then deformed in a 'Denison' testing machine. A record was made of the loads and reductions in thickness of the samples. A graph was plotted showing the relative stresses and strains for the materials (Figure 60).

As expected, the steel had the highest stress to strain ratio, followed by copper, and then aluminium.

3.8) Plunger Variation

Two of the main problems with the bulge forming process are friction and the material build-up opposite the branch in a tee piece. Friction hinders the flow of the material into the deformation zone, and limits the height of the branch. The build-up of material inside the tube is an unwanted side-effect of the basic bulge forming process. In the manufacturing process, this build-up has to be removed by a secondary machining operation, which is both time consuming and costly. If this unwanted material could be forced into the deformation zone, or away from the centre of the tube, it would aid the process by increasing the bulge height.

The problem of friction can be improved with the use of lubricants, as is shown in the results in the next section.

Three approaches were used in an attempt to remove the material build-up, which were:

1) the material was forced into the deformation zone,

2) the material was sheared from inside the tube, and,

3) the material was allowed to flow away and not build up opposite the branch.

The plungers used for all of the initial tests had a 0.1 degree taper on the section which entered the tube (Figure 10). When the tube was sealed, most of the tapered part of the plungers were in contact with the

inner wall (the inner diameter of the tube was the same as the end of the plunger, so when the plungers were advanced they made an interference contact with the tube). During the deformation process, the sides of the tube in contact with the plungers (end 15 mm) were also in contact with the die-block (the tube walls being pressed between the two), and this greatly increased the frictional force. Also, the tips of the plungers acted as rams and forced the material building-up inside the tube ahead of them. This effect concentrated the built-up area (it appeared as a stepped section in the centre of the tube, 15 mm from either end), so the greater the branch height, the greater the build-up.

Modified plungers were used (Plate 6) where the lower half of the section that entered the tube was drawn out to a round nose. When the tubes were fully-formed, the plunger tips almost met in the centre. This prevented the material building-up in the lower section and forced it up into the deformation zone. Although the principle worked, the plungers had the effect of moving the 'stepped' area away from the bottom of the tube and into the sides. There was still the same amount of friction as the geometry of the plungers was unaltered except for the added 'nose'. The bulge height was not noticeably improved, and the new plungers still left a stepped area which needed to be machined in a secondary operation.

The second type of plungers used were ones which had shearing tips (Plate 6). They had the same

finely tapered initial section, but had additional cutting tips at the end. These tips were of a length where they were 1 mm apart when the tubes were fully formed. A chip of material was left in the middle of the tube which could be removed after the process by forcing a rod through. However, when tested, the plungers did shear through the built-up material, but the process created such forces in the tube that small micro-cracks were found opposite the branch. Unlike ones found in previous tests, these passed completely through the wall and made the components unusable in an industrial application. The gap between the tips was increased, but the same problem was encountered, and the process had to be drastically altered.

In the new method, the components were formed as normal, and then a shearing process used with a separate machine. The tubes were supported end on, and a specially designed plunger, with a greatly extended cutting tip, forced through. This plunger removed the built-up material and was much more convenient than the old method.

The final method used was the one which proved the most successful. The original plungers were reground so that the new angle of taper was 3 degrees. Only the section of the plungers before the sealing step were in contact with the tube (last 1 mm), and this meant that the frictional force was the same along the whole length of the tube. When the tubes were deformed, the material built up along the entire length

and did not appear as a step. There was an increase in thickness towards the centre of the tube, but this was only about 30% to 50% of the thickness at the ends (with the old plungers, the stepped area thickness could be in the order of 300% that of the ends). Although no material was forced into the deformation zone, the effect of reducing the friction was most noticeable. Not only were greater bulge heights achieved, but in some cases it was possible to form components at higher internal pressures. For example, with an axial load of 43 kN and internal pressure of 48.30 N/mm^2, the old plungers produced a bulge height of 4.38 mm and a minimum wall thickness of 71%. However, the new plungers produced a bulge height of 13.29 mm and a minimum wall thickness ratio of 76% (an increase in bulge height of over 200%). For a load of 128 kN, the respective values were 21.58 mm to 28.51 mm (32% increase), and 68% to 77% (13% increase).

Figures 61 to 71 show the improvements created by the new plungers over all ranges of compressive axial load and internal pressure.

3.9) Lubrication

In the bulge forming process, the amount of friction acting between the tube blank and the die-blocks determines the extent of deformation. The whole process is reliant on the internal pressure in the tube being large enough to prevent the axial load buckling the tube. However, this internal pressure forces the tube walls against the sides of the die-blocks and hence maximises the resistive nature of the co-efficient of friction. Friction limits the extent of the bulging process, since the material cannot flow as easily into the side branch. Also, the build-up of material on the opposite side of the tube to the branch is increased if the material cannot flow as easily across the deformation zone.

Any method which can be used to reduce the co-efficient of friction must improve the bulge forming process, as greater bulge heights can be achieved for lower combinations of compressive axial load and internal pressure. The alteration of the plunger tapers has been shown to reduce the area over which the ends of the tube are forced against the die-blocks. This enhances the process, but cannot affect the formation of the bulge within the branch (it merely allows more material to be forced into the deformation zone).

Under normal circumstances, the tubes are formed with the hydraulic oil used as the pressurising medium acting as a lubricant (it is difficult to keep the oil off the die-block surfaces, because each time a

component is unsealed after the process, its contents are spilled over the dies).

Four lubricants were used to analyse the effect on the components, and these were compared against the standard tests done with the normal hydraulic oil. Three of the lubricants were oil based, whereas the fourth was a P.T.F.E. solution in aerosol form. The lubricants were coded 'A', 'B', 'C' and 'D', and were as follows:

Lubricant 'A'- A base oil with an I.S.O. viscosity of 32, containing 2% of oleic acid.

Lubricant 'B'- The same base oil with 2% of P.T.F.E. (the P.T.F.E. would not stay in suspension, and the oil had to agitated prior to use).

Lubricant 'C'- The base oil with 2% friction modifier (as used in wet-brake applications).

Lubricant 'D'- The P.T.F.E. in an aerosol spray.

The hydraulic oil used in the process was 'Silkolene Derwent 32', and is coded as 'Lubricant N'. As the viscosities of lubricants 'A', 'B' and 'C' were the same as the hydraulic oil, it would have been theoretically possible to incorporate the additives into the main fluid system. However, the suspension of P.T.F.E. could not be used without extensive alterations to the filtration system, because it required constant agitation to remain in suspension. For the purpose of these tests however, it was not feasible to introduce any additives into the systems

hydraulic fluid.

The tubes used were of annealed copper; 94.14 mm in length, 16.86 mm outside diameter and 0.95 mm wall thickness. Prior to being placed in the machine, the tubes were totally immersed in the lubricants and the excess allowed to drain off (except in the case of the P.T.F.E. spray when they were evenly coated and allowed to dry). The bulge forming process was then carried out as normally.

The compressive axial loads applied to the tubes were: 26 kN (merely a sealing load), 43 kN, 64 kN and 85 kN. For each of these axial loads, the internal pressures were increased from 20.70 N/mm^2 up to rupture, in 6.90 N/mm^2 increments. All of the samples were then analysed, except for those which were buckled or ruptured.

After each set of tests, the die-blocks were thoroughly cleaned with alcohol to remove any traces of the lubricants. When a set of tests were to be carried out, several components would be formed with the relevant lubricant to coat all of the die-block surfaces prior to the samples to be analysed.

Table 2 (page 210) shows the maximum forming values for the tests along with the respective tube dimensions.

The analysis of the tubes followed the same pattern as previous investigations, with close attention being paid to the bulge heights, wall thicknesses and the tube lengths. All of the lubricants

were capable of forming tee piece components.

In order to analyse the results, those obtained from the components formed using lubricants were compared against the standard (Lubricant N) set. Results were compiled which indicated the differences between relevant components (those formed with the same internal pressures and compressive axial loads). Although in some cases the standard samples gave better results than those with lubrication, it was apparent that the components formed with additional lubrication had improved features. For each axial load, the cumulative bulge height differences were tabulated and in all but one of the sixteen cases, positive values were obtained. These values, which are shown in Table 3 (page 211), were compared and it was found that the P.T.F.E. spray gave the most consistent improvement in bulge height (1.10 mm), followed by the P.T.F.E. film (0.625 mm), friction modifier (0.57 mm) and finally the oleic acid (0.415 mm). The values were minimums, because it was usually the case that the standard samples burst at the lowest internal pressures, and so the corresponding lubricated components could not be compared.

However, when a different approach was used, the trends altered slightly. Instead of comparing the results over the full range of tests, only those combinations of axial load and internal pressure which produced fully-formed tee pieces were considered. The values compared were: 64 kN with 41.40 N/mm^2 and

48.30 N/mm^2, and 85 kN with 41.40 N/mm^2 and 48.30 N/mm^2. The results are shown in Table 4 (page 211).

The change in values obtained when considering the smaller range of loads and pressures indicated that the P.T.F.E. film produced greater average bulge heights than the P.T.F.E. spray, with the other lubricants showing the same trends as in Table 3.

The analysis of the wall thicknesses showed no clear trends, but the fact that the components could be formed at higher internal pressures when lubricants were used on them, suggested that the walls did not thin as much. As stated previously, the wall thicknesses were similar for the various combinations of axial load and internal pressure.

The variation in the final lengths of the tubes gave the same trends as had been experienced in the other tests. The reduction in length was relatively constant for any given axial load, and the effect of the lubricants not noticeable.

Figures 72 to 88 show the graphical representations of the results.

3.9.1) Determination of the Coefficient of Friction

In order to relate the results obtained from the lubrication tests to the theory which had been developed to predict the required compressive axial loads, it was necessary to obtain a value for the co-efficient of friction between the die-blocks and the copper tubes. This was achieved by carrying out tests

on the machine using a solid cylinder of copper (a standard copper tube could not be used, as the process required the blank to be axially loaded from one direction only, and without internal pressure the tube would be crumpled and not stay in contact with the die-blocks).

The billet was 24.20 mm in outside diameter (it was slightly larger than the standard tubes so that it could be clamped in place between the die-blocks) and 107 mm in length. One of the plungers was removed from the machine, so that the axial load was only applied from one side. The billet was clamped in the die-blocks, and then the plunger advanced until it touched it (the pressure to the cylinder was just sufficient to advance the plunger, but not to push the billet through the die-blocks). The pressure to the cylinder was then increased until the plunger started to move the billet. This procedure was repeated several times, with the loads and displacements monitored on the ultra-violet recorder.

When the loads were analysed and averaged, the value obtained for the coefficient of friction was 0.3.

3.10) The Effect of Altering the Branch Radius

Four sets of die-blocks were manufactured which were identical in every respect except for the branch radius. The radius in question is that at the intersection of the central passage and the side branch. When the dies are manufactured, the curves of interpenetration result in 'knife-edges'. Components cannot be formed with die-blocks such as these, because the edges shear the metal at very low axial loads and internal pressures. Therefore, all die-blocks have a radius along these curves, to prevent the above happening. The following tests were carried out to investigate the effect of varying this radius.

The radii selected were 2 mm, 3 mm, 4 mm and 5 mm. This range was selected because, for any value below 2 mm, the tubes ruptured at the intersection because of the severity of the corner angle. Die-blocks were not manufactured with a radius in excess of 5 mm because the formed components were visually unsatisfactory with respect to an industrial application (the crisp tee piece shape was lost).

All of the die-blocks were tested over the same range: compressive axial loads of 85 kN, 106 kN, 128 kN and 149 kN and internal pressures of 27.60 N/mm^2 and incrementing in 6.90 N/mm^2 steps. Most of the samples withstood the highest internal pressure the machine could produce, although there were two exceptions when the tubes burst at 55.20 N/mm^2. The maximum forming values and the respective tube

dimensions are shown in Table 5 (page 212).

Figures 89 to 94 show the graphical representations for tubes formed with a compressive axial load of 85 kN and various internal pressures. Although the bulge heights obtained for the four values of branch radii are similar, the 2 mm radius provides a branch with the highest value of the percentage of original wall thickness at the dome centre, followed by the 3 mm radius, with maximum reductions in thickness being obtained with the 4 mm and 5 mm radii.

Figures 95 to 100 depict the results for a compressive axial load of 106 kN. The trends are similar to the above, except that the 2 mm and 3 mm radii tend to give greater bulge heights than the 4 mm and 5 mm ones.

Figures 101 to 106 depict the results for a load of 128 kN. The trends are the same as for the 106 kN load.

Figures 107 to 112 depict the results for a load of 149 kN. Again the results are similar to those for the 106 kN and 128 kN loads.

Table 5 shows the components which burst or buckled, and these are not included in the graphical representations.

Figure 113 shows that the ratio of final to initial length of the tube decreases as the compressive axial load increases. However, varying the value of the branch radius does not produce any apparent trends.

Figure 114 depicts how the ratio of final

bulge height/original radius varies with internal pressure and axial load. The internal pressure only produces a small improvement in the value of $\bar{H}/R_0$, whereas the compressive axial load produces a noticeable increase in the ratio. With loads of 149 kN, 128 kN and 106 kN, the smaller the branch radius, the higher the value of $\bar{H}/R_0$. However, with the 85 kN load the trend is reversed.

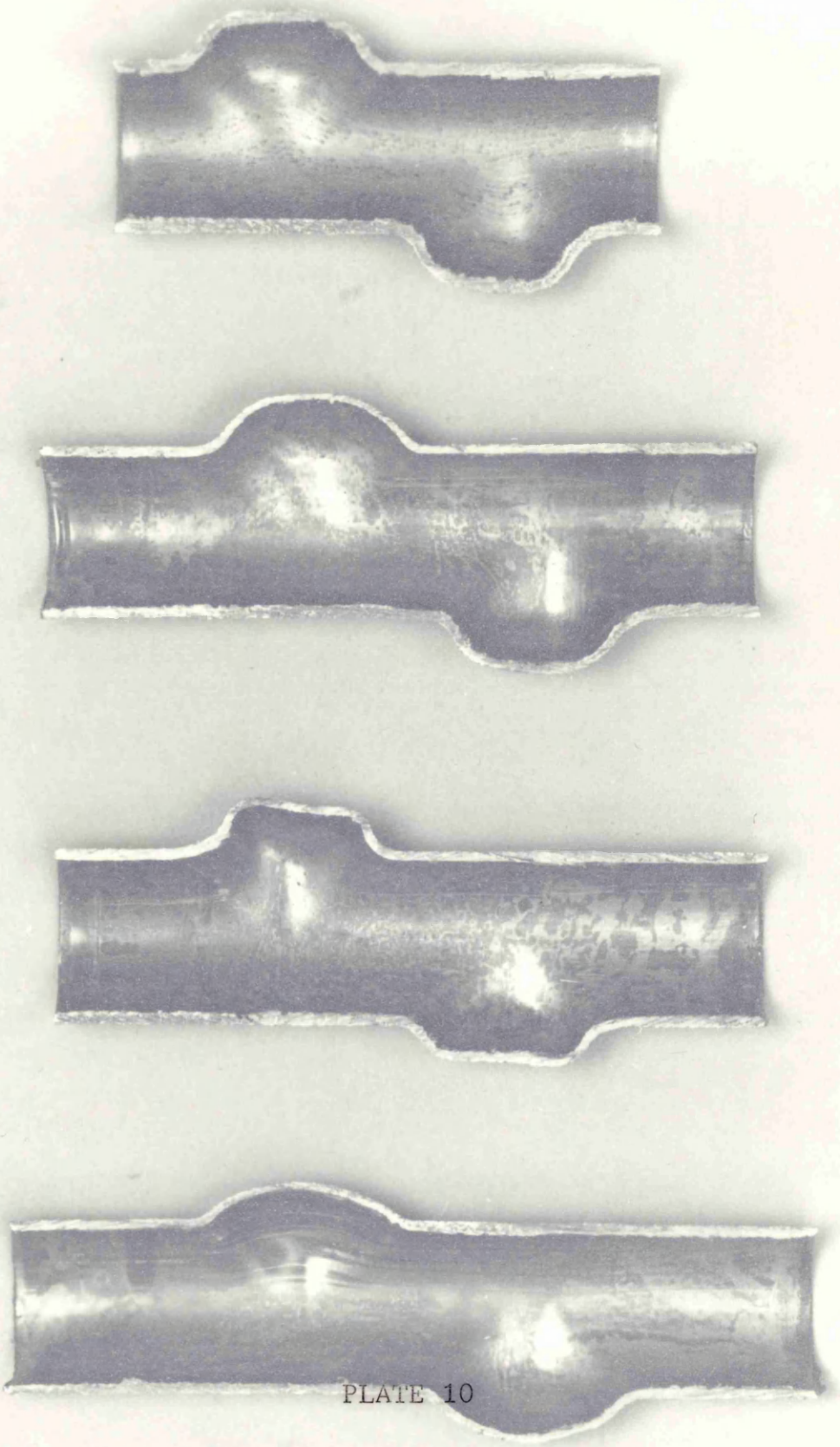

PLATE 10

OFF-SET JOINT TUBE HALVES

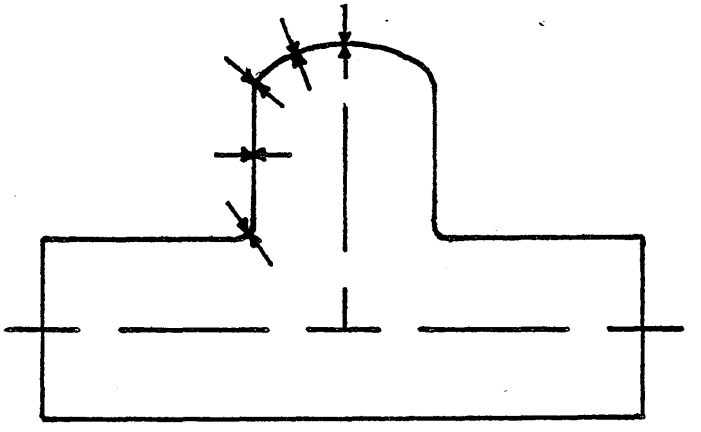

FIGURE 13(a)

A Tee Piece During Forming.

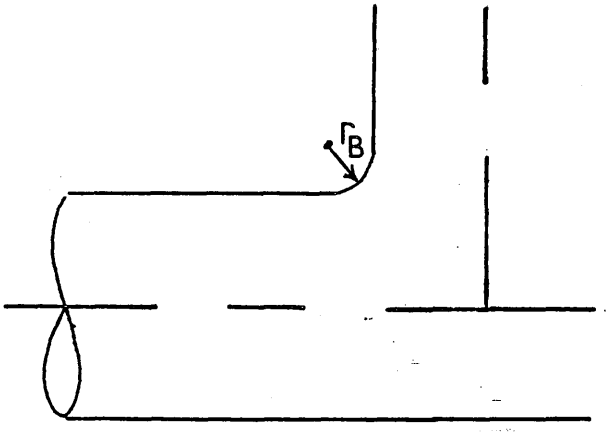

FIGURE 13(b)

Elememt Of Tee Piece During Forming.

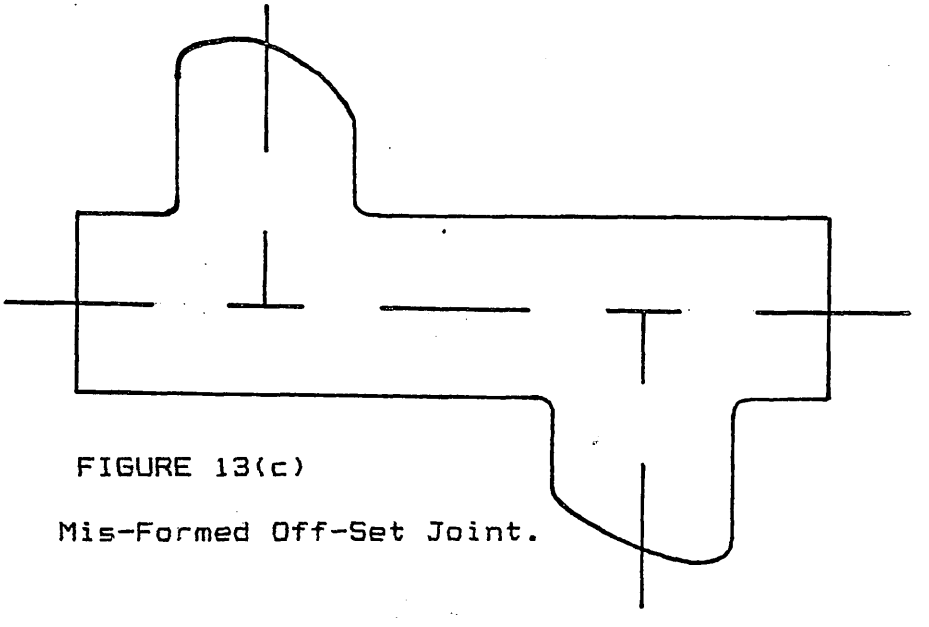

FIGURE 13(c)

Mis-Formed Off-Set Joint.

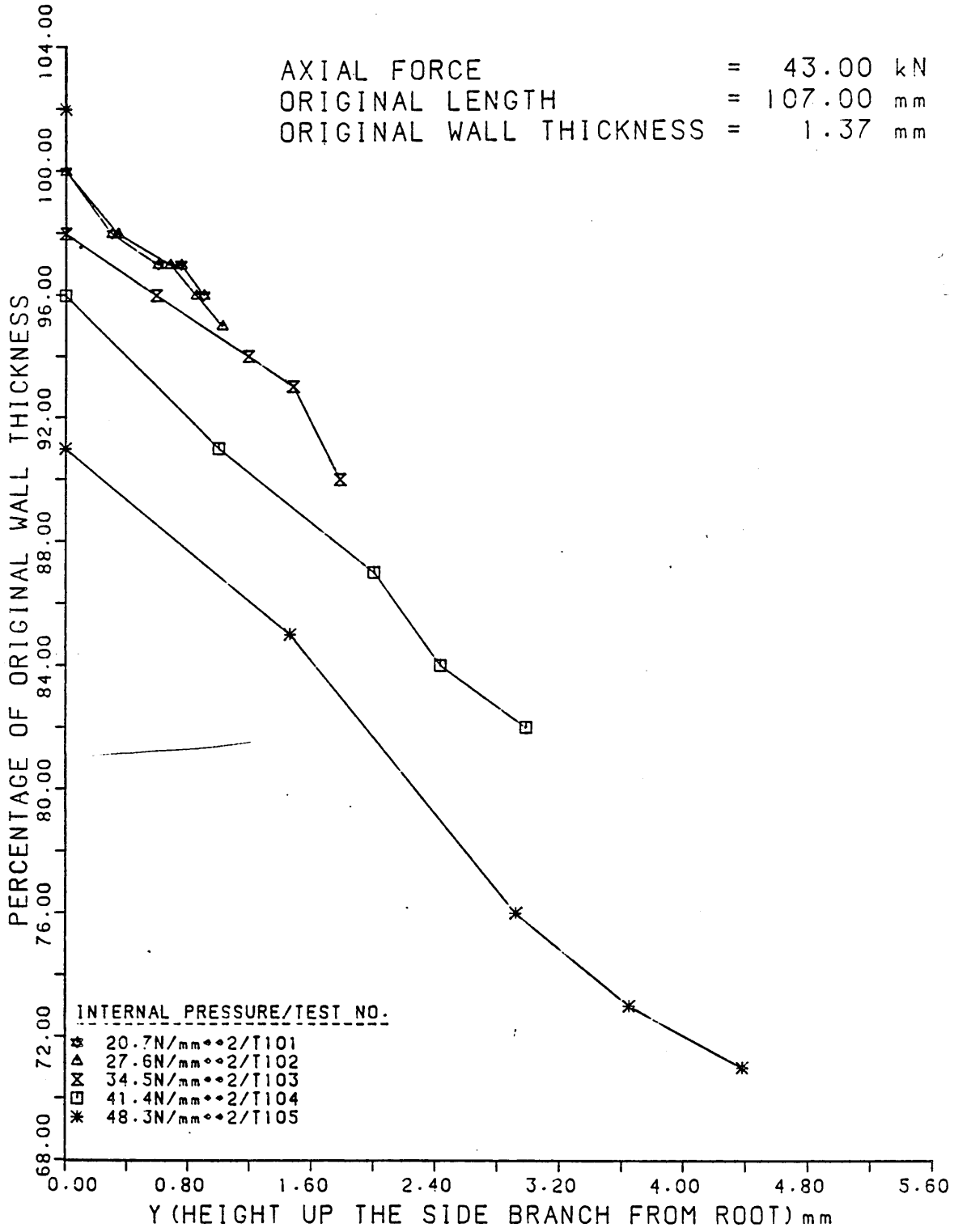

FIGURE 14

The Wall Thickness Distributions Along The Side Branches And Domes Of Tee Pieces Formed At Various Internal Pressures.

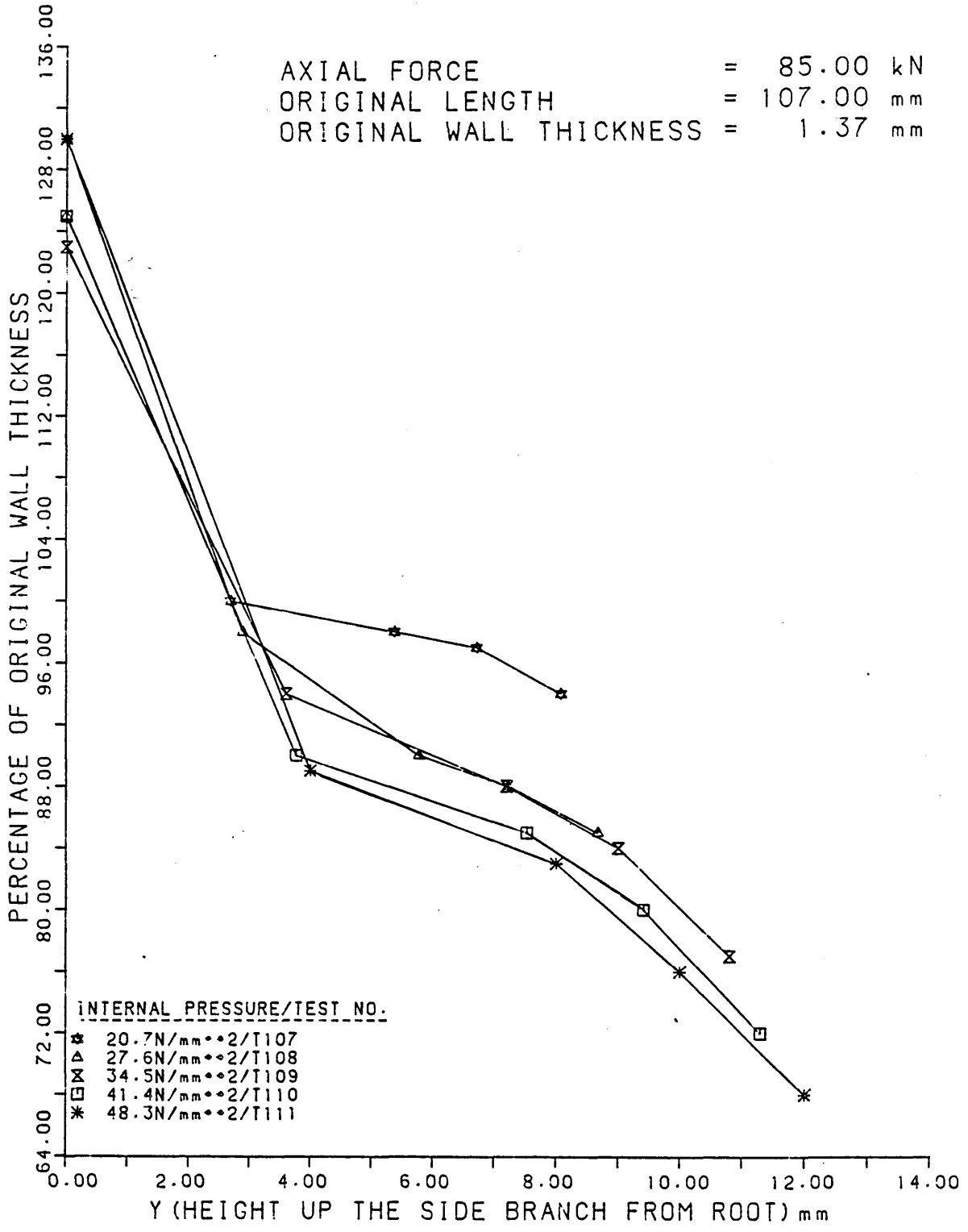

FIGURE 15

The Wall Thickness Distributions Along The Side Branches And Domes Of Tee Pieces Formed At Various Internal Pressures.

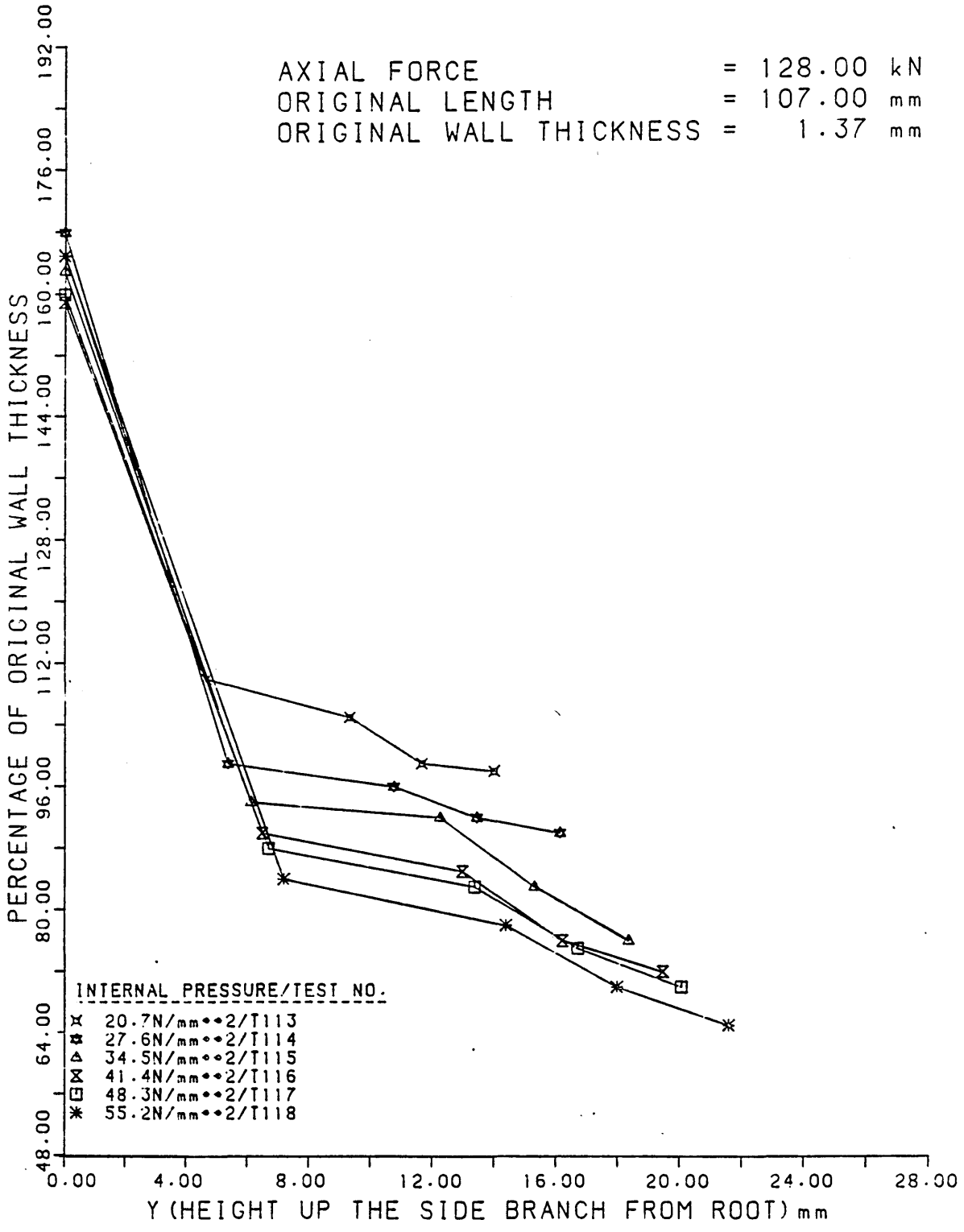

FIGURE 16

The Wall Thickness Distributions Along The Side Branches And Domes Of Tee Pieces Formed At Various Internal Pressures.

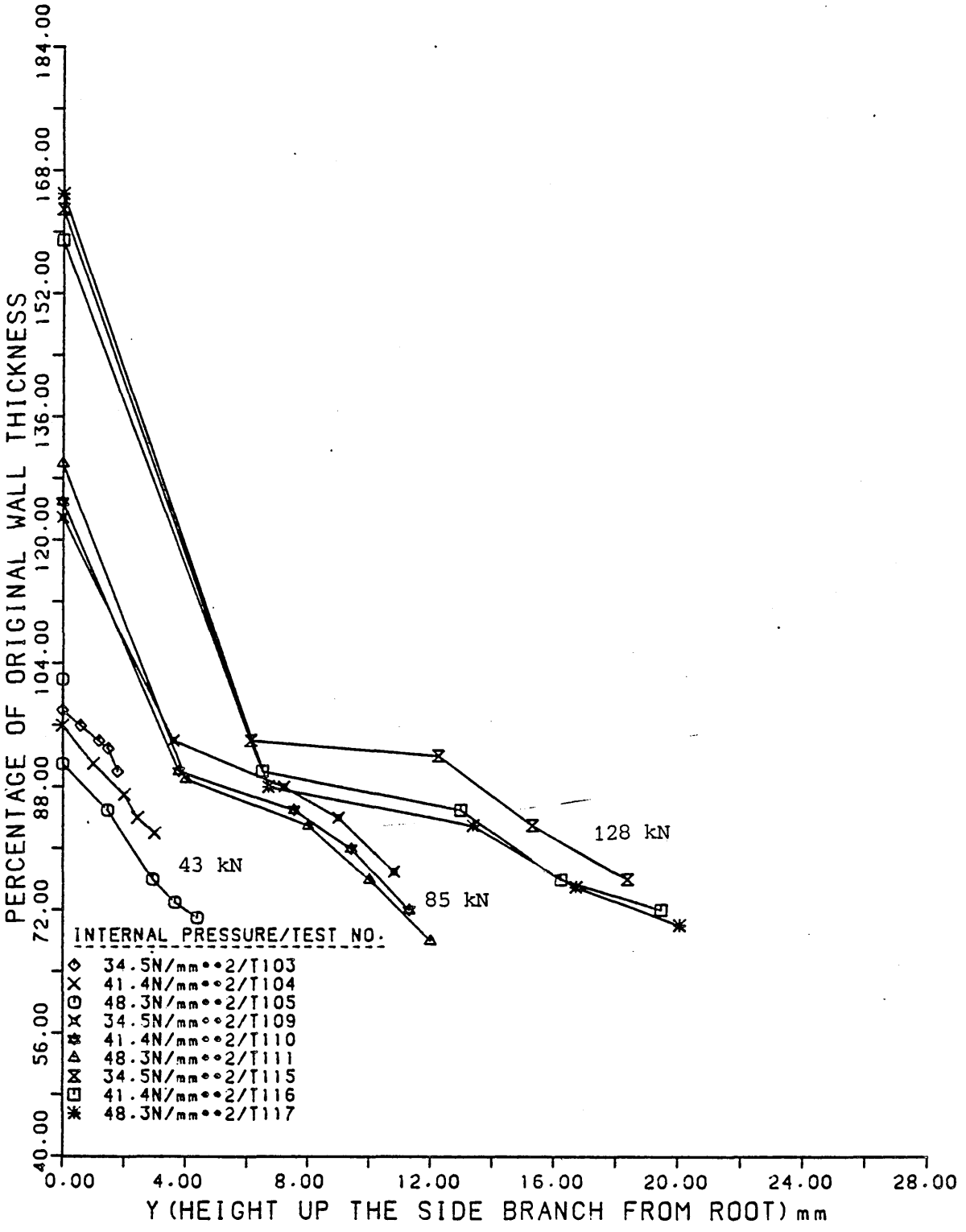

FIGURE 17

The Wall Thickness Distributions Along The Side Branches And Domes Of Tee Pieces Formed At Various Internal Pressures And With Various Compressive Axial Loads.

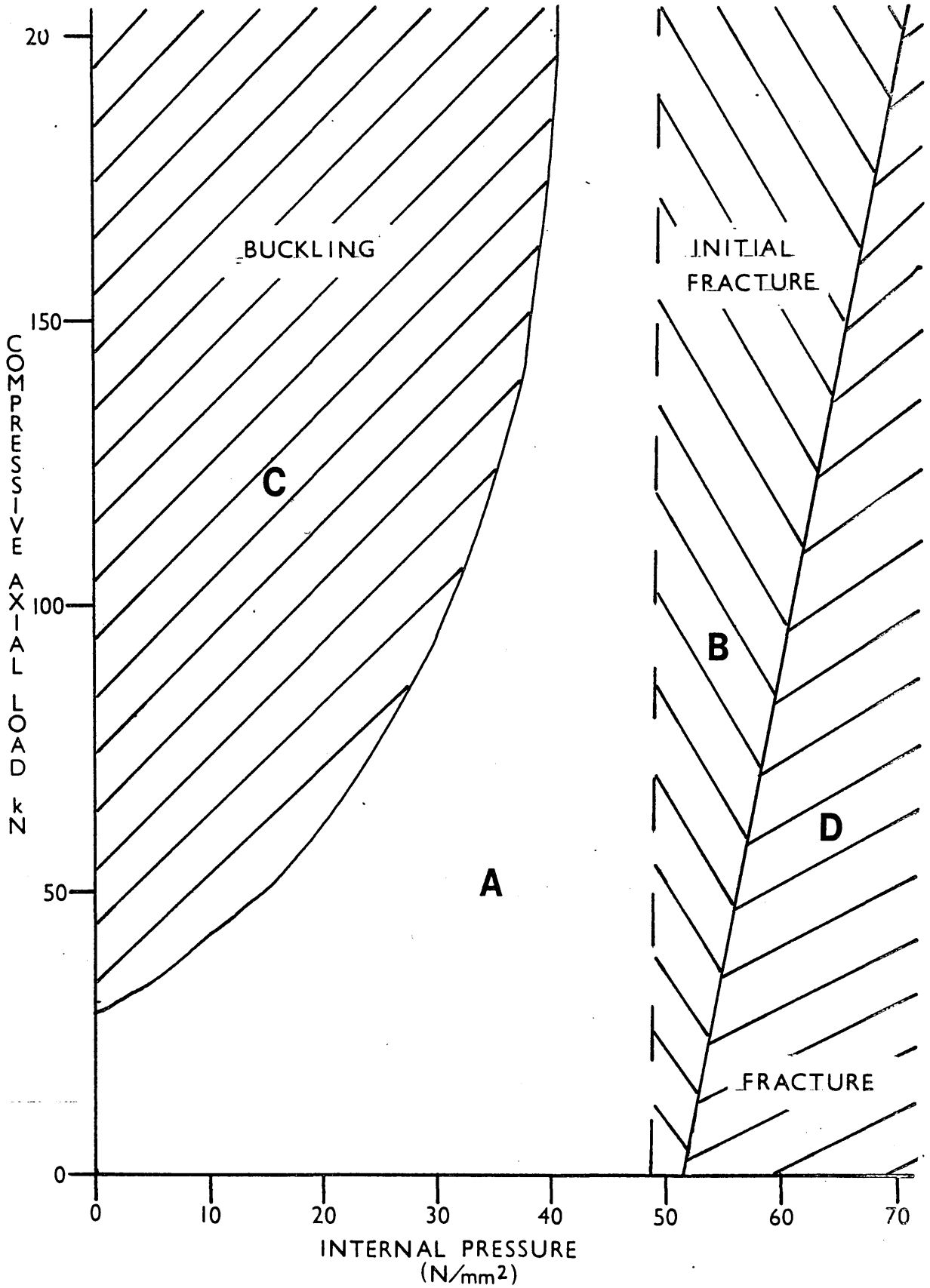

FIGURE 18

The Forming Limits For A Tube Of Wall Thickness:

t_o = 1.37 mm.

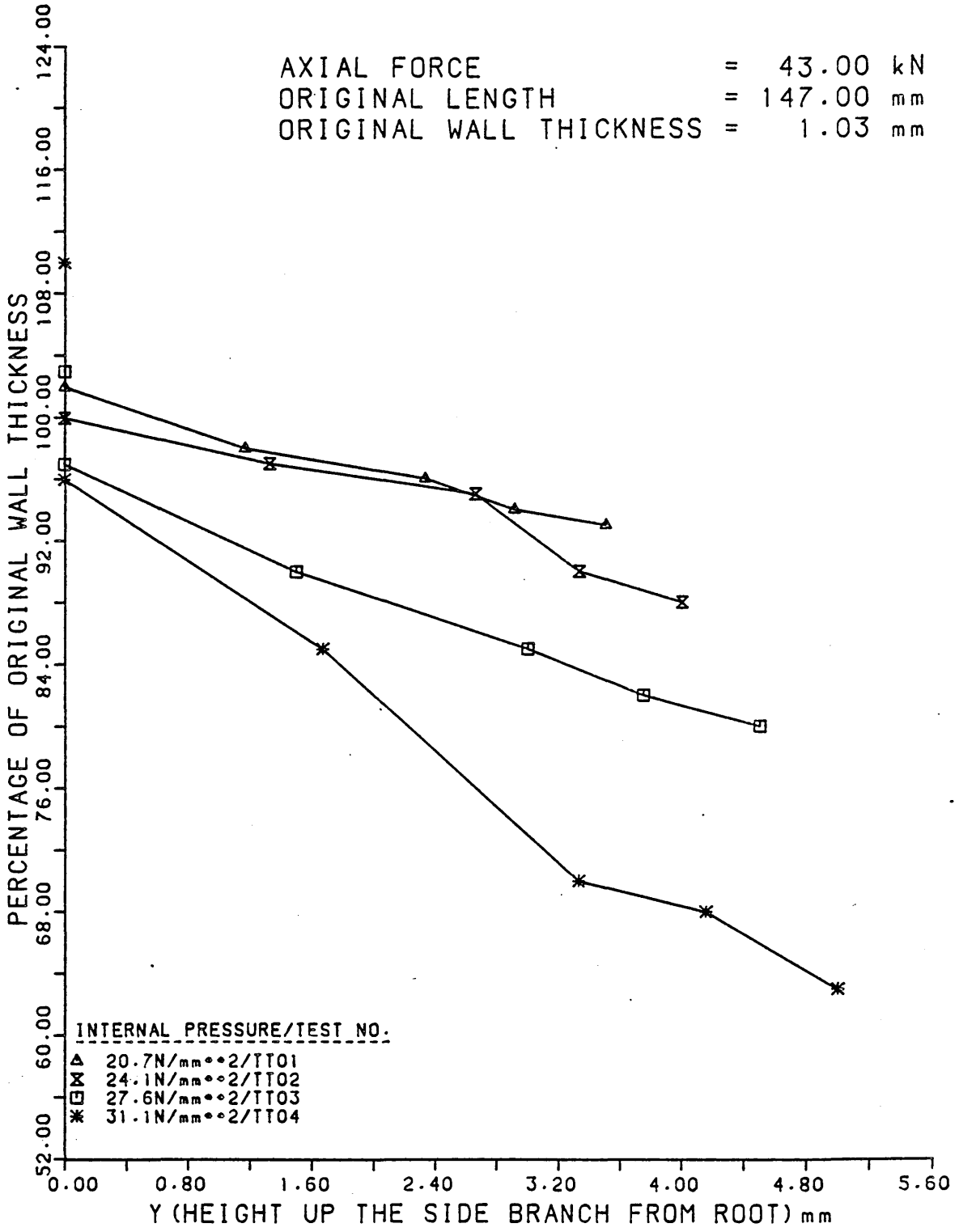

FIGURE 19

The Wall Thickness Distributions Along The Side Branches And Domes Of Tee Pieces Formed At Various Internal Pressures.

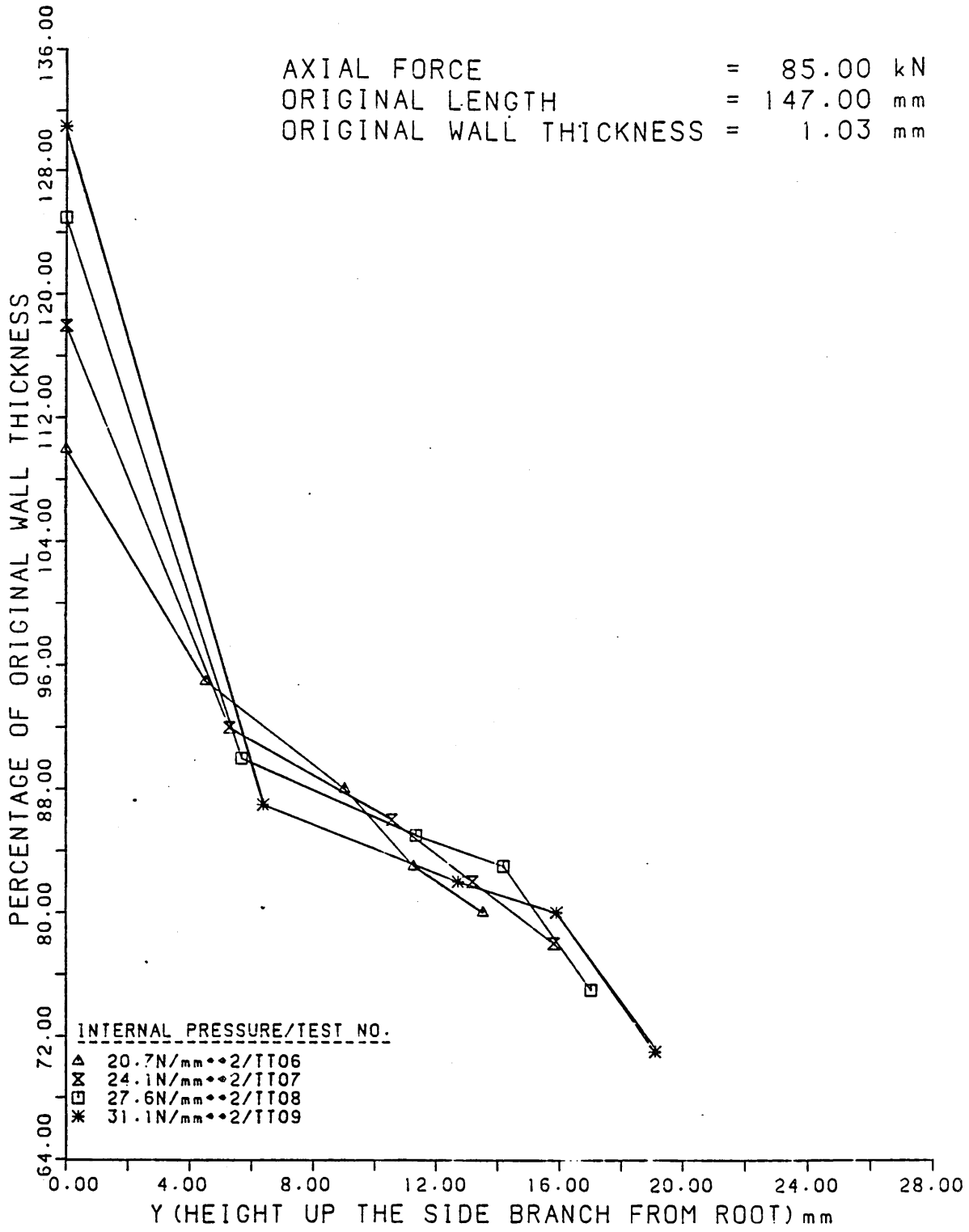

FIGURE 20

The Wall Thickness Distributions Along The Side Branches And Domes Of Tee Pieces Formed At Various Internal Pressures.

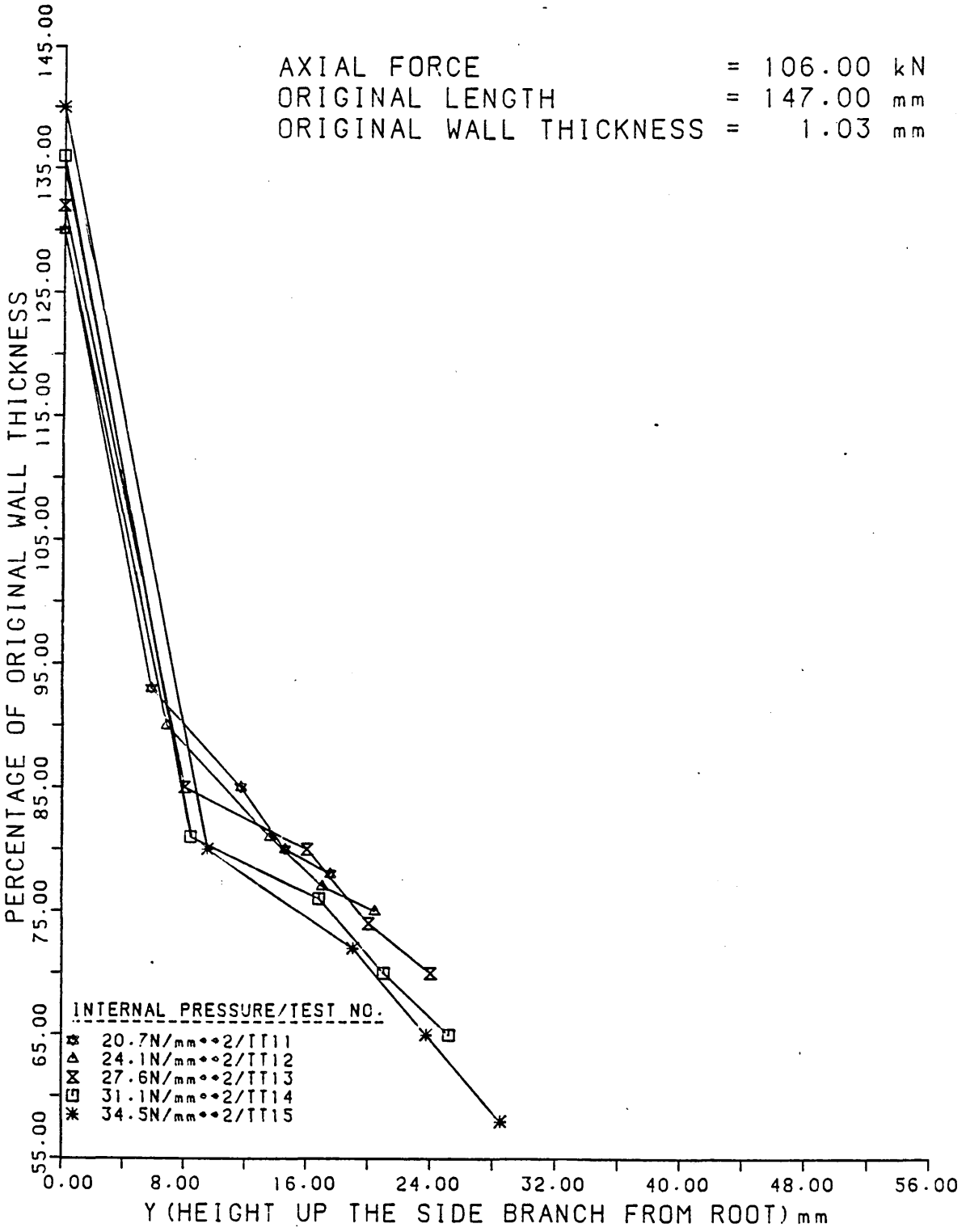

FIGURE 21

The Wall Thickness Distributions Along The Side Branches And Domes Of Tee Pieces Formed At Various Internal Pressures.

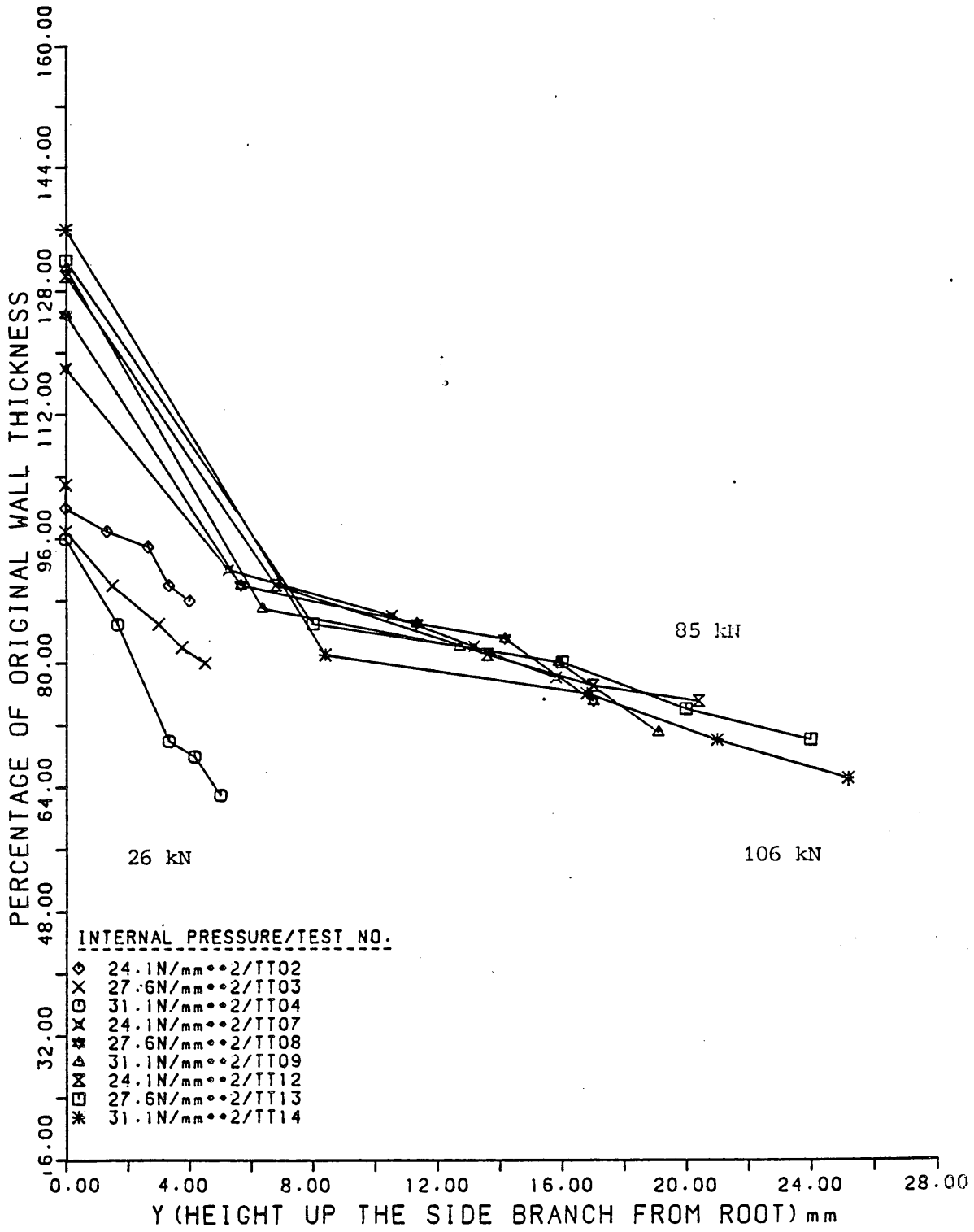

FIGURE 22

The Wall Thickness Distributions Along The Side Branches And Domes Of Tee Pieces Formed At Various Internal Pressures And With Various Compressive Axial Loads.

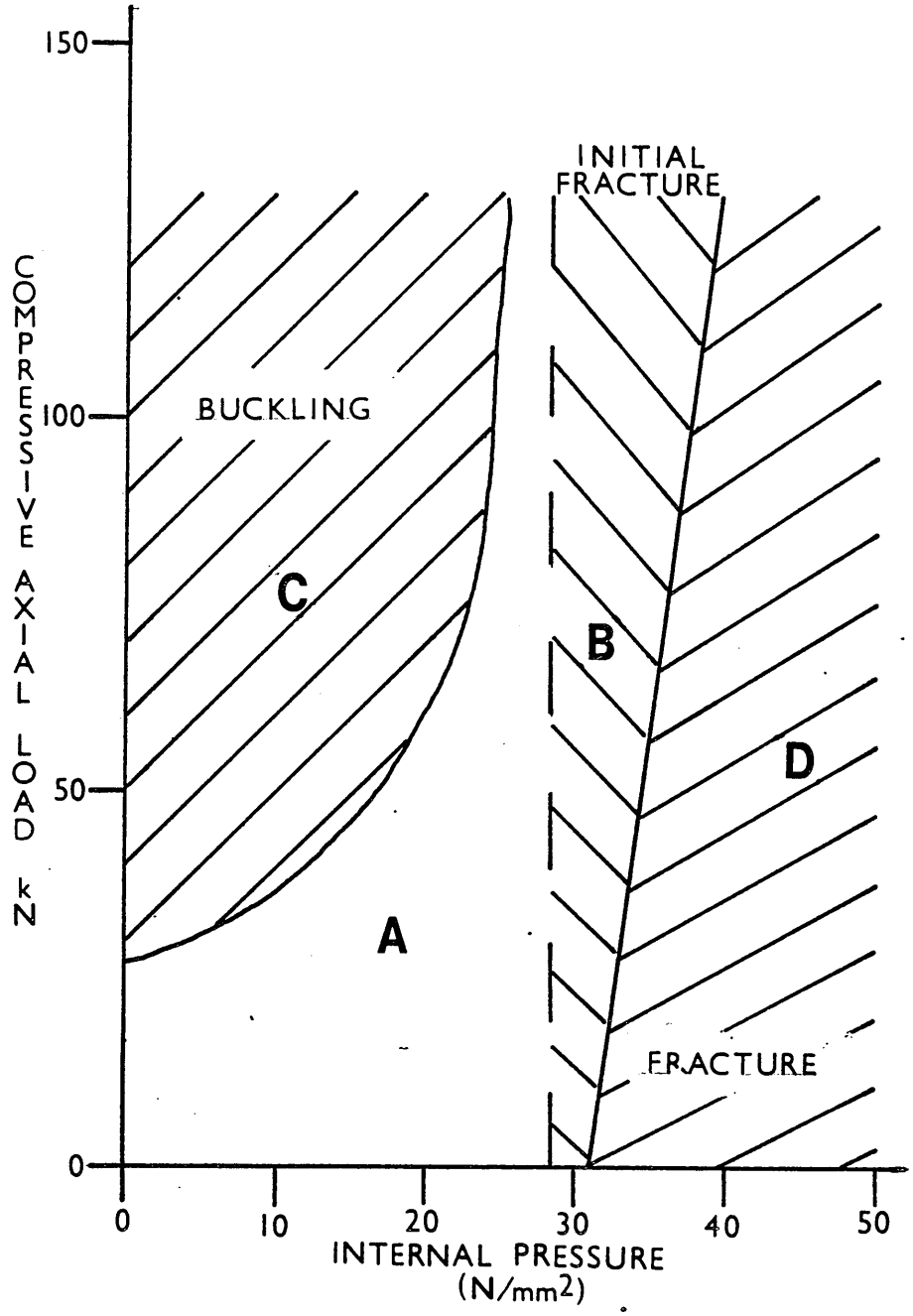

FIGURE 23

The Forming Limits For A Tube Of Wall Thickness:

t_o = 1.03 mm.

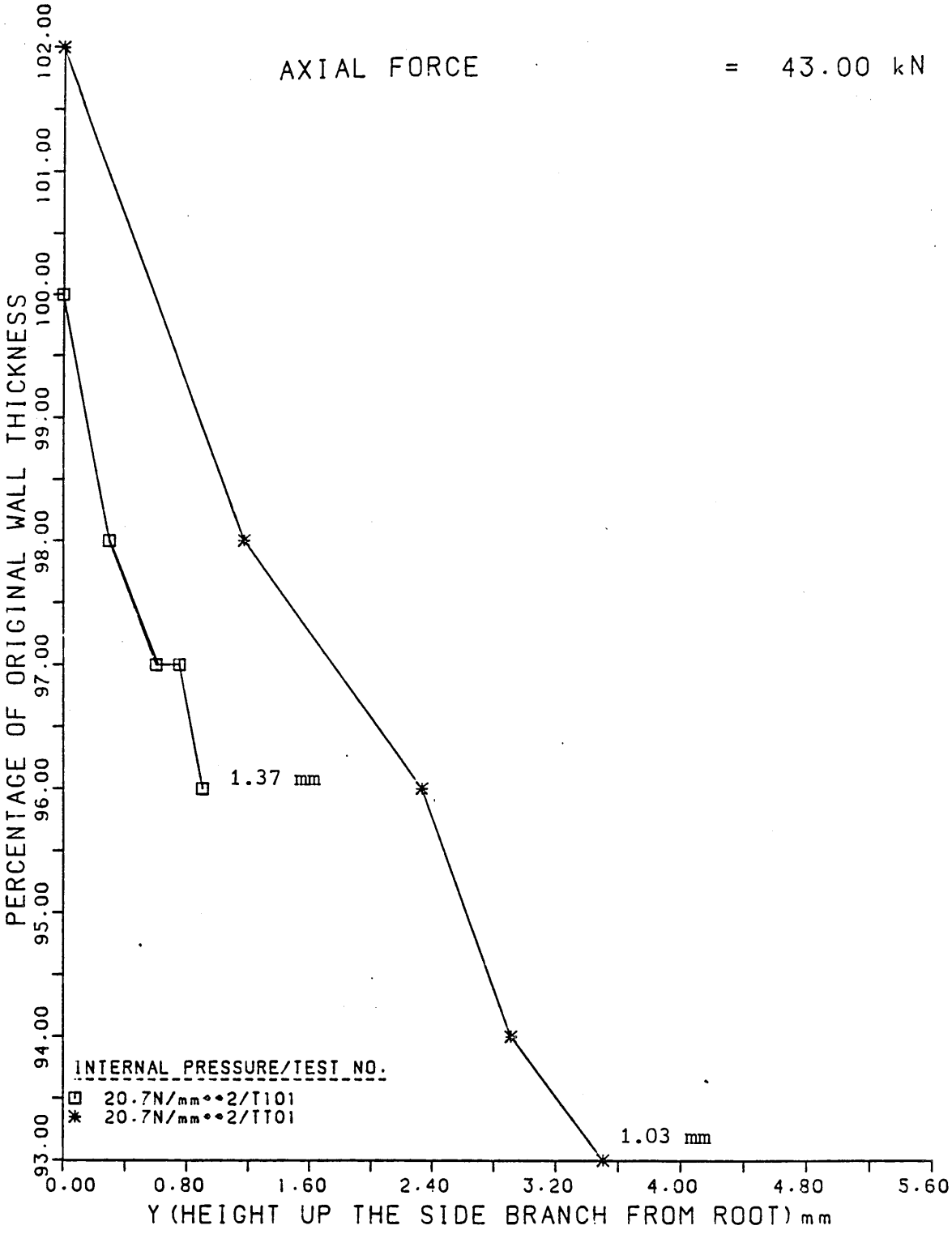

FIGURE 24

The Wall Thickness Distributions Along The Side Branches And Domes Of Tee Pieces Formed From Tubes With Different Initial Wall Thicknesses.

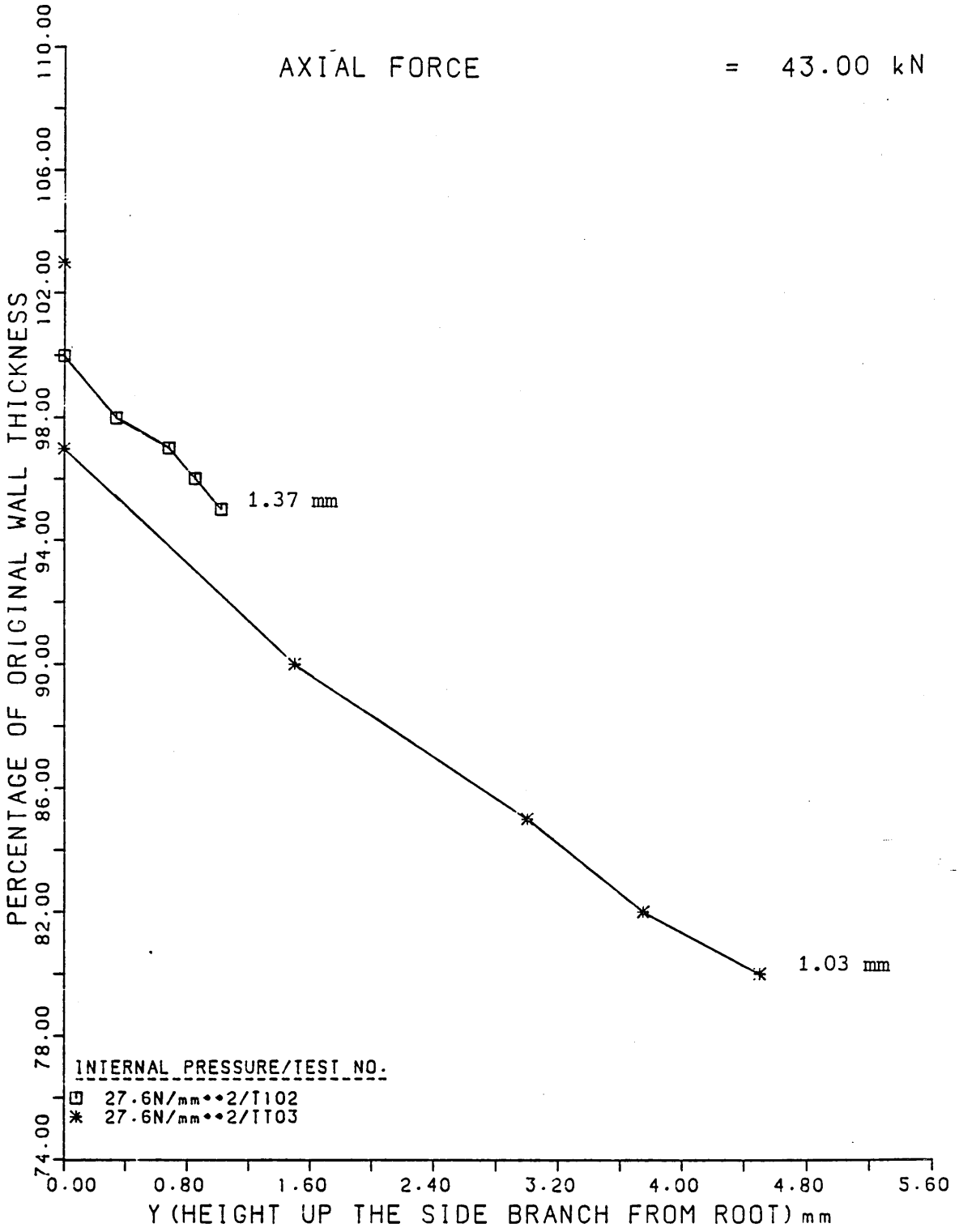

FIGURE 25

The Wall Thickness Distributions Along The Side Branches And Domes Of Tee Pieces Formed From Tubes With Different Initial Wall Thicknesses.

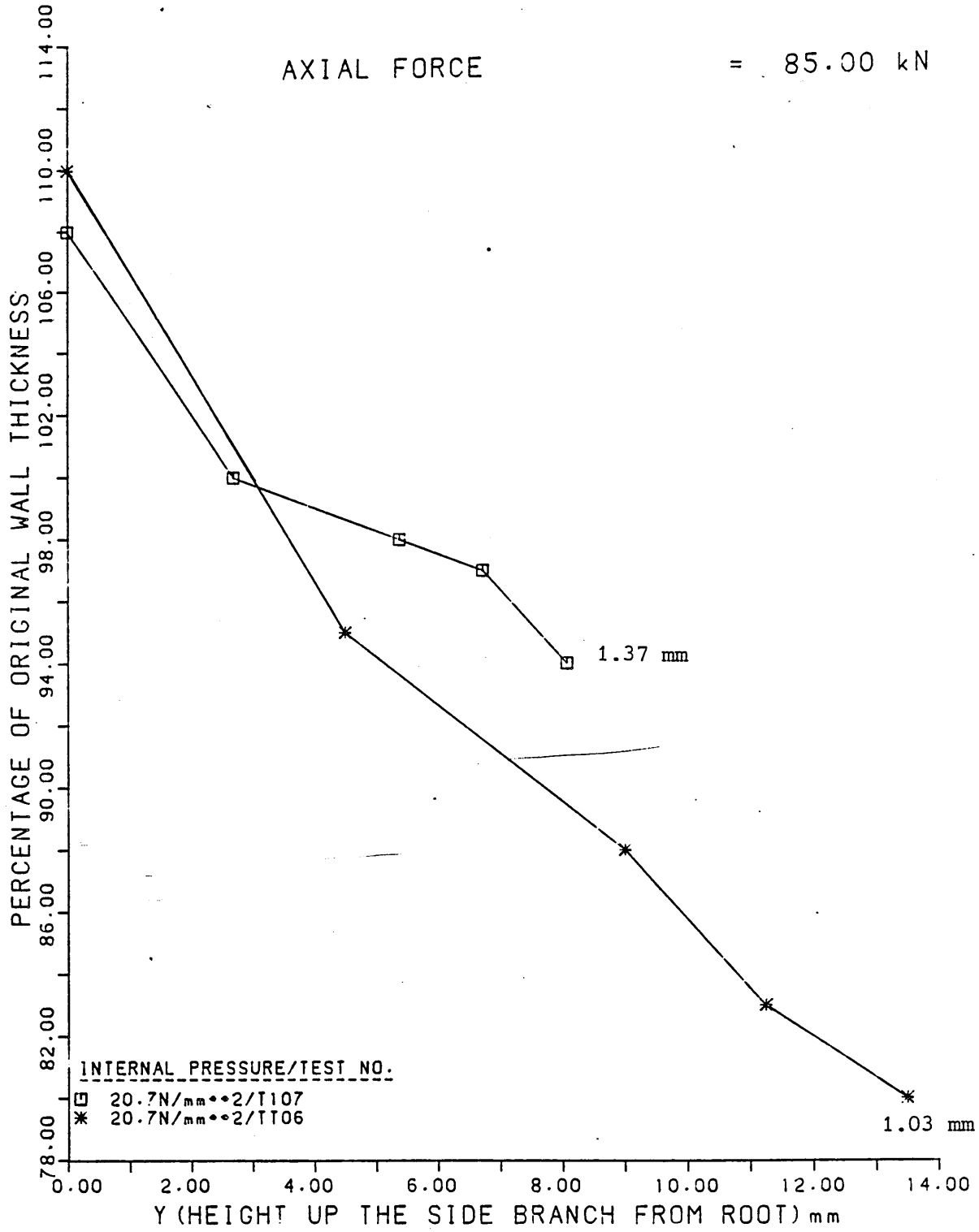

FIGURE 26

The Wall Thickness Distributions Along The Side Branches And Domes Of Tee Pieces Formed From Tubes With Different Initial Wall Thicknesses.

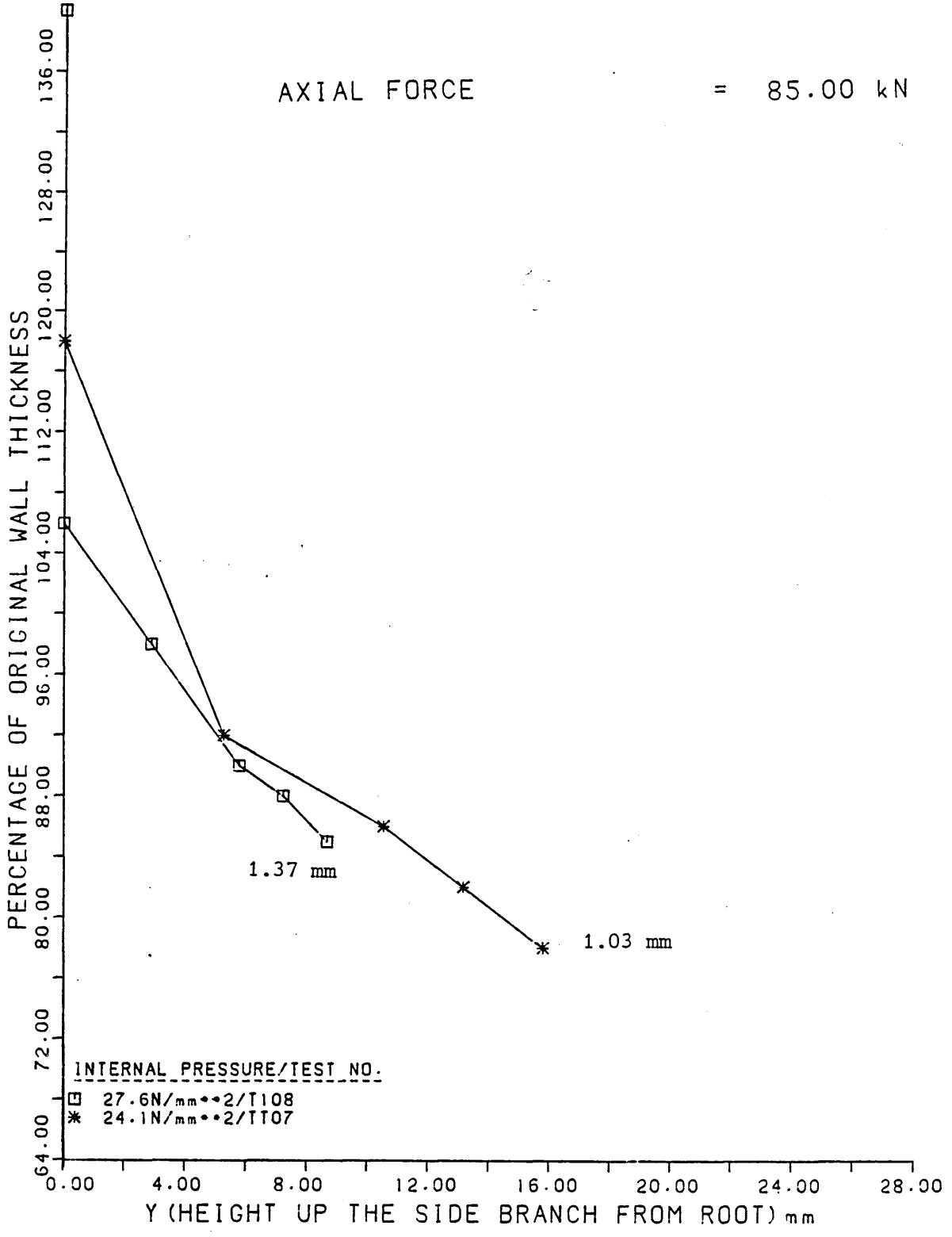

FIGURE 27

The Wall Thickness Distributions Along The Side Branches And Domes Of Tee Pieces Formed From Tubes With Different Initial Wall Thicknesses.

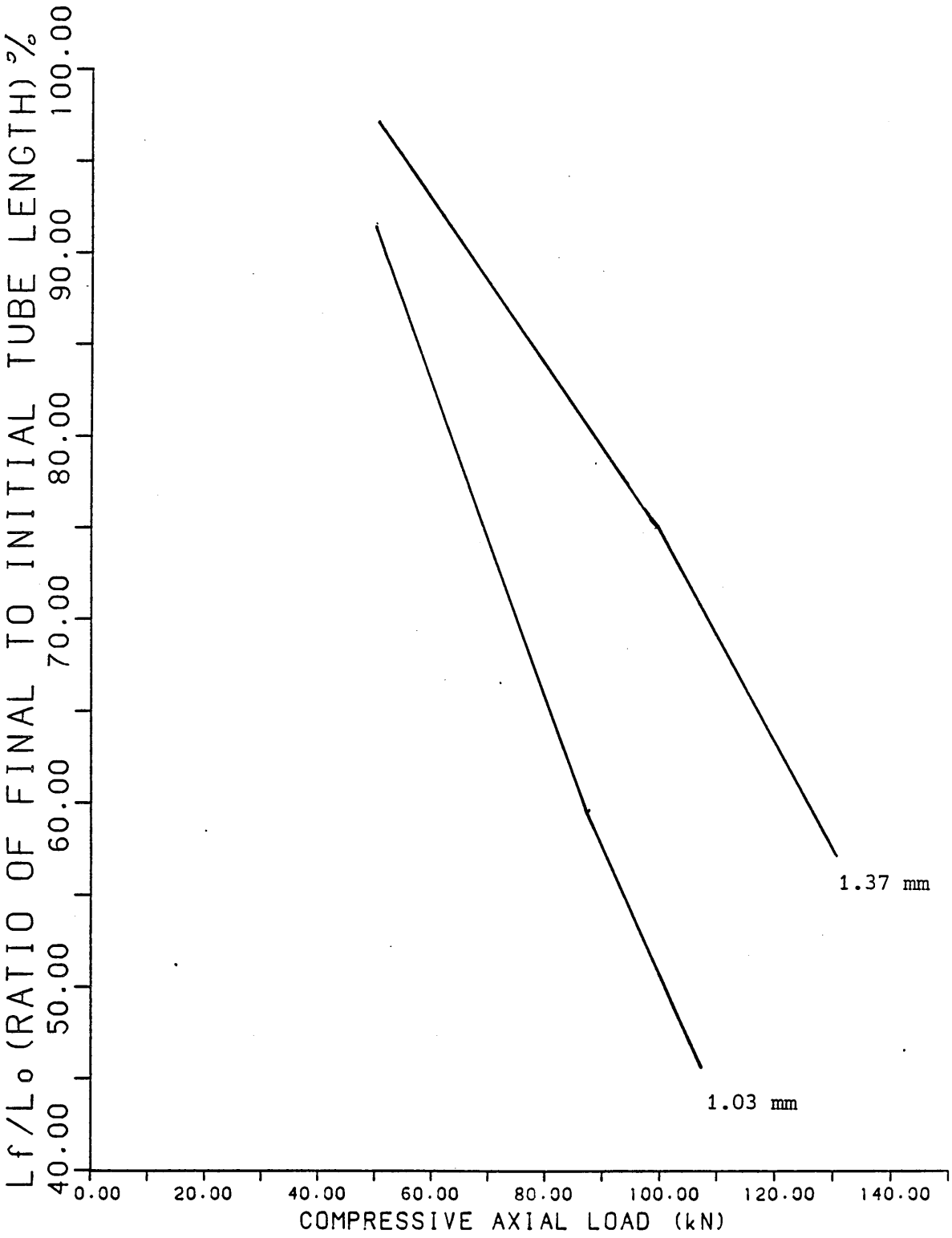

FIGURE 28

The Final To Original Tube Length Variation Against Compressive Axial Load For Tee Pieces Formed From Tubes Of Different Wall Thicknesses.

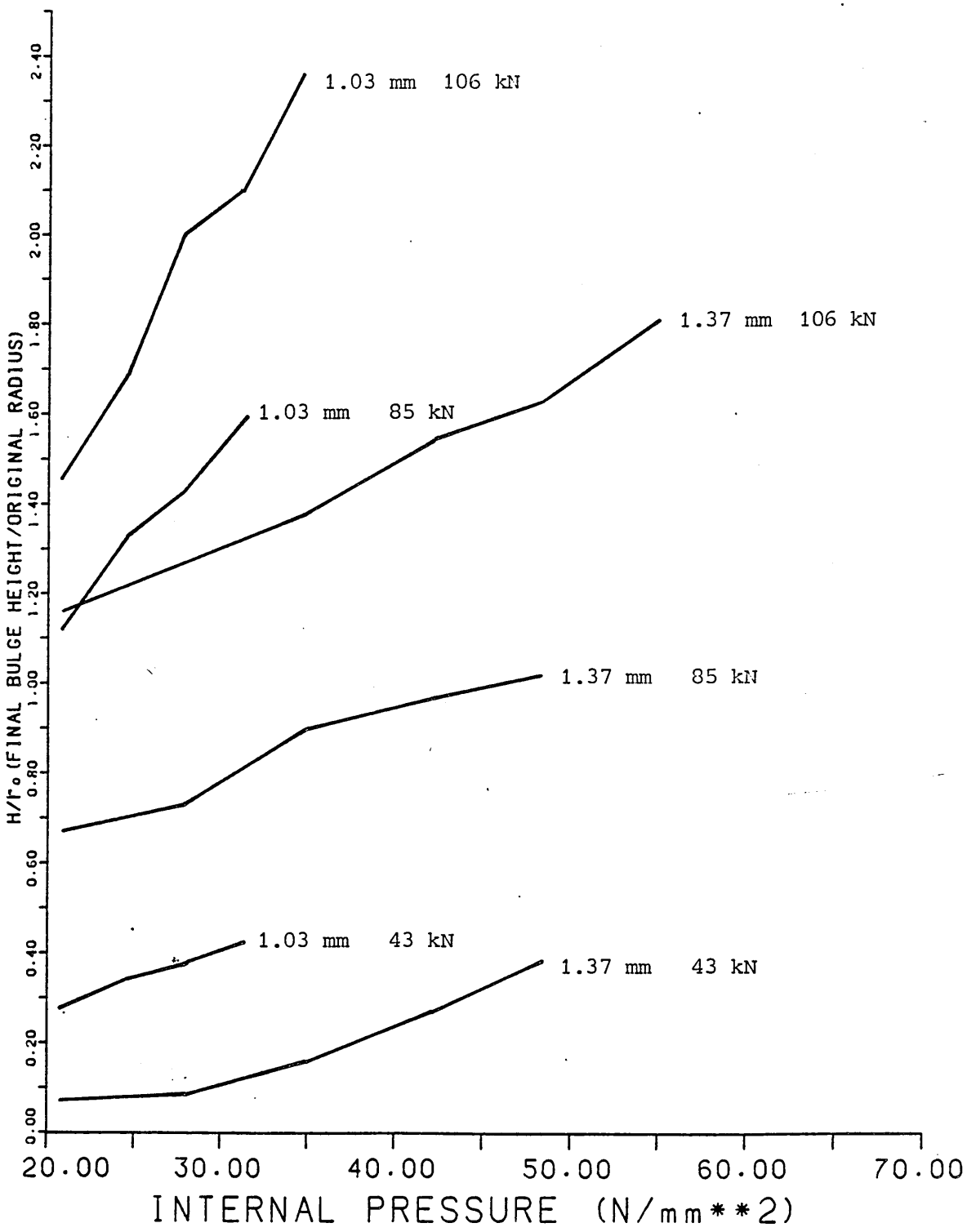

FIGURE 29

The Bulge Height To Original Tube Radius Variation Against Internal Pressure For Tee Pieces Formed From Tubes With Different Wall Thicknesses.

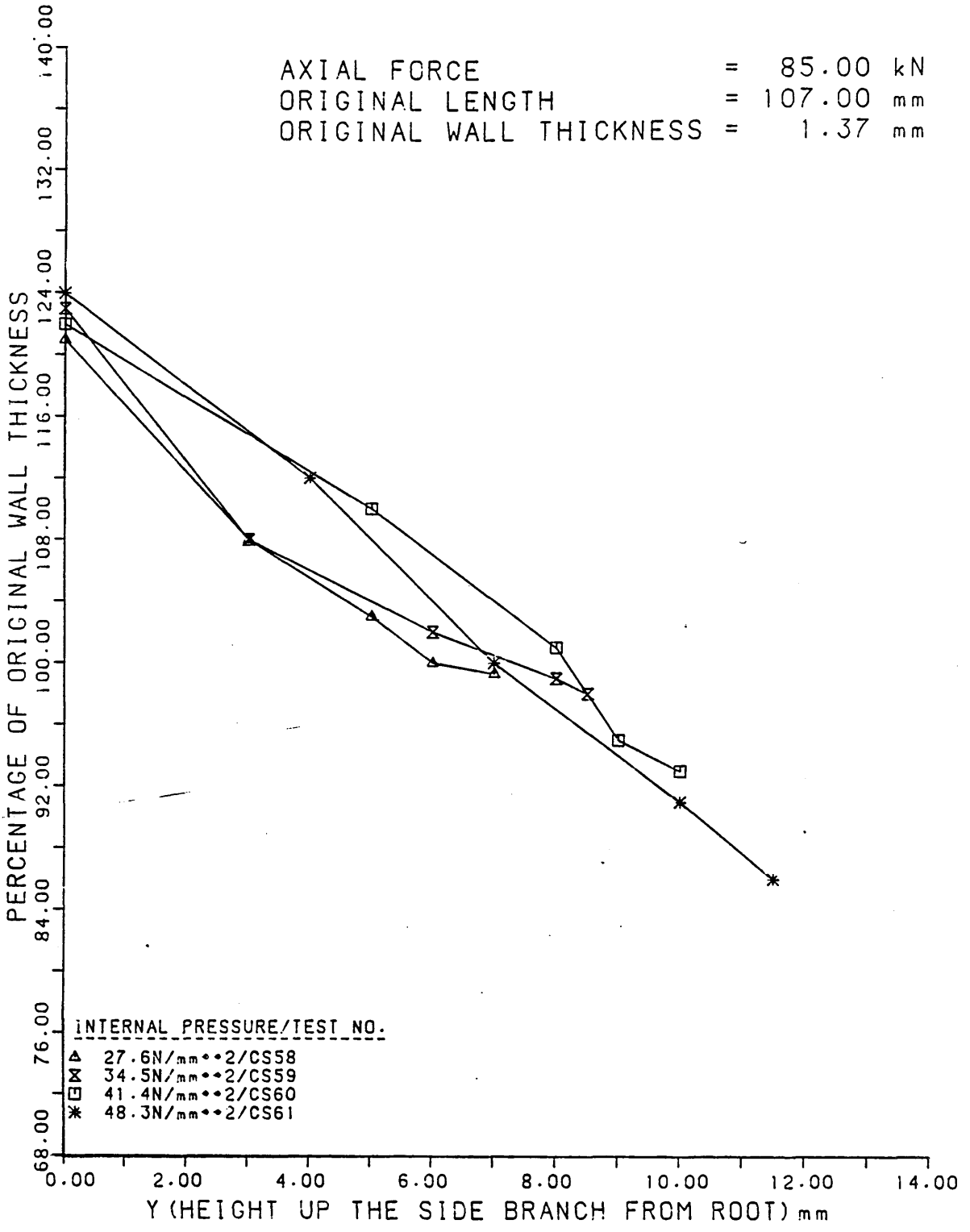

FIGURE 30

The Wall Thickness Distributions Along The Side Branches And Domes Of Cross Joints Formed At Various Internal Pressures.

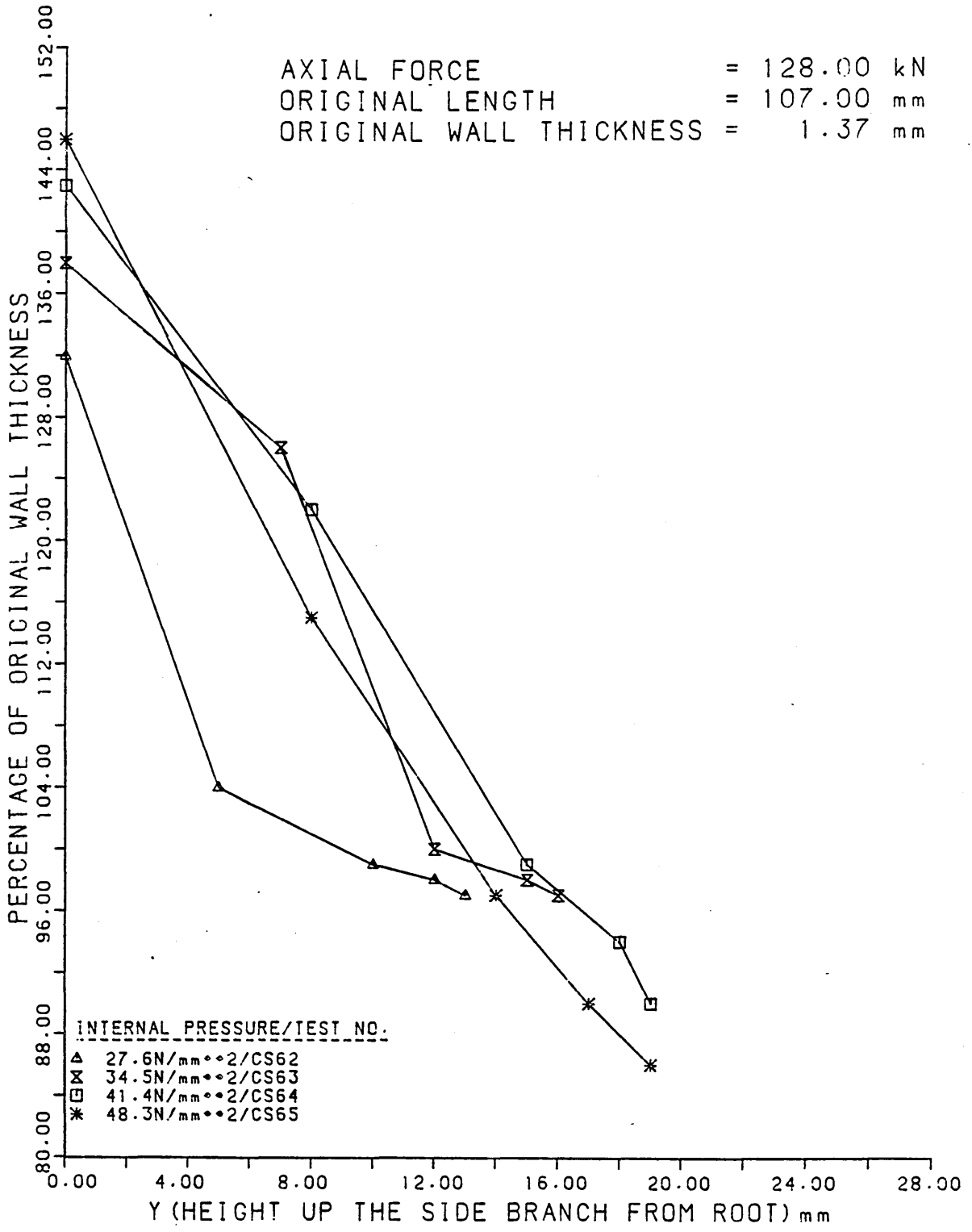

FIGURE 31

The Wall Thickness Distributions Along The Side Branches And Domes Of Cross Joints Formed At Various Internal Pressures.

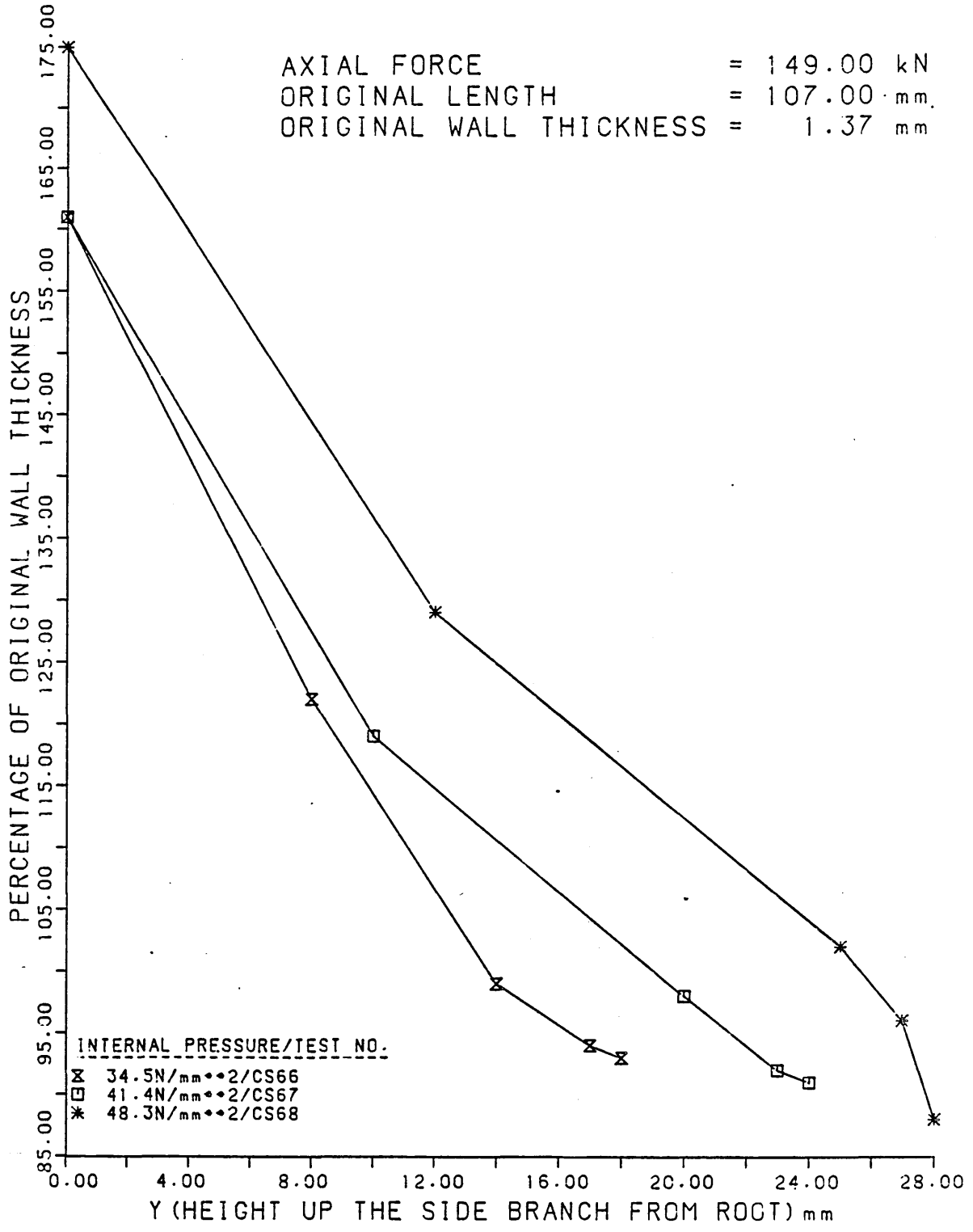

FIGURE 32

The Wall Thickness Distributions Along The Side Branches And Domes Of Cross Joints Formed At Various Internal Pressures.

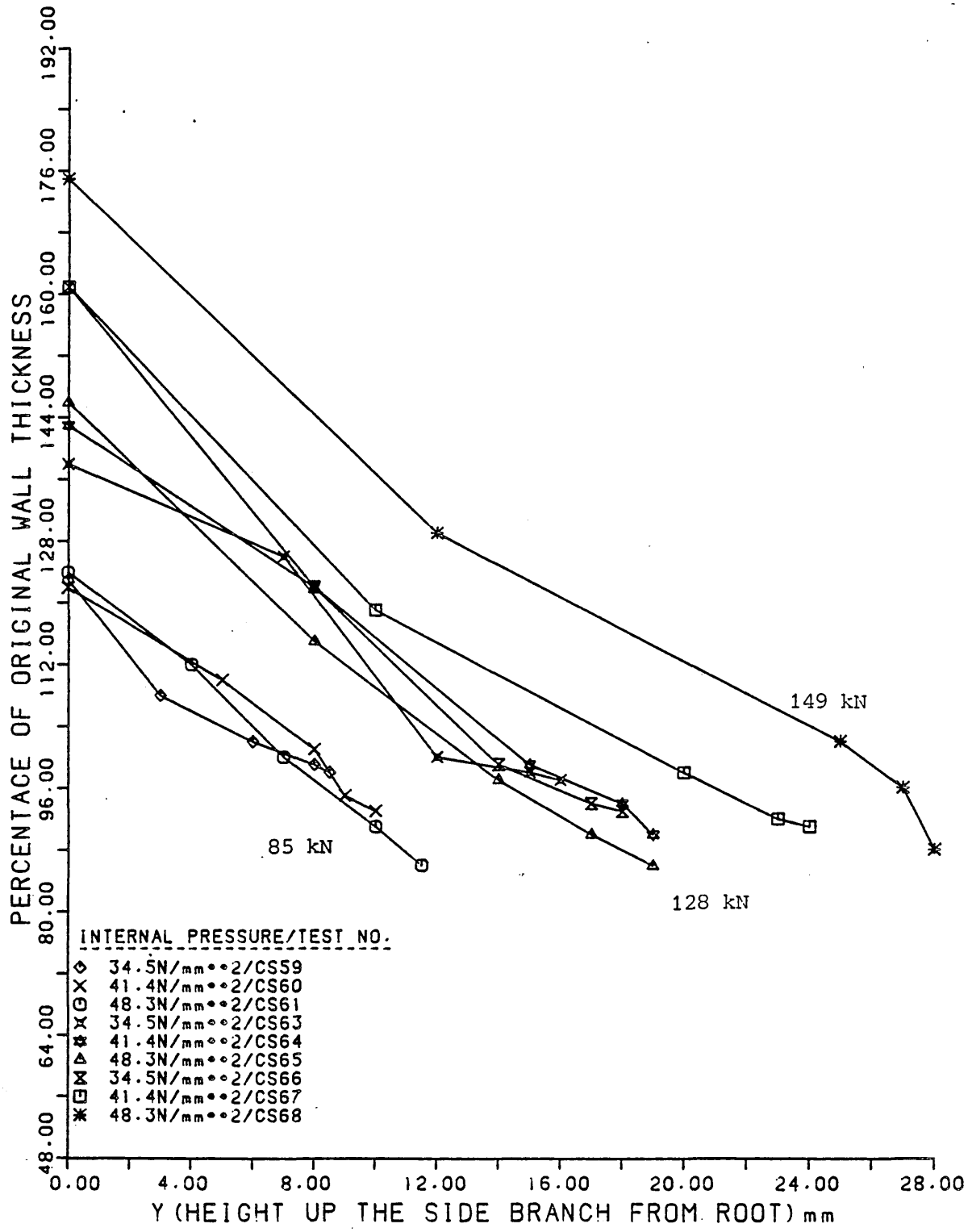

FIGURE 33

The Wall Thickness Distributions Along The Side Branches And Domes Of Cross Joints Formed At Various Internal Pressures And With Various Compressive Axial Loads.

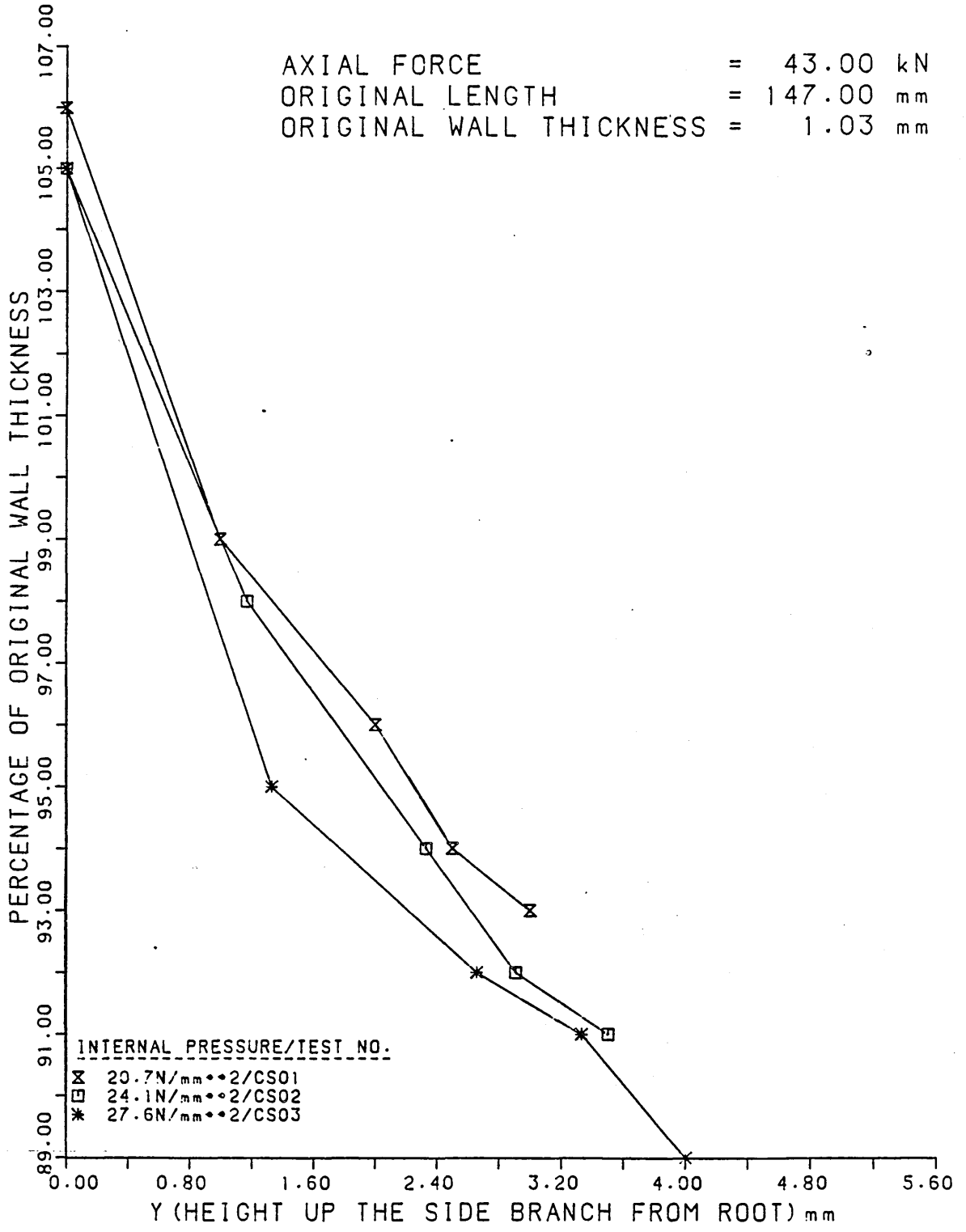

FIGURE 34

The Wall Thickness Distributions Along The Side Branches And Domes Of Cross Joints Formed At Various Internal Pressures.

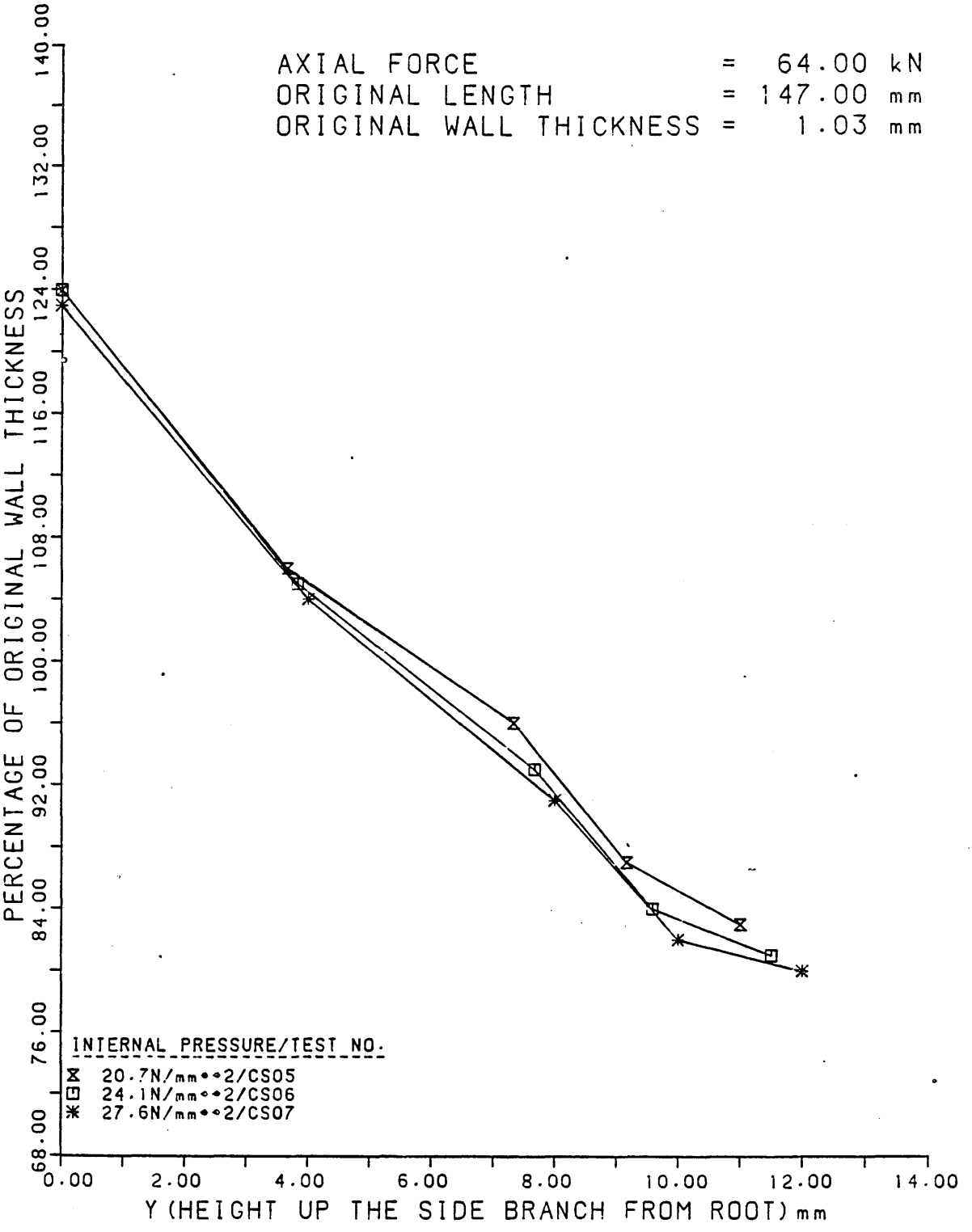

FIGURE 35

The Wall Thickness Distributions Along The Side Branches And Domes Of Cross Joints Formed At Various Internal Pressures.

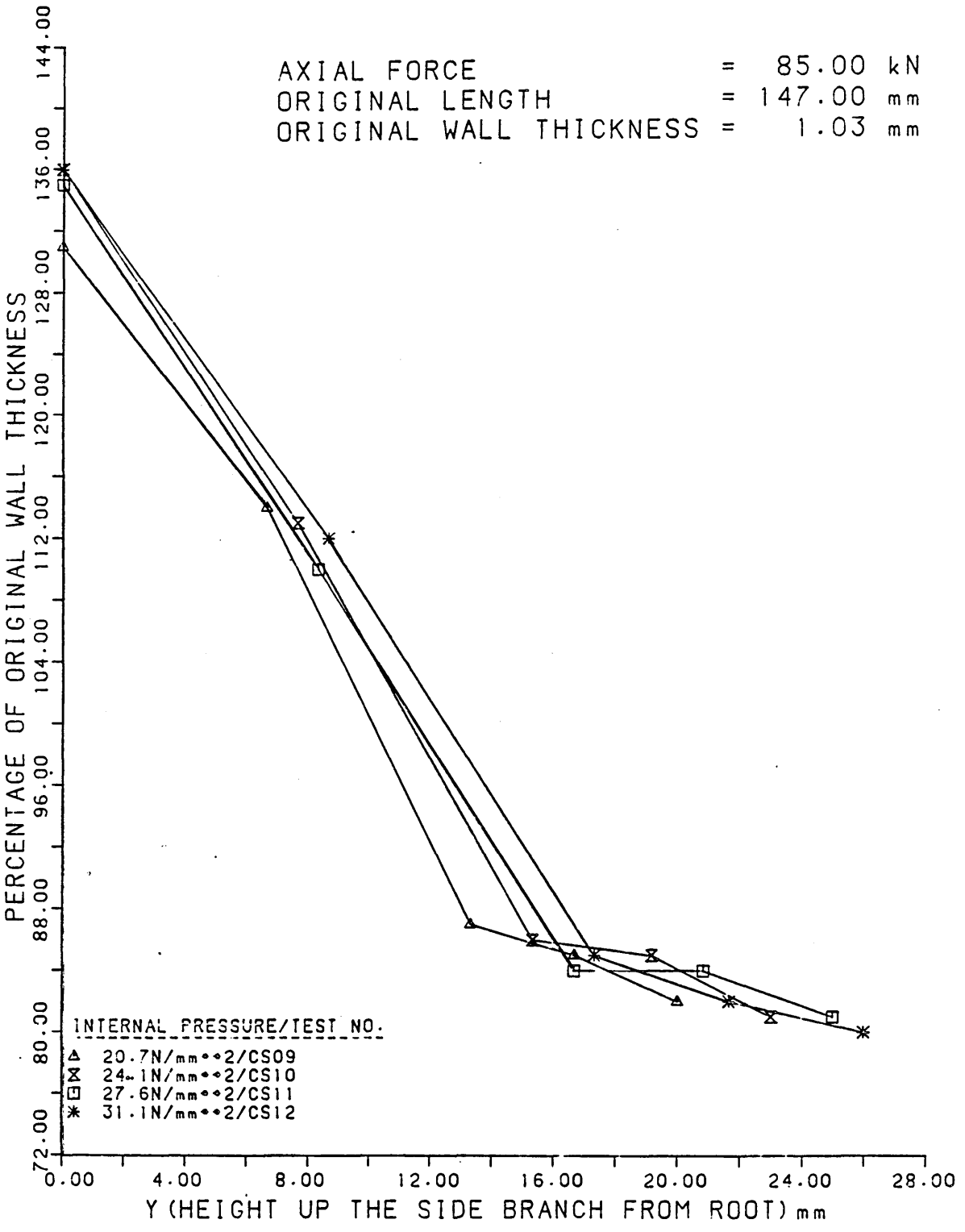

FIGURE 36

The Wall Thickness Distributions Along The Side Branches And Domes Of Cross Joints Formed At Various Internal Pressures.

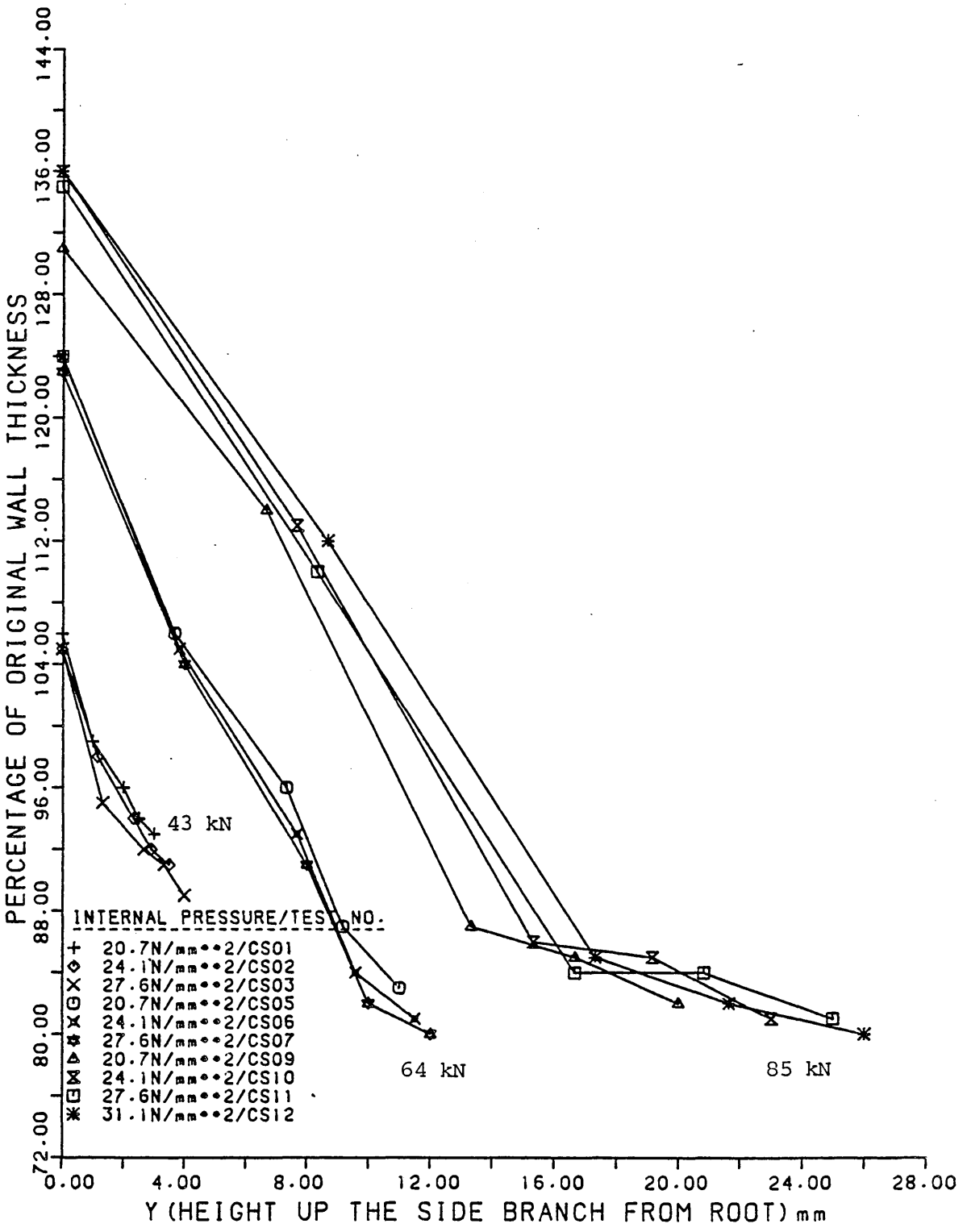

FIGURE 37

The Wall Thickness Distributions Along The Side Branches And Domes Of Cross Joints Formed At Various Internal Pressures And With Various Compressive Axial Loads.

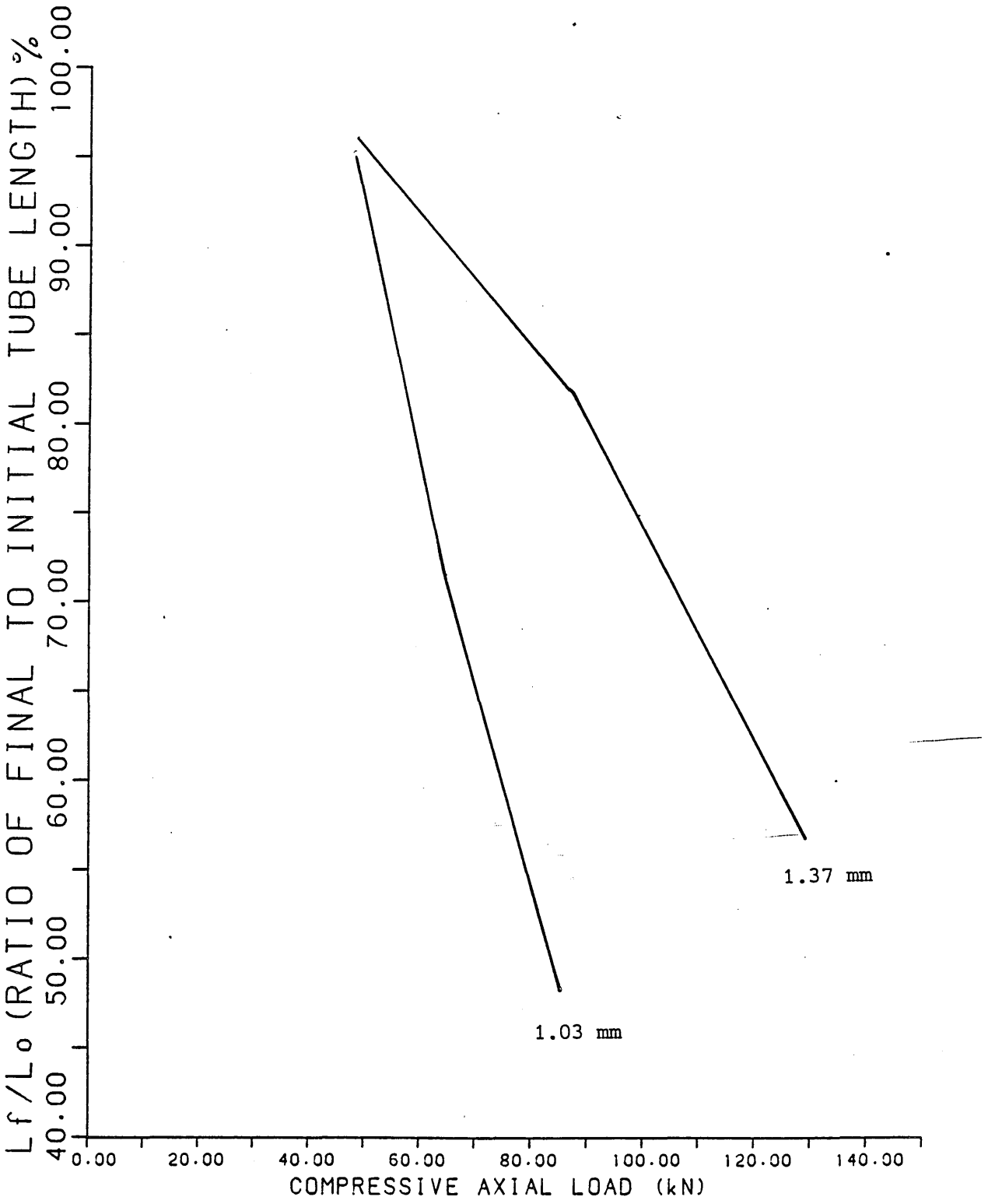

FIGURE 38

The Final To Original Tube Length Variation Against Compressive Axial Load For Cross Joints Formed From Tubes Of Different Wall Thicknesses.

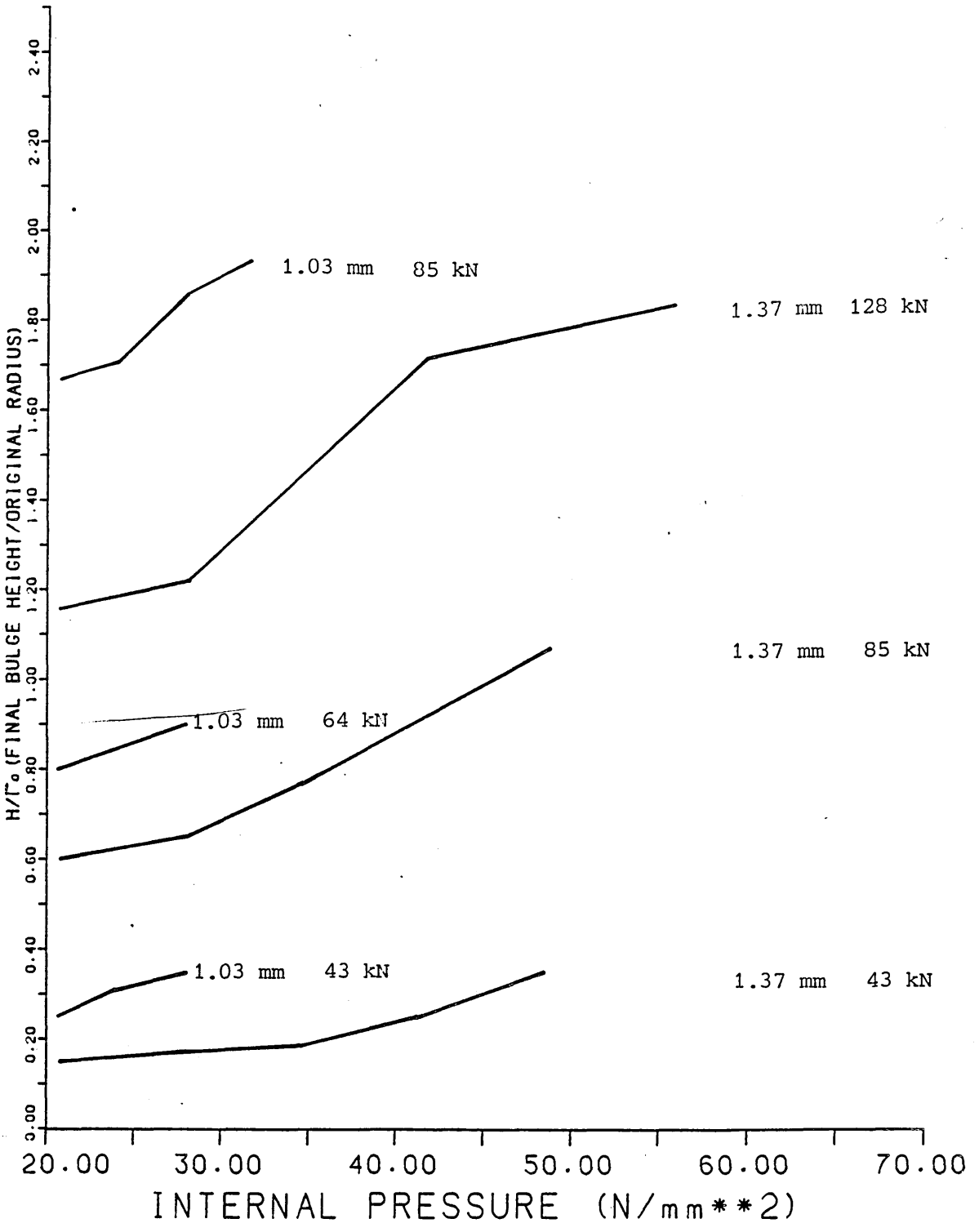

FIGURE 39

The Bulge Height To Original Tube Radius Variation Against Internal Pressure For Cross Joints Formed From Tubes With Different Wall Thicknesses.

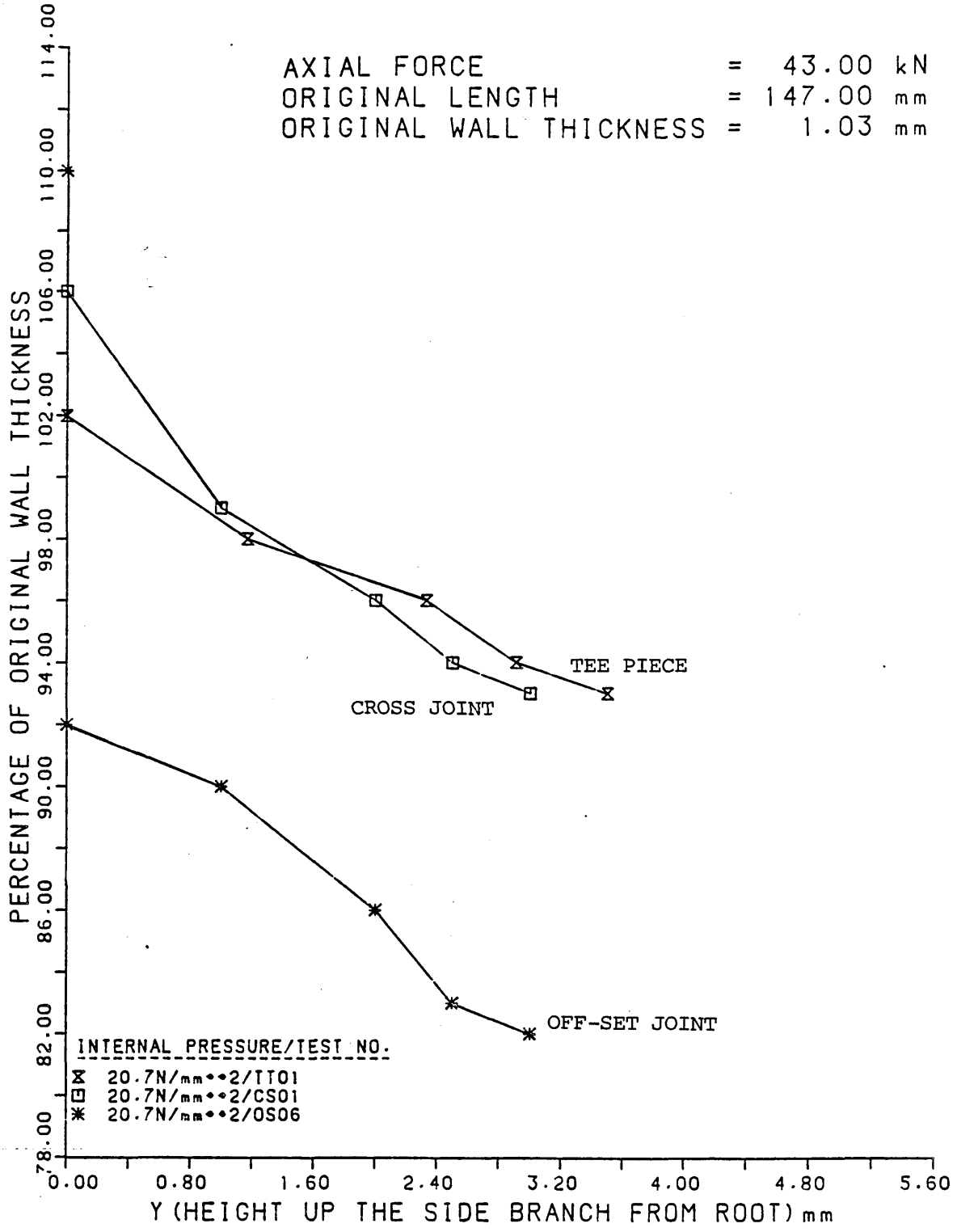

FIGURE 40

The Wall Thickness Distributions Along The Side Branches And Domes Of Tee Pieces, Cross Joints And Off-Set Pieces.

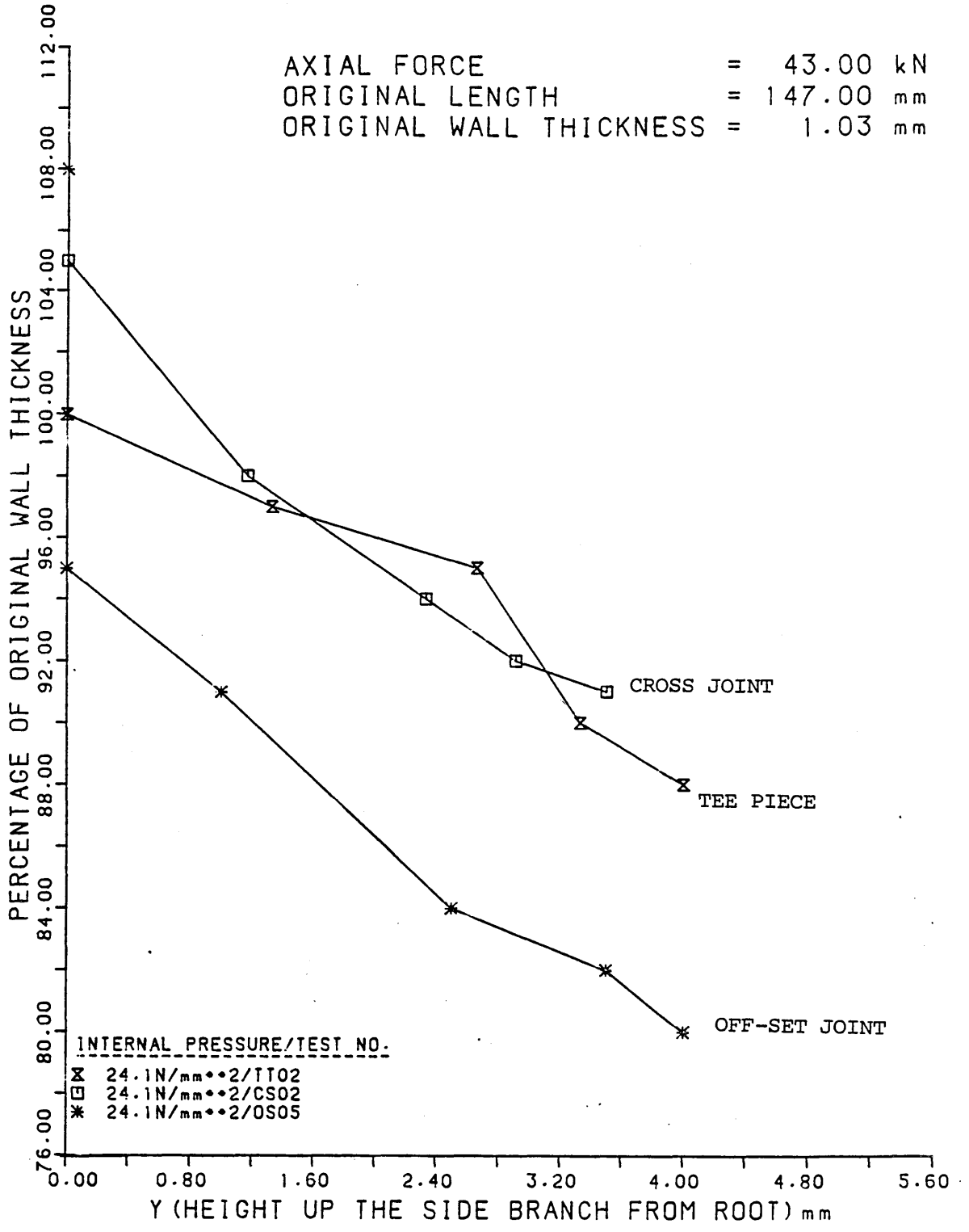

FIGURE 41

The Wall Thickness Distributions Along The Side Branches And Domes Of Tee Pieces, Cross Joints And Off-Set Pieces.

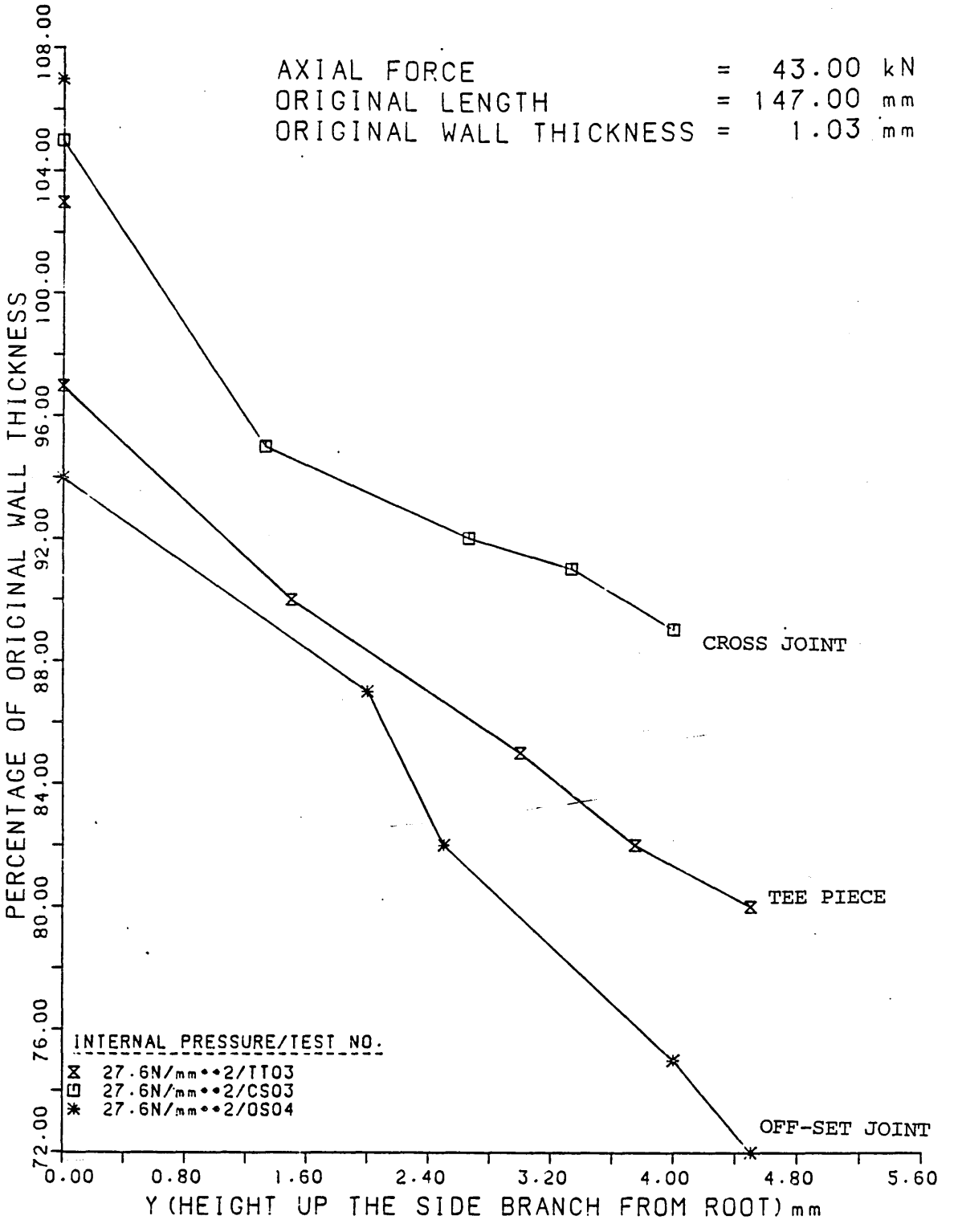

FIGURE 42

The Wall Thickness Distributions Along The Side Branches And Domes Of Tee Pieces, Cross Joints And Off-Set Pieces.

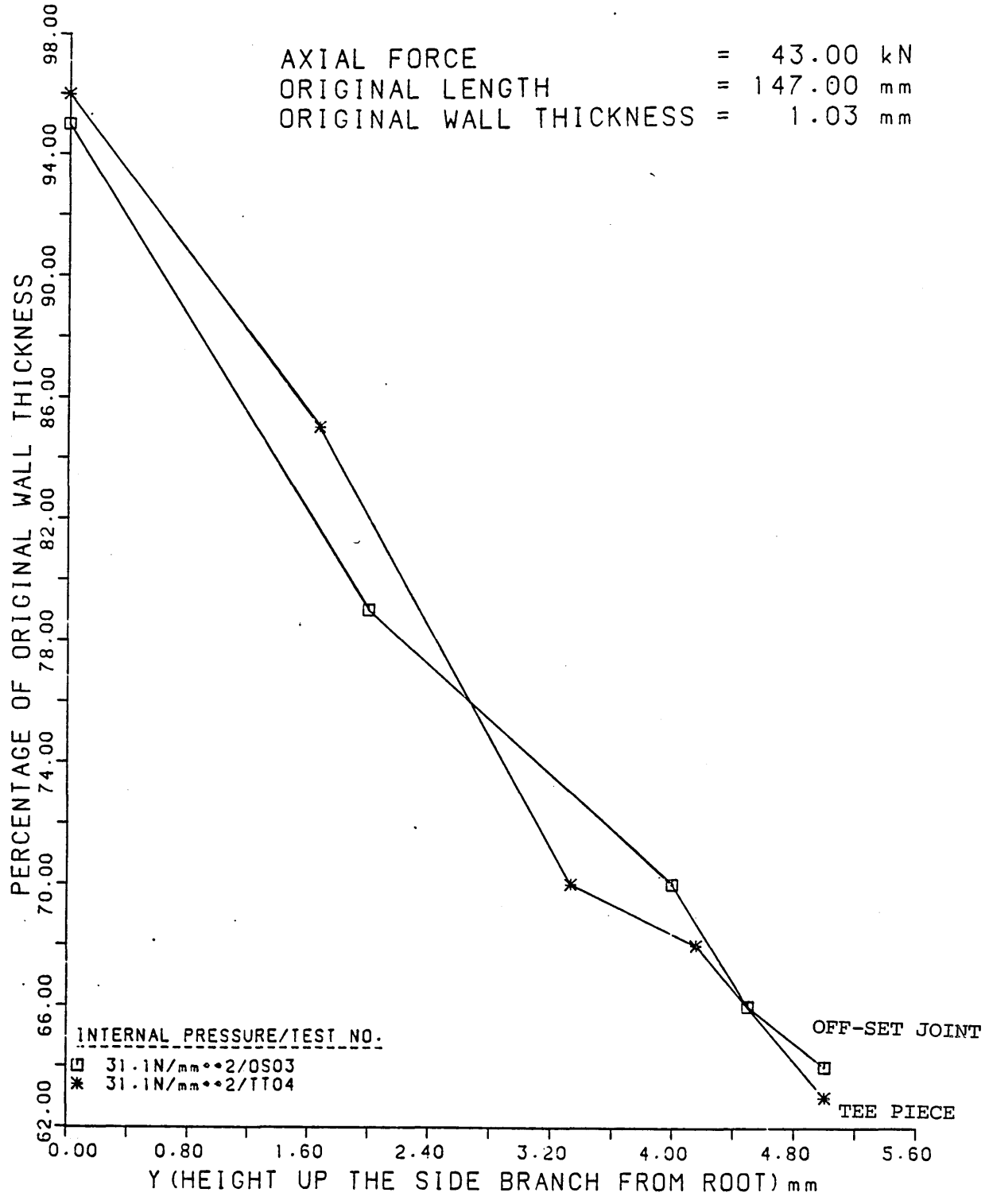

FIGURE 43

The Wall Thickness Distributions Along The Side Branches And Domes Of Tee Pieces, Cross Joints And Off-Set Pieces.

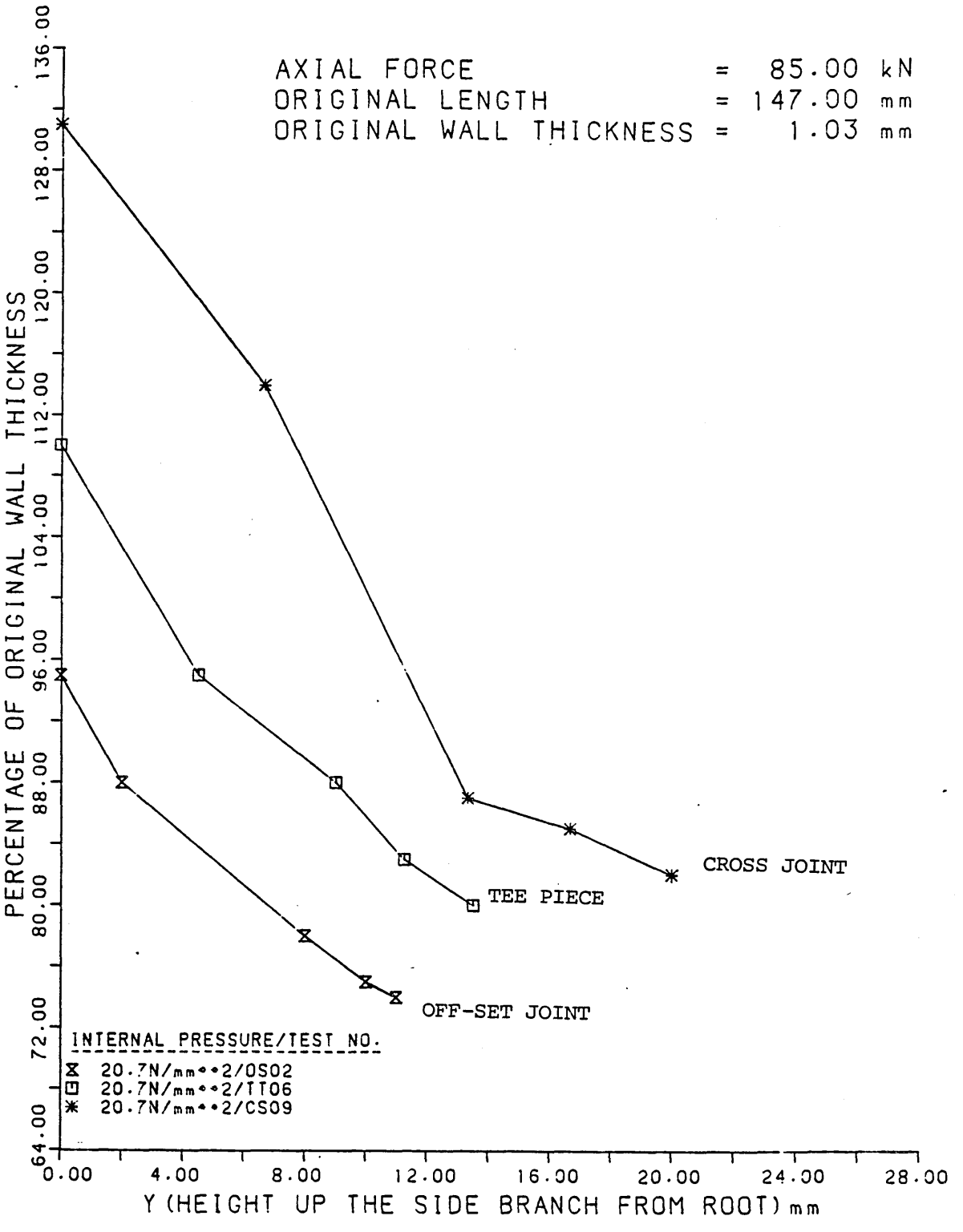

FIGURE 44

The Wall Thickness Distributions Along The Side Branches And Domes Of Tee Pieces, Cross Joints And Off-Set Pieces.

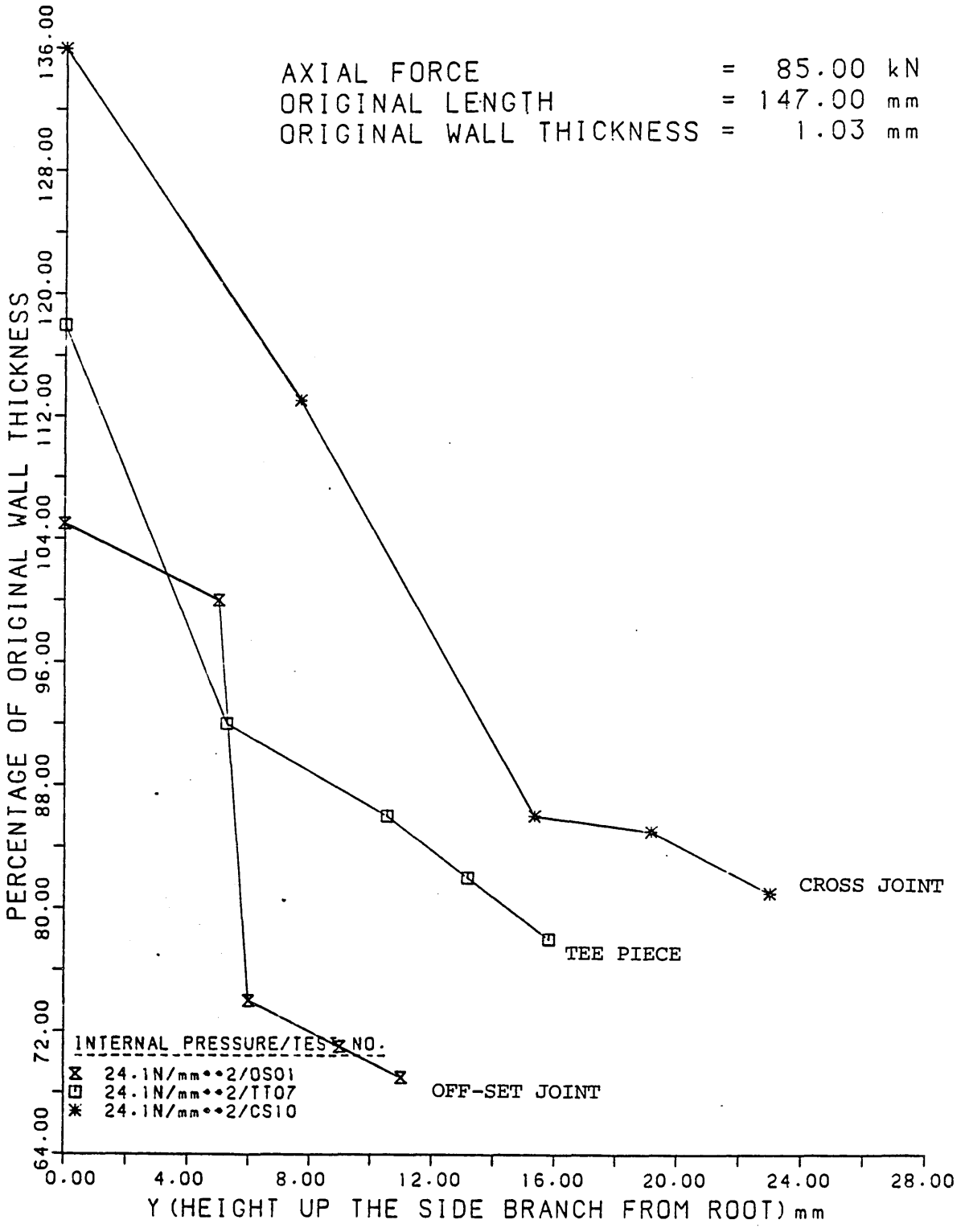

FIGURE 45

The Wall Thickness Distributions Along The Side Branches And Domes Of Tee Pieces, Cross Joints And Off-Set Pieces.

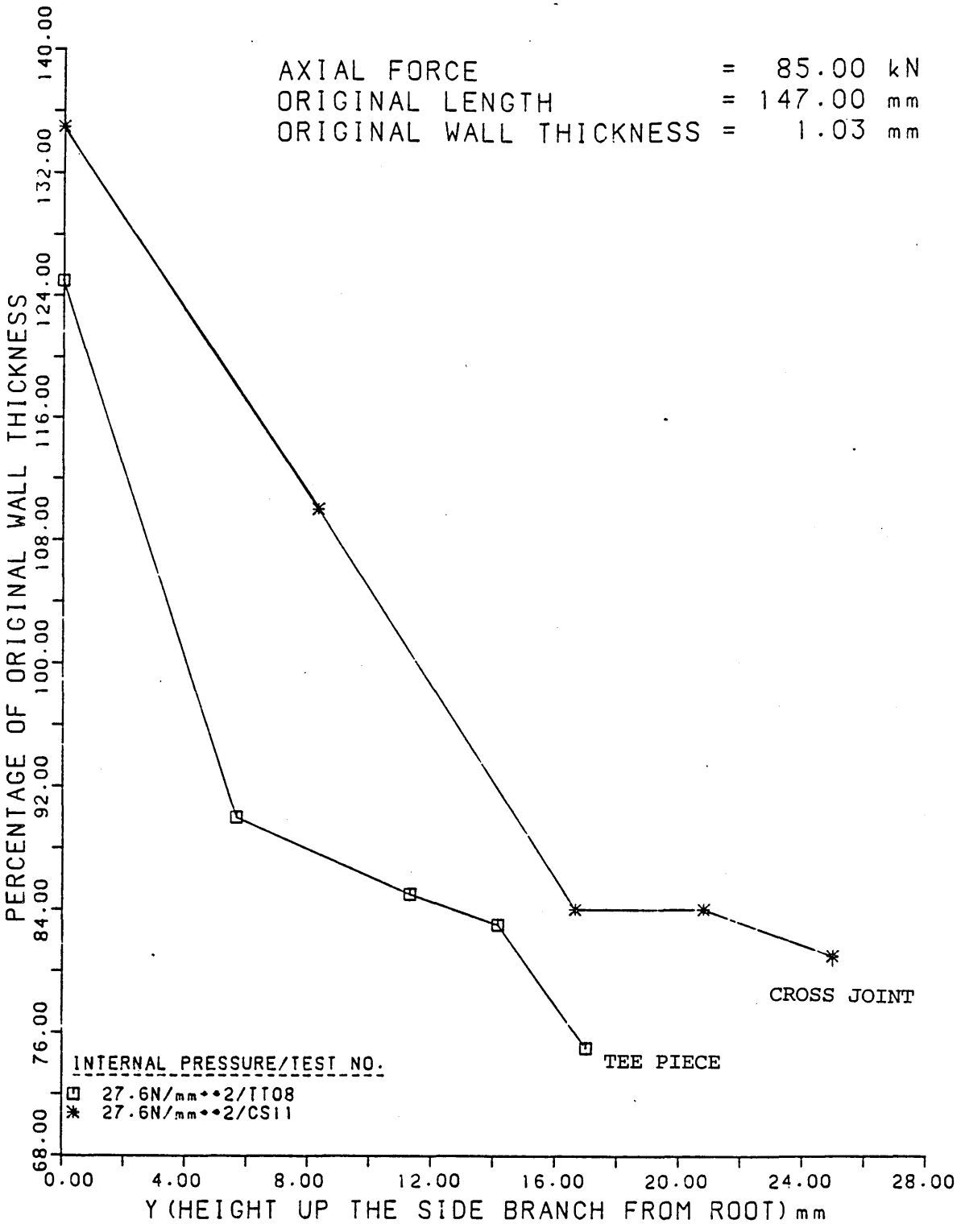

FIGURE 46

The Wall Thickness Distributions Along The Side Branches And Domes Of Tee Pieces, Cross Joints And Off-Set Pieces.

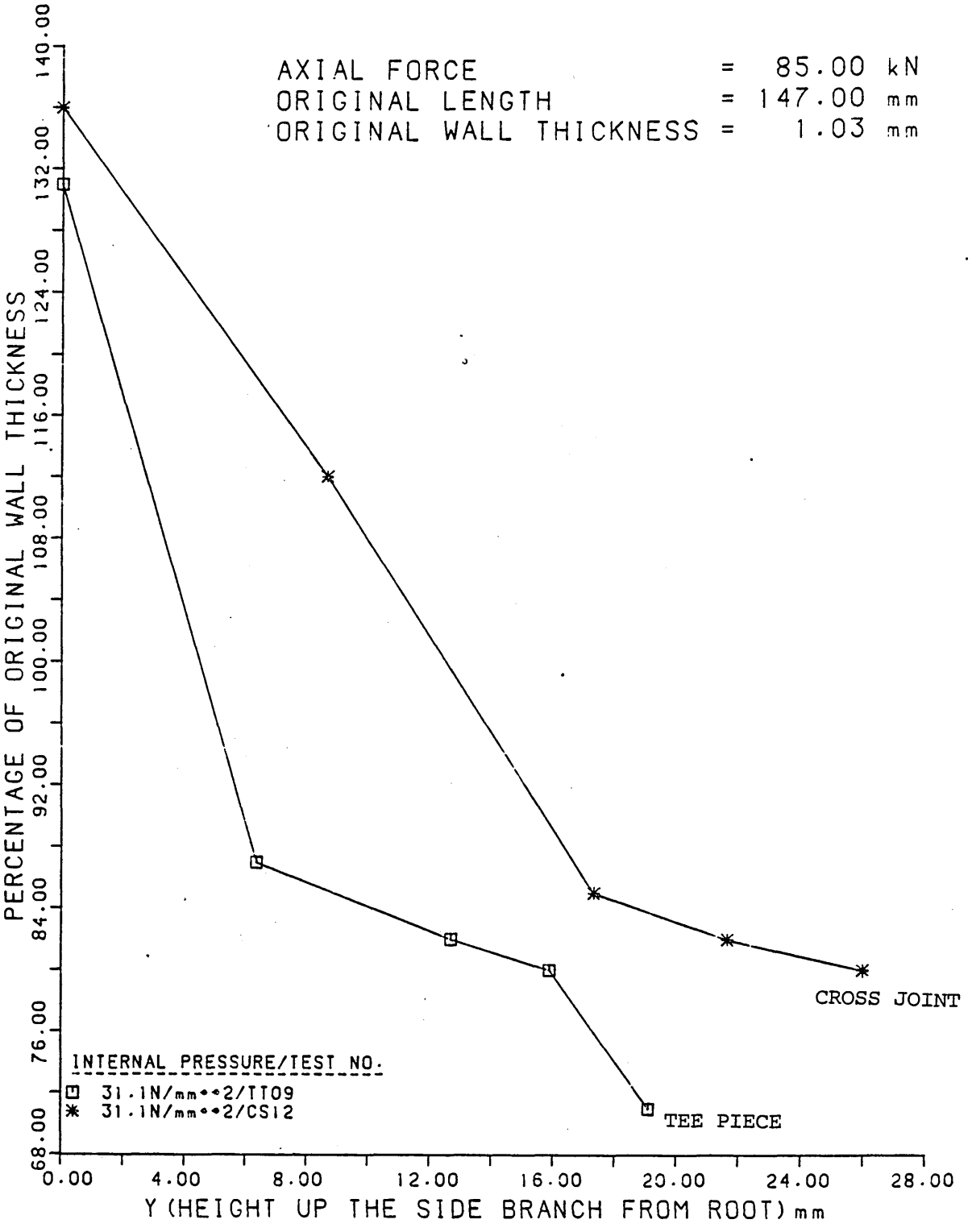

FIGURE 47

The Wall Thickness Distributions Along The Side Branches And Domes Of Tee Pieces, Cross Joints And Off-Set Pieces.

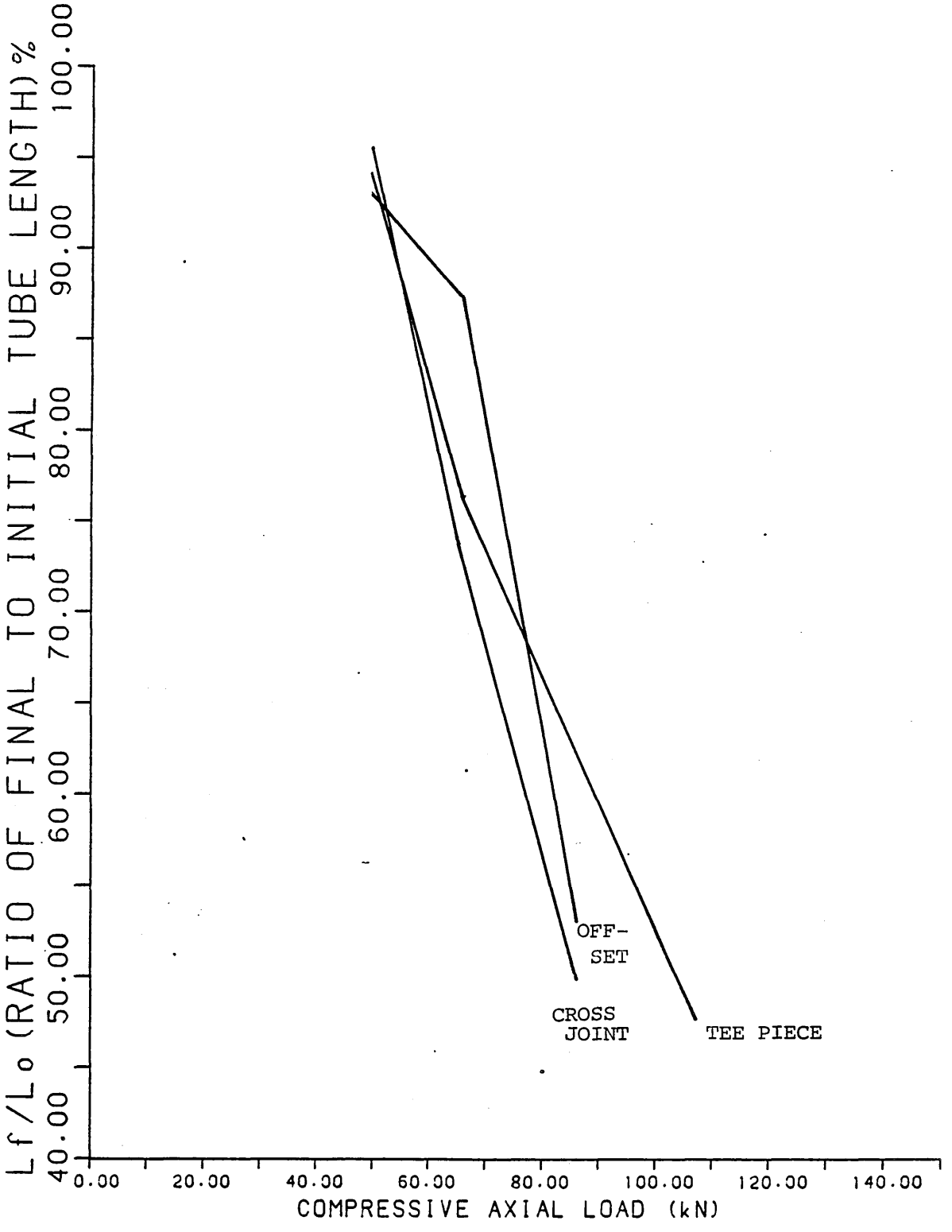

FIGURE 48

The Final To Original Tube Length Variation

Against Compressive Axial Load For Tee Pieces,

Cross Joints And Off-Set Pieces.

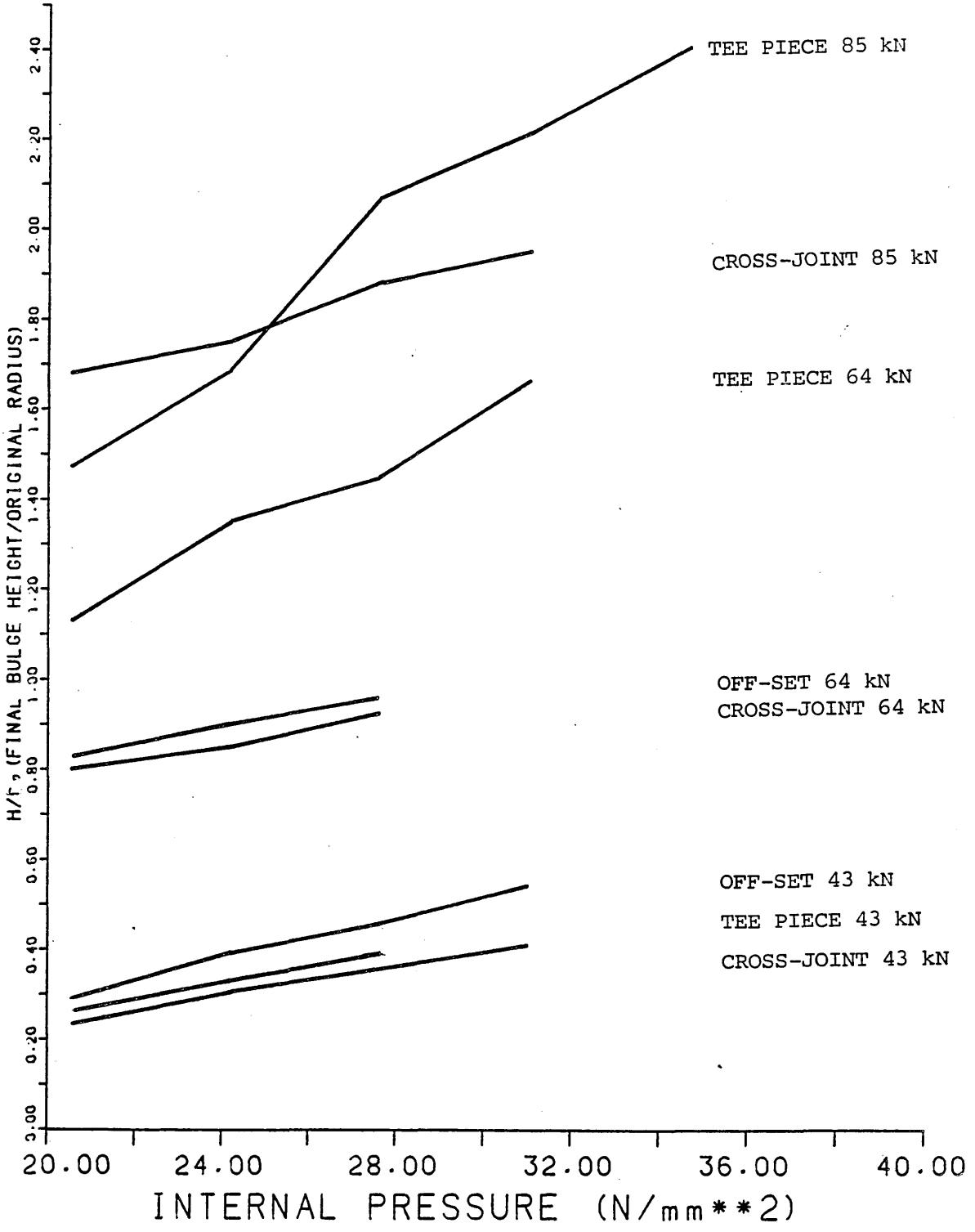

FIGURE 49

The Bulge Height To Original Tube Radius Variation Against Internal Pressure For Tee Pieces, Cross Joints And Off-Set Pieces.

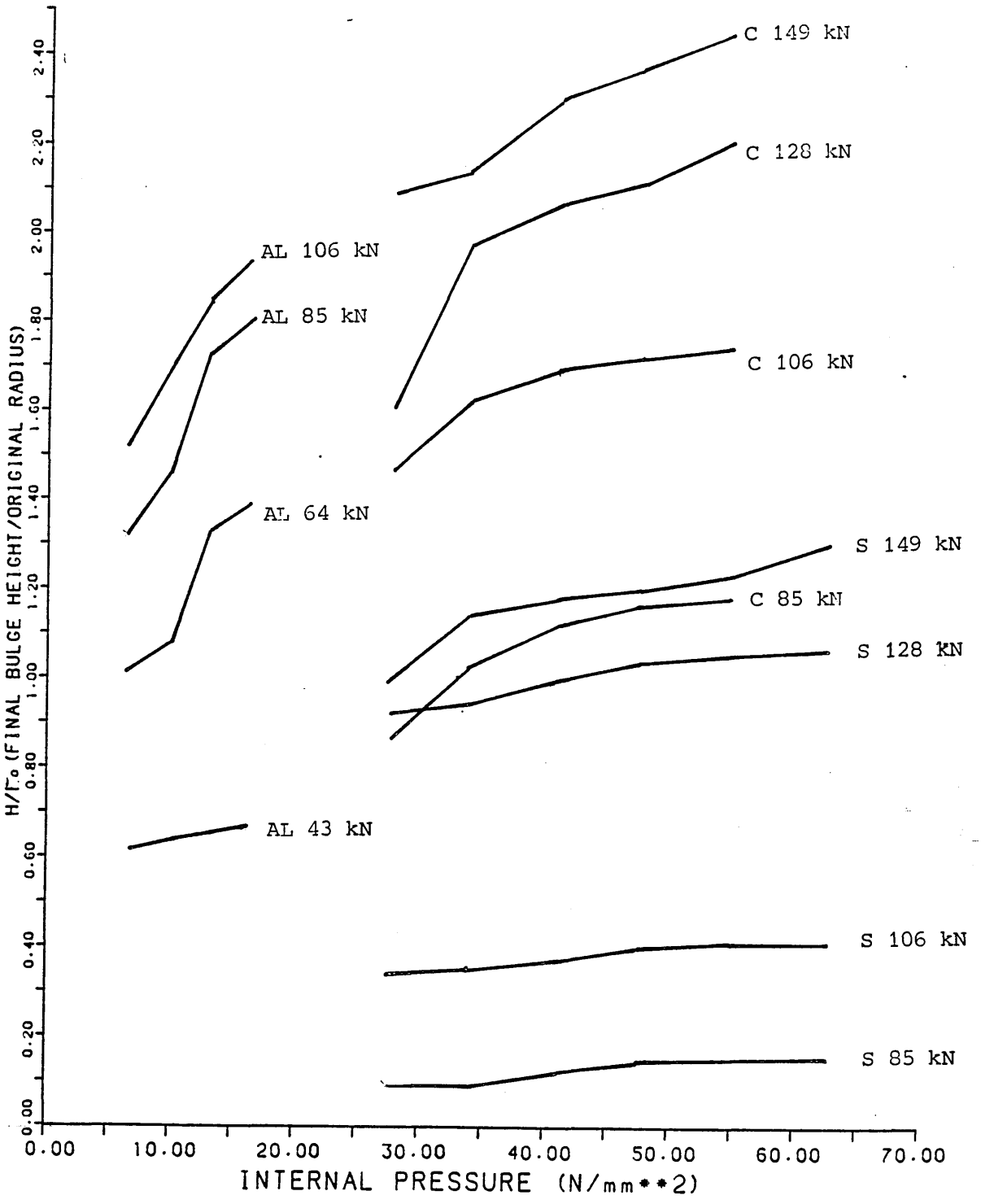

FIGURE 50

The Bulge Height To Original Tube Radius Variation Against Internal Pressure For Tee Pieces Formed From Aluminium, Copper And Steel.

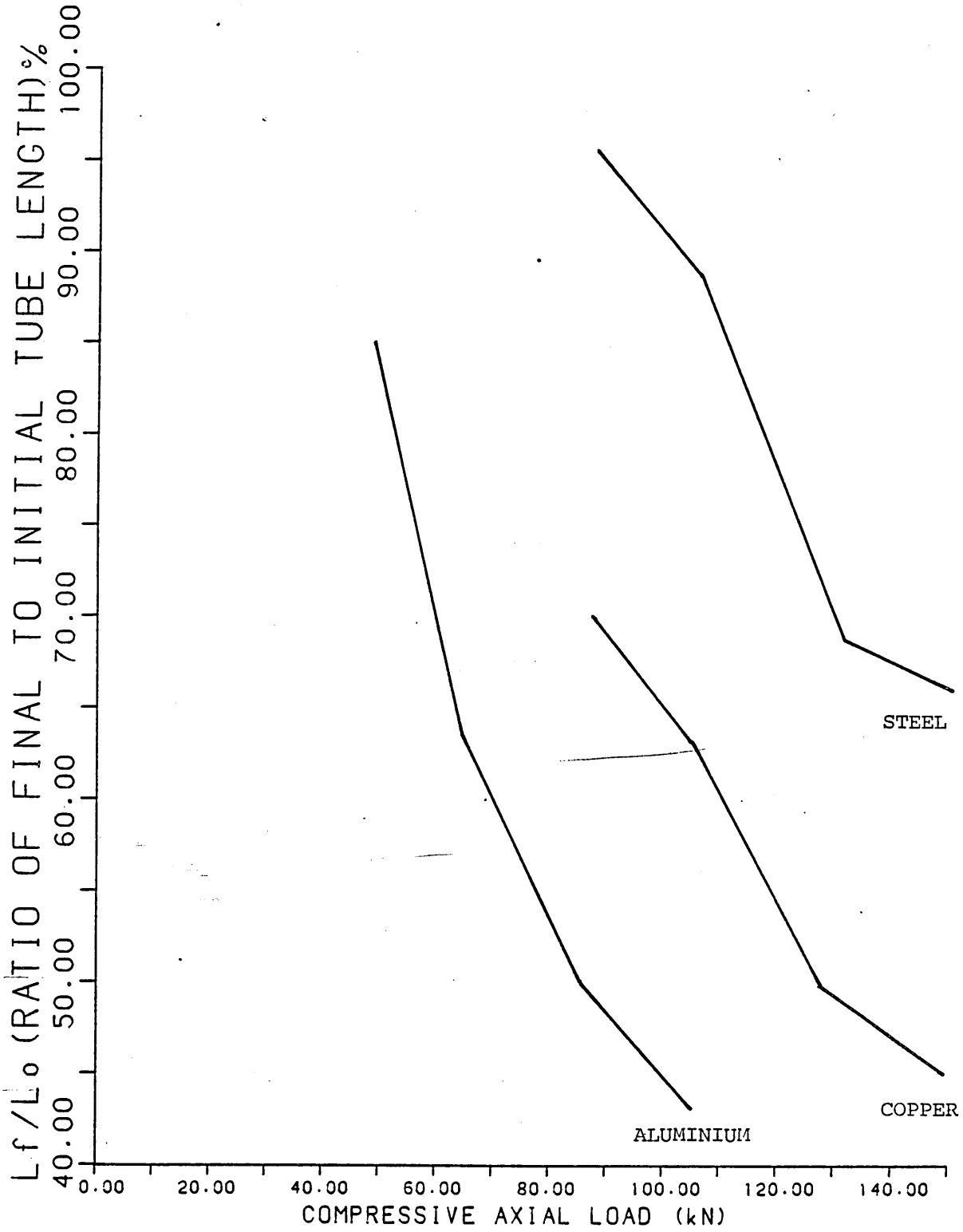

FIGURE 51

The Final To Original Tube Length Variation Against Compressive Axial Load For Tee Pieces Formed From Aluminium, Copper And Steel.

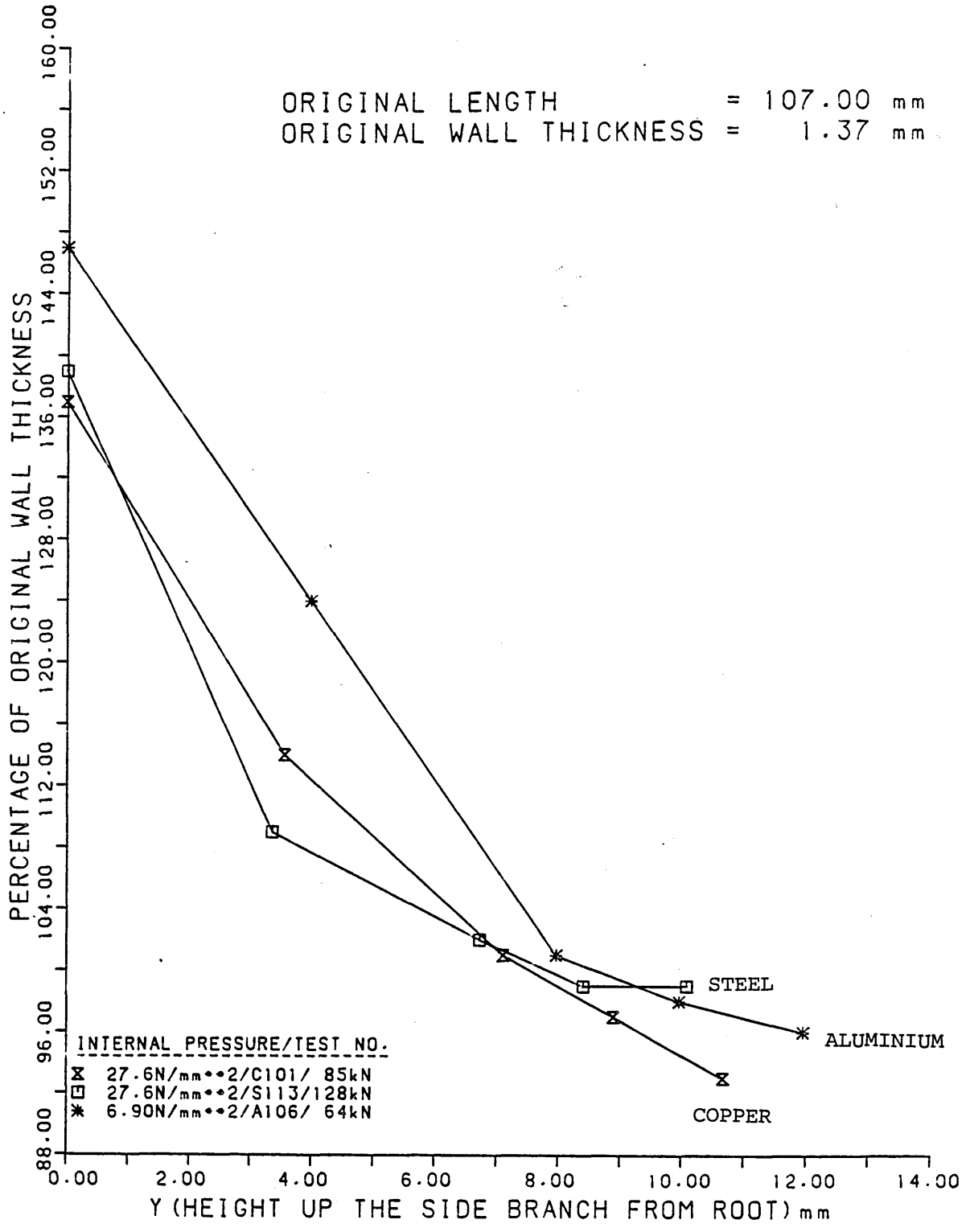

FIGURE 52

The Wall Thickness Distributions Along The Side Branches And Domes Of Tee Pieces Formed From Aluminium, Copper And Steel.

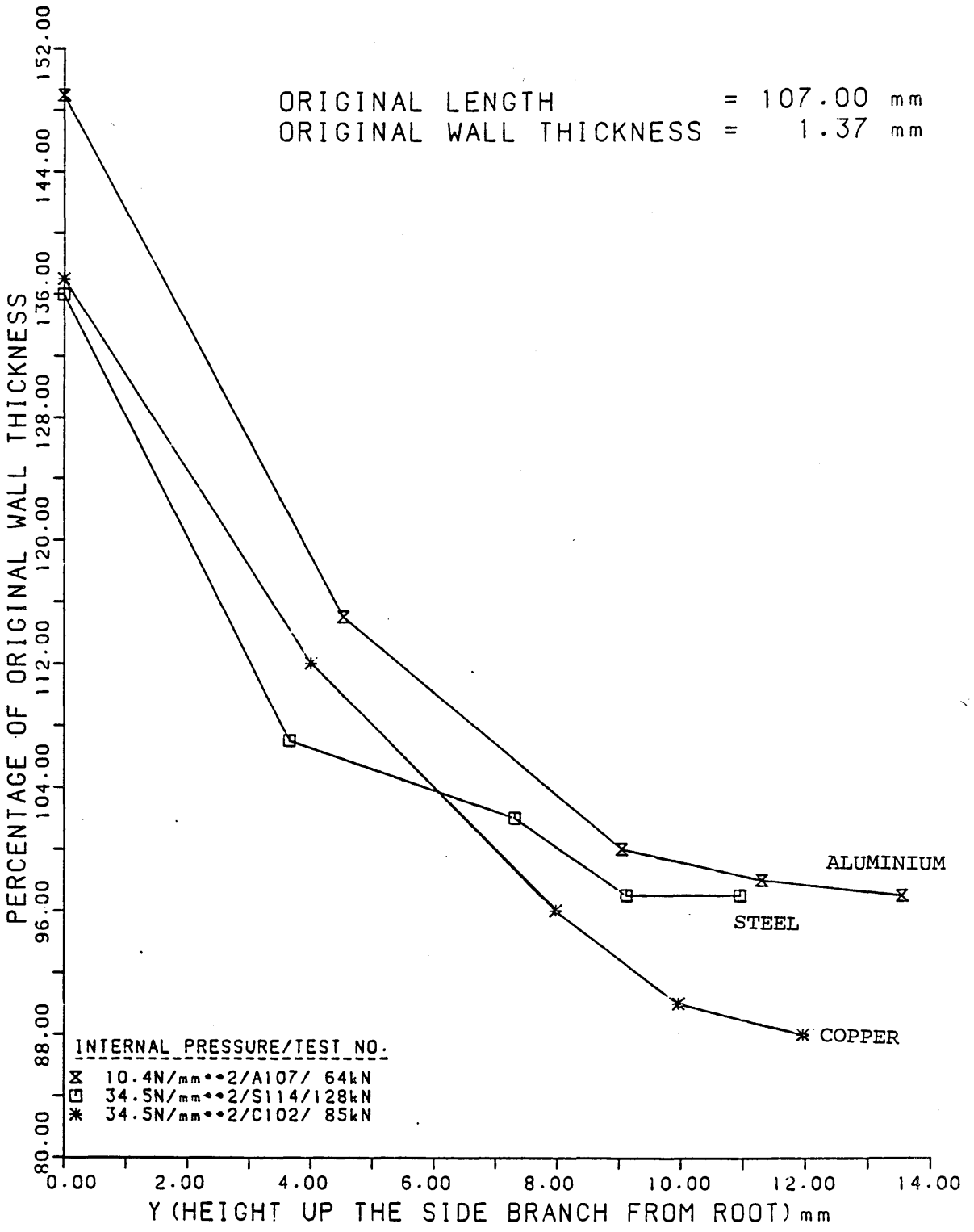

FIGURE 53

The Wall Thickness Distributions Along The Side Branches And Domes Of Tee Pieces Formed From Aluminium, Copper And Steel.

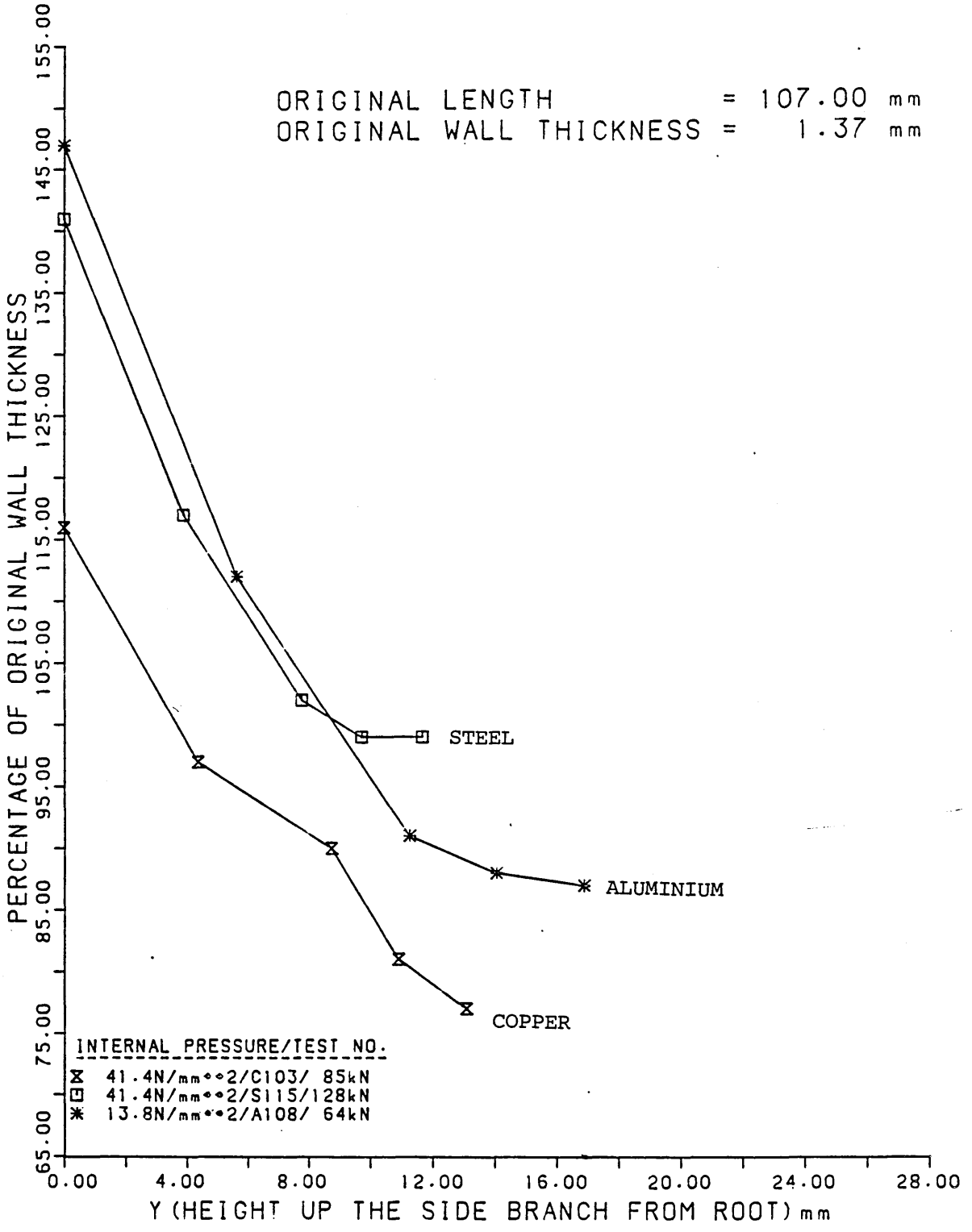

FIGURE 54

The Wall Thickness Distributions Along The Side Branches And Domes Of Tee Pieces Formed From Aluminium, Copper And Steel.

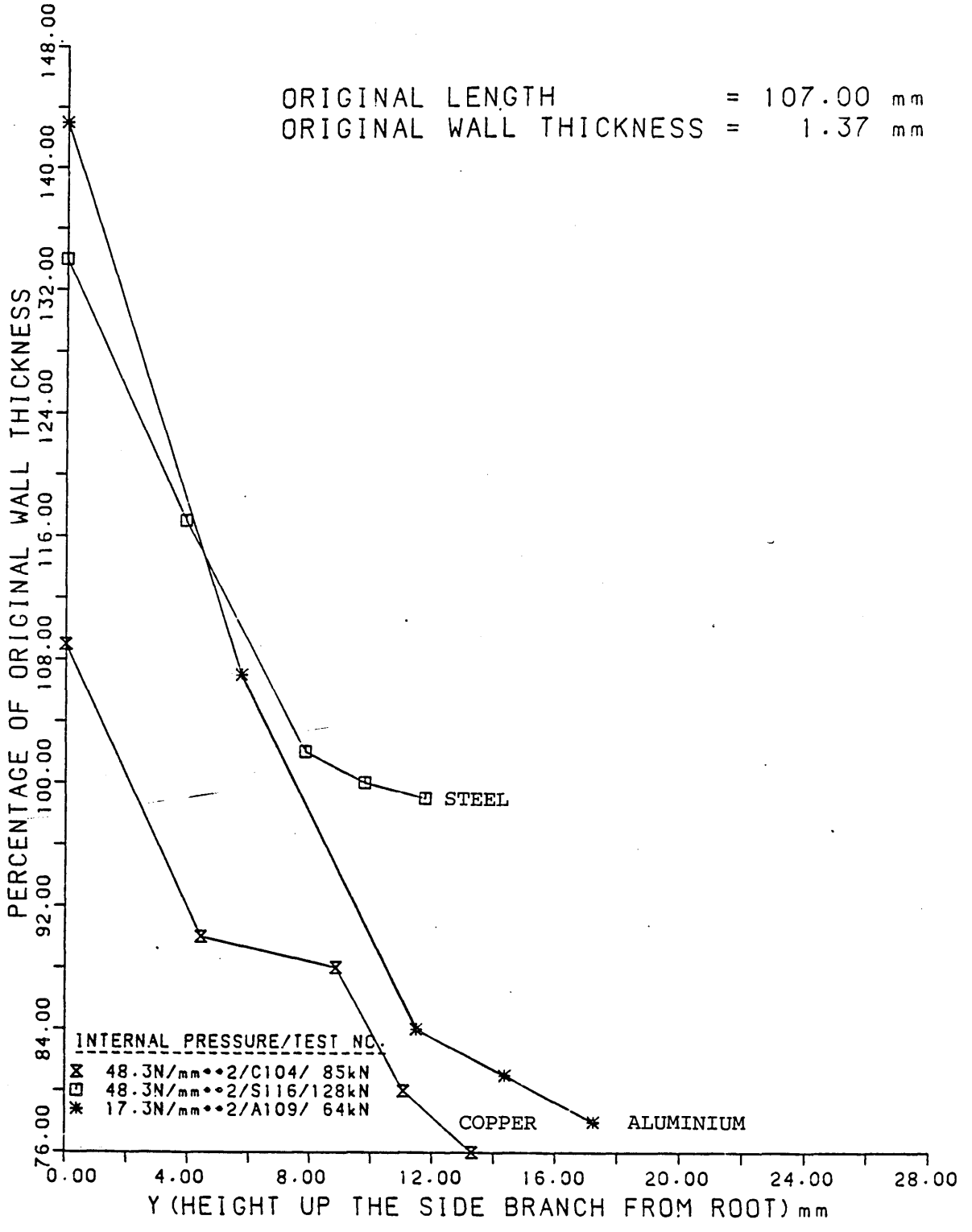

FIGURE 55

The Wall Thickness Distributions Along The Side Branches And Domes Of Tee Pieces Formed From Aluminium, Copper And Steel.

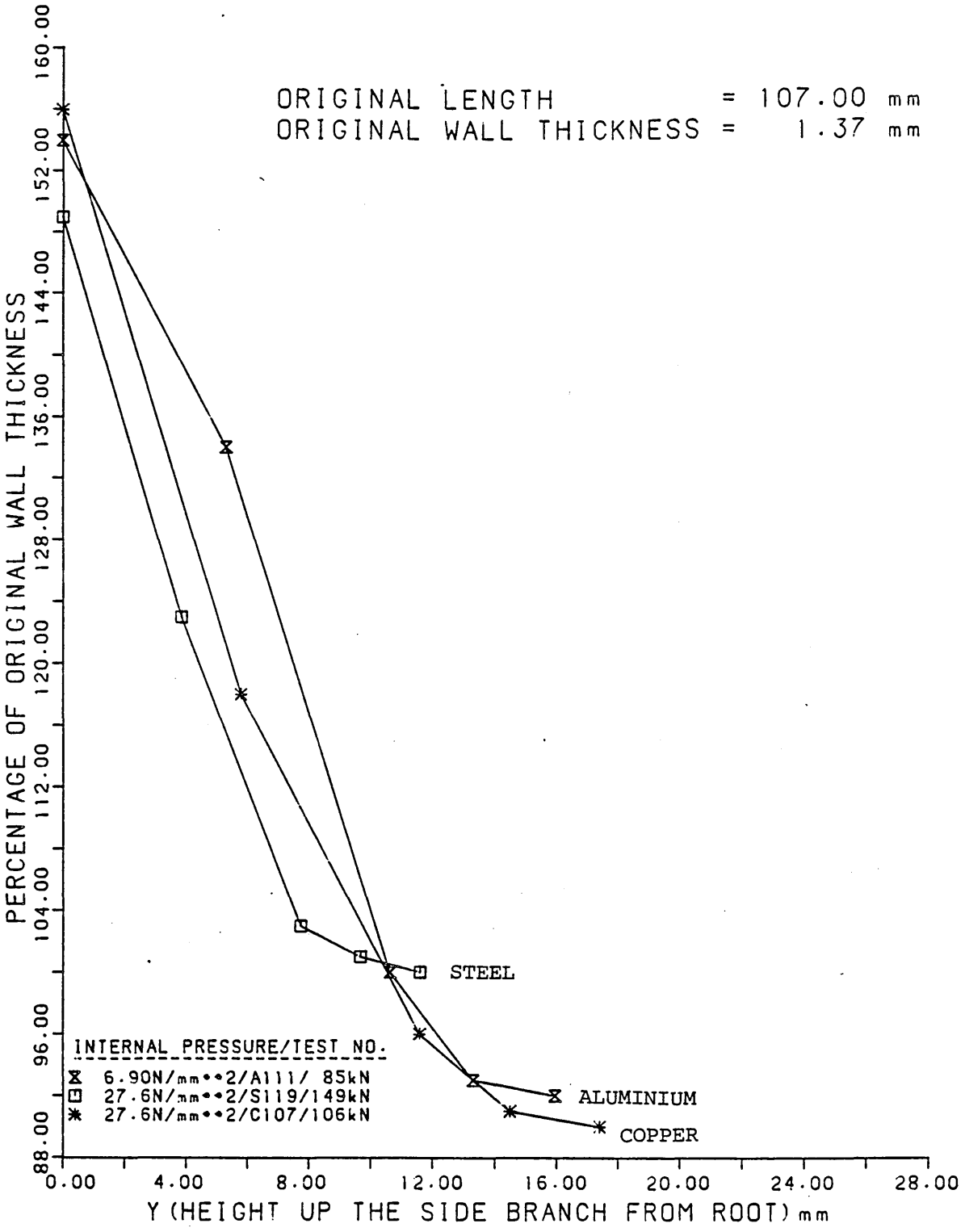

FIGURE 56

The Wall Thickness Distributions Along The Side Branches And Domes Of Tee Pieces Formed From Aluminium, Copper And Steel.

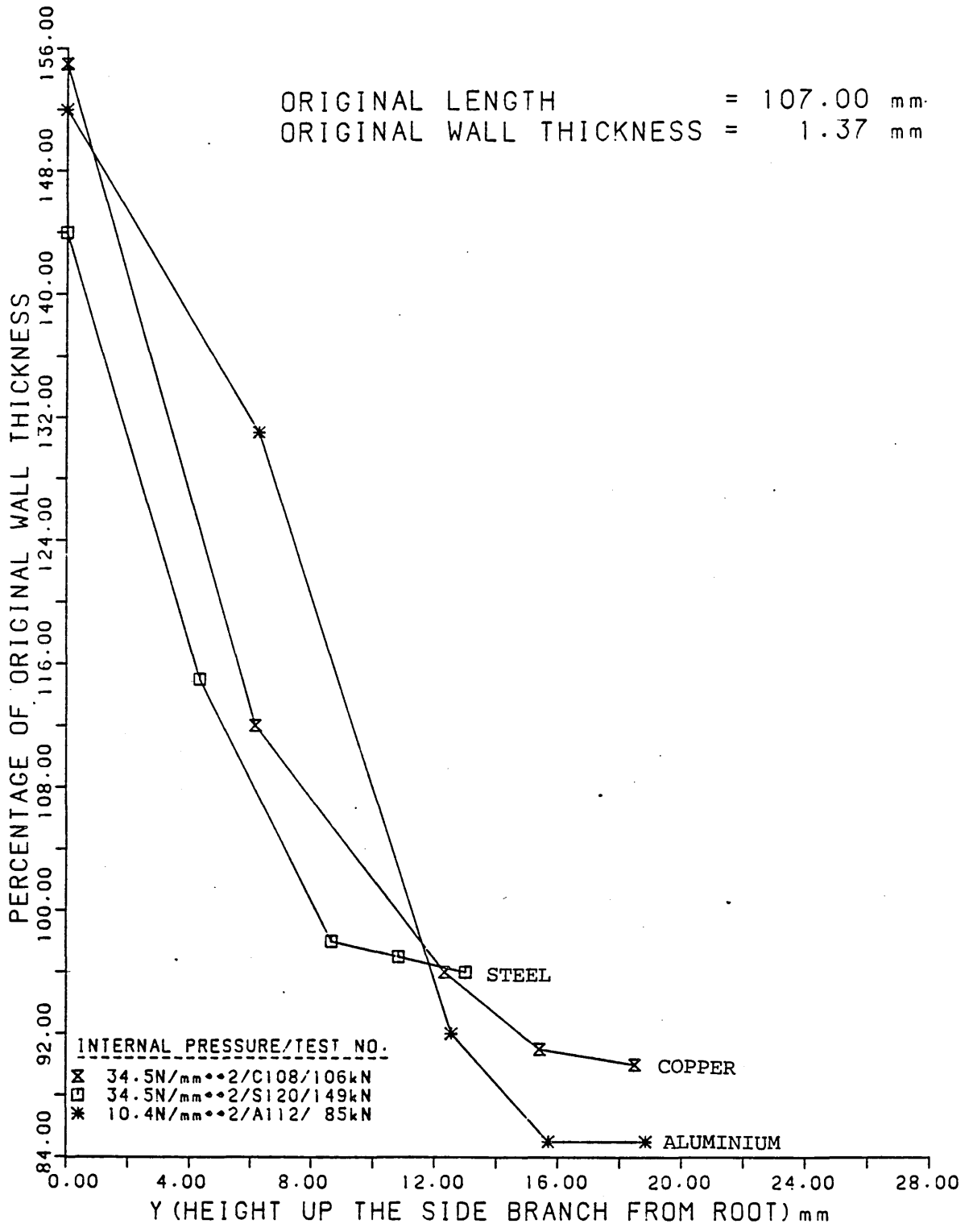

FIGURE 57

The Wall Thickness Distributions Along The Side Branches And Domes Of Tee Pieces Formed From Aluminium, Copper And Steel.

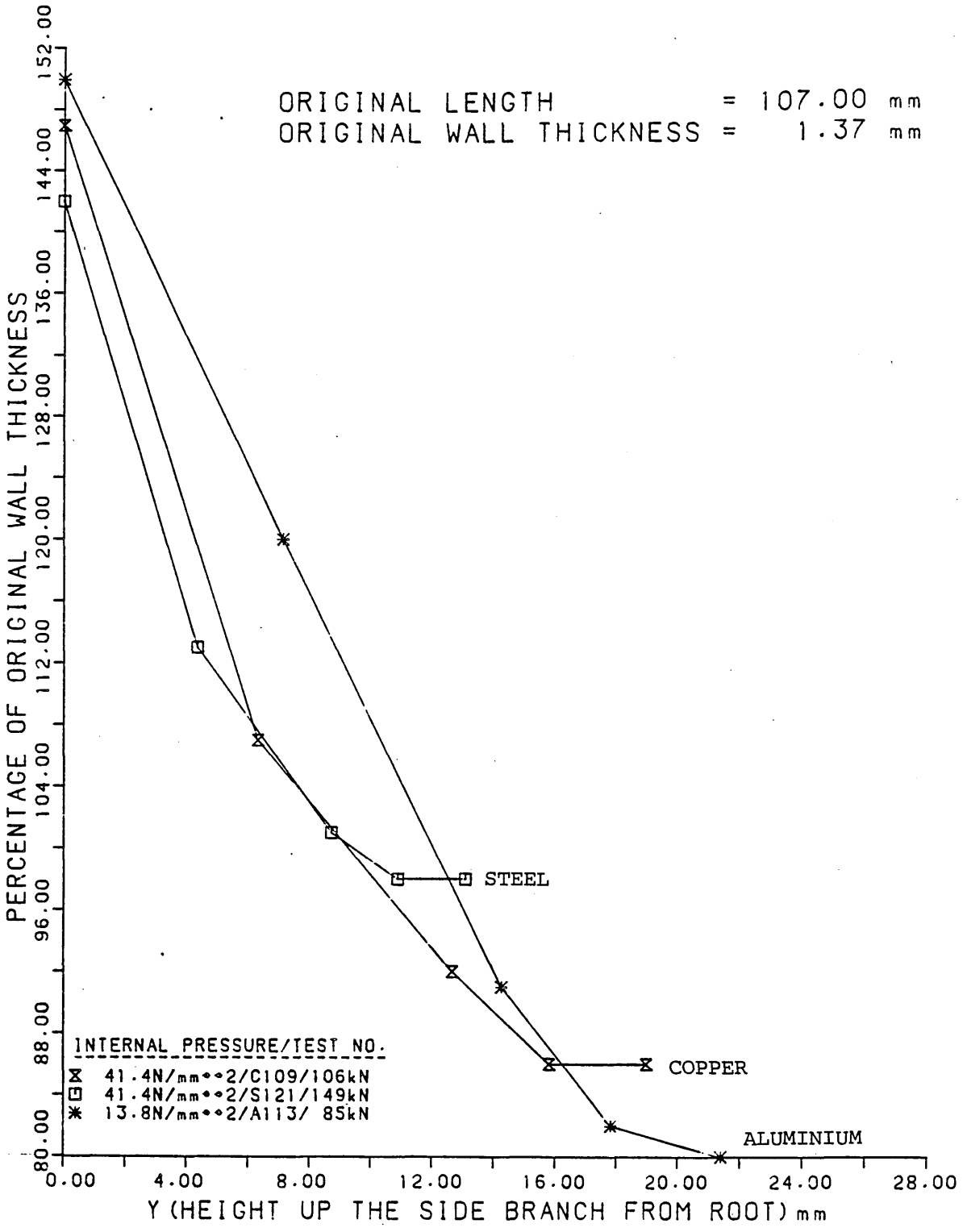

FIGURE 58

The Wall Thickness Distributions Along The Side Branches And Domes Of Tee Pieces Formed From Aluminium, Copper And Steel.

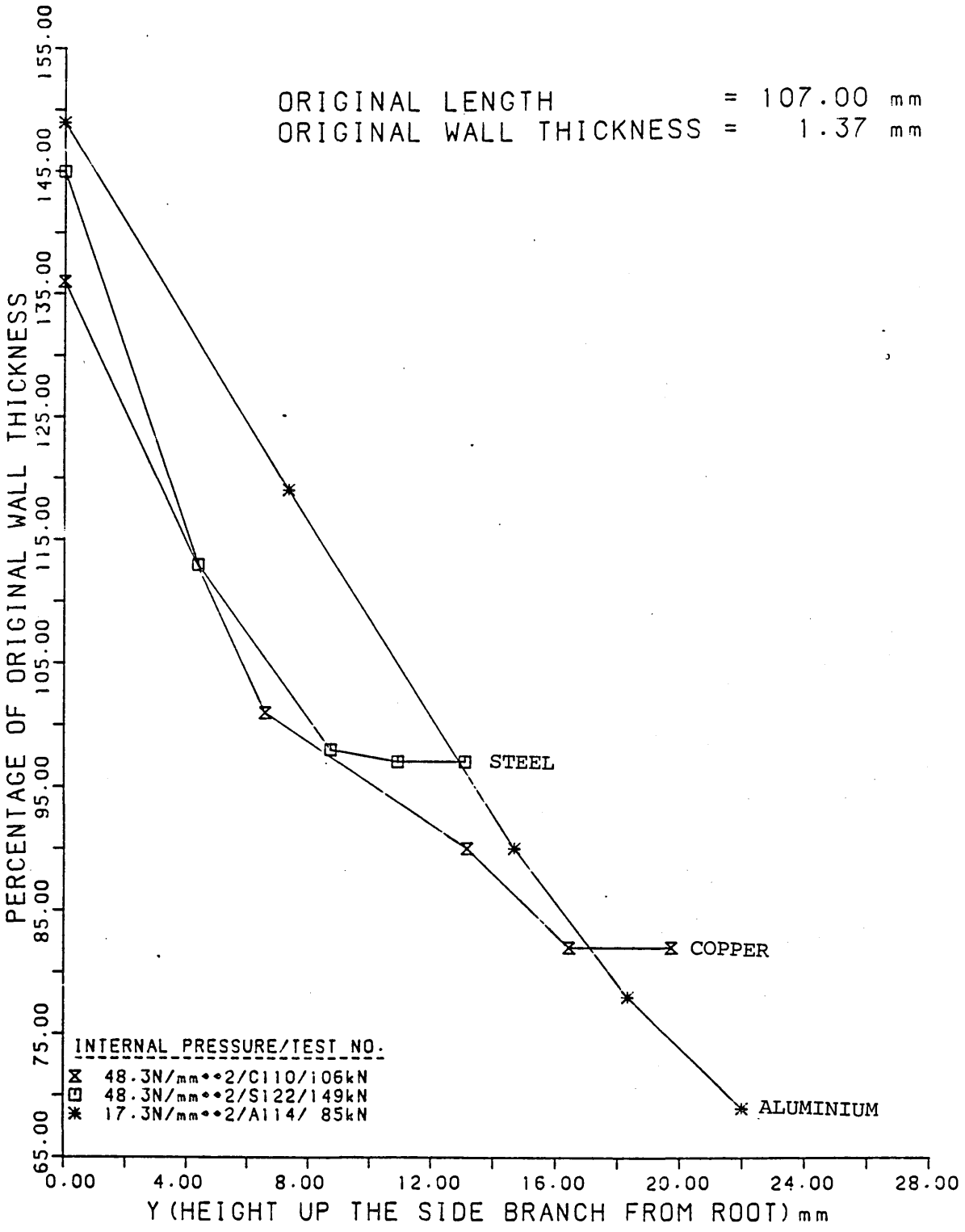

FIGURE 59

The Wall Thickness Distributions Along The Side Branches And Domes Of Tee Pieces Formed From Aluminium, Copper And Steel.

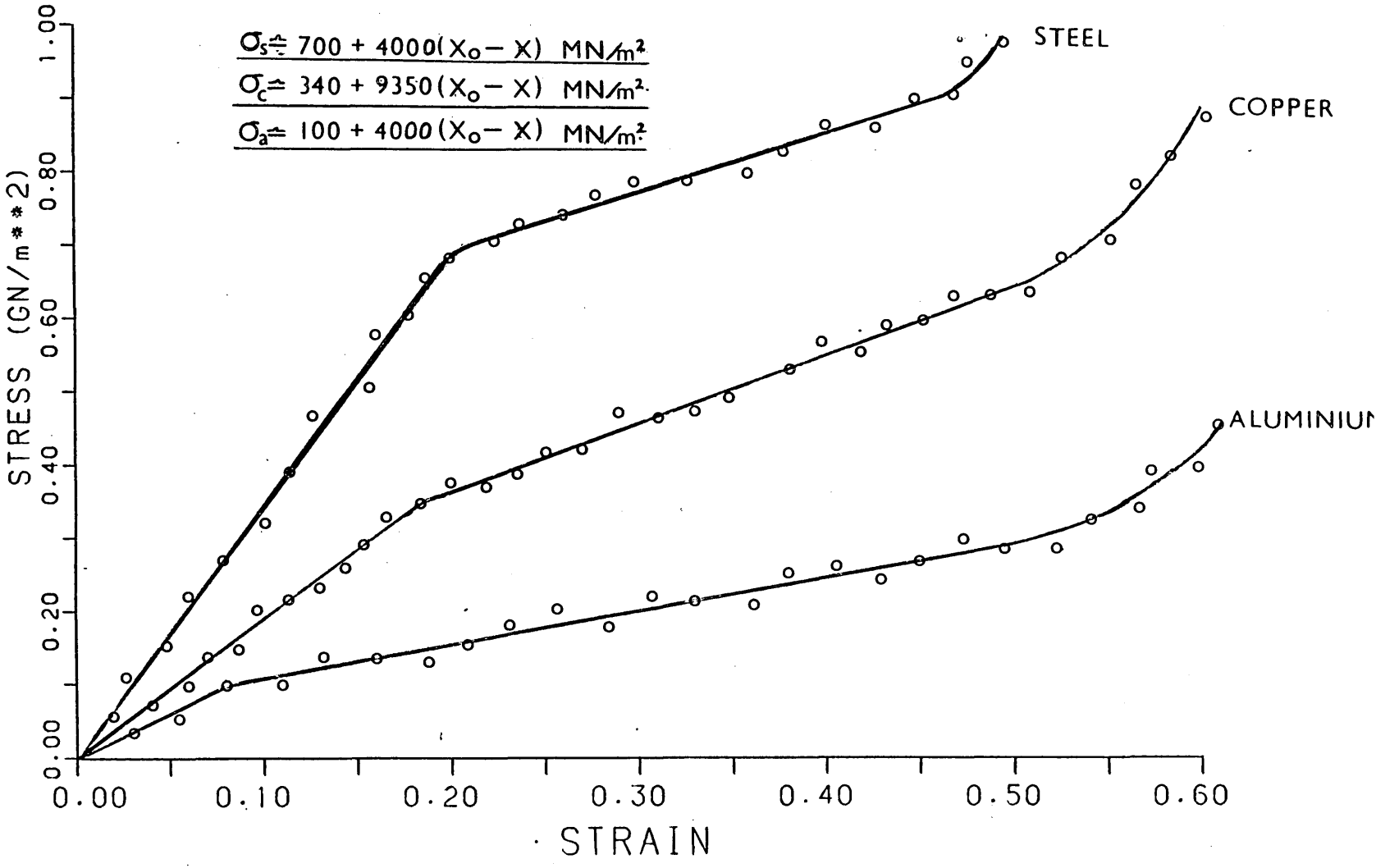

FIGURE 60 : The Stress-Strain Relationships For Compression Tests On Aluminium, Copper And Steel Rings.

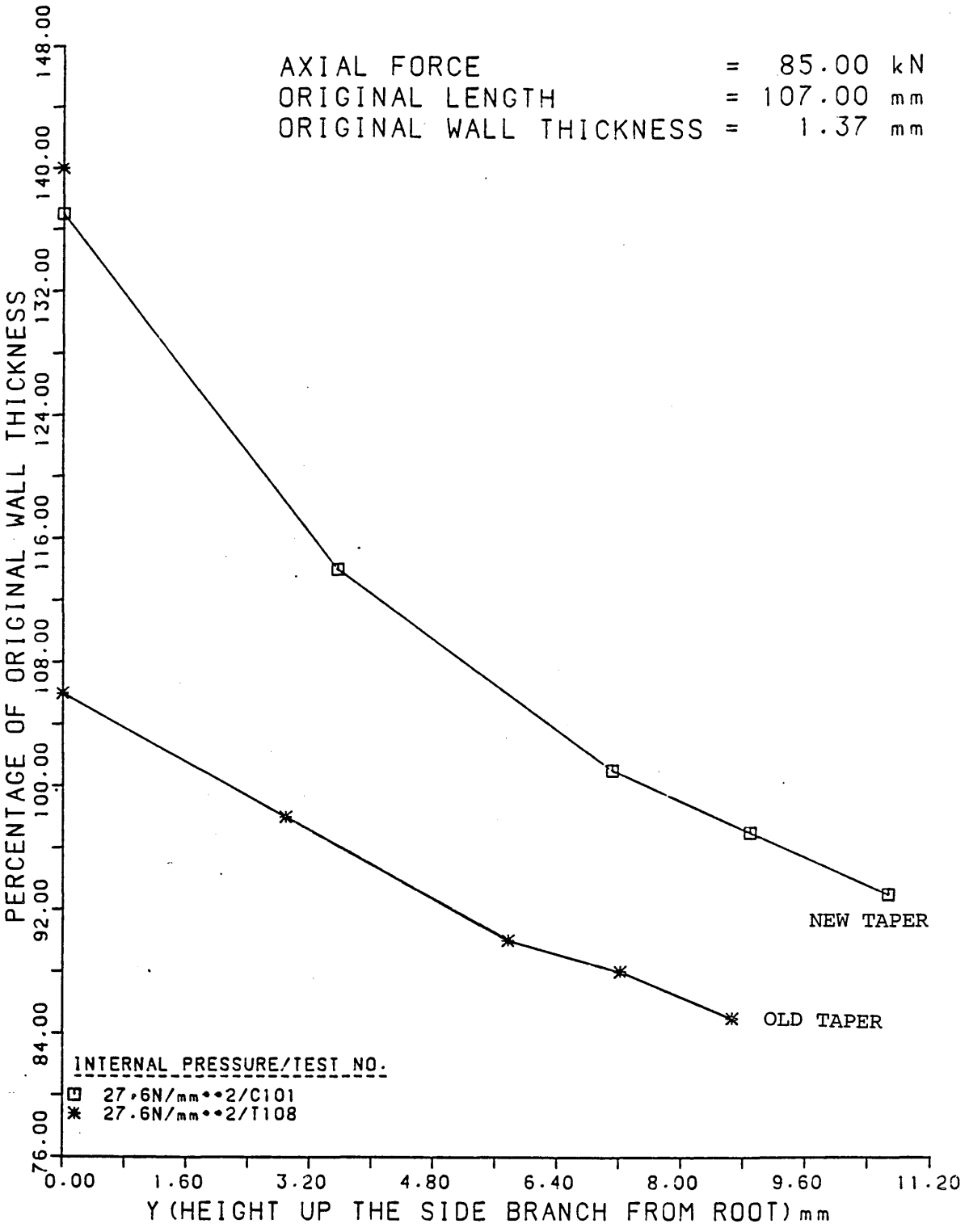

FIGURE 61

.The Wall Thickness Distributions Along The Side Branches And Domes Of Tee Pieces Formed With Plungers With Different End Tapers.

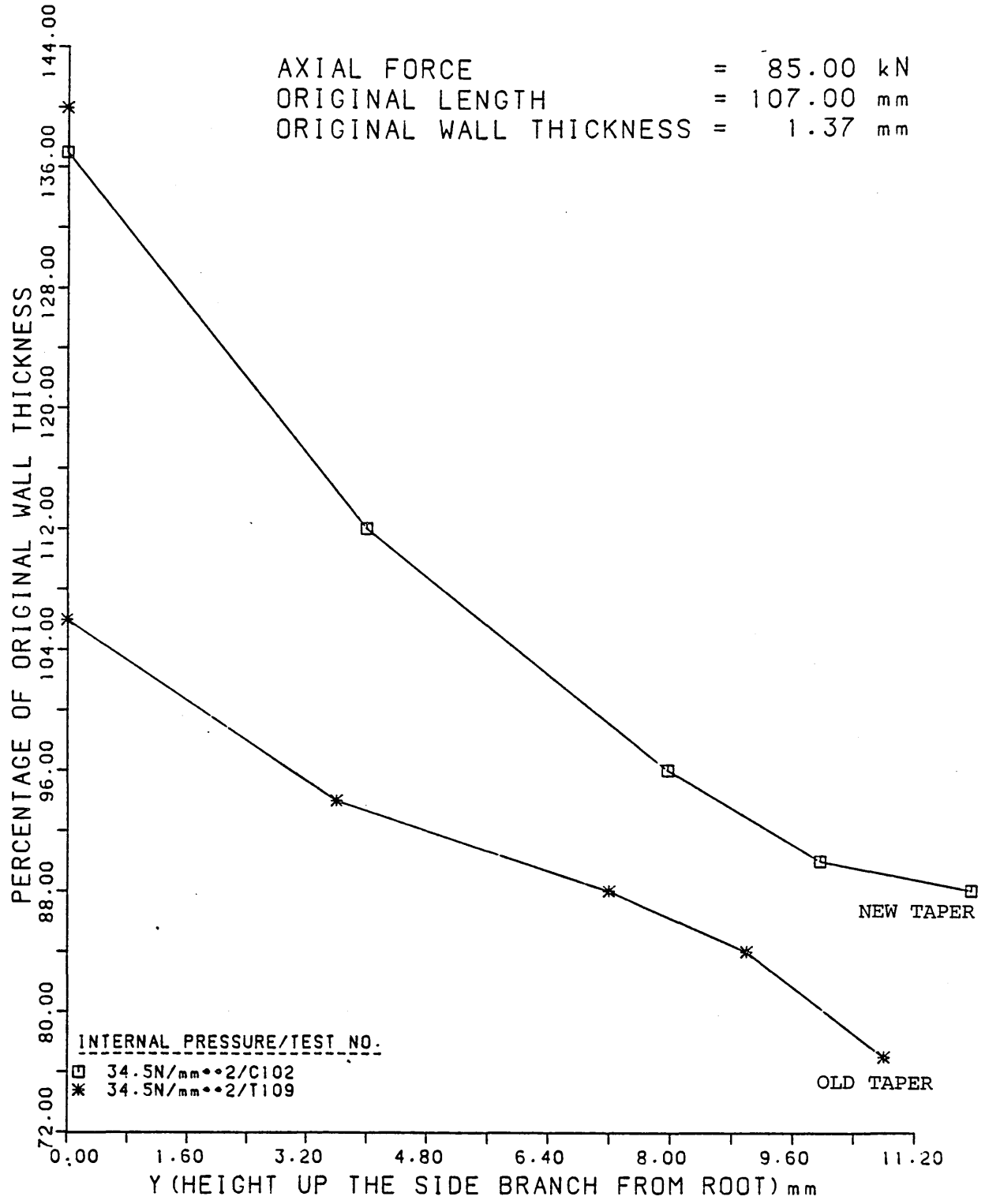

FIGURE 62

The Wall Thickness Distributions Along The Side Branches And Domes Of Tee Pieces Formed With Plungers With Different End Tapers.

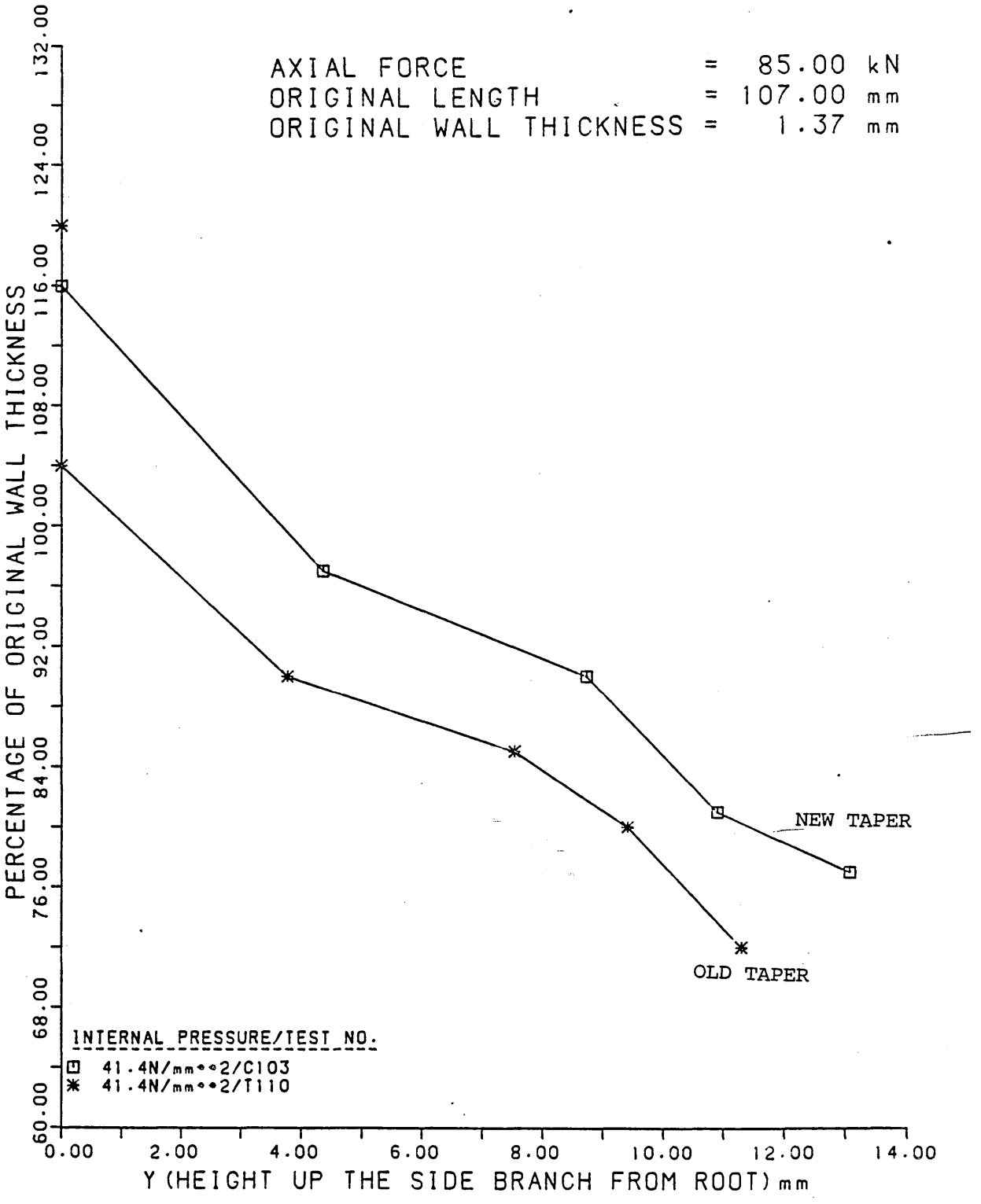

FIGURE 63

The Wall Thickness Distributions Along The Side Branches And Domes Of Tee Pieces Formed With Plungers With Different End Tapers.

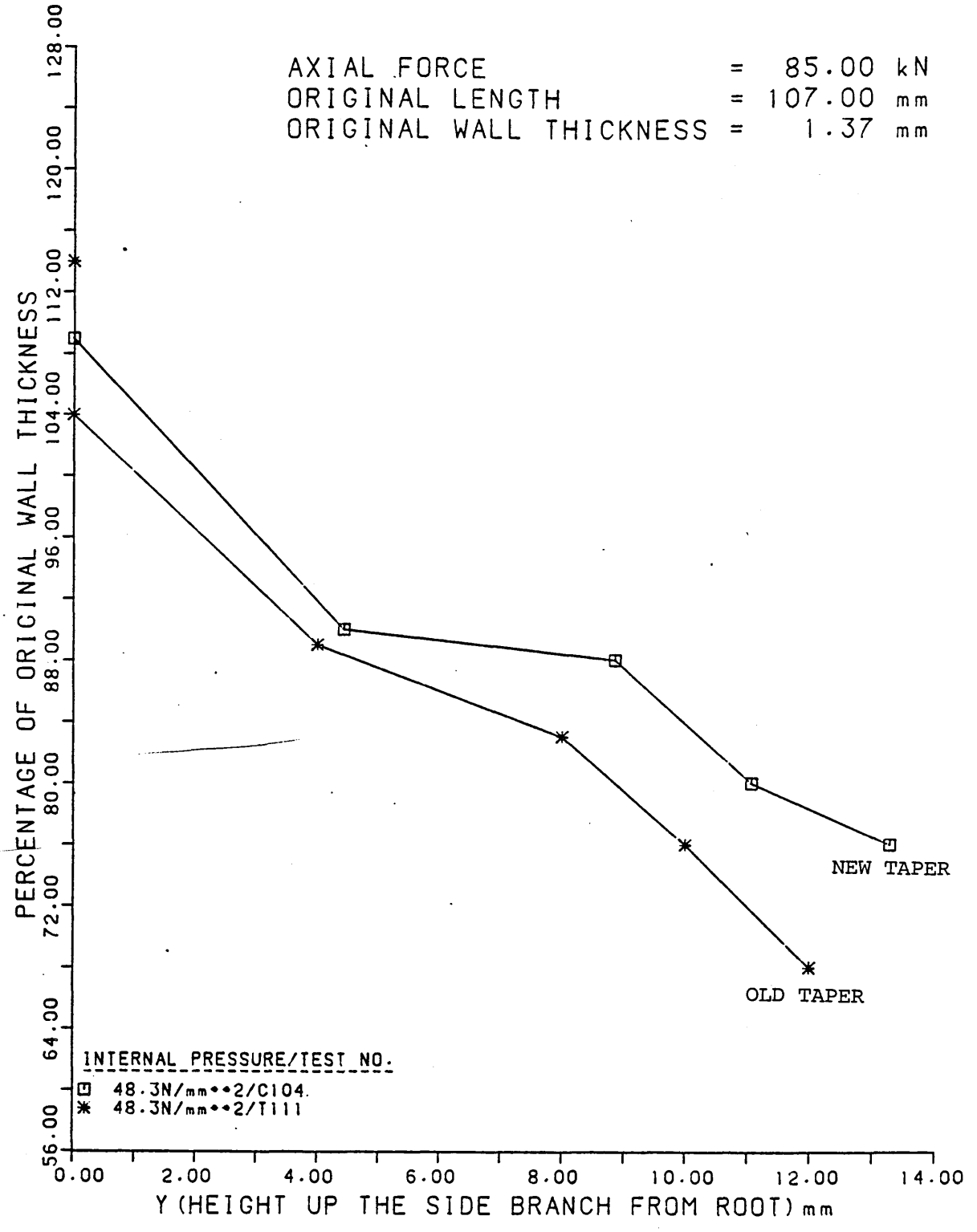

FIGURE 64

The Wall Thickness Distributions Along The Side Branches And Domes Of Tee Pieces Formed With Plungers With Different End Tapers.

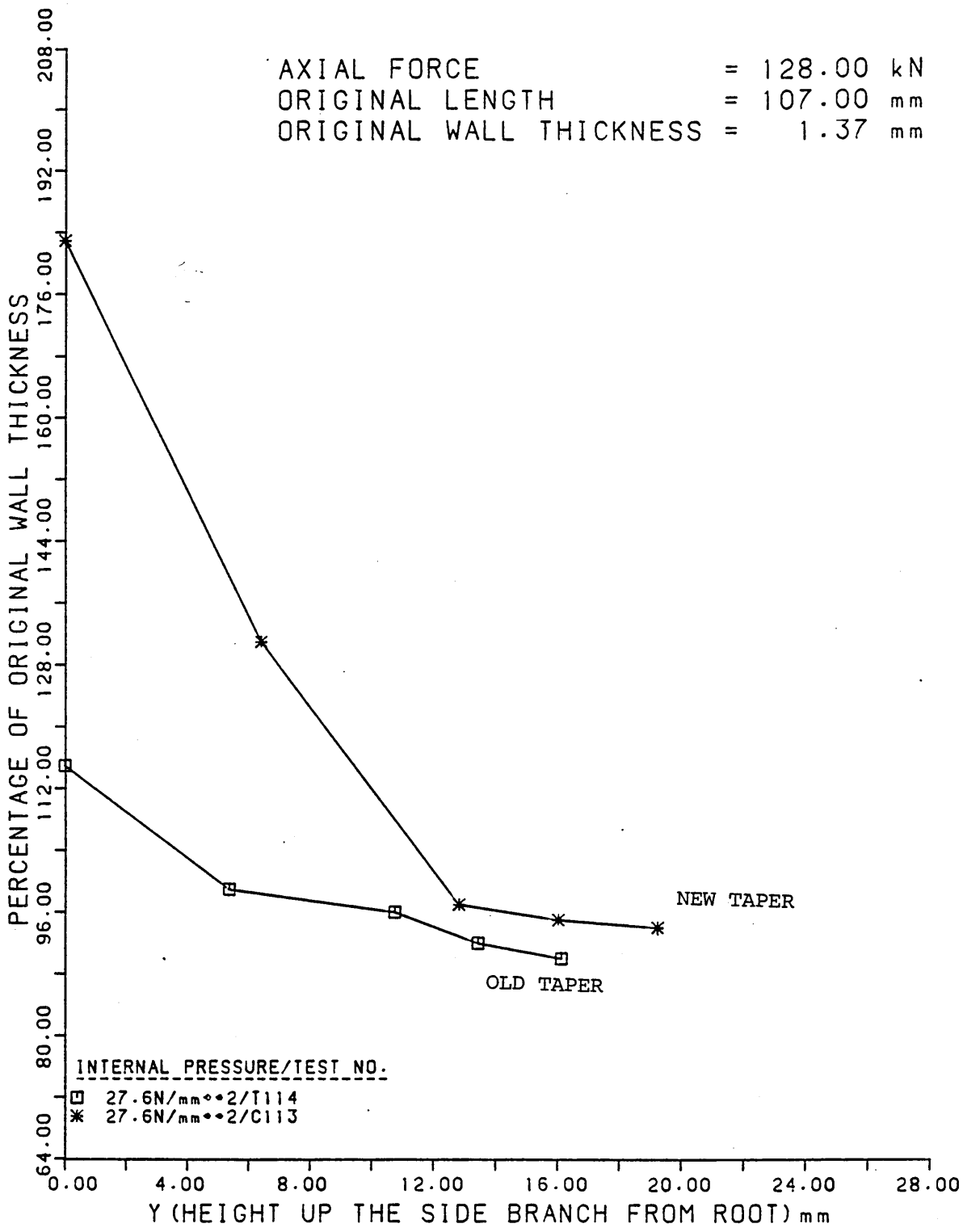

FIGURE 65

The Wall Thickness Distributions Along The Side Branches And Domes Of Tee Pieces Formed With Plungers With Different End Tapers.

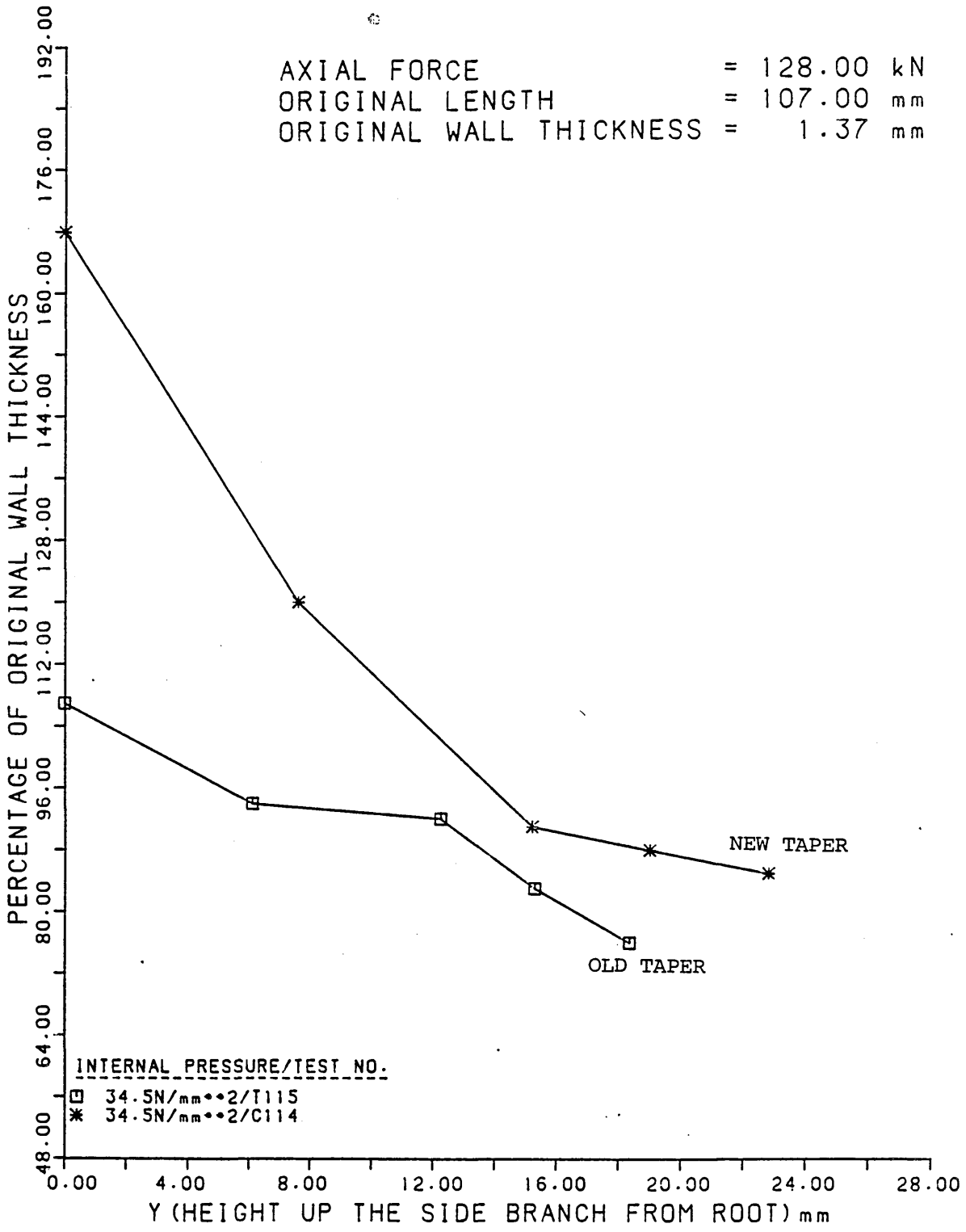

FIGURE 66

The Wall Thickness Distributions Along The Side Branches And Domes Of Tee Pieces Formed With Plungers With Different End Tapers.

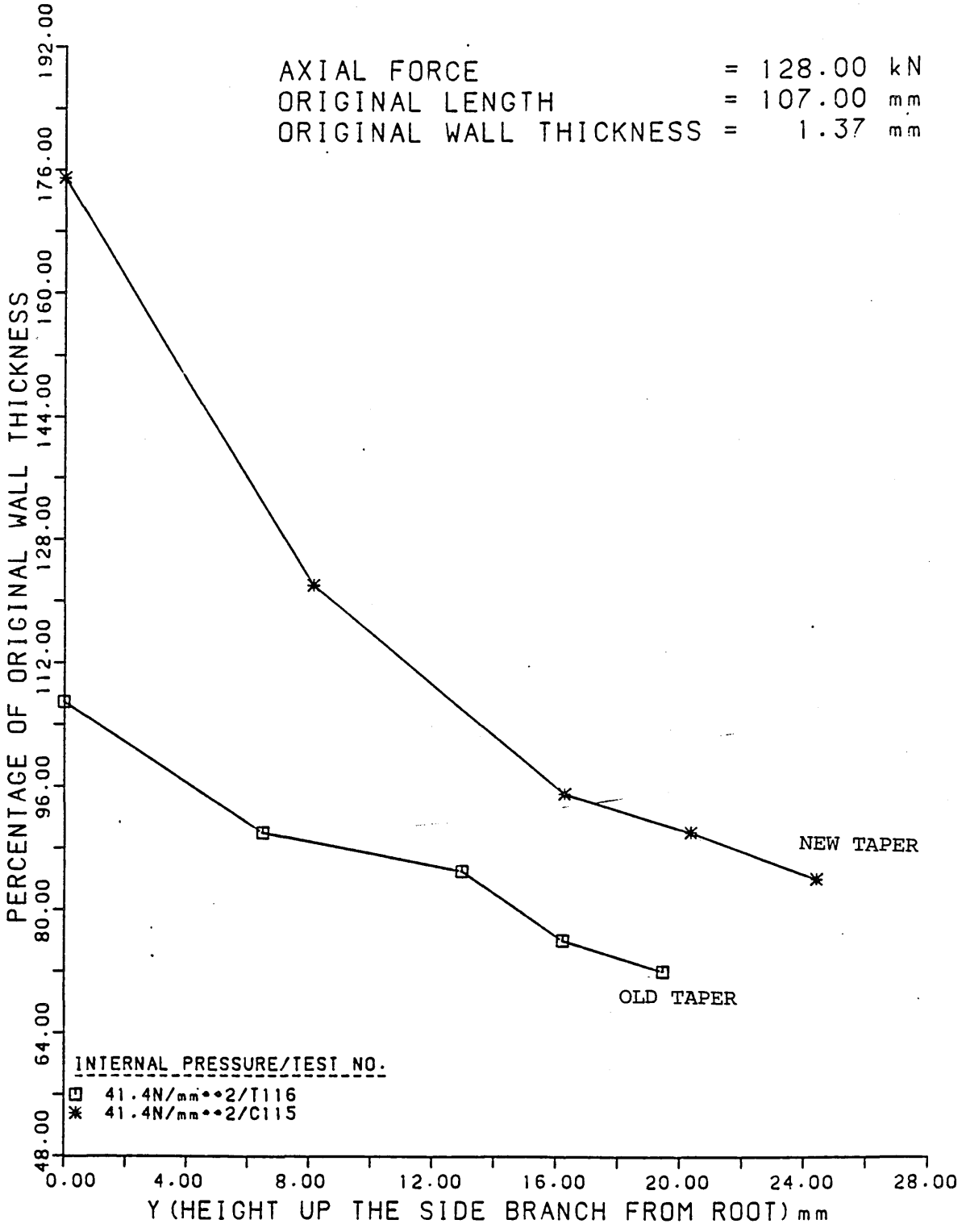

FIGURE 67

The Wall Thickness Distributions Along The Side Branches And Domes Of Tee Pieces Formed With Plungers With Different End Tapers.

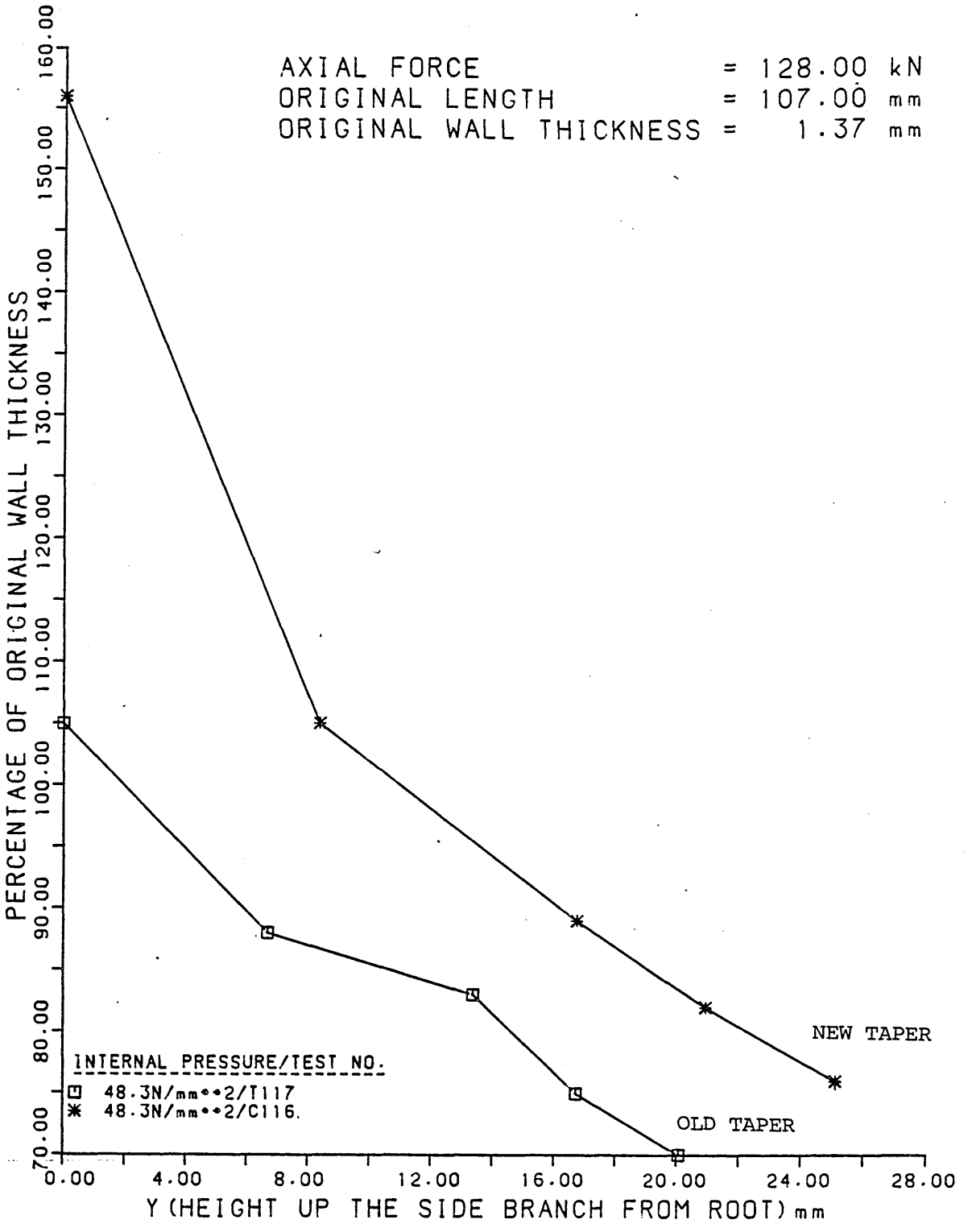

FIGURE 68

The Wall Thickness Distributions Along The Side Branches And Domes Of Tee Pieces Formed With Plungers With Different End Tapers.

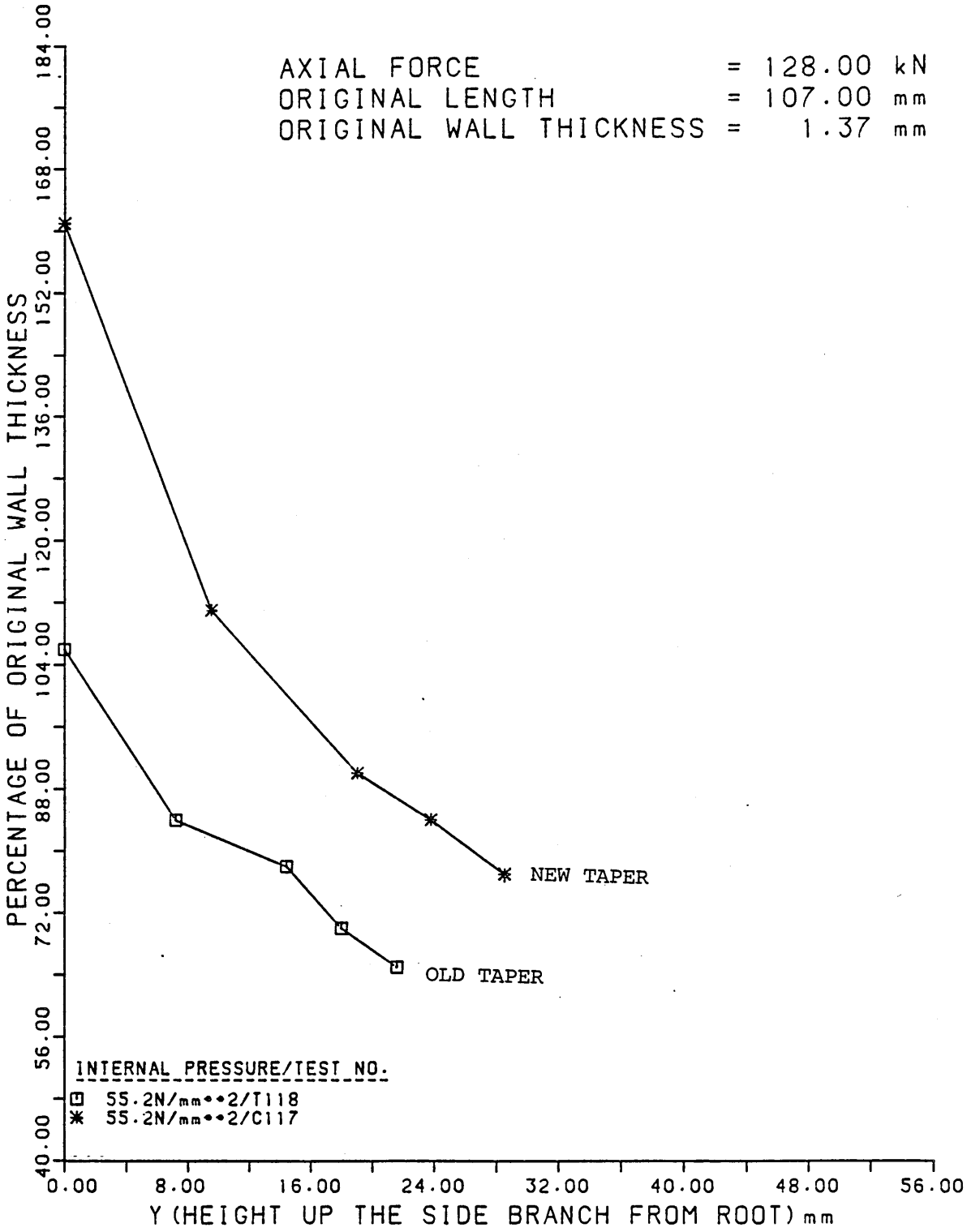

FIGURE 69

The Wall Thickness Distributions Along The Side Branches And Domes Of Tee Pieces Formed With Plungers With Different End Tapers.

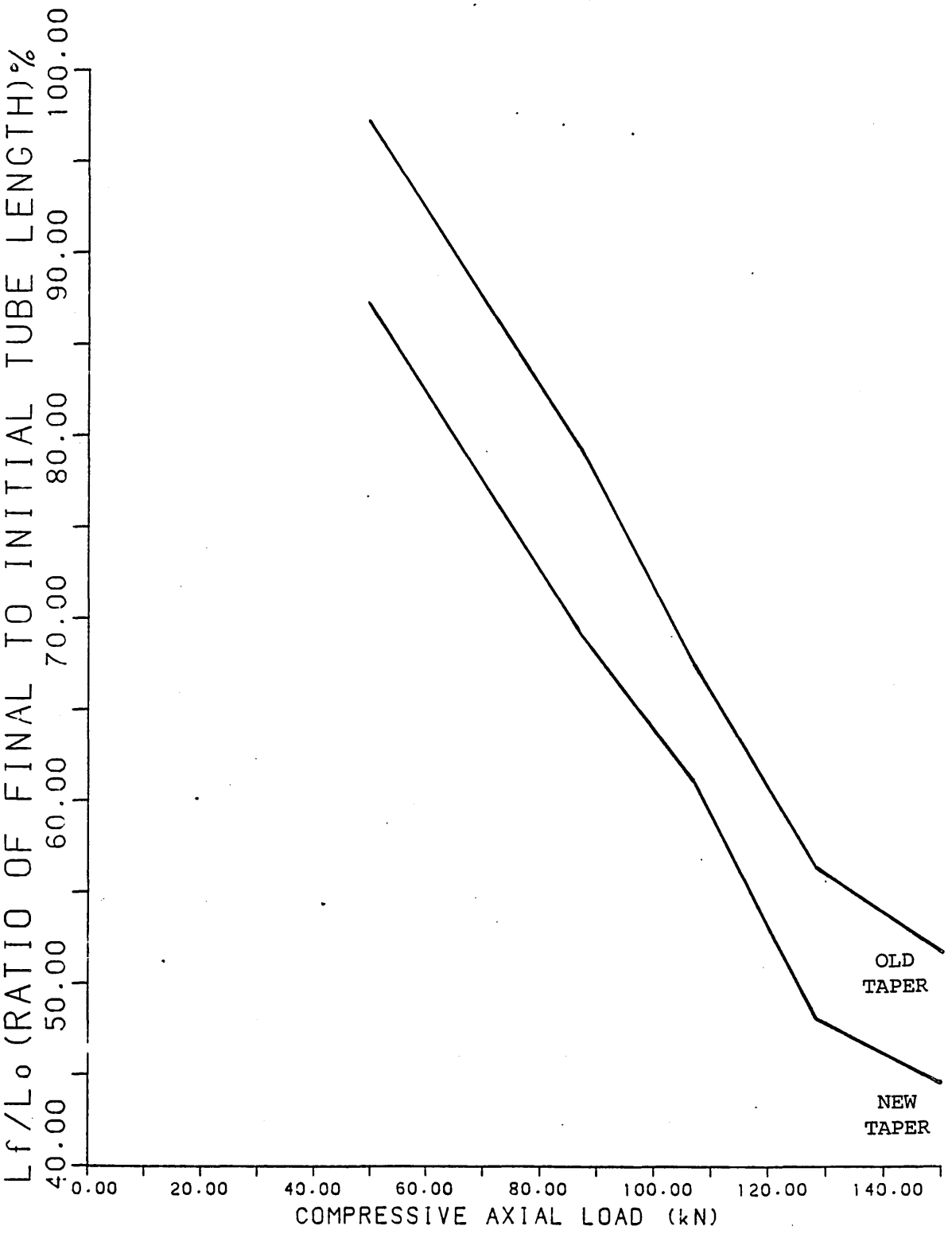

FIGURE 70

The Final To Original Tube Length Variation Against Compressive Axial Load For Tee Pieces Formed With Plungers With Different End Tapers.

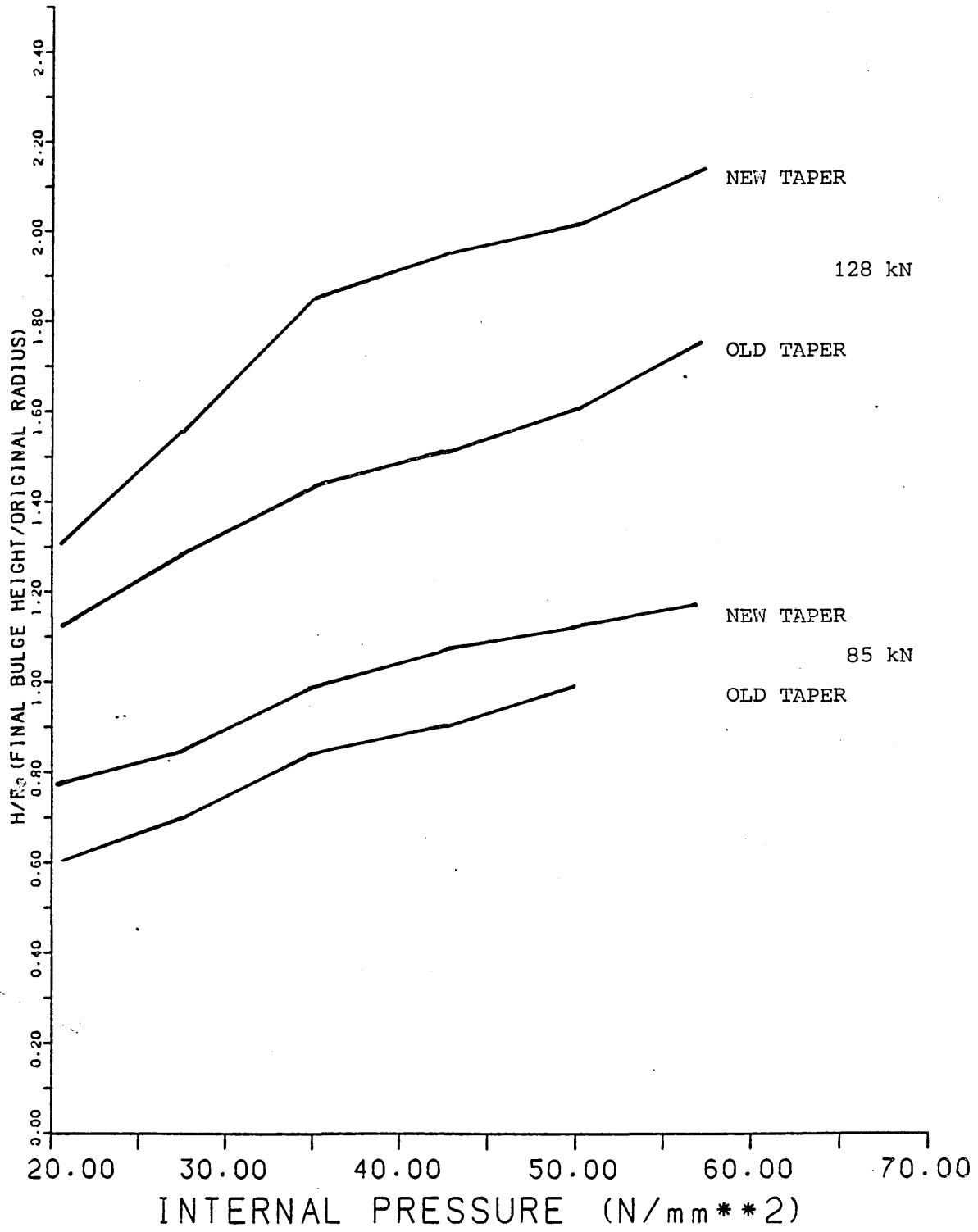

FIGURE 71

The Bulge Height To Original Tube Radius Variation Against Internal Pressure For Tee Pieces Formed With Plungers With Different End Tapers.

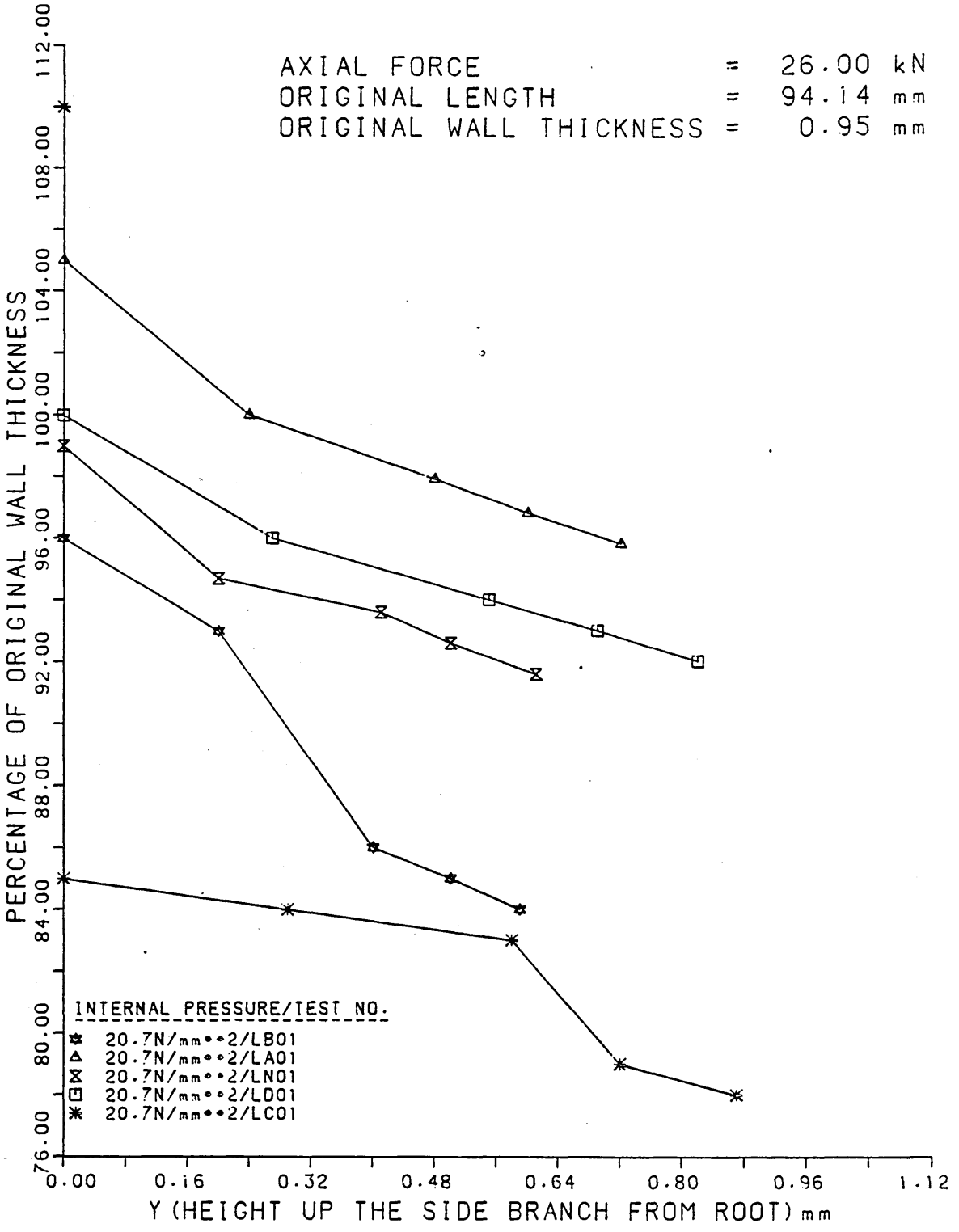

FIGURE 72

The Wall Thickness Distributions Along The Side Branches And Domes Of Tee Pieces Formed Using Various Lubricants.

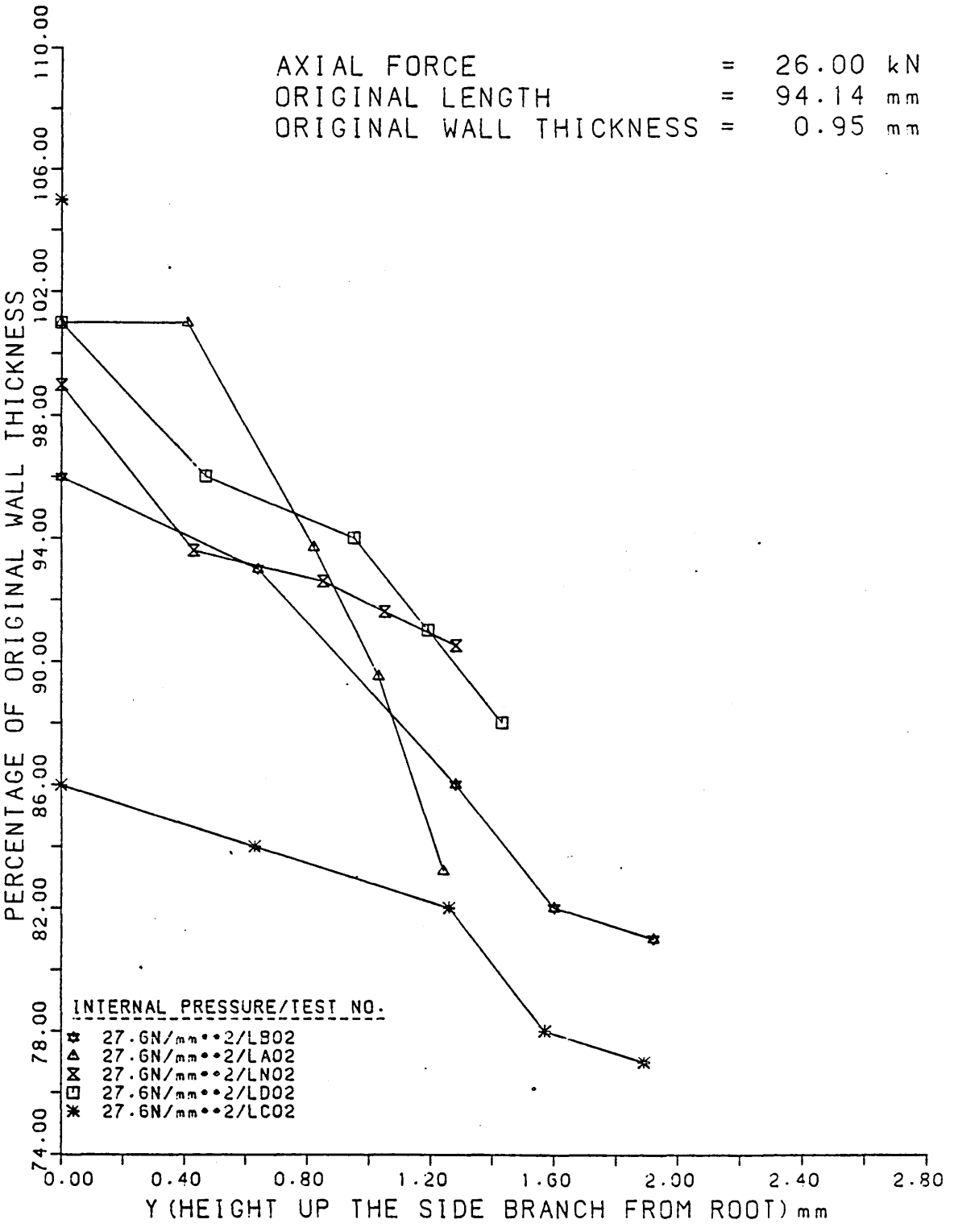

FIGURE 73

The Wall Thickness Distributions Along The Side Branches And Domes Of Tee Pieces Formed Using Various Lubricants.

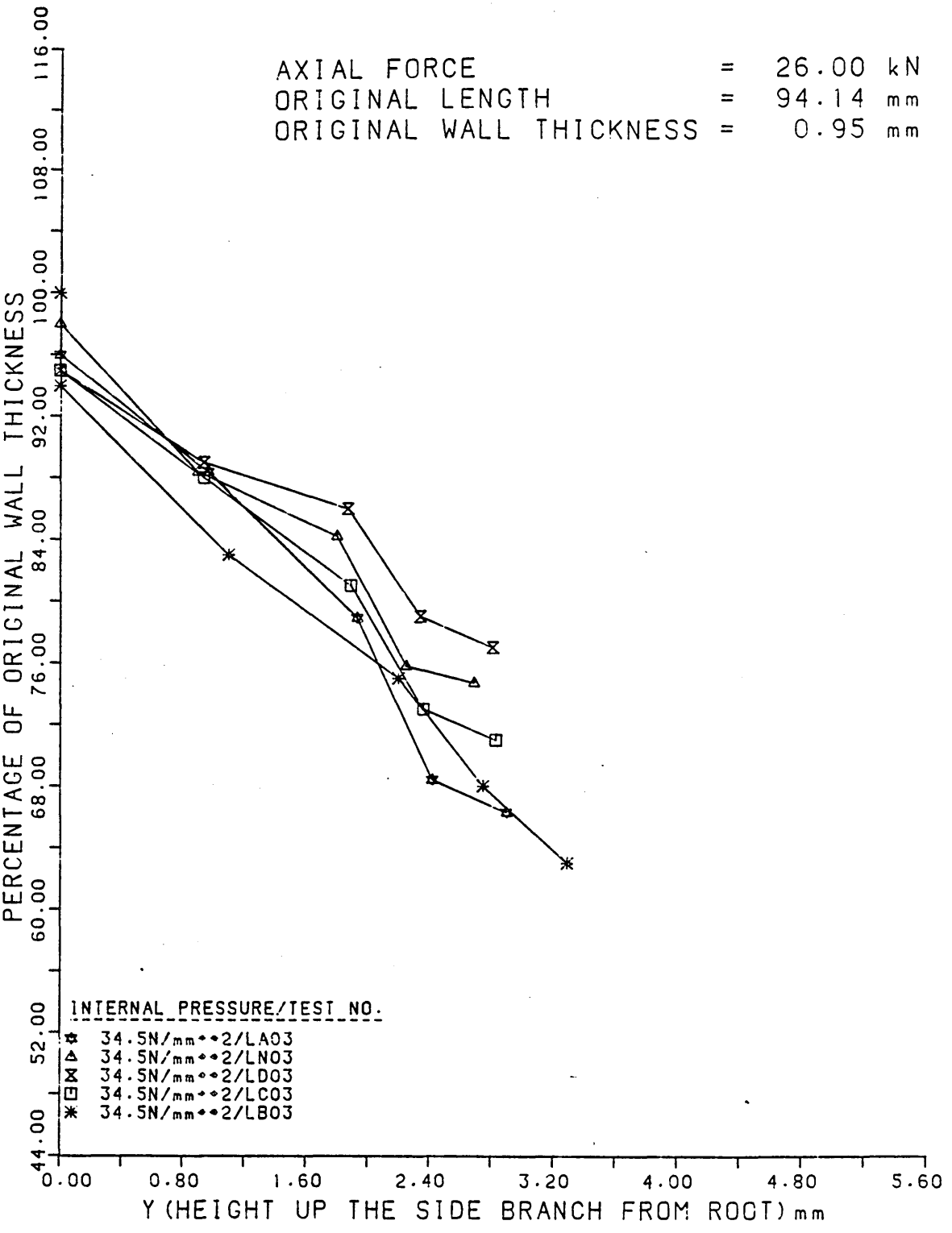

FIGURE 74

The Wall Thickness Distributions Along The Side Branches And Domes Of Tee Pieces Formed Using Various Lubricants.

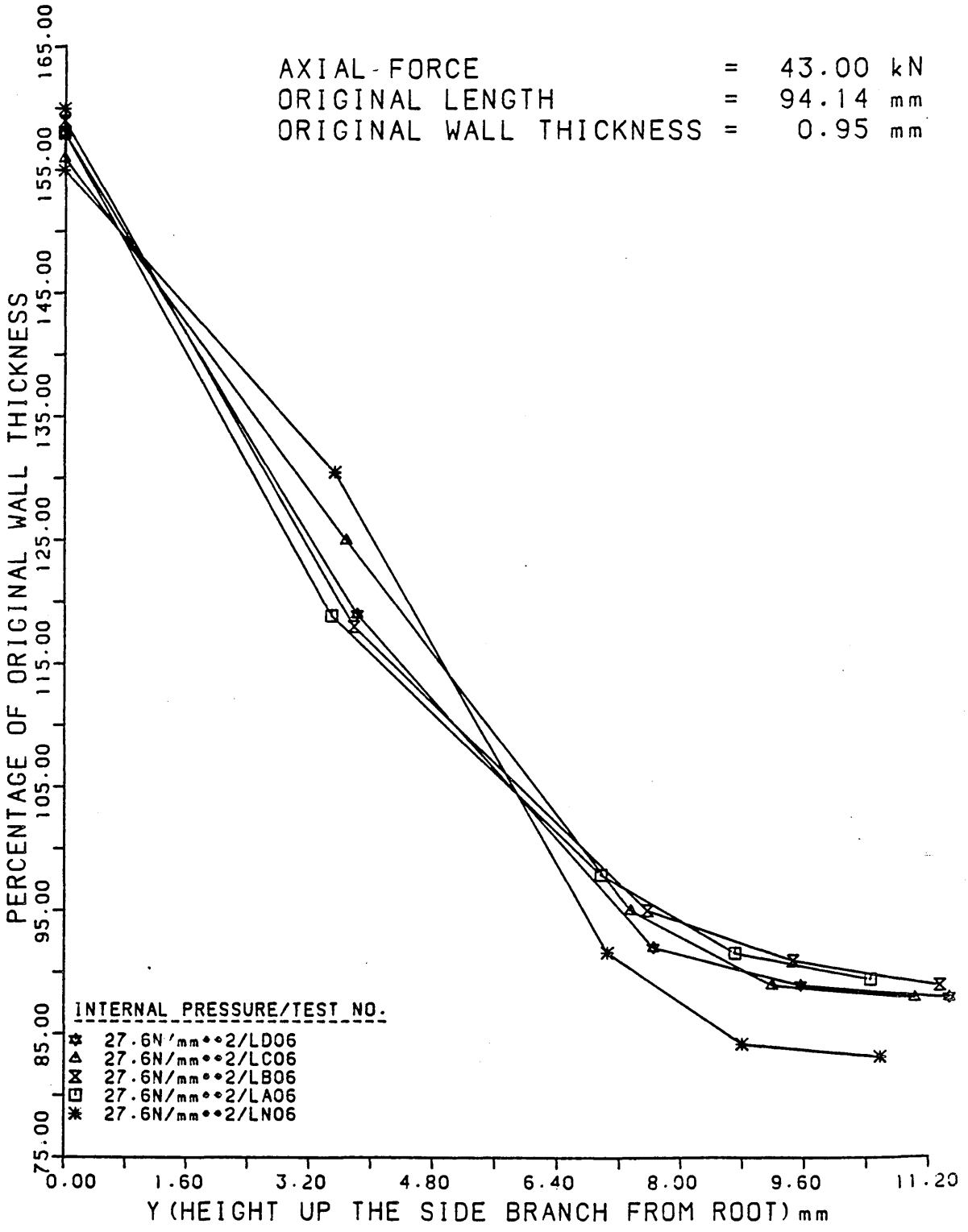

FIGURE 75

The Wall Thickness Distributions Along The Side Branches And Domes Of Tee Pieces Formed Using Various Lubricants.

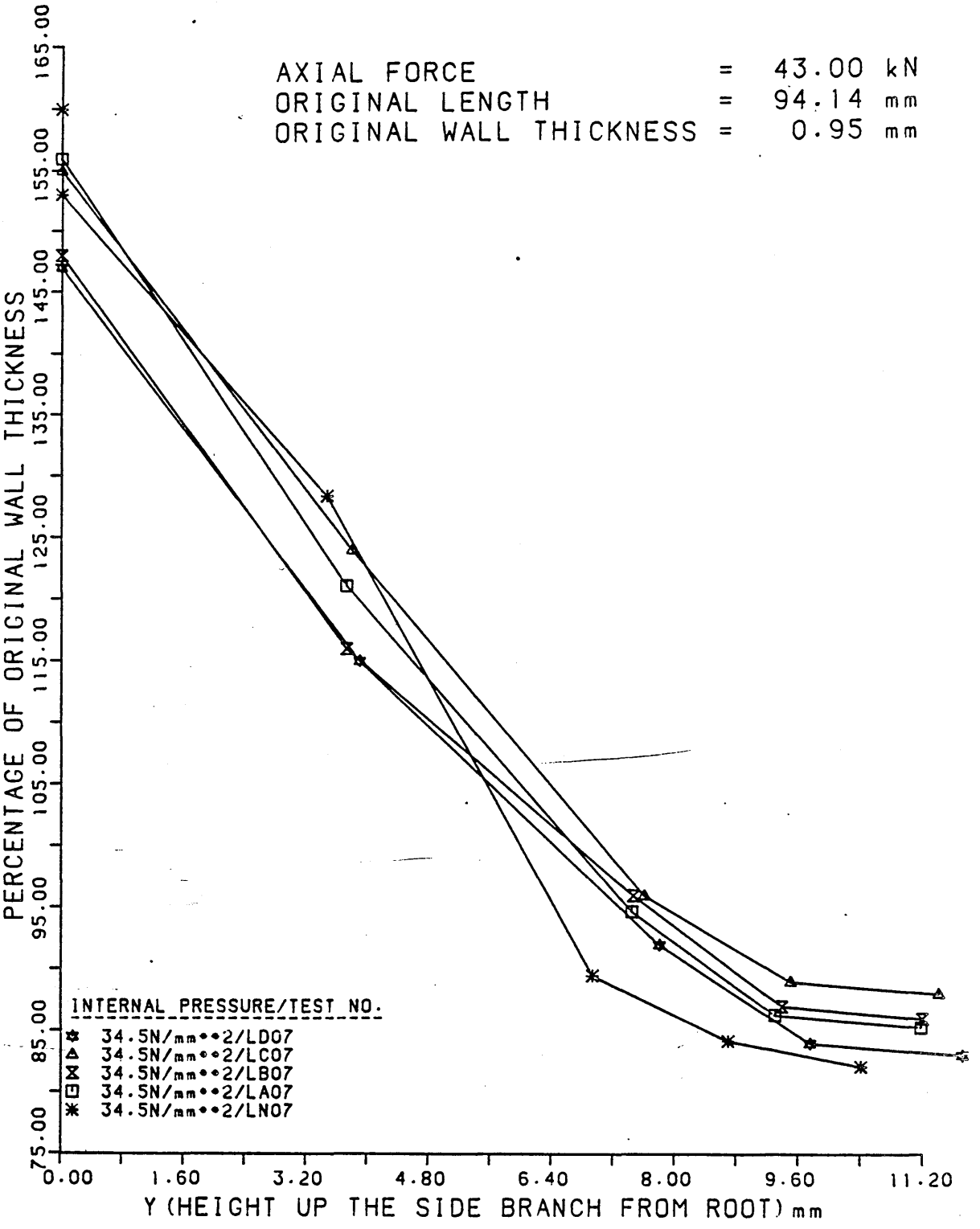

FIGURE 76

The Wall Thickness Distributions Along The Side Branches And Domes Of Tee Pieces Formed Using Various Lubricants.

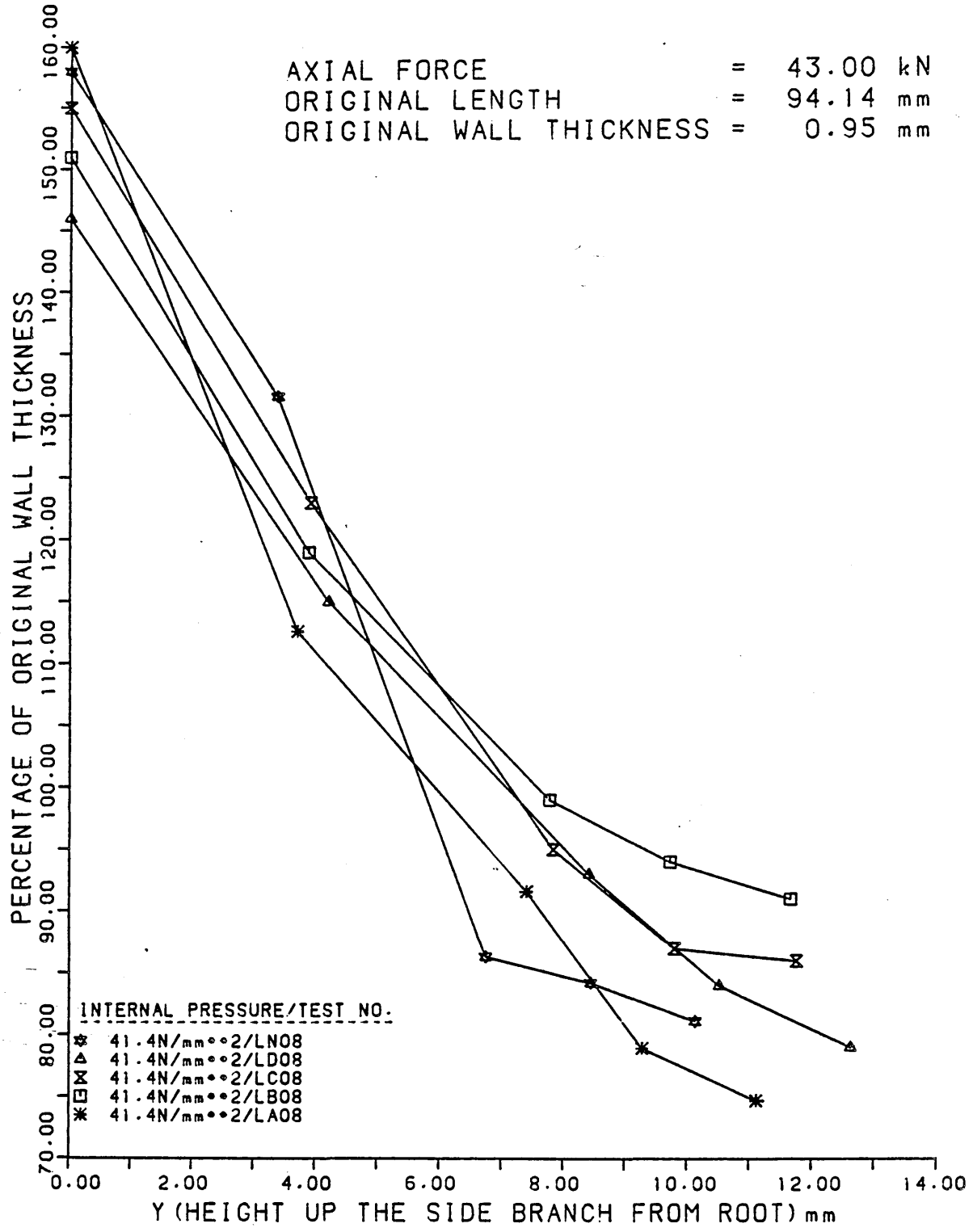

FIGURE 77

The Wall Thickness Distributions Along The Side Branches And Domes Of Tee Pieces Formed Using Various Lubricants.

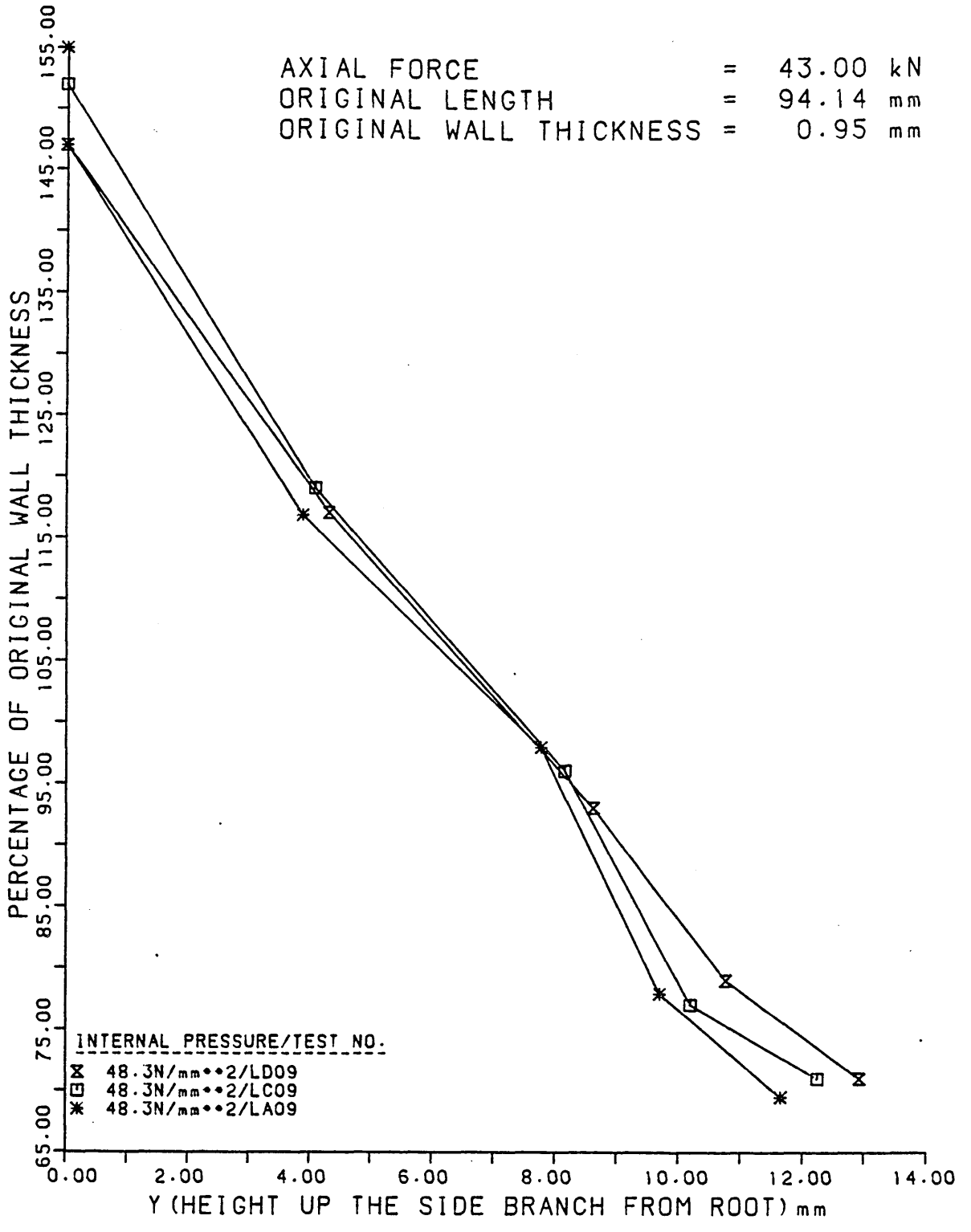

FIGURE 78

The Wall Thickness Distributions Along The Side Branches And Domes Of Tee Pieces Formed Using Various Lubricants.

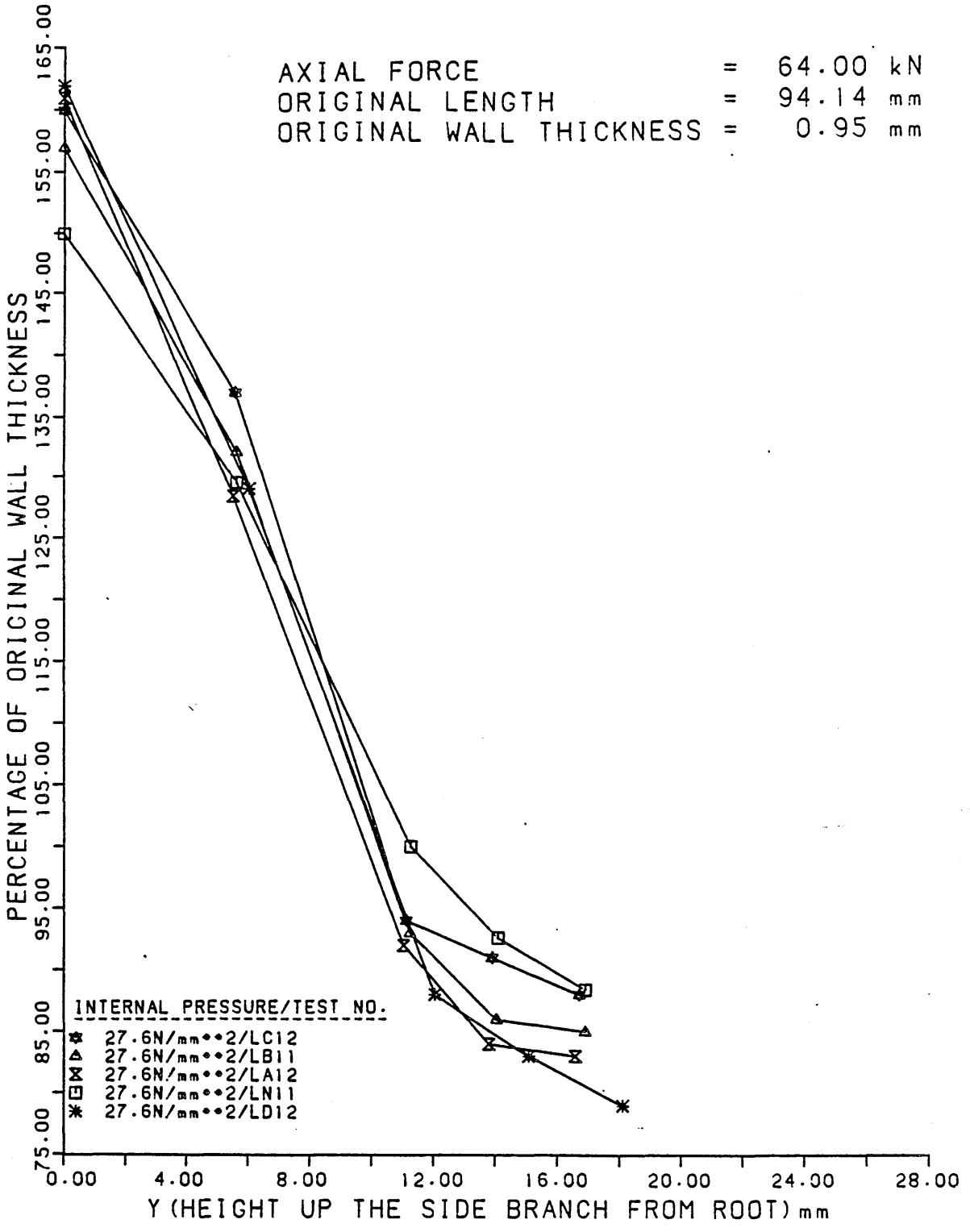

FIGURE 79

The Wall Thickness Distributions Along The Side Branches And Domes Of Tee Pieces Formed Using Various Lubricants.

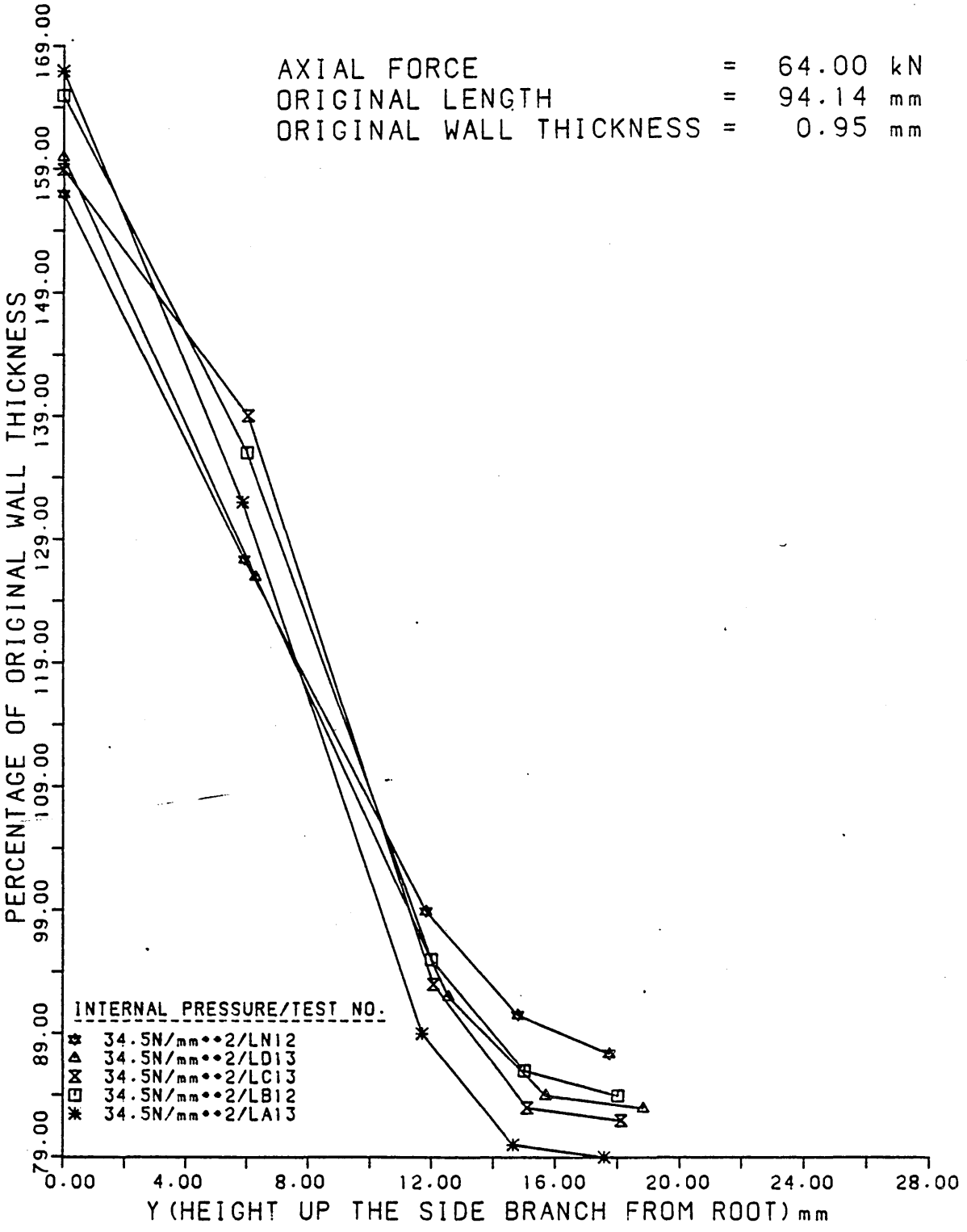

FIGURE 80

The Wall Thickness Distributions Along The Side Branches And Domes Of Tee Pieces Formed Using Various Lubricants.

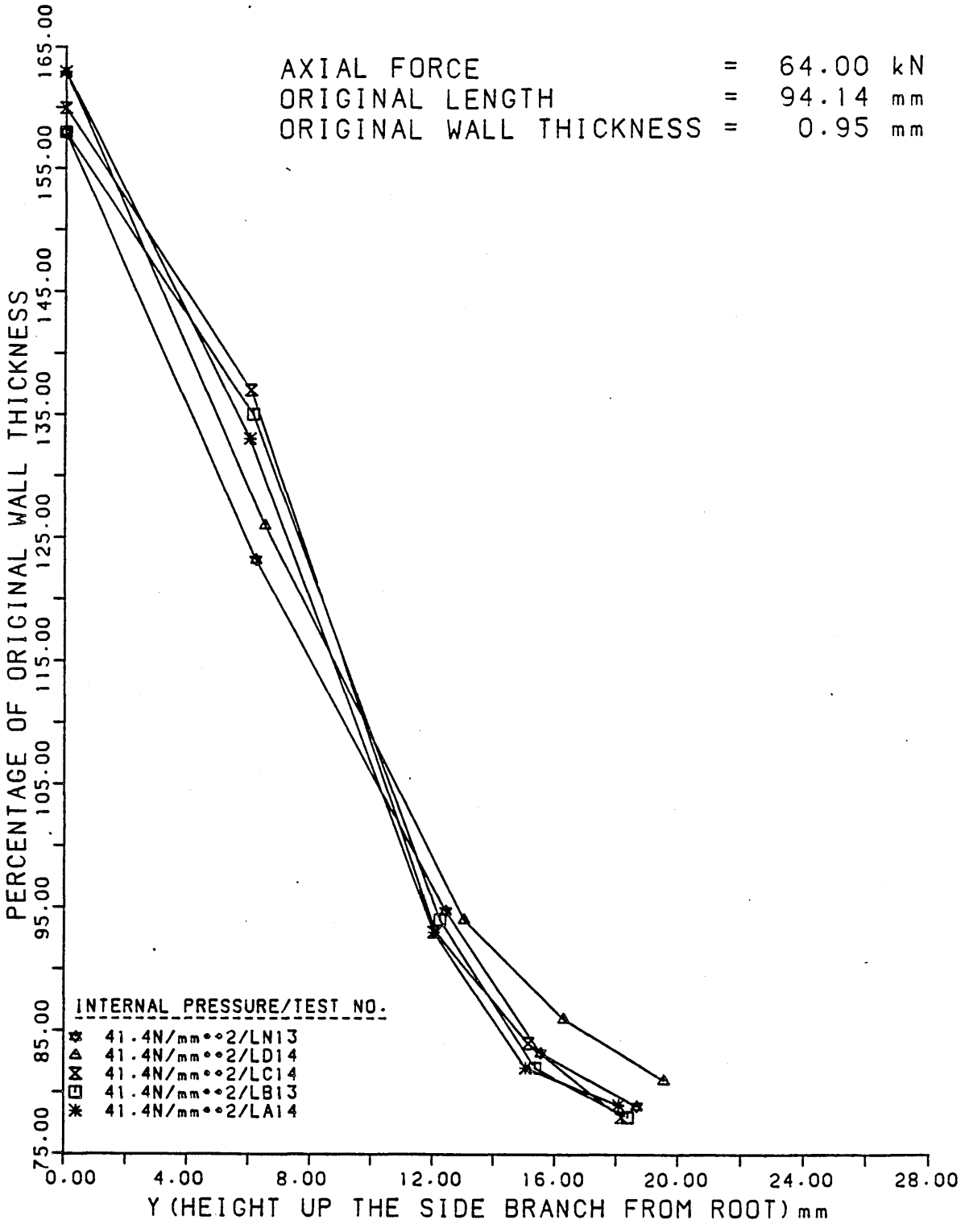

FIGURE 81

The Wall Thickness Distributions Along The Side Branches And Domes Of Tee Pieces Formed Using Various Lubricants.

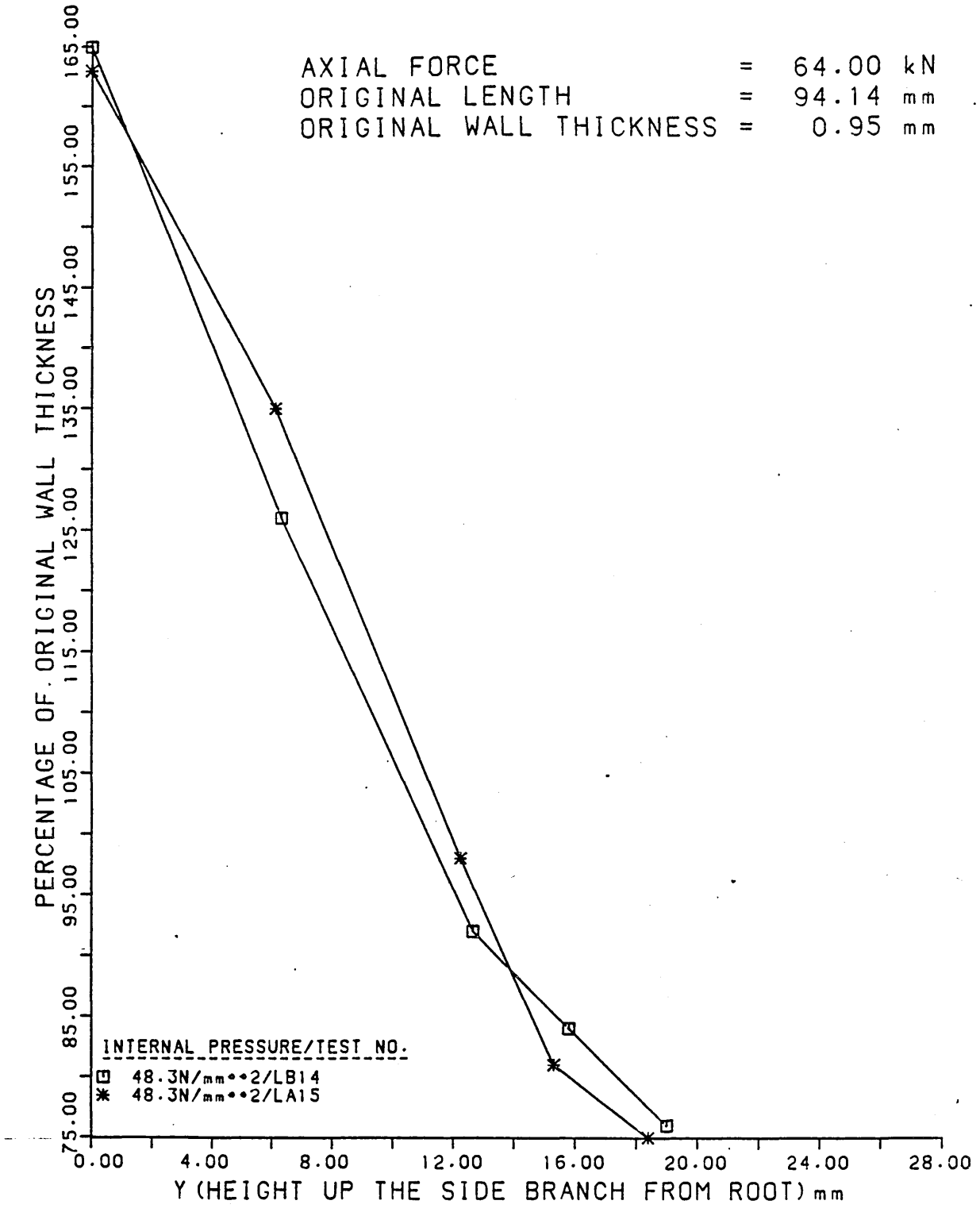

FIGURE 82

The Wall Thickness Distributions Along The Side Branches And Domes Of Tee Pieces Formed Using Various Lubricants.

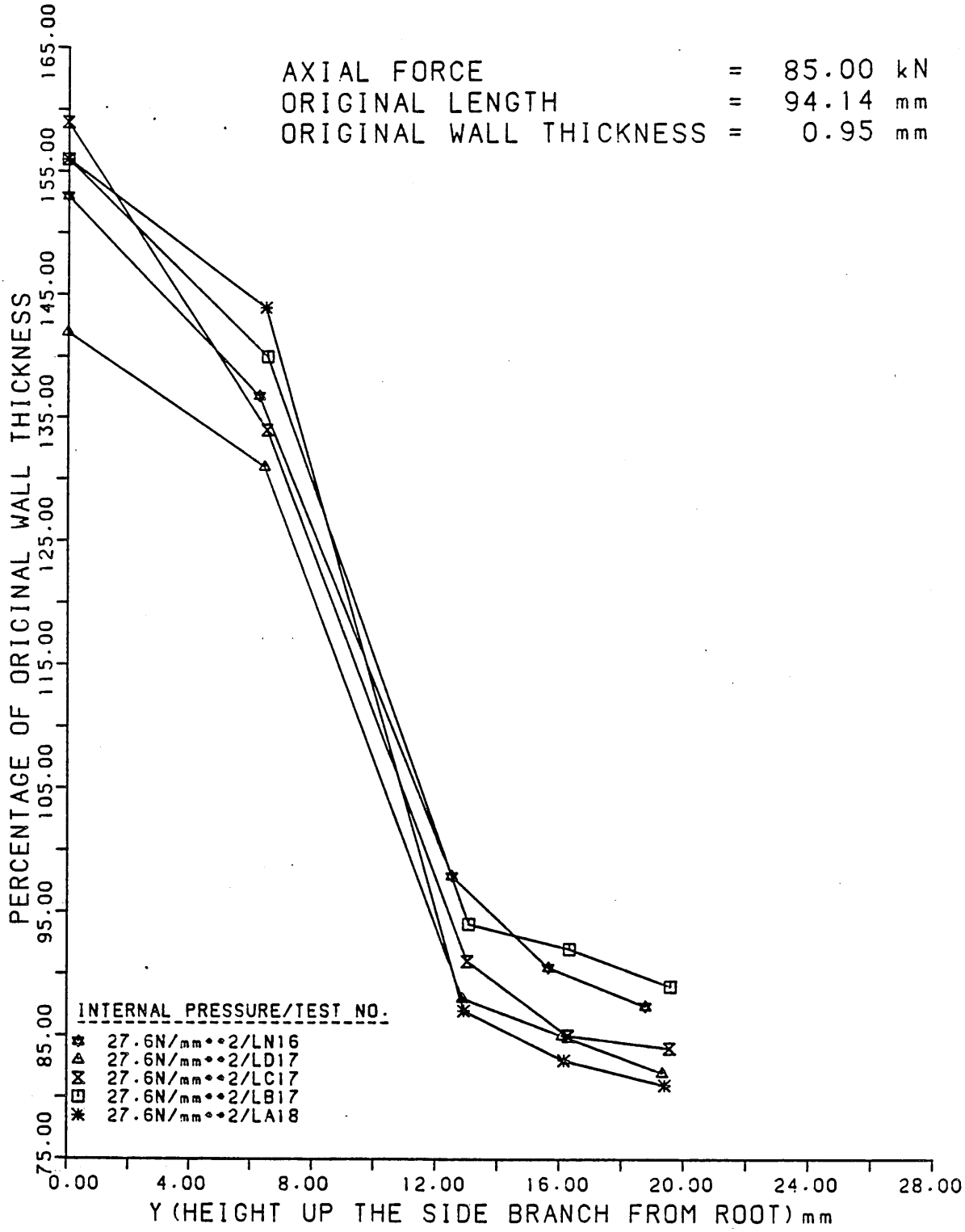

FIGURE 83

The Wall Thickness Distributions Along The Side Branches And Domes Of Tee Pieces Formed Using Various Lubricants.

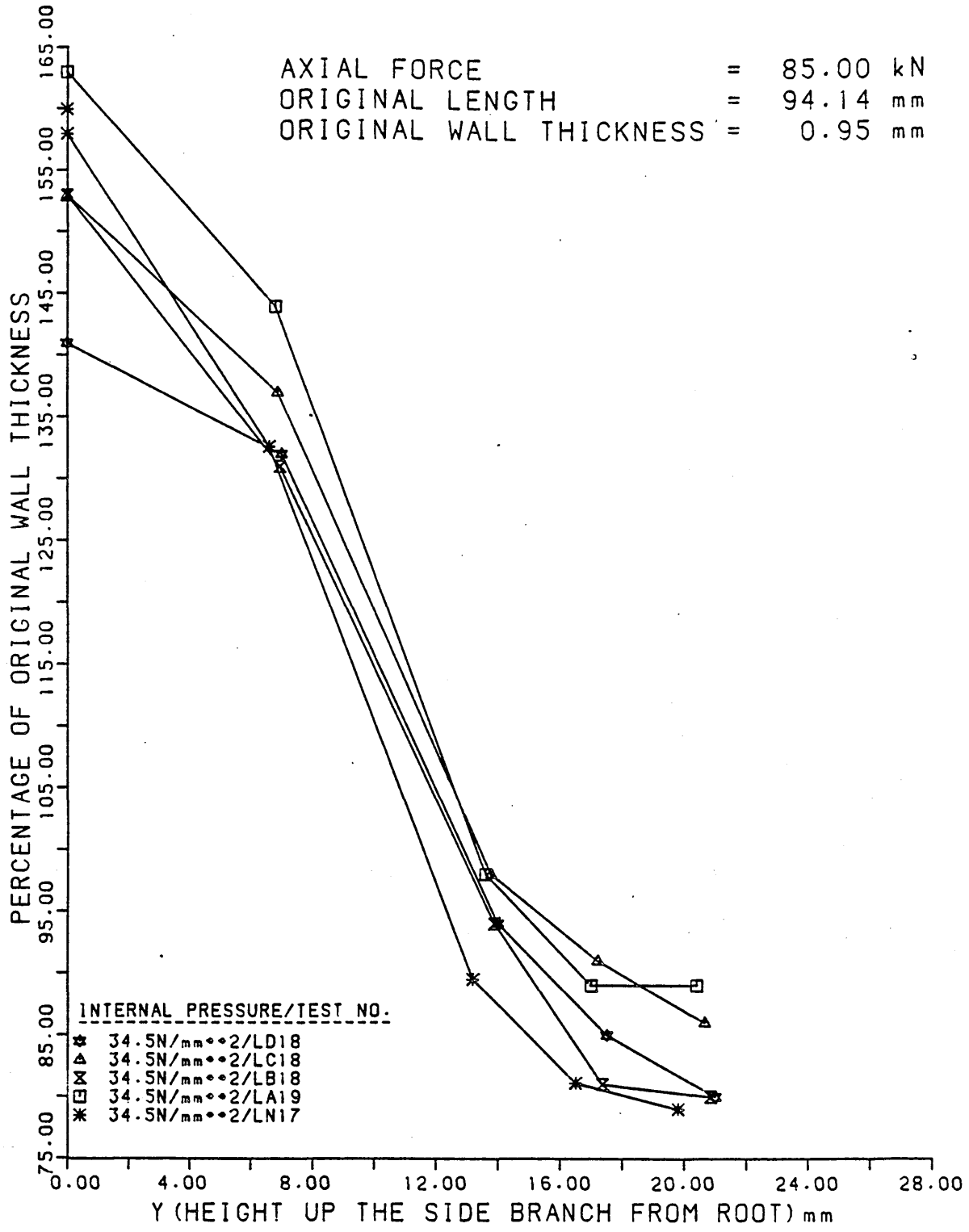

FIGURE 84

The Wall Thickness Distributions Along The Side Branches And Domes Of Tee Pieces Formed Using Various Lubricants.

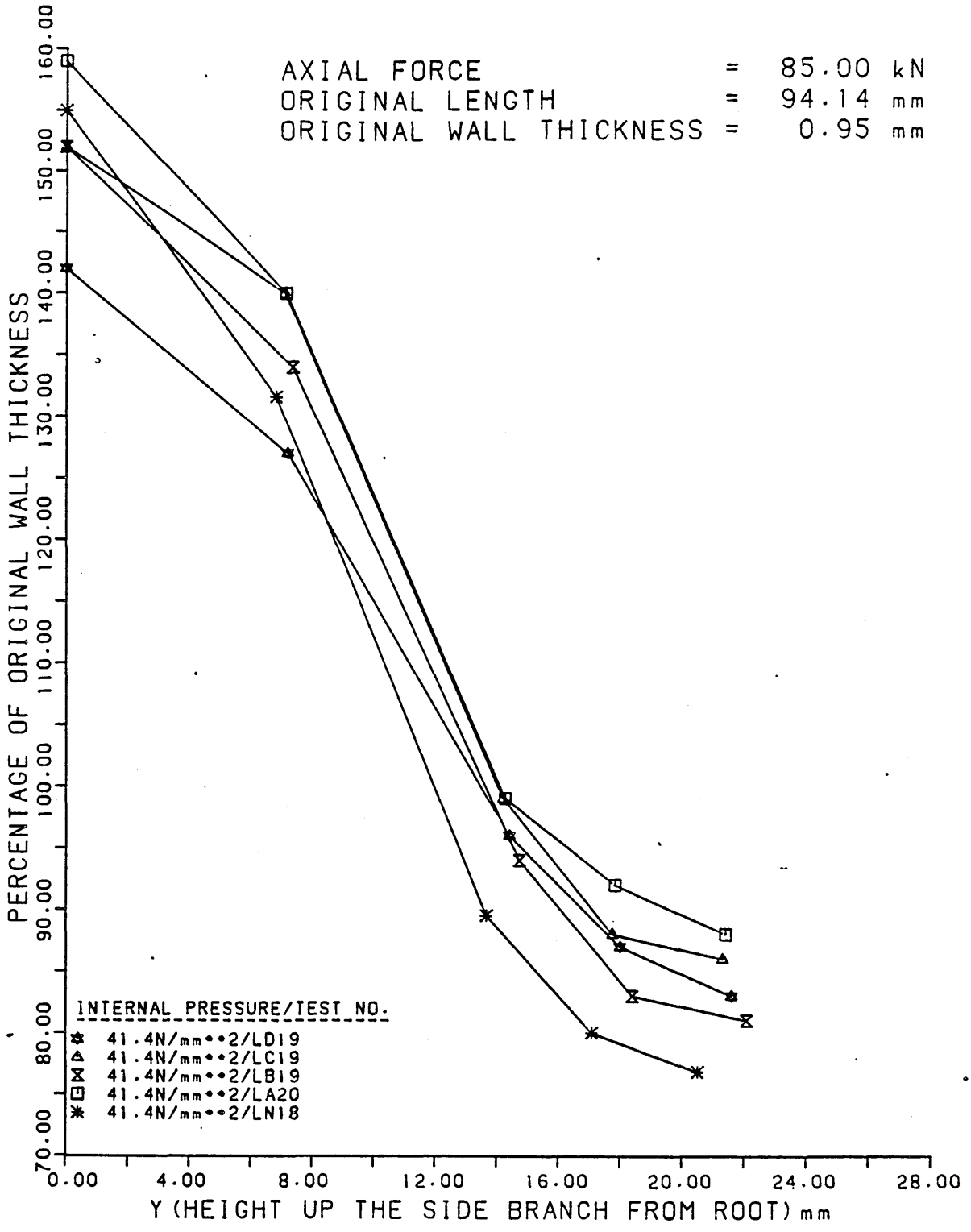

FIGURE 85

The Wall Thickness Distributions Along The Side Branches And Domes Of Tee Pieces Formed Using Various Lubricants.

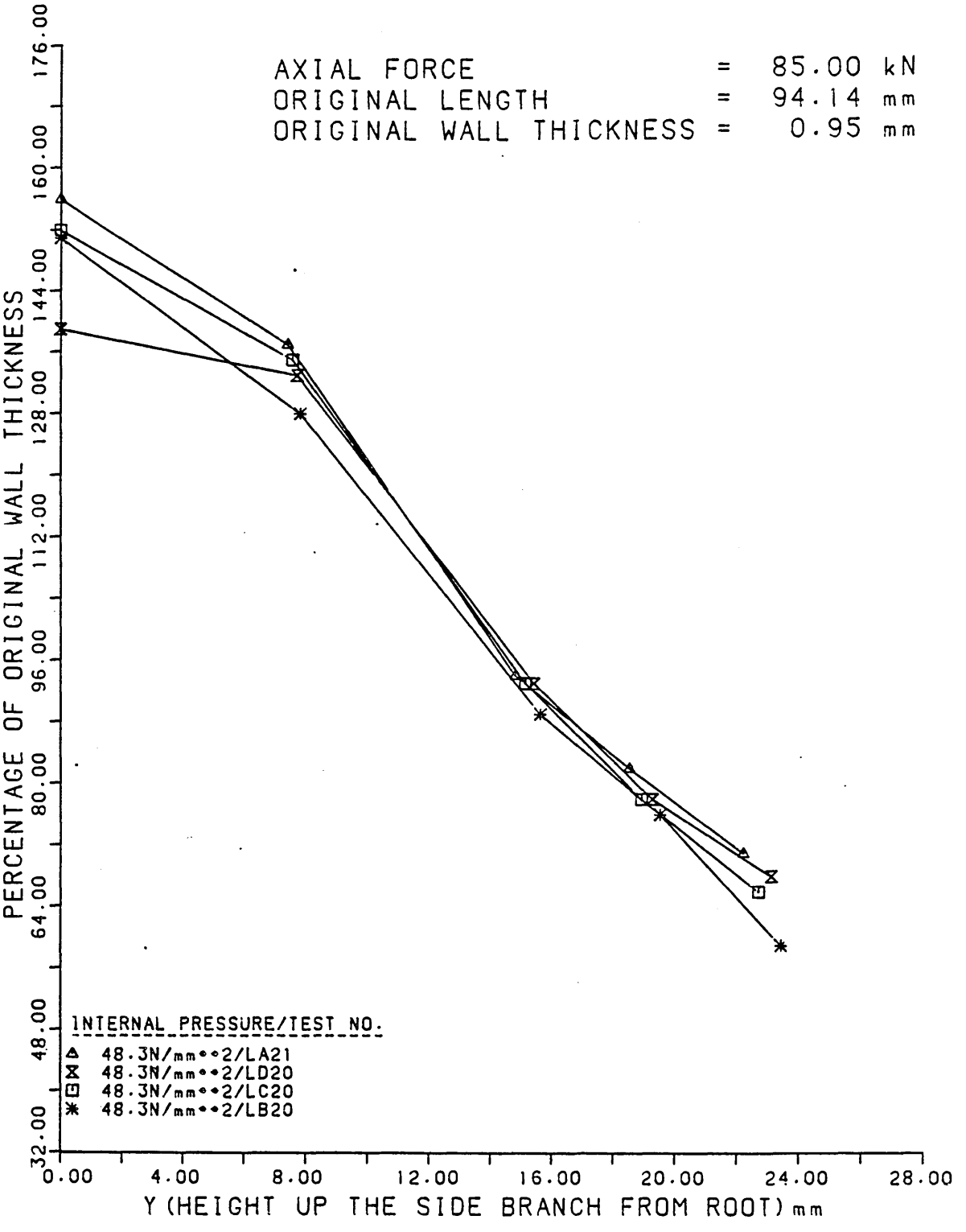

FIGURE 86

The Wall Thickness Distributions Along The Side Branches And Domes Of Tee Pieces Formed Using Various Lubricants.

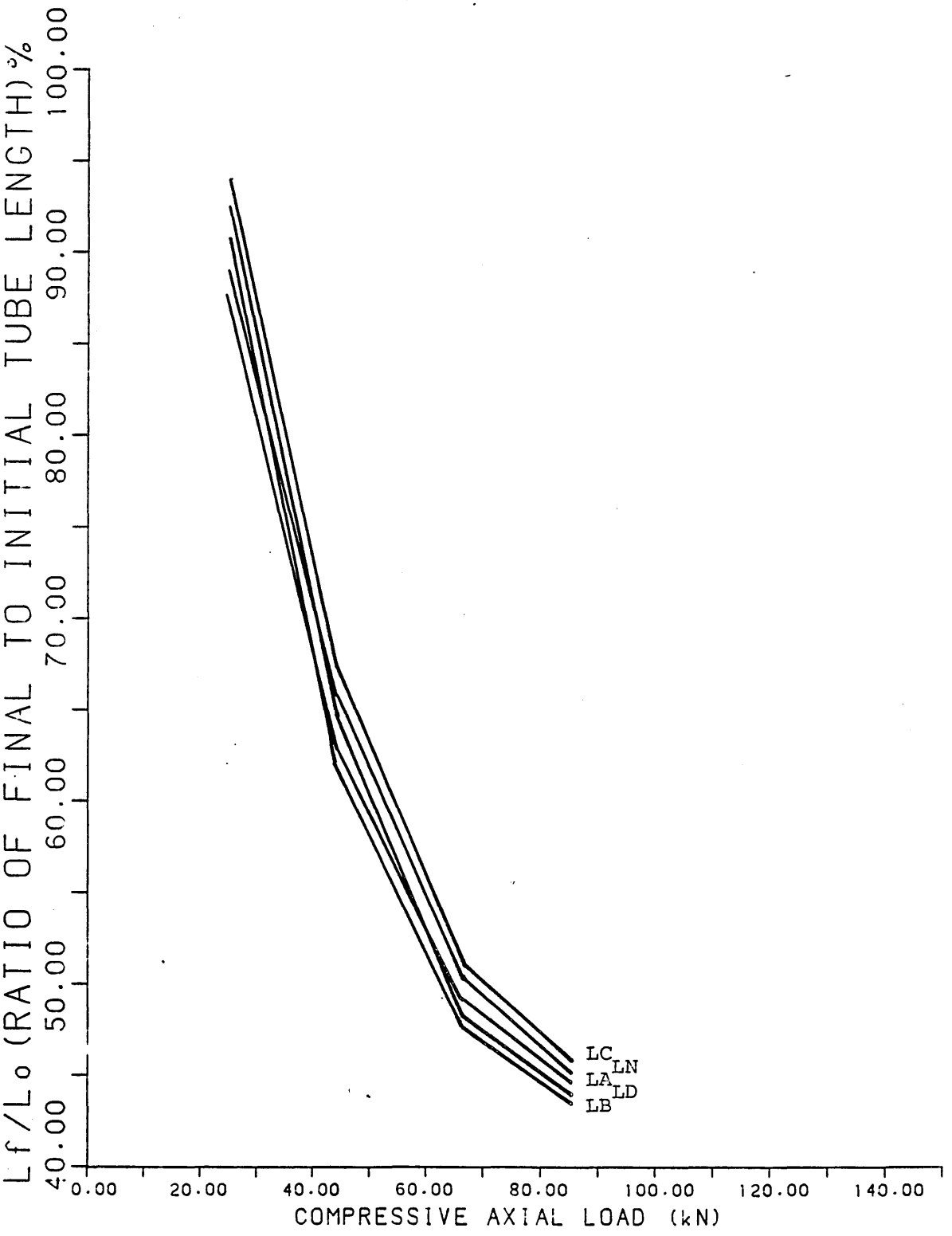

FIGURE 87

The Final To Original Tube Length Variation

Against Compressive Axial Load For Tee Pieces

Formed Using Various Lubricants.

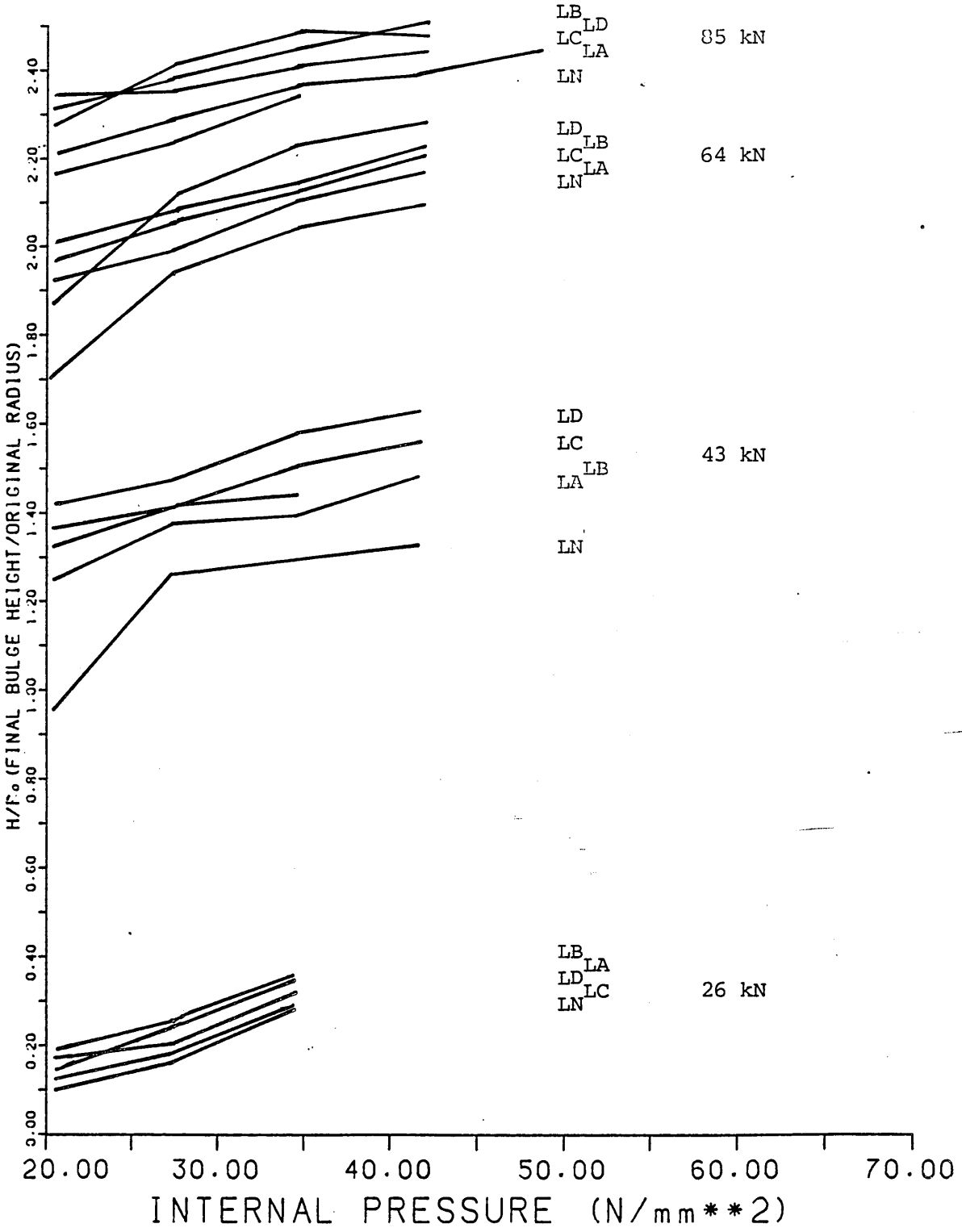

FIGURE 88

The Bulge Height To Original Tube Radius Variation Against Internal Pressure For Tee Pieces Formed Using Various Lubricants.

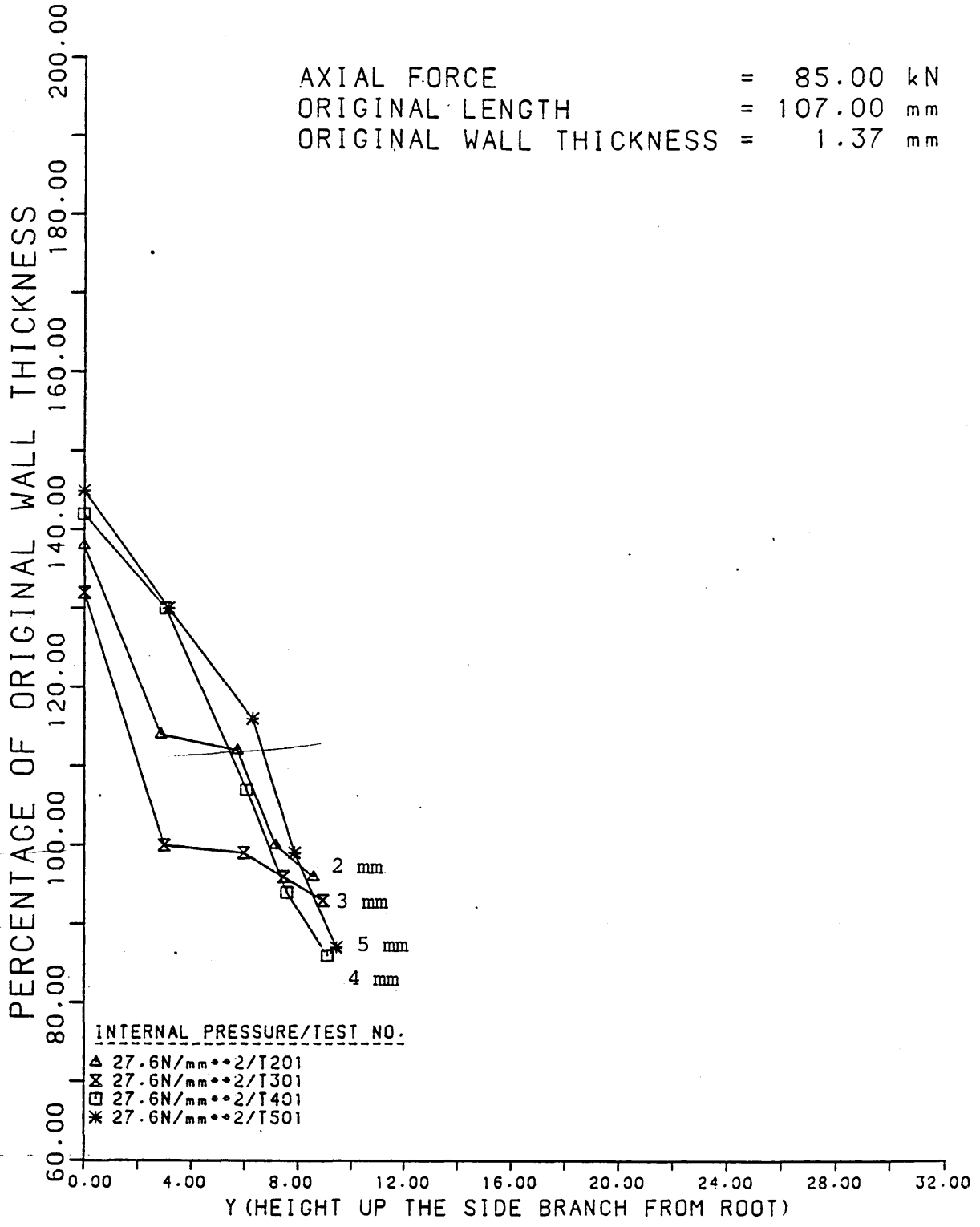

FIGURE 89

The Wall Thickness Distributions Along The Side Branches And Domes Of Tee Pieces Formed With Various Branch Radii.

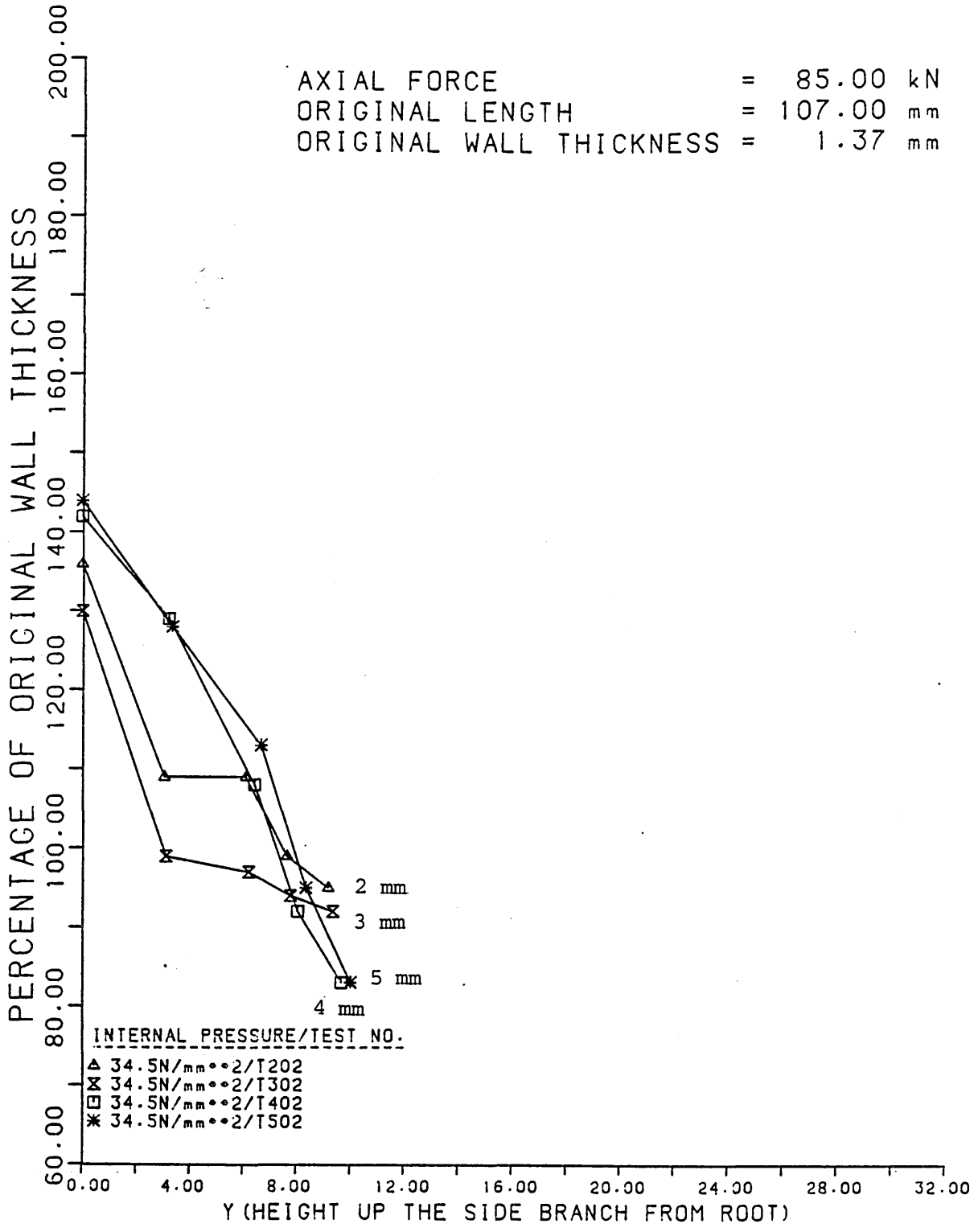

FIGURE 90

The Wall Thickness Distributions Along The Side Branches And Domes Of Tee Pieces Formed With Various Branch Radii.

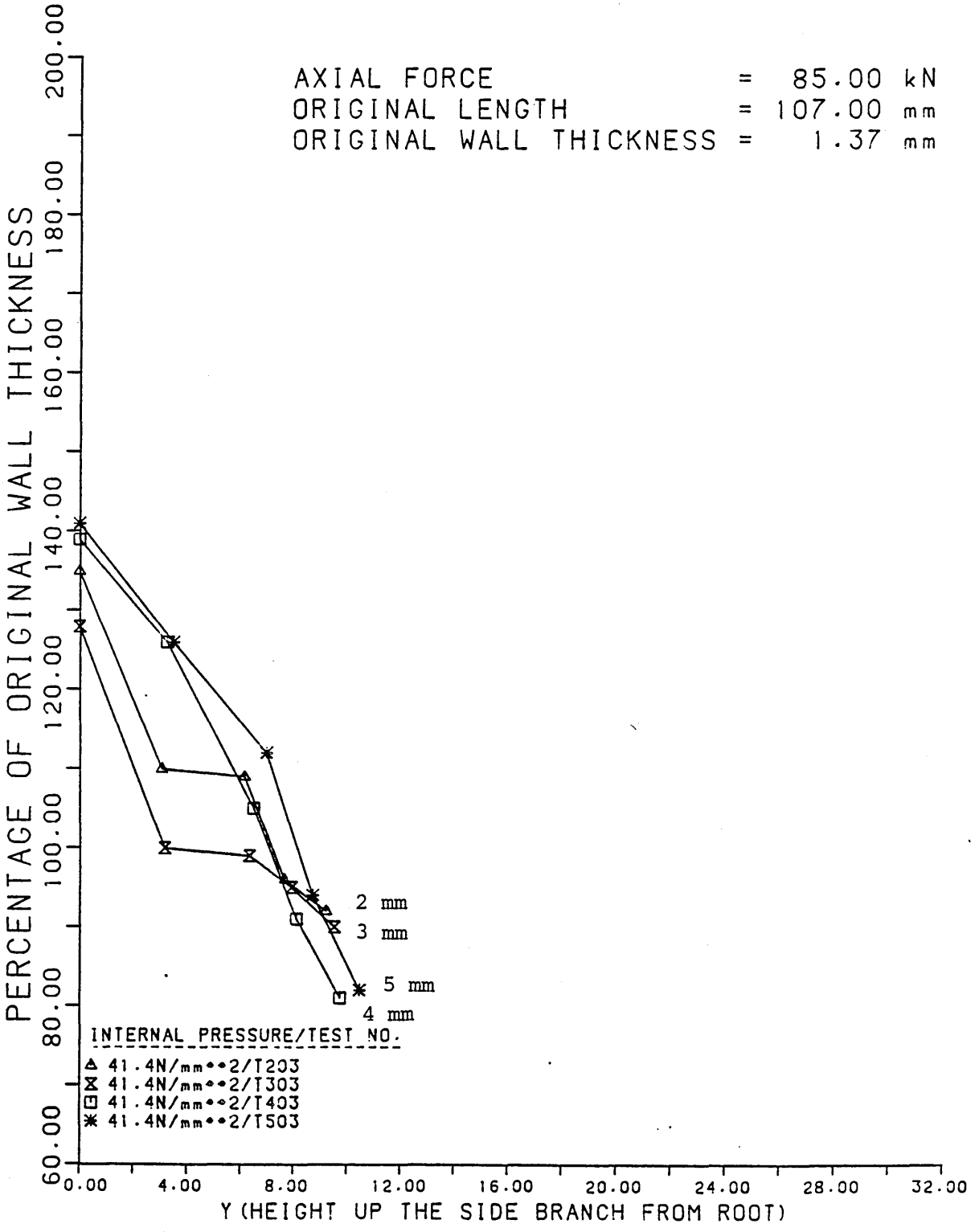

FIGURE 91

The Wall Thickness Distributions Along The Side Branches And Domes Of Tee Pieces Formed With Various Branch Radii.

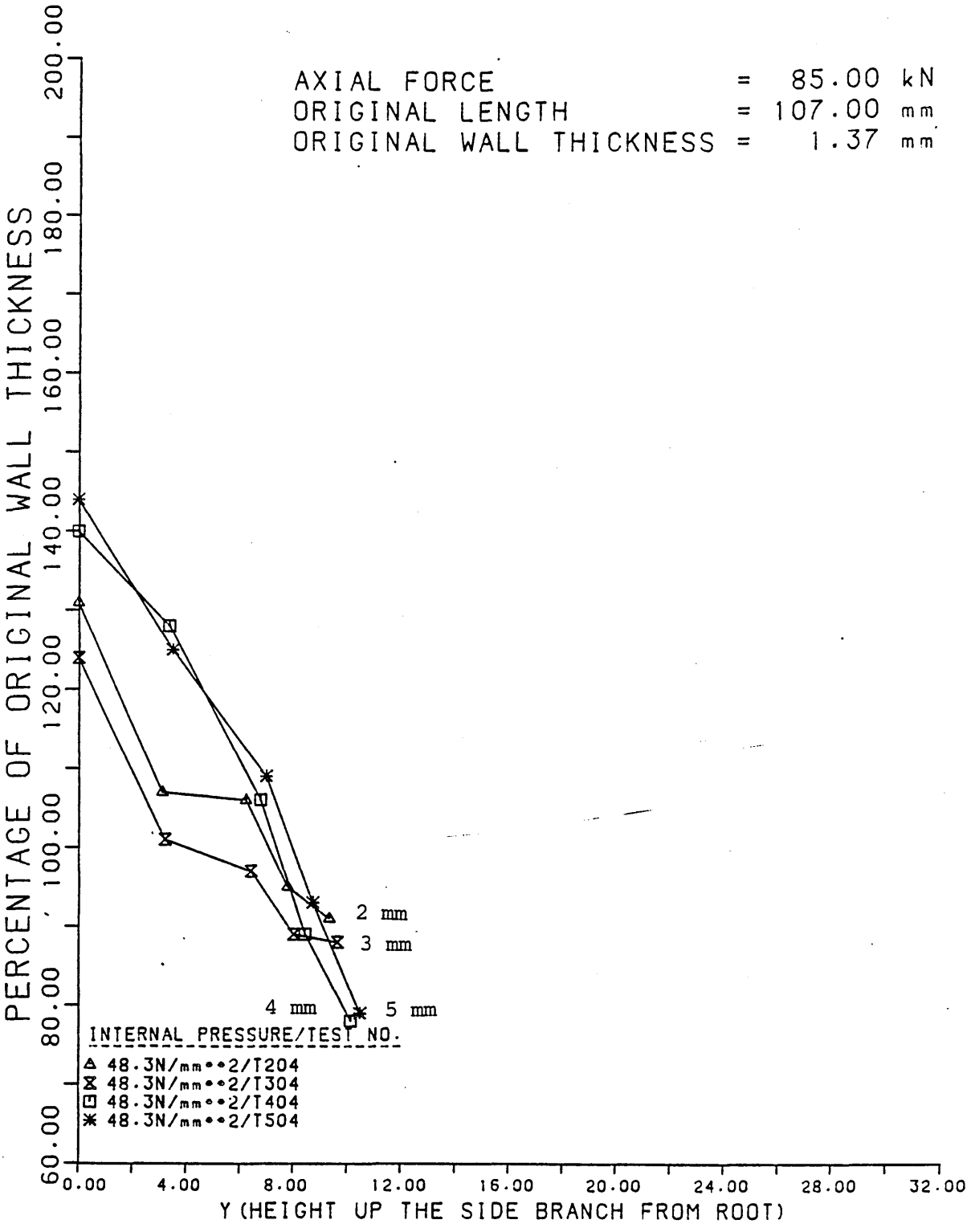

FIGURE 92

The Wall Thickness Distributions Along The Side Branches And Domes Of Tee Pieces Formed With Various Branch Radii.

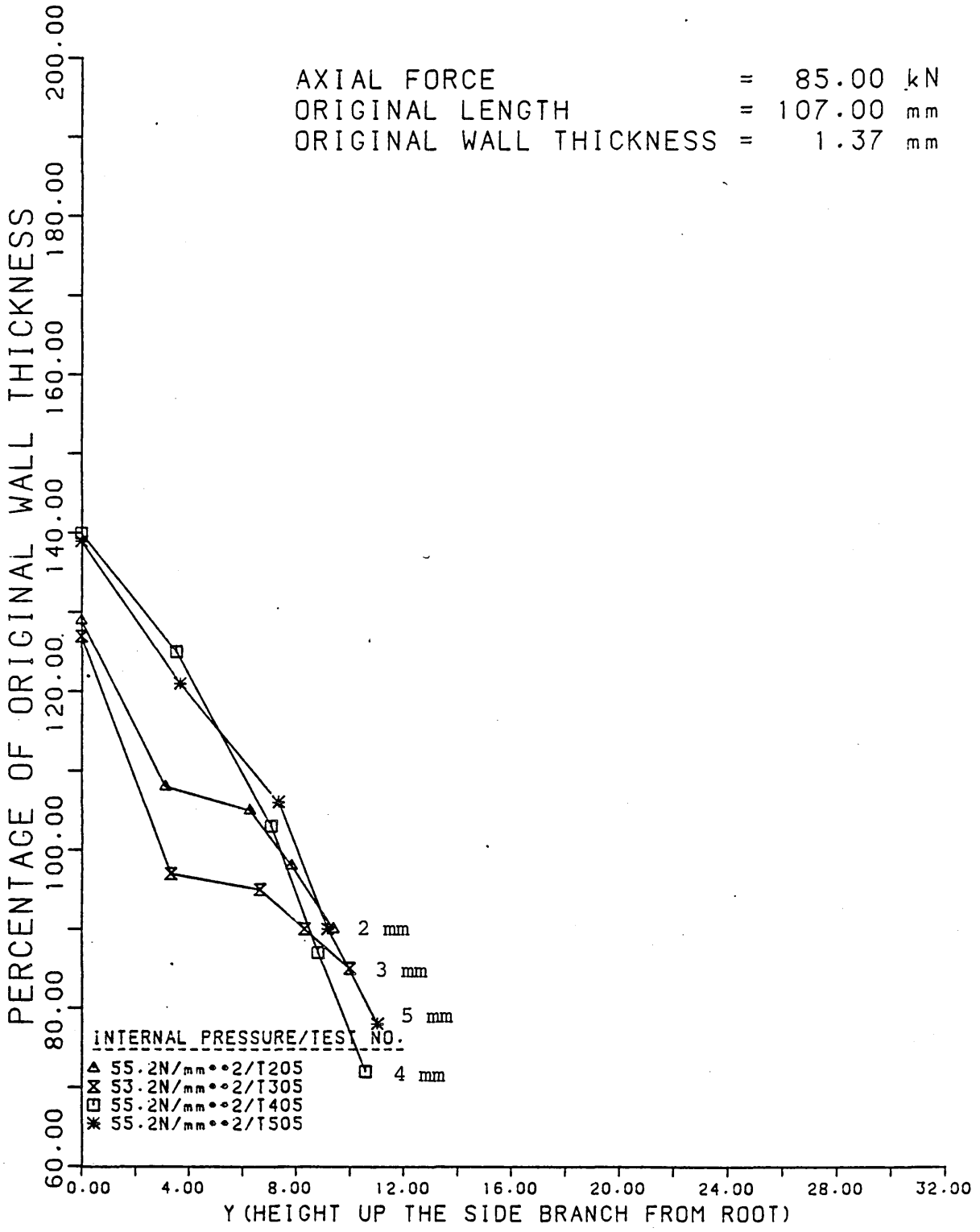

FIGURE 93

The Wall Thickness Distributions Along The Side Branches And Domes Of Tee Pieces Formed With Various Branch Radii.

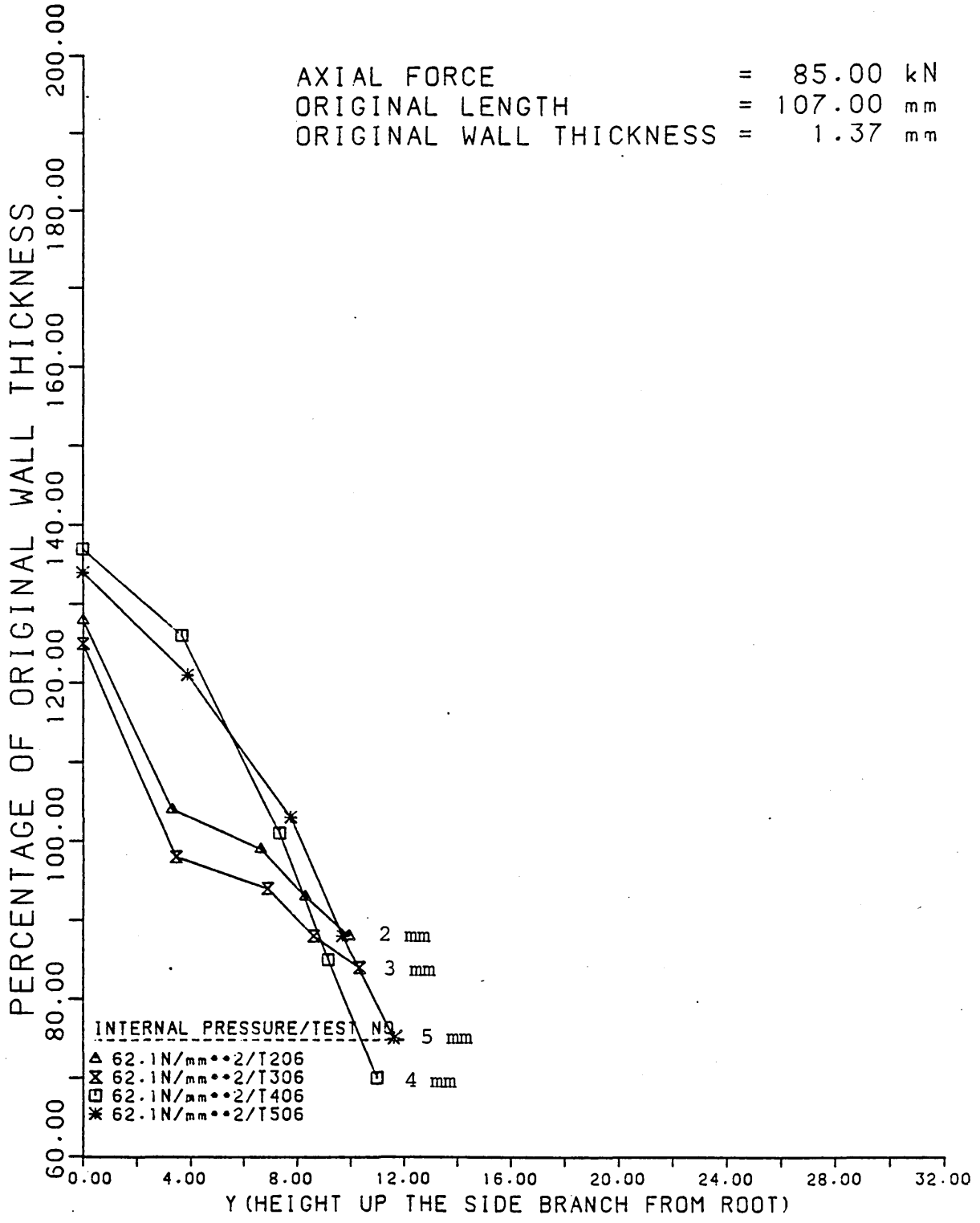

FIGURE 94

The Wall Thickness Distributions Along The Side Branches And Domes Of Tee Pieces Formed With Various Branch Radii.

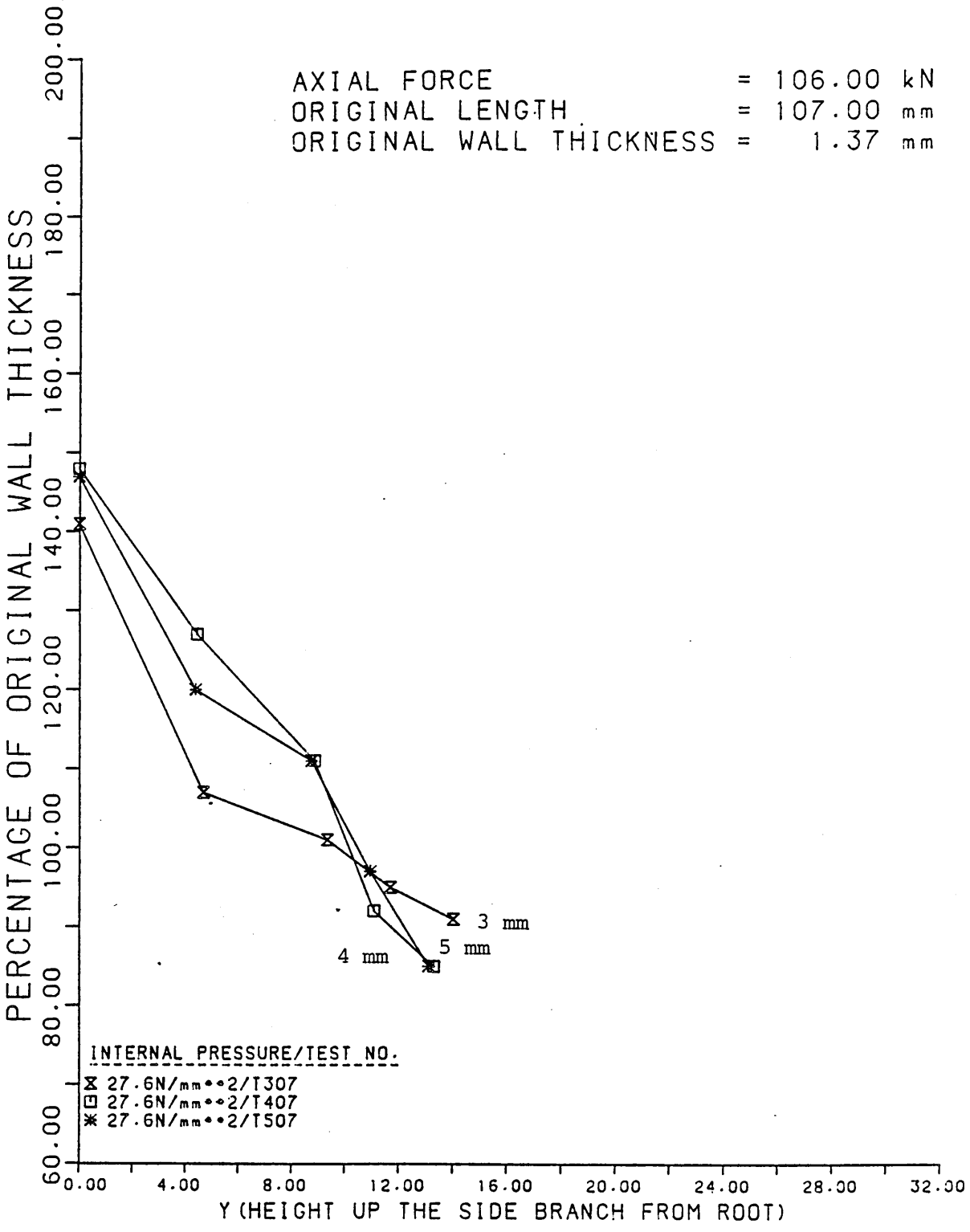

FIGURE 95

The Wall Thickness Distributions Along The Side Branches And Domes Of Tee Pieces Formed With Various Branch Radii.

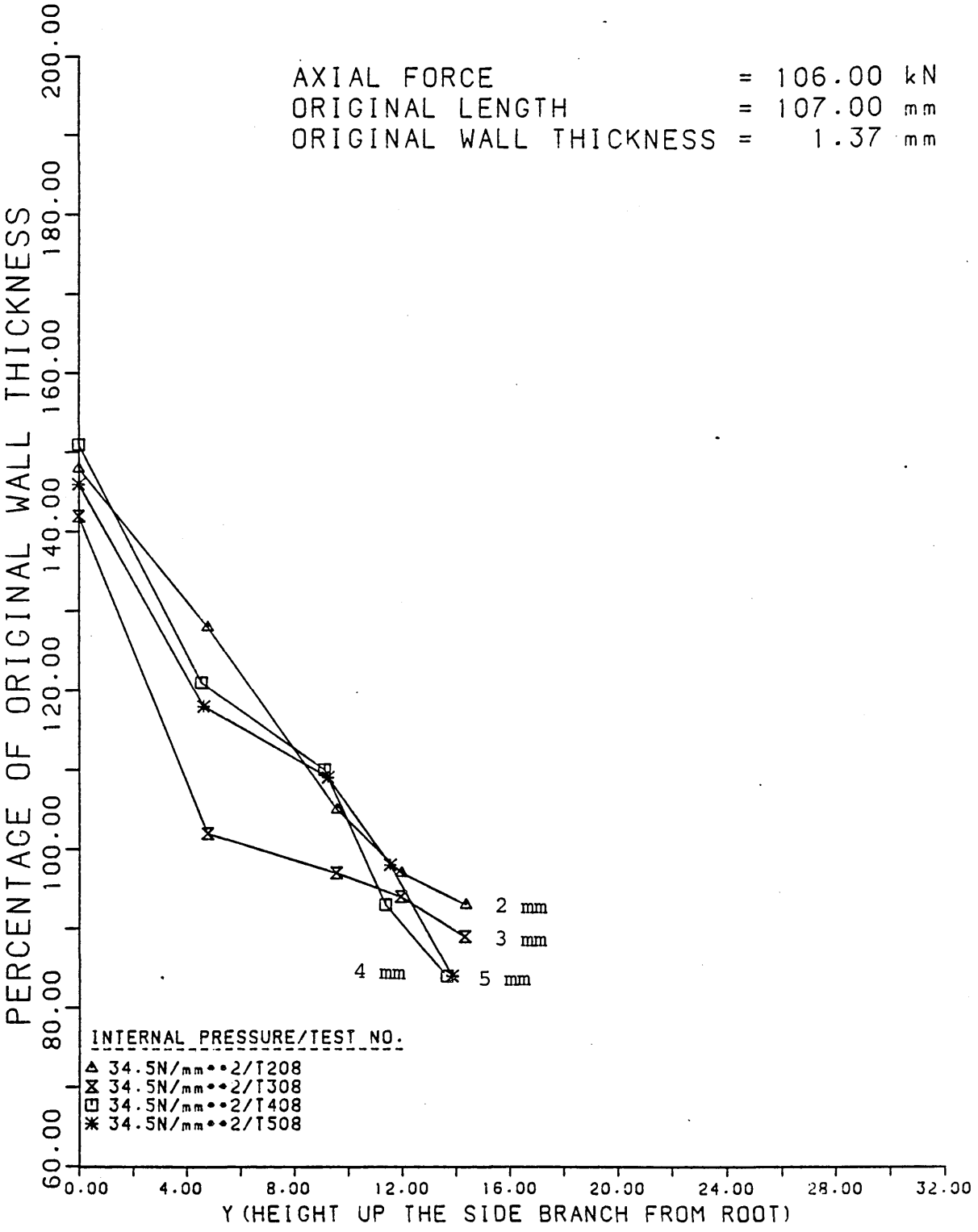

FIGURE 96

The Wall Thickness Distributions Along The Side Branches And Domes Of Tee Pieces Formed With Various Branch Radii.

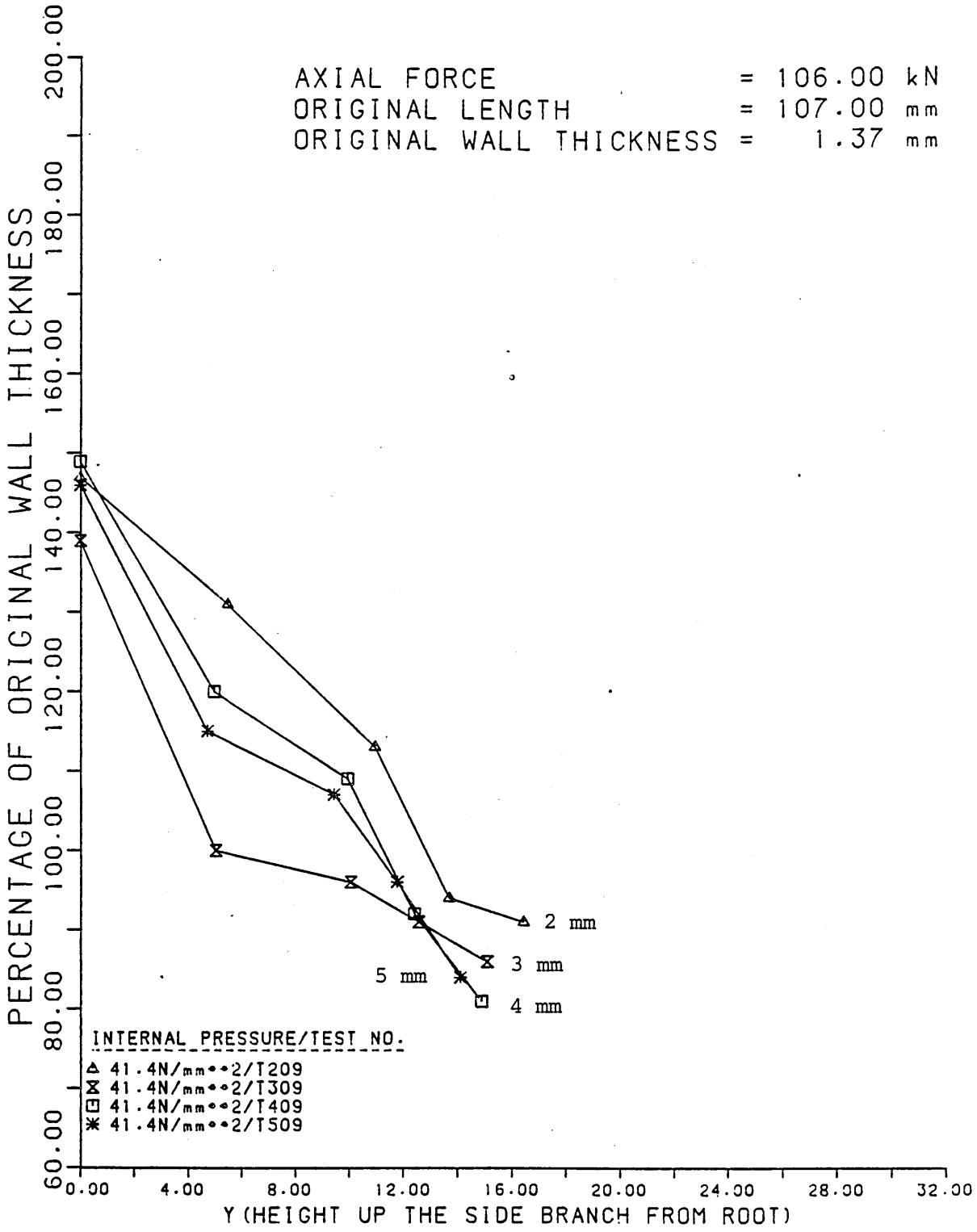

FIGURE 97

The Wall Thickness Distributions Along The Side Branches And Domes Of Tee Pieces Formed With Various Branch Radii.

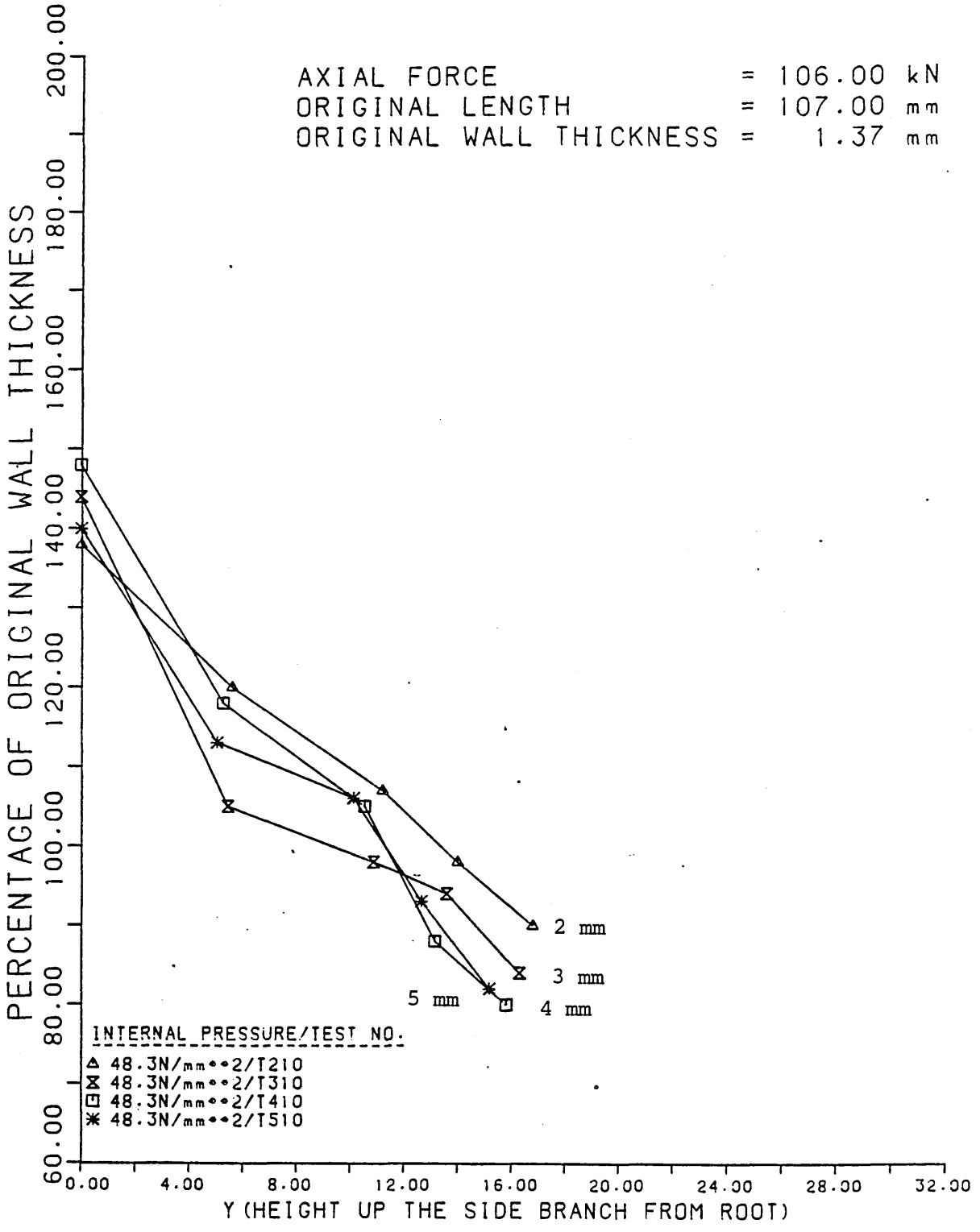

FIGURE 98

The Wall Thickness Distributions Along The Side Branches And Domes Of Tee Pieces Formed With Various Branch Radii.

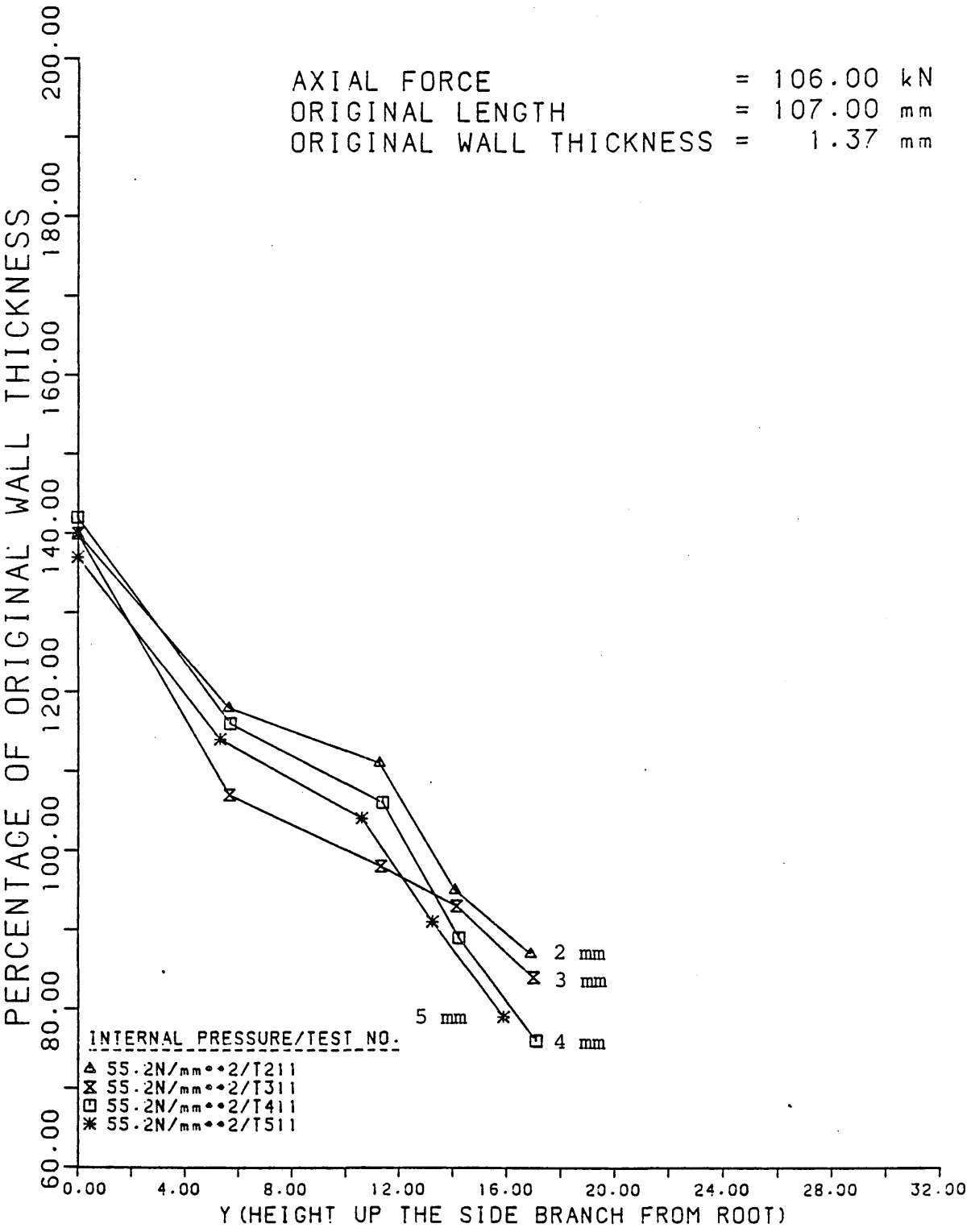

FIGURE 99

The Wall Thickness Distributions Along The Side Branches And Domes Of Tee Pieces Formed With Various Branch Radii.

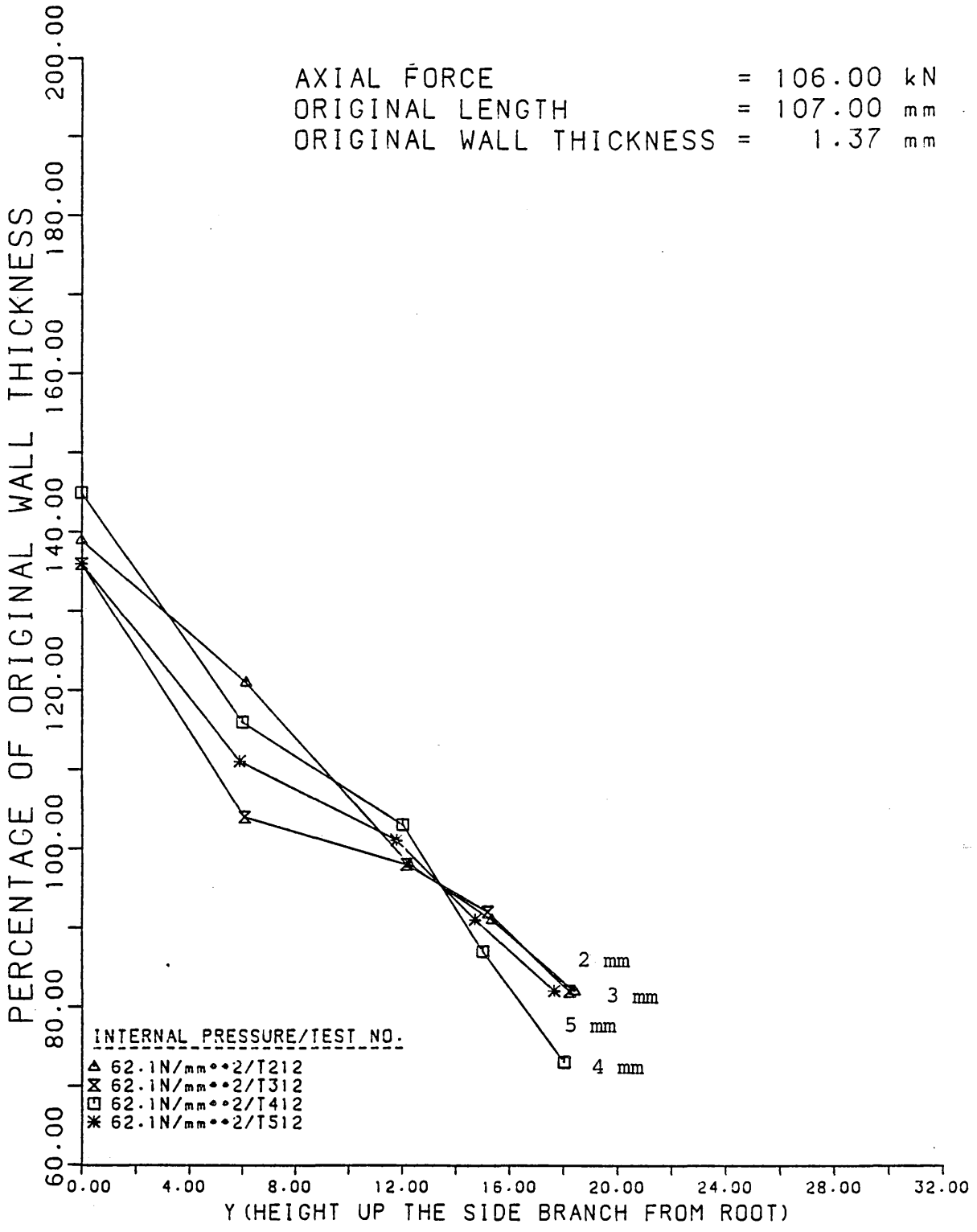

FIGURE 100

The Wall Thickness Distributions Along The Side Branches And Domes Of Tee Pieces Formed With Various Branch Radii.

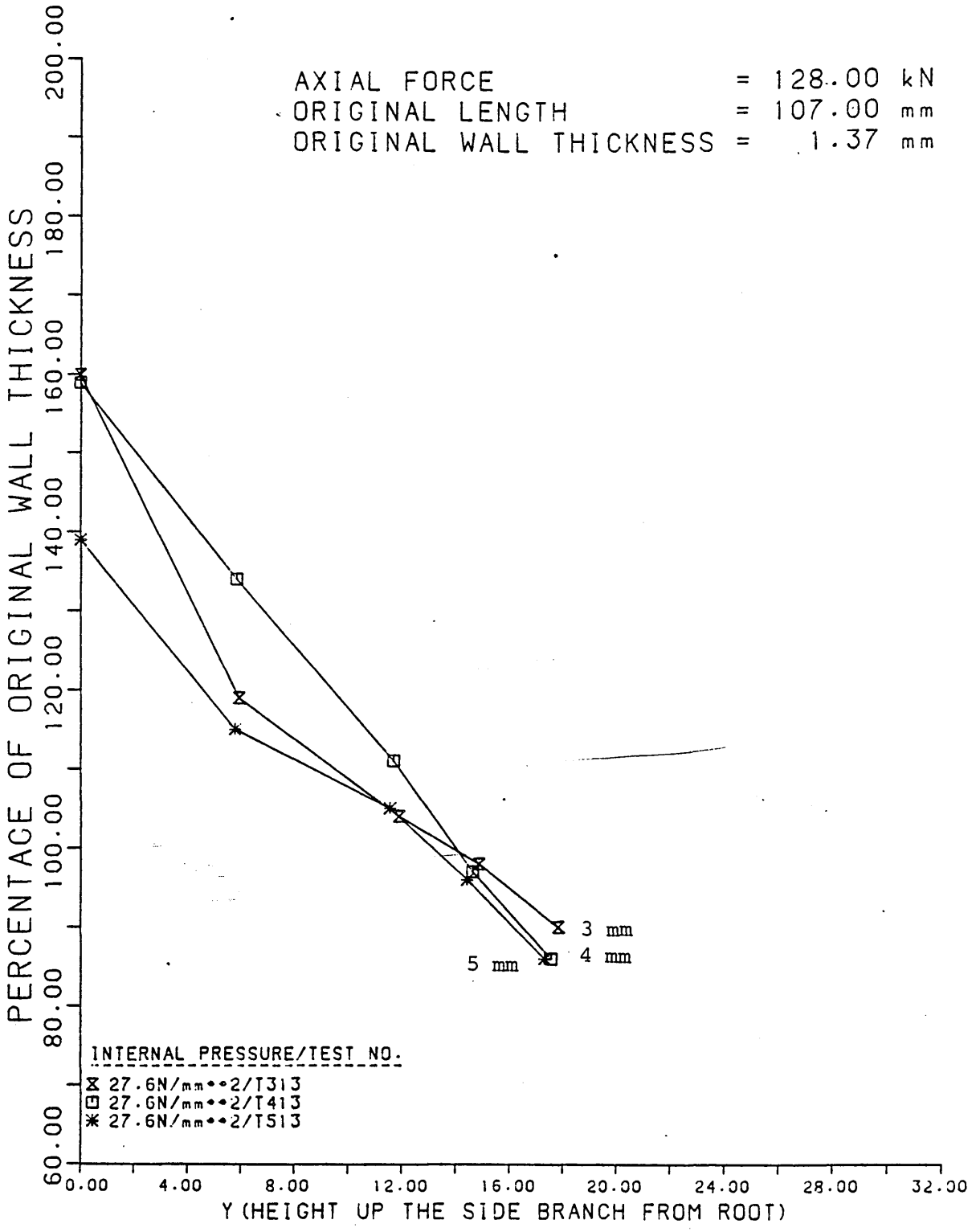

FIGURE 101

The Wall Thickness Distributions Along The Side Branches And Domes Of Tee Pieces Formed With Various Branch Radii.

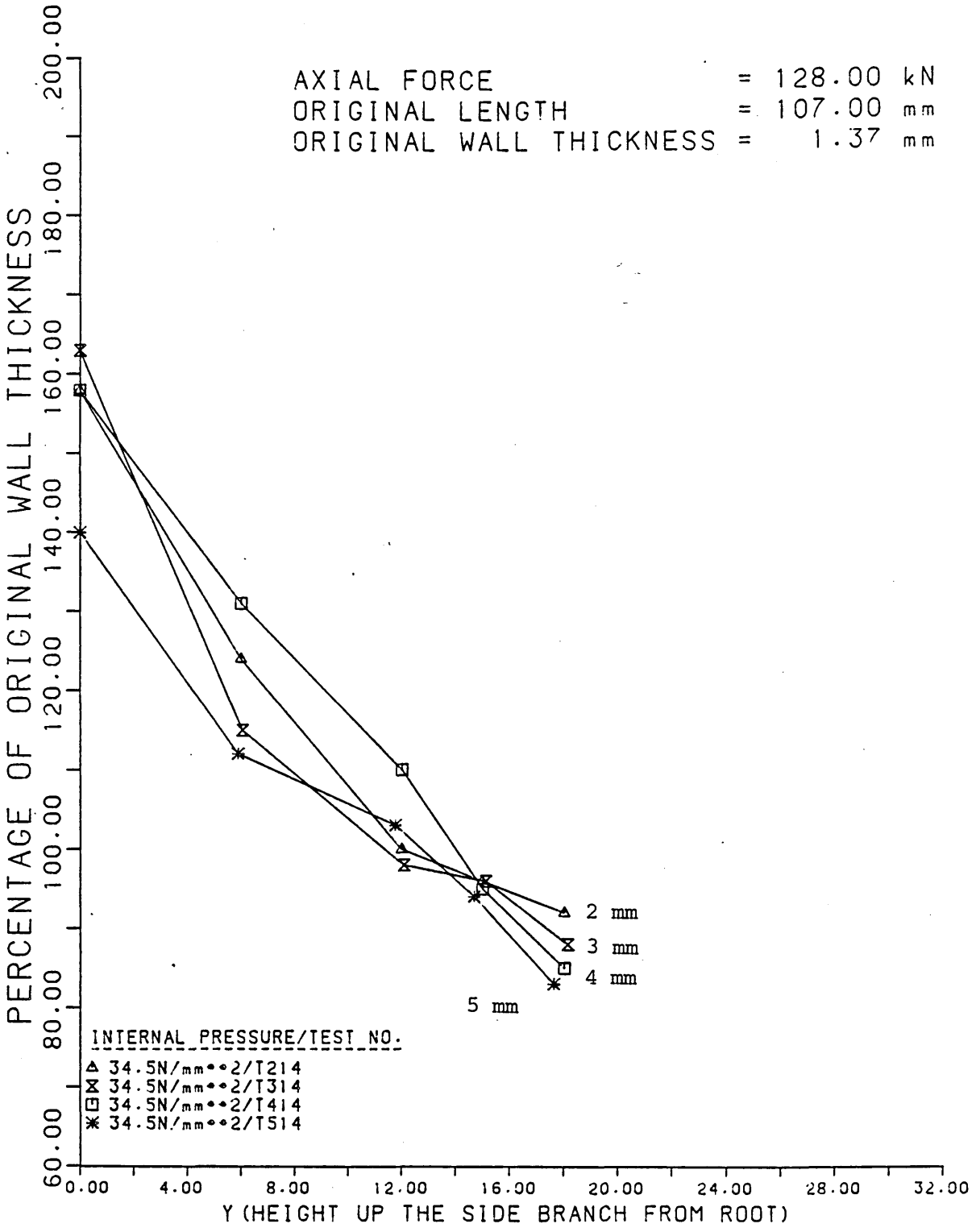

FIGURE 102

The Wall Thickness Distributions Along The Side Branches And Domes Of Tee Pieces Formed With Various Branch Radii.

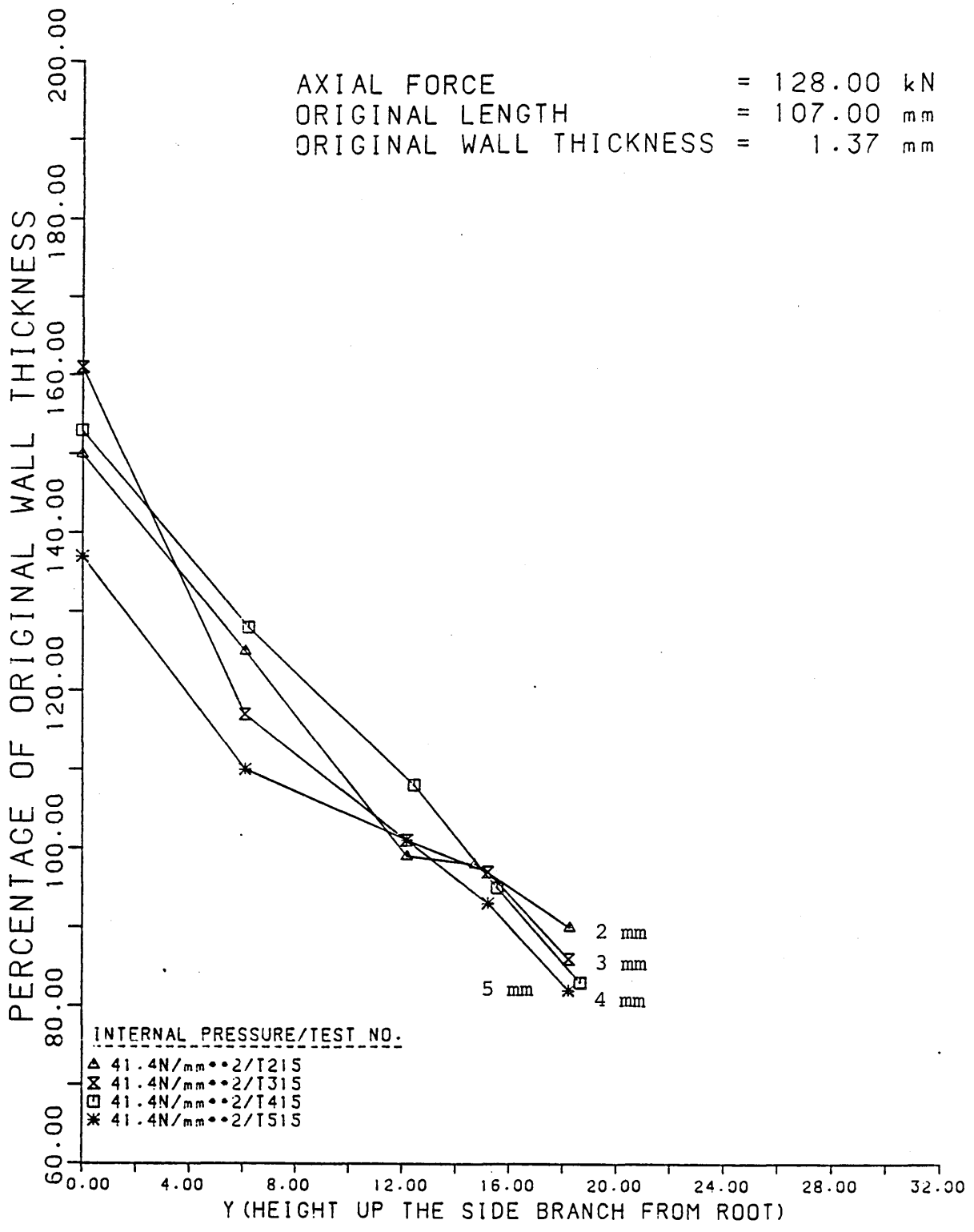

FIGURE 103

The Wall Thickness Distributions Along The Side Branches And Domes Of Tee Pieces Formed With Various Branch Radii.

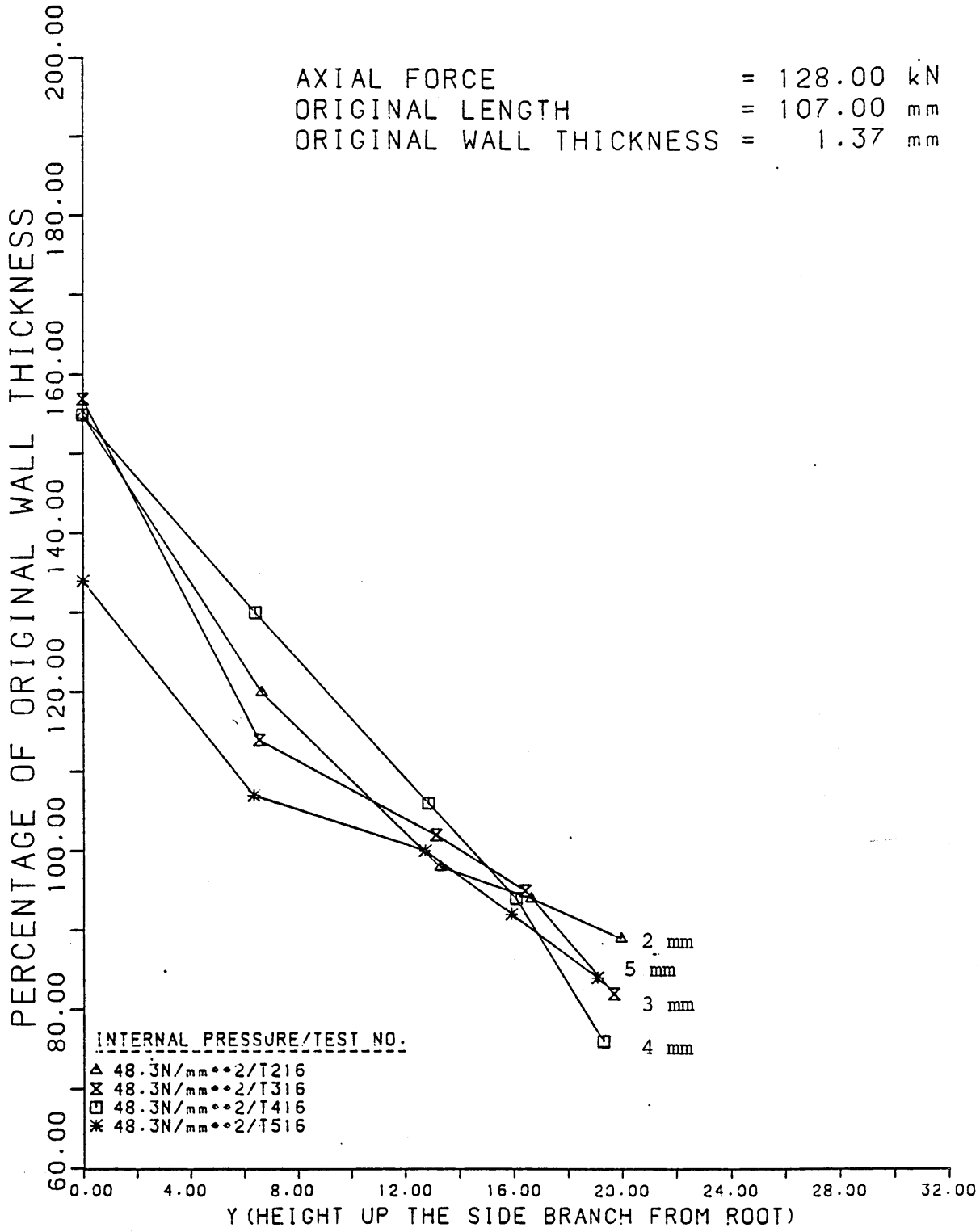

FIGURE 104

The Wall Thickness Distributions Along The Side Branches And Domes Of Tee Pieces Formed With Various Branch Radii.

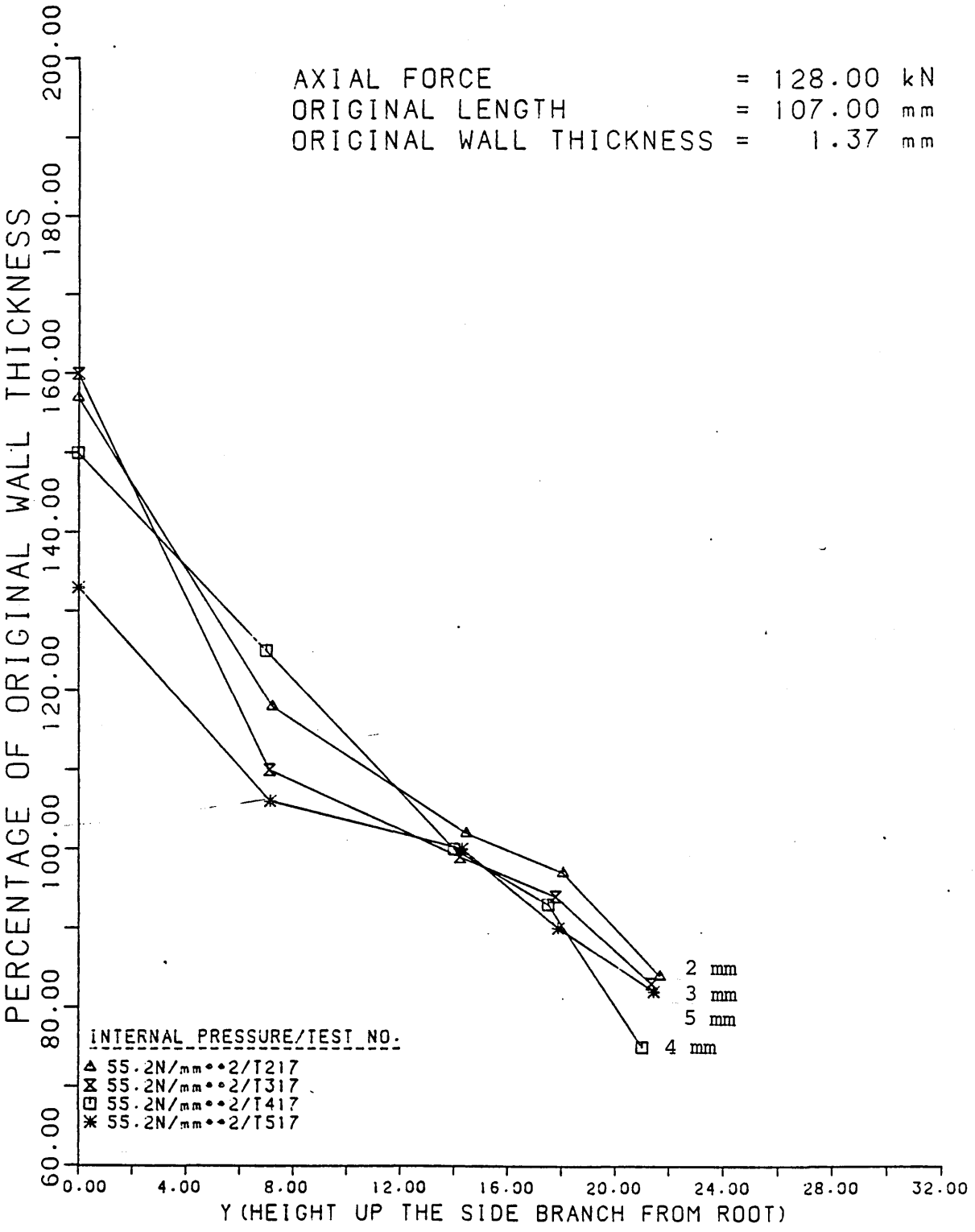

FIGURE 105

The Wall Thickness Distributions Along The Side Branches And Domes Of Tee Pieces Formed With Various Branch Radii.

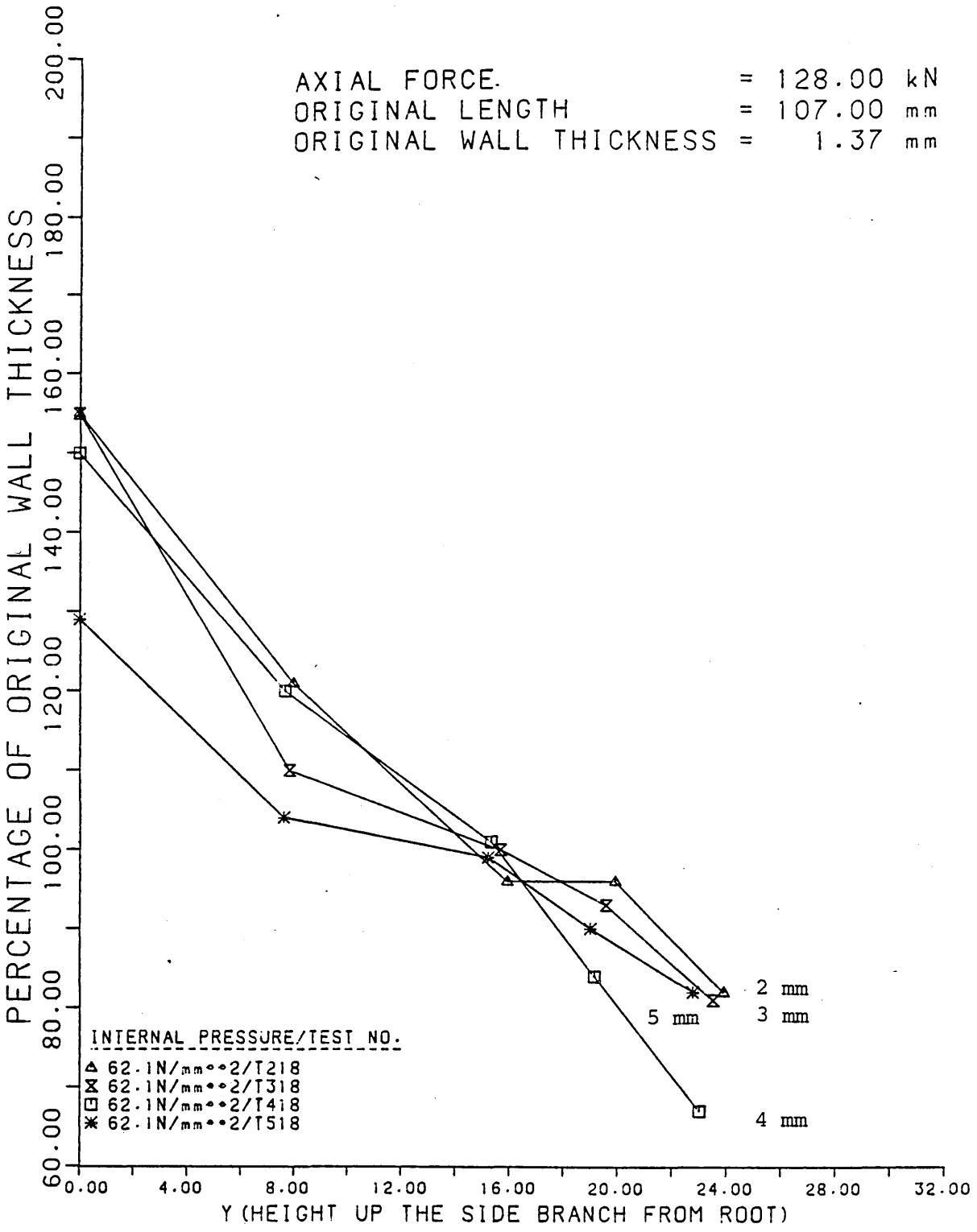

FIGURE 106

The Wall Thickness Distributions Along The Side Branches And Domes Of Tee Pieces Formed With Various Branch Radii.

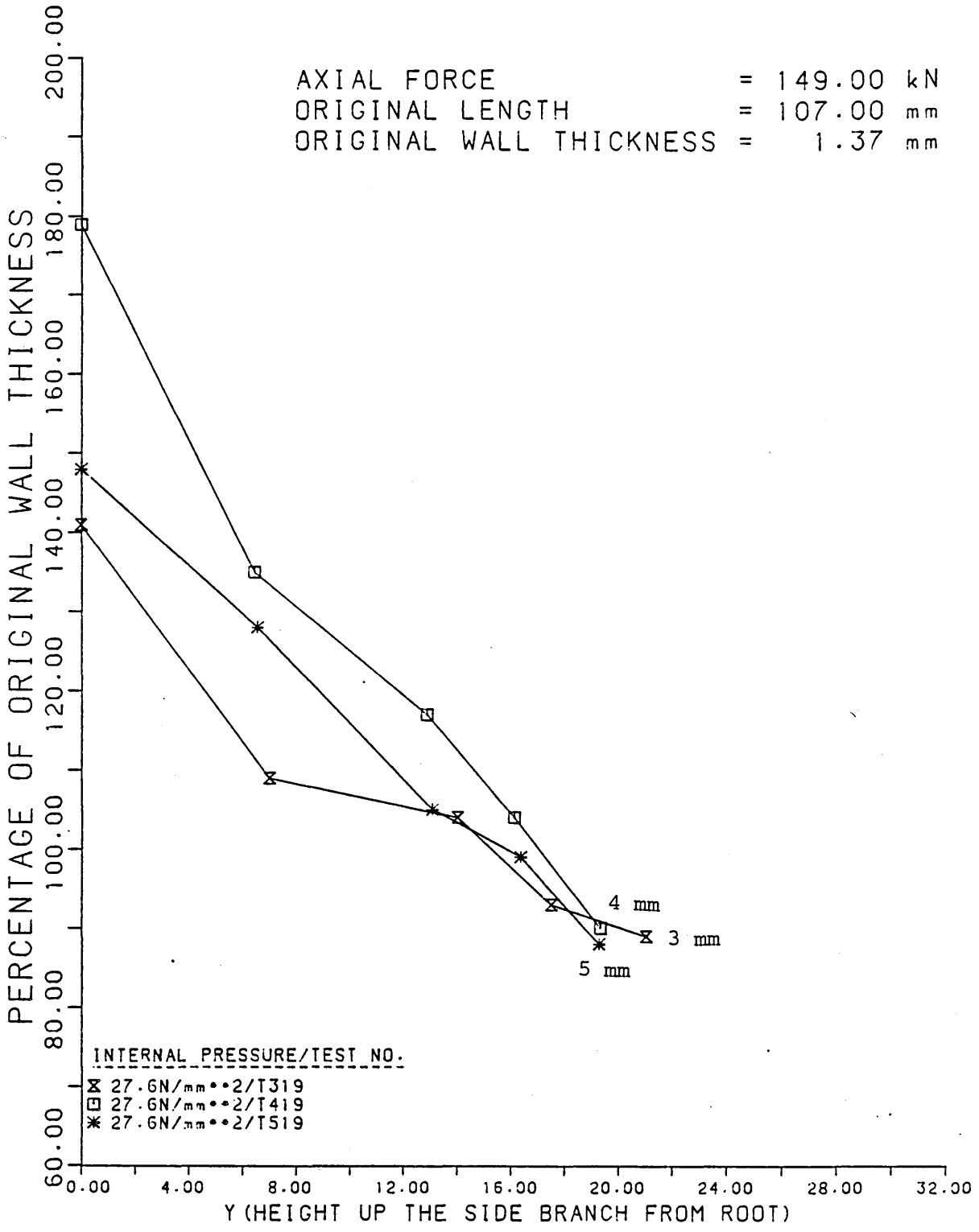

FIGURE 107

The Wall Thickness Distributions Along The Side Branches And Domes Of Tee Pieces Formed With Various Branch Radii.

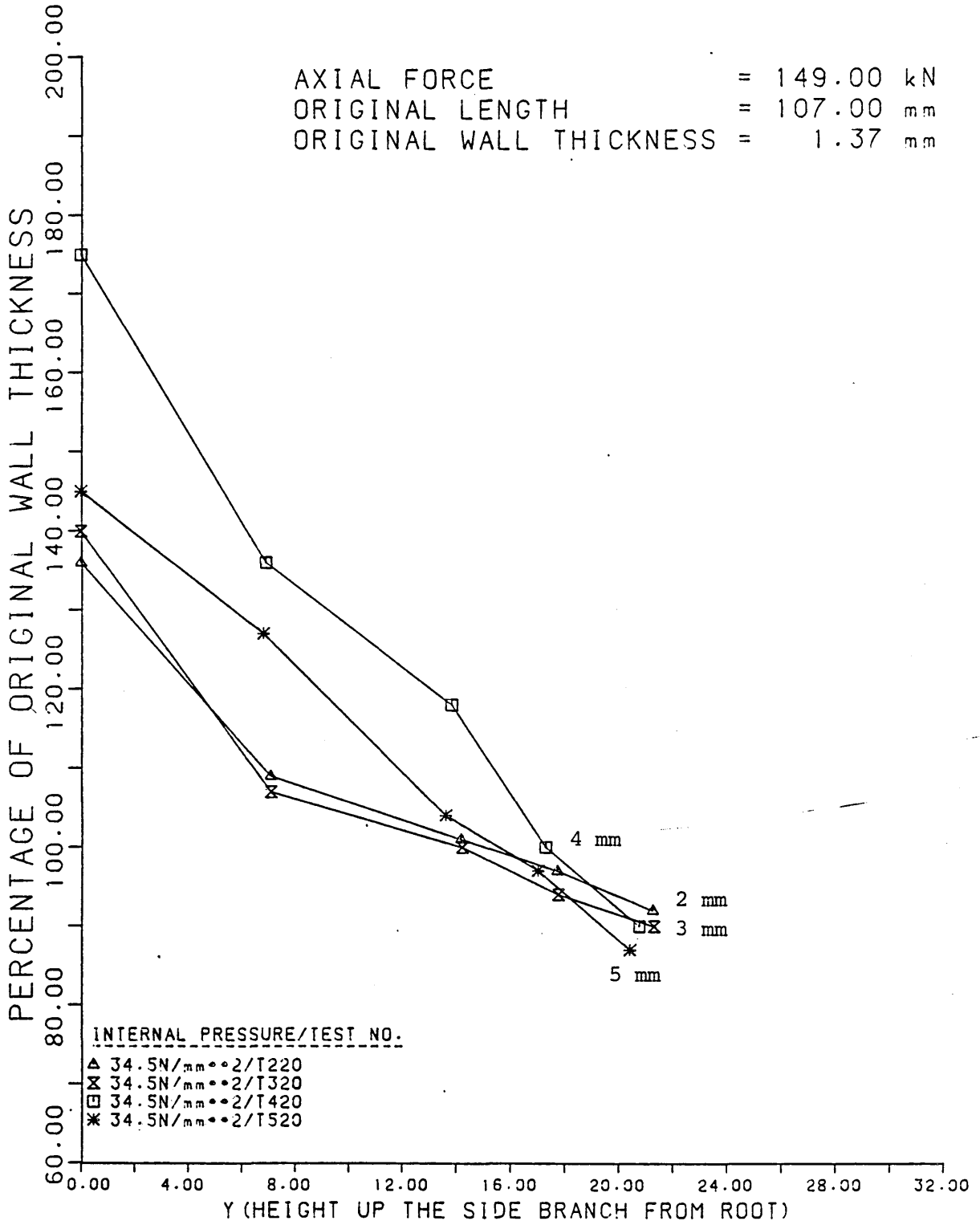

FIGURE 108

The Wall Thickness Distributions Along The Side Branches And Domes Of Tee Pieces Formed With Various Branch Radii.

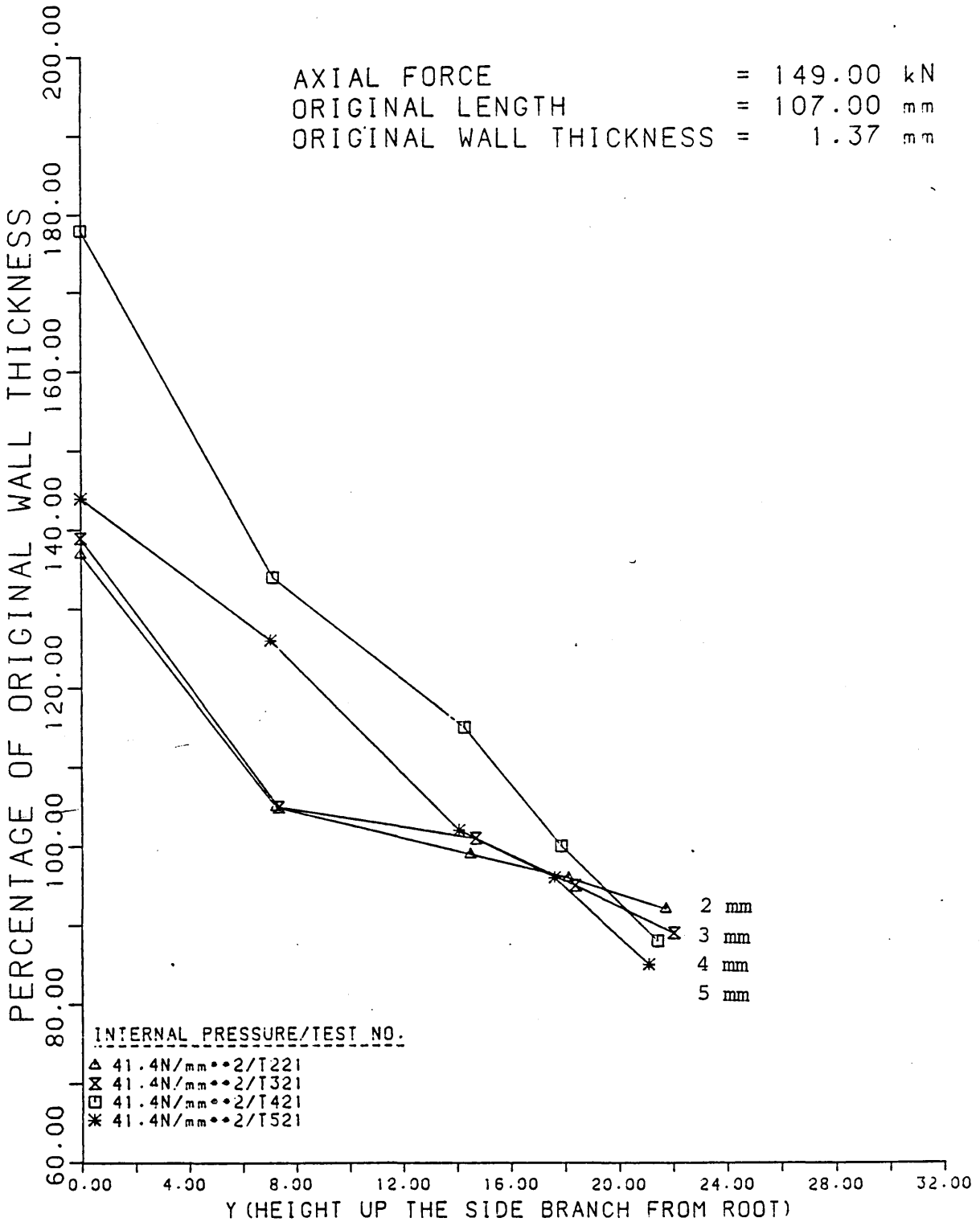

FIGURE 109

The Wall Thickness Distributions Along The Side Branches And Domes Of Tee Pieces Formed With Various Branch Radii.

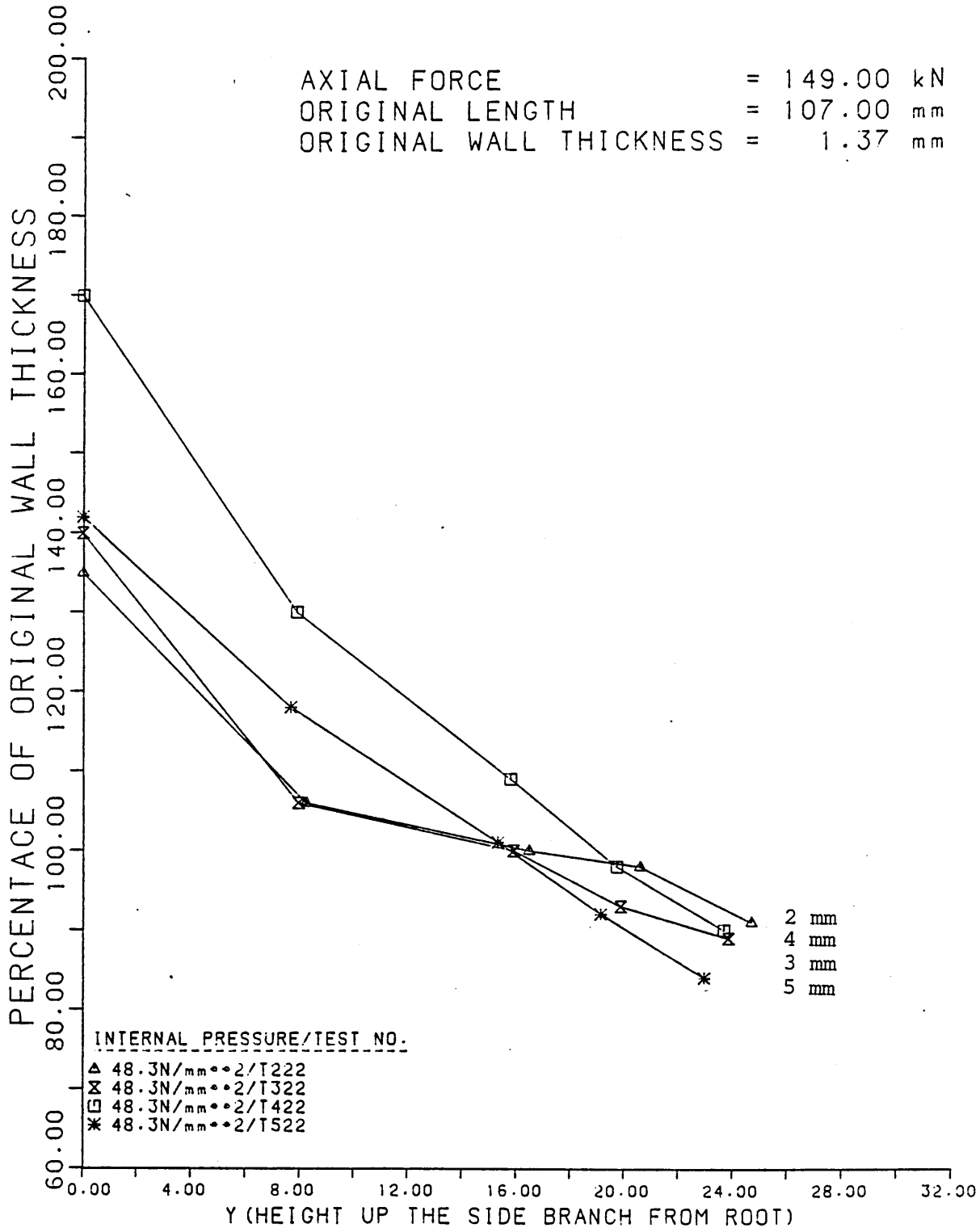

FIGURE 110

The Wall Thickness Distributions Along The Side Branches And Domes Of Tee Pieces Formed With Various Branch Radii.

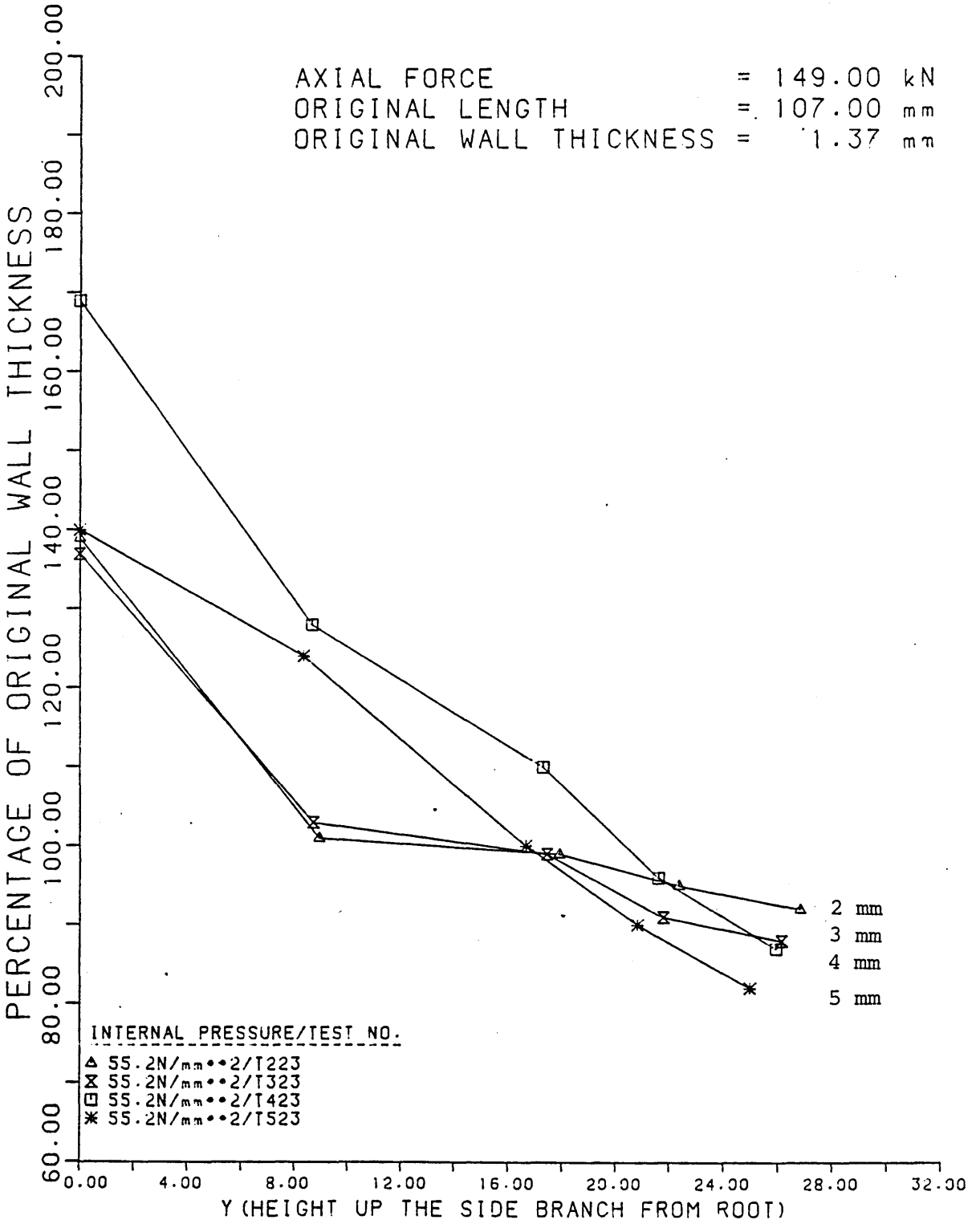

FIGURE 111

The Wall Thickness Distributions Along The Side Branches And Domes Of Tee Pieces Formed With Various Branch Radii.

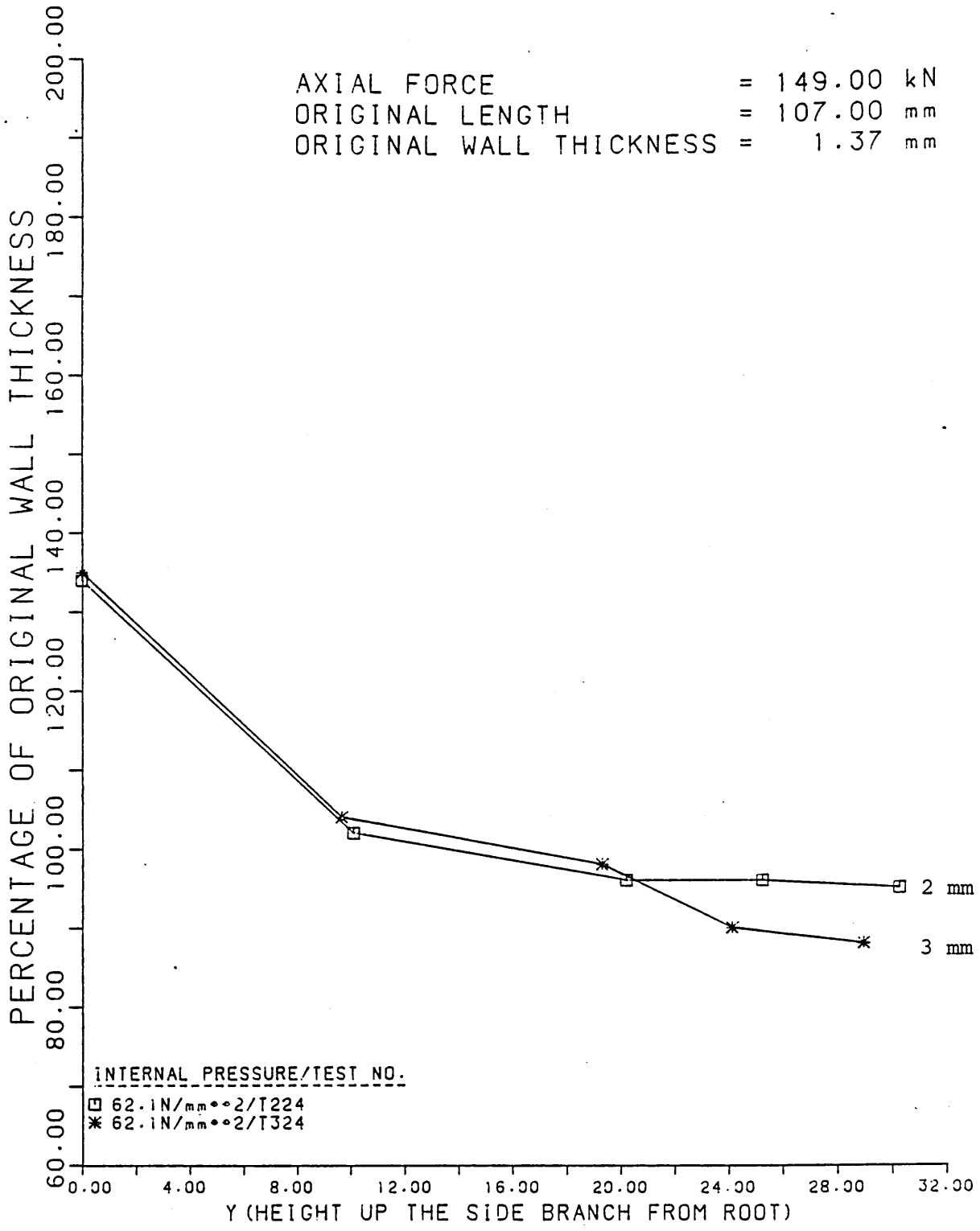

FIGURE 112

The Wall Thickness Distributions Along The Side Branches And Domes Of Tee Pieces Formed With Various Branch Radii.

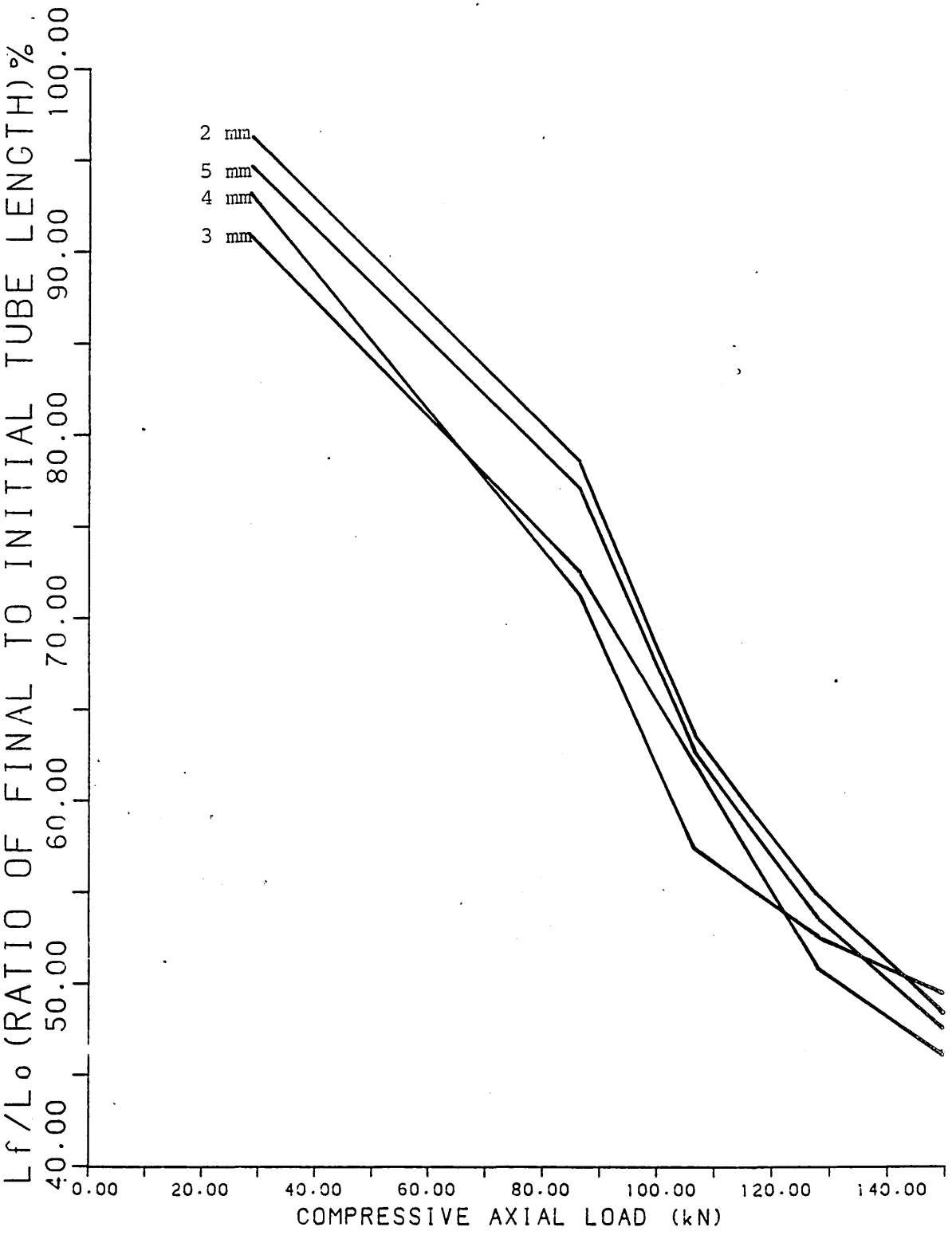

FIGURE 113

The Final To Original Tube Length Variation

Against Compressive Axial Load For Tee Pieces

Formed With Various Branch Radii.

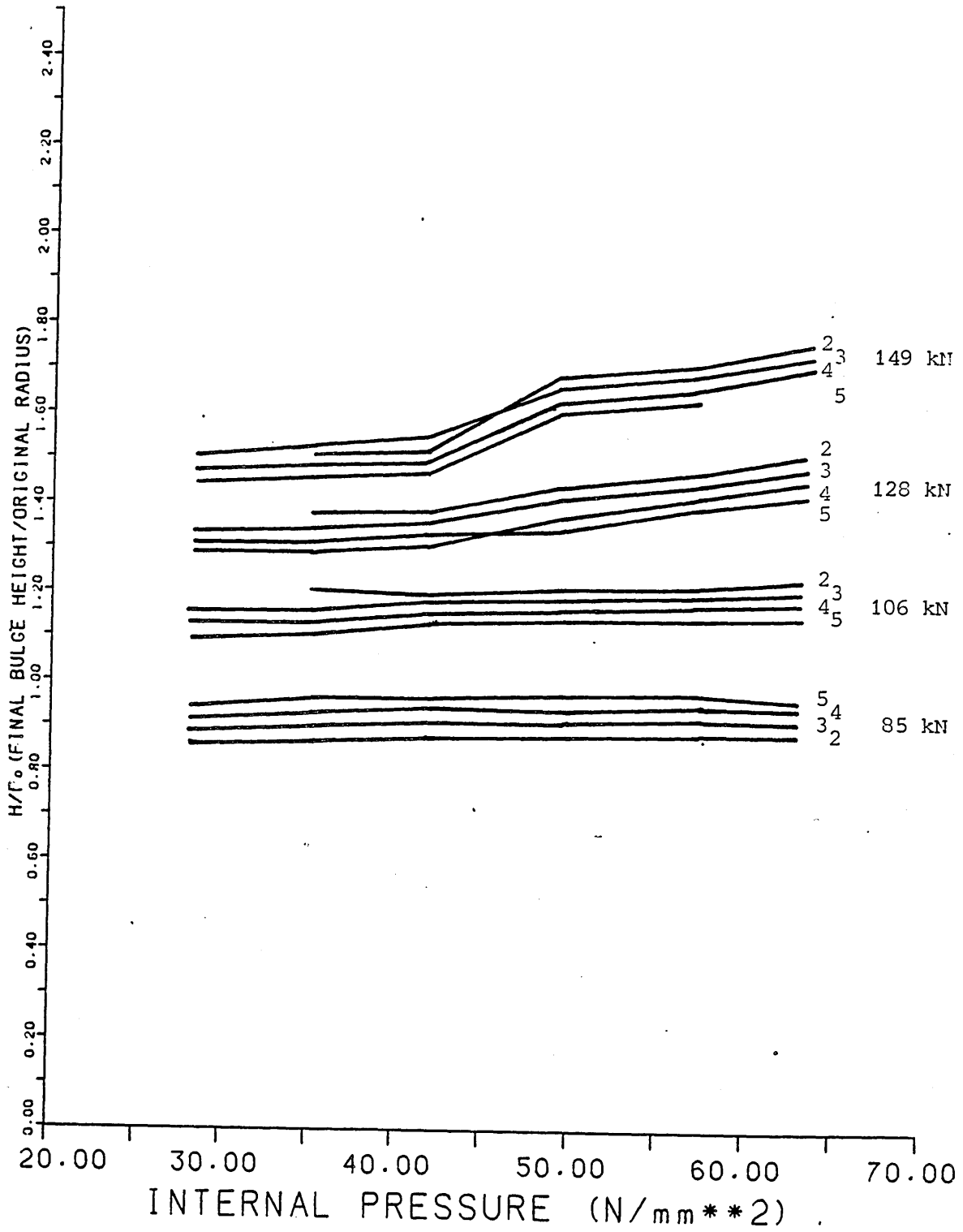

FIGURE 114

The Bulge Height To Original Tube Radius Variation Against Internal Pressure For Tee Pieces Formed With Various Branch Radii.

Table 1. Forming Ranges for Different Tube Materials

Material	Compressive Axial Load (kN)	Maximum Bulge Height (mm)	Minimum Wall Thickness Ratio (%)	Maximum Internal Pressure (N/mm^2)	Bursting Pressure (N/mm^2)
Aluminium	43	8.14	82	17.25	20.7
Aluminium	64	17.23	78	17.25	20.7
Aluminium	85	22.00	69	17.25	20.7
Copper	85	13.60	67	55.20	62.1
Steel	85	1.88	98	62.10	----
Aluminium	106	26.51	78	17.25	20.7
Copper	106	20.00	65	55.20	62.1
Steel	106	4.88	96	62.10	----
Copper	128	28.51	77	55.20	62.1
Steel	128	12.10	98	62.10	----
Copper	149	27.97	84	55.20	62.1
Steel	149	13.51	95	62.10	----

Table 2. Forming Ranges for the Different Lubricants.

Lubricant	Compressive Axial Load (kN)	Maximum Bulge Height (mm)	Minimum Wall Thickness Ratio (%)	Maximum Internal Pressure (N/mm^2)	Bursting Pressure (N/mm^2)	Maximum Buckling Pressure (N/mm^2)	Figure
LN	26	2.69	75	34.5	41.4	----	74
LA	26	2.90	66	34.5	41.4	----	74
LB	26	3.29	63	34.5	41.4	----	74
LC	26	2.83	71	34.5	41.4	----	74
LD	26	2.81	71	34.5	41.4	----	74
LN	43	10.13	81	41.4	48.3	20.7	77
LA	43	11.65	70	48.3	55.2	20.7	78
LB	43	11.67	91	41.4	48.3	20.7	77
LC	43	12.24	71	48.3	55.2	20.7	78
LD	43	12.93	71	48.3	55.2	20.7	78
LN	64	18.65	79	41.4	48.3	20.7	81
LA	64	18.38	75	48.3	55.2	20.7	82
LB	64	18.99	76	48.3	55.2	20.7	82
LC	64	18.15	78	41.4	48.3	20.7	81
LD	64	19.54	81	41.4	48.3	20.7	81
LN	85	20.5	77	41.4	48.3	20.7	85
LA	85	22.23	71	48.3	55.2	20.7	86
LB	85	23.45	59	48.3	55.2	20.7	86
LC	85	22.72	66	48.3	55.2	20.7	86
LD	85	23.14	68	48.3	55.2	20.7	86

Table 3. Averaged Bulge Height Variations (mm) from Standard Tests.

Compressive Axial Load / Lubricant	26 (kN)	43 (kN)	64 (kN)	85 (kN)	Compressive Axial Loads Averaged
LA	+0.09	+0.52	-0.14	+1.19	+0.415
LB	+0.41	+0.78	+0.10	+1.26	+0.625
LC	+0.37	+0.95	+0.39	+0.57	+0.570
LD	+0.22	+1.49	+0.57	+1.38	+1.100

Table 4. Bulge Heights (mm) for Selected Pressures & Loads

Load/Pressure ($kN \sim N/mm^2$) / Lubricant	64 & 41.4	64 & 48.3	85 & 41.4	85 & 48.3
LN	18.65	-----	20.5	-----
LA	18.06	18.38	21.41	22.23
LB	18.36	18.99	22.09	23.45
LC	18.15	-----	21.31	22.72
LD	19.54	-----	21.60	23.14

Table 5. Forming Ranges for Various Branch Radii.

Branch Radius (mm)	Compressive Axial Load (kN)	Maximum Bulge Height (mm)	Minimum Wall Thickness Ratio (%)	Maximum Internal Pressure (N/mm^2)	Bursting Pressure (N/mm^2)	Maximum Buckling Pressure (N/mm^2)	Figur
2	85	9.93	88	62.1	-----	-----	94
3	85	10.31	84	62.1	-----	-----	94
4	85	10.97	70	62.1	-----	-----	94
5	85	11.62	75	62.1	-----	-----	94
2	106	18.39	82	62.1	-----	27.60	100
3	106	18.20	82	62.1	-----	-----	100
4	106	18.01	73	62.1	-----	-----	100
5	106	17.64	82	62.1	-----	-----	100
2	128	23.91	82	62.1	-----	27.60	106
3	128	23.52	81	62.1	-----	-----	106
4	128	23.02	67	62.1	-----	-----	106
5	128	22.79	82	62.1	-----	-----	106
2	149	30.29	95	62.1	-----	27.60	112
3	149	28.97	88	62.1	-----	-----	112
4	149	25.94	87	55.2	62.10	-----	111
5	149	24.97	82	55.2	62.10	-----	111

4. THEORETICAL ANALYSIS

4.1) Theoretical Wall Thickness Distribution

The following geometrical analysis is an extension of the analysis to predict the variation in the wall thickness around the bulge profile presented in references **29**, **30** and **31**. The theory deals with the expansion of a tubular blank into an axisymmetric component i.e. one having the same expansion all around the axis, in addition to forming into a side branch. In order to analyse these two cases of bulge forming, the following assumptions are made:

1) the deformation profile at any instant can be described by a circular arc,

and 2) the effect of additional material fed into the deformation zone may be taken into account by introducing an apparent strain factor (ASF).

4.1.1) Expansion of a Curved Surface

Referring to Figure 115a, the arc **ABC** of initial uniform thickness t_1, polar height H_1 and radius of curvature $\mathcal{C}_1$, expands to an arc **A'B'C'** of polar height H_2, and radius of curvature $\mathcal{C}_2$. Unlike the previous analysis where it had been assumed that the new arc would have had points **A** and **C** (hence **AB'C**) in common with the initial arc, this theory takes into account the radius of the junction between the tube and the branch (Figure 115b). Practically, it is known that if the angle between the tube and the branch is 90^{o}, and there is no radius on the corners, the component

will be ruptured at this point. These corners must have a slight radius on them to allow the material to flow into the branch, and so in this theory, the branch radius is represented by 'r_B'.

Consider a point distance x_1 from the axis and a height h_1 from the chord **AC** on the undeformed arc **ABC**. On the expanded arc **A'B'C'**, this same point has an axial position of x_2 and height h_2 from the chord **AC** (the chord **AC** has the same '**Y**' co-ordinate as **A'C'**; only the '**X**' co-ordinates have changed).

From the geometry:

$$\frac{x_2}{x_o} = \frac{(h_2 + y_2)}{y_2} ,$$

and

$$\frac{x_1}{x_o} = \frac{(h_1 + y_1)}{y_1} .$$

Combining these two equations gives:

$$\frac{x_2}{x_1} = \frac{y_1(h_2 + y_2)}{y_2(h_1 + y_1)} \qquad \ldots\ldots(1).$$

However, from the geometry,

$$y_2H_2 = (a - r_B)^2 \text{ and } y_1H_1 = a^2.$$

Combining these two equations gives:

$$\frac{y_2}{y_1} = \frac{H_1(a - r_B)^2}{H_2a^2} \qquad \ldots\ldots(2).$$

Substituting for y_1 and y_2 in (1) gives:

$$\frac{x_2}{x_1} = \frac{a^2H_2(h_2 + (a - r_B)^2/H_2)}{(a - r_B)^2H_1(h_1 + a^2/H_1)}$$

which becomes,

$$\frac{x_2}{x_1} = \frac{a^2H_1H_2(H_2h_2 + (a - r_B)^2)}{(a - r_B)^2H_1H_2(H_1h_1 + a^2)} \ldots\ldots(3).$$

Also from the geometry,

$$y_1 + h_1 = \frac{x_1^2}{(H_1 - h_1)} \qquad \ldots\ldots(4),$$

and

$$y_2 + h_2 = \frac{x_2^2}{(H_2 - h_2)} \qquad \ldots\ldots(5).$$

Combining equations (4) and (5) with equation (1) gives:

$$\frac{x_2}{x_1} = \frac{y_2(H_2 - h_2)}{y_1(H_1 - h_1)} .$$

But, from equation (2),

$$\frac{y_2}{y_1} = \frac{H_1(a - r_B)^2}{H_2 a^2} ,$$

thus:

$$\frac{x_2}{x_1} = \frac{H_1(a - r_B)^2(H_2 - h_2)}{H_2 a^2(H_1 - h_1)} \qquad \ldots\ldots(6).$$

Combining equations (3) and (6) gives:

$$\frac{a^2 H_1 H_2(H_2 h_2 + (a - r_B)^2)}{(a - r_B)^2 H_1 H_2(H_1 h_1 + a^2)} = \frac{H_1(a - r_B)^2(H_2 - h_2)}{H_2 a^2(H_1 - h_1)} ,$$

$$\frac{a^2(H_2 h_2 + (a - r_B)^2)}{(a - r_B)^2(H_1 h_1 + a^2)} = \frac{H_1(a - r_B)^2(H_2 - h_2)}{H_2 a^2(H_1 - h_1)} ,$$

$$H_2 a^4(H_1 - h_1)(H_2 h_2 + (a - r_B)^2) = H_1(a - r_B)^4(H_2 - h_2)(H_1 h_1 + a^2) ,$$

$$H_1 H_2 a^4(H_2 h_2 + (a - r_B)^2) - h_1 H_2 a^4(H_2 h_2 + (a - r_B)^2) = H_1^2 h_1(a - r_B)^4(H_2 - h_2) + a^2 H_1(a - r_B)^4(H_2 - h_2) ,$$

$$H_1H_2a^4(H_2h_2 + (a - r_B)) - a^2H_1(a - r_B)^4(H_2 - h_2)$$
$$= H_1^2h_1(a - r_B)^4(H_2 - h_2) + h_1H_2a^4(H_2h_2 + (a - r_B)^2),$$

$$H_1a^2[a^2H_2(H_2h_2 + (a - r_B)^2) - (a - r_B)^4(H_2 - h_2)]$$
$$= h_1[H_1^2(a - r_B)^4(H_2 - h_2) + H_2a^4(H_2h_2 + (a - r_B)^2)],$$

$$h_1 = \frac{H_1a^2[a^2H_2(H_2h_2 + (a - r_B)^2) - (a - r_B)^4(H_2 - h_2)]}{H_1^2(a - r_B)^4(H_2 - h_2) + H_2a^4(H_2h_2 + (a - r_B)^2)} \quad \ldots\ldots(7).$$

Substituting for h_1 in equation (3):

$$\frac{x_2}{x_1} = \frac{a^2(H_2h_2 + (a - r_B)^2)}{(a - r_B)^2(H_1h_1 + a^2)},$$

$$\frac{x_2}{x_1} = \frac{a^2(H_2h_2 + (a - r_B)^2)[H_1^2(a - r_B)^4(H_2 - h_2) + H_2a^4(H_2h_2 + (a - r_B)^2]}{\left[(a - r_B)^2[H_1^2a^2(a^2H_2(H_2h_2 + (a - r_B)^2) - (a - r_B)^4(H_2 - h_2)] + a^2[H_1^2(a - r_B)^4(H_2 - h_2) + H_2a^4(H_2h_2 + (a - r_B)^2)]\right]}.$$

However, if it is assumed that all the components are formed from cylindrical tubes with no prior bulging (which is the case for all of the tests done), H_1 can be taken as zero ($H_1 = 0$).

The equation therefore simplifies to:

$$\frac{x_2}{x_1} = \frac{a^2(H_2h_2 + (a - r_B)^2)[H_2a^4(H_2h_2 + (a - r_B)^2)]}{(a - r_B)^2a^2[H_2a^4(H_2h_2 + (a - r_B)^2)]},$$

$$\frac{x_2}{x_1} = \frac{(H_2h_2 + (a - r_B)^2)}{(a - r_B)^2}.$$

$$\text{i.e. } \frac{x_2}{x_1} = 1 + \frac{H_2h_2}{(a - r_B)^2} \quad \ldots\ldots(8).$$

4.1.2) Axisymmetric Expansion of a Tubular Branch

Referring to Figure 115c, force equilibrium in

the meridional direction of an element of the deformed profile gives:

$$\frac{d(\sigma_L t)}{dr} = \frac{(\sigma_\phi - \sigma_L)t}{r} \qquad \text{.....(9).}$$

Similarly, the force equilibrium in the normal direction is given by:

$$\frac{P}{t} = \frac{\sigma_\phi}{\phi_\phi} + \frac{\sigma_L}{\phi_L} \qquad \text{.....(10).}$$

At this point we assume that during the entire deformation process σ_ϕ and σ_L will be connected by:

$$\sigma_\phi = K\sigma_L \qquad \text{.....(11),}$$

$$\text{where } K = (2 - \phi_\phi/\phi_L).$$

Substituting for σ_ϕ in equation (9), integrating and also noting that $\sigma_L = \sigma_{L,0}$ and $t = t_0$ at $r = r_0$, we obtain,

$$\sigma_L = \sigma_{L,0} t_0 \phi_\phi \exp[(r_0 - \phi_\phi)/P_L] \qquad \text{.....(12),}$$

where r_0 is the original tube radius, and t_0 is the original thickness.

Similarly, substituting for σ_ϕ in equation (10) and simplifying gives,

$$\frac{P}{t} = \frac{2\sigma_L}{\phi_\phi} \qquad \text{.....(13).}$$

Now, the global force equilibrium of the bulged portion of the tube for radius $r \geq r_0$ can be shown to yield:

$$\sigma_{L,0} = P\phi_L/t_0 \qquad \text{.....(14).}$$

We shall now make use of the Levy-Mises

plastic flow rule which may be written as:

$$\frac{\epsilon_1}{\sigma_1'} = \frac{\epsilon_2}{\sigma_2'} = \frac{\epsilon_3}{\sigma_3'} = \lambda \qquad \ldots\ldots(15)$$

where $\epsilon_1 = \ln\left[\frac{x_2}{x_1}\right]$, $\epsilon_2 = \ln\left[\frac{r}{r_0}\right]$ and $\epsilon_3 = \ln\left[\frac{t}{t_0}\right]$

and σ_1', σ_2' and σ_3' are the deviatoric components of the principal stresses $\sigma_1 = \sigma_L$, $\sigma_2 = \sigma_\phi$ and $\sigma_3 = -P$ respectively. The hydrostatic components of the principal stresses are given by $(\sigma_1 + \sigma_2)/3$ where $\sigma_3 = -P$ and is considered negligibly small in comparison to σ_1 and σ_2.

Thus:

$$\sigma_1' = \sigma_L - (\sigma_L + \sigma_\phi)/3 ,$$

and $$\sigma_2' = \sigma_\phi - (\sigma_L + \sigma_\phi)/3 .$$

Substituting for σ_1' and σ_2' in equation (15) we obtain:

$$\frac{\epsilon_2}{\epsilon_1} = \frac{\sigma_\phi - (\sigma_L + \sigma_\phi)/3}{\sigma_L - (\sigma_L + \sigma_\phi)/3} ,$$

$$= \frac{3\sigma_\phi - \sigma_L - \sigma_\phi}{3\sigma_L - \sigma_L - \sigma_\phi} ,$$

$$= \frac{2\sigma_\phi - \sigma_L}{2\sigma_L - \sigma_\phi} \qquad \ldots\ldots(16).$$

Substituting for σ_ϕ from equation (11) gives:

$$\frac{\epsilon_2}{\epsilon_1} = \frac{2K\sigma_L - \sigma_L}{2\sigma_L - K\sigma_L} ,$$

$$= \frac{2K - 1}{2 - K} .$$

But $K = (2 - \phi_\phi/\phi_L)$, so:

$$\frac{\epsilon_2}{\epsilon_1} = \frac{2(2 - \phi_\phi/\phi_L) - 1}{2 - (2 - \phi_\phi/\phi_L)} ,$$

$$= \frac{4 - 2\phi_o/\phi_L - 1}{\phi_o/\phi_L},$$

$$= \frac{3 - 2\phi_o/\phi_L}{\phi_o/\phi_L}.$$

or $\epsilon_2 = m\epsilon_1$ .....(17),

where $m = (3 - 2\phi_o/\phi_L)/(\phi_o/\phi_L)$ .....(18).

From the principle of volume constancy:

$$\epsilon_1 + \epsilon_2 + \epsilon_3 = 0$$

Substituting for ϵ_2 from equation (17) and re-arranging gives:

$$\epsilon_3 = -(1 + m)\epsilon_1 \quad \text{.....(19),}$$

but $\epsilon_3 = \ln\left[\frac{t}{t_0}\right]$ and $\epsilon_1 = \ln\left[\frac{x_2}{x_1}\right]$.

Hence, equation (19) becomes:

$$\ln\left[\frac{t}{t_0}\right] = -(1 + m)\ln\left[\frac{x_2}{x_1}\right],$$

$$= \ln\left[\left[\frac{(x_1)}{(x_2)}\right]^{(1 + m)}\right],$$

so that $t = t_0\left[\frac{(x_1)}{(x_2)}\right]^{(1 + m)}$ .....(20).

Substituting for (x_1/x_2) from equation (8), the current thickness at any point $h_2 = (r - r_0)$ on the bulged profile can be expressed as:

$$t = \frac{t_0}{\left[1 + \frac{H_2 h_2}{(a - r_B)^2}\right]^{(1 + m)}} \quad \text{.....(21),}$$

or $$\frac{t}{t_0} = \frac{1}{\left[1 + \frac{H_2 h_2}{(a - r_B)^2}\right]^{(1 + m)}}.$$

4.1.3) Asymmetric Bulging of a Tube into a Side Cavity

The theory considers the bulging of a tubular blank such that a side branch is formed having a diameter equal to that of the blank. The successive deformation mode is illustrated schematically in Figure 116.

During the initial process, the chord length **DEF** in the axial direction starts to form a radius of $\phi_L = \infty$ to ϕ_S. In the transverse direction the curved length starts to deform from $\phi_\bullet = r_0$ to ϕ_S. ϕ_S is the radius of curvature of the common spherical dome that is formed, with a height of H_S. This radius remains constant for the rest of the expansion process.

Referring to Figure 116, and considering the geometry in the axial direction:

$$r_0^2 = (2\phi_S - H_S)H_S \quad ,$$

$$\phi_S = 0.5(r_0^2/H_S + H_S) \quad ,$$

$$= \frac{r_0^2 + H_S^2}{2H_S} \qquad \text{.....(22).}$$

In the circumferential direction:

$$\phi_S = r_0 + H_S \qquad \text{.....(23),}$$

where H_S is the polar height of the dome when $\phi_L = \phi_\bullet = \phi_S$. Hence, combining equations (22) and (23):

$$r_0 + H_S = \frac{r_0^2 + H_S^2}{2H_S} \quad ,$$

$$2H_S r_0 + 2H_S^2 - H_S^2 - r_0^2 = 0 \quad ,$$

$$H_S^2 + 2H_S r_0 - r_0^2 = 0 \quad .$$

Solving this quadratic equation for H_S gives:

$$H_S = (\sqrt{2} - 1)r_0 \text{ or } (-\sqrt{2} - 1)r_0 \quad .$$

As H_S must be positive:

$$H_S = (\sqrt{2} - 1)r_0 \qquad \ldots\ldots(24).$$

Substituting H_S into equation (23):

$$\text{¢}_S = r_0 + (\sqrt{2} - 1)r_0 \quad ,$$

$$\text{¢}_S = \sqrt{2}r_0 \qquad \ldots\ldots(25).$$

During the initial stages of buckling, until the polar height becomes H_S, the thickness distribution along the profile in the axial direction is given by equation (21). At any intermediate stage the value of m is calculated from equation (18) using the prevailing values of ¢_L and $\text{¢}_\bullet$. When the spherical dome of height H_S has formed, with a radius of curvature ¢_S, then $\text{¢}_L = \text{¢}_\bullet = \text{¢}_S$ and therefore m = 1.

Hence, equation (21) becomes:

$$t = \frac{t_0}{\left[1 + \frac{H_S h_2}{(a - r_B)^2}\right]^2} \qquad \ldots\ldots(26).$$

This gives the thickness distribution along the deformed profile of the spherical cap.

4.1.4) Bulging After $\text{¢}_\bullet = \text{¢}_S$

Once a spherical cap of radius of curvature ¢_S is formed, any further expansion takes place in a mode depicted in Figure 116, such that part of the tubular branch is formed with a spherical cap of radius of curvature ¢_S.

An element 'dl' of the bulged spherical cap expands and takes the form of the ring element of the

tubular branch. Applying the principle of volume constancy,

$$2\pi x.dl.t = 2\pi r_0.dl.t_1 ,$$

where t_1 is the wall-thickness of the ring element of the tubular branch. Re-arranging and taking $\log_e$ yields,

$$\ln (r_0/x) + \ln (t_1/t) + \ln (dL/dl) = 0 \quad .....(27).$$

But, for this type of deformation, previous work by Hashmi(31) has shown that $\ln (r_0/x) = \ln (dL/dl)$ at any point, hence,

$$\ln (t/t_1) = \ln (r_0/x)^2$$

so that

$$t_1 = t.(x/r_0)^2 \quad .....(28).$$

Also, since $\ln (r_0/x) = \ln (dL/dl)$, we have

$$r_0/x = dL/dl.$$

But from the geometry, $x = \phi_S \sin\theta$ and $dl = \phi_S d\theta$,

hence, $\dfrac{r_0}{x} = \dfrac{r_0}{\phi_S \sin\theta} = \dfrac{dL}{\phi_S d\theta}$,

so that,

$$r_0 \operatorname{cosec}\theta d\theta = dL \quad .....(29).$$

Integrating equation (29) and noting that $L = 0$ for $\theta = \theta_0$ and $L = -L_0$ for $\theta = \theta_L$, the angle giving arc length $\phi_S\theta_L$ on the curved surface which actually forms the wall of the tubular branch of height L_0; we obtain:

$$\ln[\tan(\theta_L/2)/\tan(\theta_0/2)] = -[L_0/r_0] ,$$

which upon rearrangement gives:

$$\theta_L = 2\tan^{-1}[\tan(\theta_0/2)\exp(-L_0/r_0)] \quad .....(30).$$

Now substituting $(x/r_0) = (\phi_S \sin\theta_L/r_0)$ in equation (28), the wall thickness at the junction of the tubular branch of length L_0 and the spherical dome of radius of curvature ϕ_S is found to be,

$$t_L = (t\phi_S^2 \sin^2\theta_L)/r_0^2 \quad .....(31)$$

where t, which is the thickness on the curved surface at $\phi = \phi_L$, is given by equation (26) after substituting,

$$h_2 = h_{\phi L} = H_S - \mathcal{C}_S(1 - \cos\phi_L).$$

Once the value of the wall thickness at the junction of the tubular branch and the spherical cap is found, the thickness distribution along the spherical cap can be determined in the same manner as described above i.e.:

$$t' = \frac{t_L}{\left[1 + \frac{H_S h_\phi}{(a - r_B)^2}\right]^2} \qquad \text{.....(32)}$$

where t' is the wall thickness of the expanded spherical cap at a height of $h_{\phi L}$ from the junction of the tubular branch and the spherical dome - see Figure 116. $h_{\phi L}$ varies from 0 at the junction, to H_S at the tip of the dome.

4.1.5) The Effect of Axial Deformation

Feeding new material into the deformation zone has two effects on the resulting bulge. The deformation causes thickening of the wall along the whole length of the blank. During initial bulging, until the spherical dome is formed, this causes thickening along the cap. Once the spherical dome of height H_S and radius of curvature $\mathcal{C}_S$ is formed, any increase in the amount of axial deformation has no effect on the cap, but is simply used to form the tubular branch. The amount of deformation that affects the thickness of the spherical cap can be evaluated by equating the displaced volume

to the volume of the bulge.

Volume due to displacement $dx_1 = \pi r_0^2 dx_1$.

The volume of the spherical cap can be obtained by integrating the circular area πx^2, between the limits $(\phi_S - H_S)$ and ϕ_S i.e.

$$dV/dh = \pi x^2 = \pi(\phi_s^2 - h^2).$$

$$\text{Volume of the spherical cap} = \int_{\phi s - Hs}^{\phi s} \pi(\phi_s^2 - h^2)dx,$$

$$= \left[\pi(\phi_s^2 h - h^3/3)\right]_{\phi s - Hs}^{\phi s},$$

$$= \pi(-\phi_S^3/3 + \phi_S^2 H_S + (\phi_S - H_S)^3/3)$$

Equating the two volumes and substituting $\phi_s = 2.r_0$ and $H_S = (\sqrt{2} - 1)r_0$ gives:

$$dx_1 = 4\sqrt{2}.r_0/3 - 2r_0 + r_0/3,$$

$$= 0.219r_0 \qquad \text{.....(33).}$$

Therefore, the axial deformation will cause an increase in the wall thickness of the cap from the start of the deformation until the axial displacement of each end of the tube equals $0.219r_0$. After this, further axial deformation will contribute towards forming the wall of the tubular branch. The thickness distribution on the spherical cap along the longitudinal axis previously obtained is multiplied by the apparent strain factor to allow for the thickening that occurs. This apparent strain factor is given by the ratio of the original length to the compressed length of the blank.

Note that this applies for the forming of both

tee pieces and cross joints. For cross joints, the deformation occurring at each end of the tube is equated to the volumes of the two spherical caps formed. For tee pieces, half the deformation at the end of the tube is equated to the volume of the one spherical cap formed. The other half of the deformation contributes to the thickening of the main branch opposite the side branch.

Axial deformation in excess of dx_1 will contribute towards forming the wall of the tubular part of the branch. The wall thickness at the root of the branch will be governed by the apparent strain factor prevailing at that stage. As each plunger moves inwards by dx_2, the wall of the blank thickens, and hence, the resulting height, L_D of the branch formed from the deformation, becomes smaller than the axial displacement, dx_2. The relationship between dx_2 and L_D may be obtained by equating the displaced volume of the tubular branch formed, of height L_D and thickness varying from t_0 at the junction with the previously formed cap, to t' at the root. Thus:

$$dx_2 t_0 = L_D(t' + t_0)/2.$$

But $t' = f.t_0$ so that:

$$dx_2 t_0 = L_D t_0(1 + f)/2 \text{ which re-arranges to:}$$

$$L_D = 2dx_2/(1 + f) \qquad \ldots\ldots(34).$$

Hence, the length of the tubular branch formed, L_D, can be obtained from the apparent strain factor, f:

where $f = \dfrac{\text{original length of the blank}}{\text{deformed length of the blank}}$.

4.1.6) Application of the Theory

For different stages in the bulging process, different equations have to be used to determine the thickness distribution around the bulge. There are three different cases that can be obtained, which are:

1) the formation of a dome of height H_2, which is less than H_S, and of radius of curvature in the longitudinal direction, ϕ_L which is greater than ϕ_S,

2) the formation of a spherical dome of height H_S, and radius of curvature ϕ_S,

3) the formation of a spherical dome of height H_S, and radius of curvature ϕ_S, and a tubular branch of length L_0.

4.1.6.1) For Case 1

The equation that applies in this case is (21):

$$\text{i.e. } t = \frac{t_0}{\left[1 + \frac{H_2 h_2}{(a - r_B)^2}\right]^{(1+m)}} \qquad \ldots\ldots(21),$$

$$\text{where } m = \frac{(3 - 2\phi_\bullet/\phi_L)}{\phi_\bullet/\phi_L} \qquad \ldots\ldots(18),$$

and $a = r_0$.

4.1.6.2) For Case 2

For this case, when $\phi_L = \phi_\bullet = \phi_S$, equation (26) applies, i.e.,

$$t = \frac{t_0}{\left[1 + \frac{H_S h_2}{(a - r_B)^2}\right]^2} \qquad \ldots\ldots(26),$$

where $H_S = (\sqrt{2} - 1) r_0$.

4.1.6.3) For Case 3

This case involves rather more calculation than the previous two cases. The original cap has been further expanded to form a new cap and a tubular branch. Now considering an element that forms part of the junction between the spherical cap and the tubular branch. On the original cap this element would have been at an angle of ϕ_L. This angle can be evaluated from equation (30),

$$\phi_L = 2\tan^{-1}[\tan(\phi_0/2)\exp(-L_0/r_0)] \quad \ldots\ldots(30),$$

where $\phi_0 = \sin^{-1}(r_0/\ell_S) = \sin^{-1}(r_0/\sqrt{2}r_0) = 45^o$

This angle corresponds to a polar height, $h_{\phi L}$ on the original spherical cap of:

$$h_{\phi L} = H_S - \ell_S(1 - \cos\phi_L).$$

The wall thickness of this element on the original cap can now be obtained, using the equation used for Case 2, and substituting $h_2 = h_{\phi L}$ i.e.,

$$t = \frac{t_0}{\left[1 + \frac{H_S h_{\phi L}}{(a - r_B)^2}\right]^2}.$$

As the cap is expanded to form a tubular branch and a new cap, the elements on the original cap expand to form part of the junction. The new thickness of this element on the expanded cap can be found from:

$$t_L = (t\ell_S^2\sin^2\phi_L)/r_0^2 \quad \ldots\ldots(31).$$

Substituting for $\ell_S = \sqrt{2}r_0$ gives:

$$t_L = 2t\sin^2\phi_L.$$

The thickness around the new cap can be found using a similar method as Case 2:

$$t' = \frac{t_L}{\left[1 + \frac{H_S h_\bullet}{(a - r_B)^2}\right]^2} .$$

To evaluate the wall thickness along the tubular branch, the process to find t_L must be repeated.

4.1.6.4) The Effect of Axial Deformation

From the theory, the initial effect of the axial deformation is to cause thickening of the cap. This continues until:

$$dx_1 = 0.219 r_0 .$$

At this stage the deformed length of the blank will be:

$$\text{Deformed Length} = X_0 - 2.dx_1 .$$

The modified values for the wall thickness are obtained by multiplying the values previously obtained by the Apparent Strain Factor (f). This is given by the ratio of the original length over the deformed length of the blank:

$$f = X_0 / X .$$

To obtain the modified wall thicknesses, the original values need simply be multiplied by f. Any additional deformation will cause a tubular branch to be formed. The theoretical length of this branch can be calculated from the amount of deformation (see Figure 117).

4.2) Theoretical Prediction of Axial Load

The following theory considers the axial load required to cause a given shortening of a cylindrical tube. The reduction in the length of the tube, the yield stress of the material, and the co-efficient of friction between the tube and the die-block are taken into account.

4.2.1) Theoretical Analysis

From the analysis of the domed portion of a thin shell, it can be shown that:

$$\frac{\sigma_{\phi}}{r_1} + \frac{\sigma_{\theta}}{r_2} = \frac{P}{t} \qquad \ldots\ldots (35)$$

However, Tresca states that

$$\sigma_y = |(\sigma_{maximum} - \sigma_{minimum})|.$$

For the case of a hemispherical dome:

$\sigma_{\phi} = \sigma_{\theta}$ and are tensile, thus:

$$\sigma_y = |(-\sigma_{\phi} + \sigma_{\theta})| \text{ or } |(0 + \sigma_{\theta})| \text{ or } |(-\sigma_{\phi} - 0)|,$$

$$= 0, \sigma_{\phi} \text{ or } \sigma_{\theta}.$$

Hence, replacing σ_{ϕ} and σ_{θ} with σ_y in equation (35) gives:

$$P = \sigma_y . t . \left[\frac{1}{r_1} + \frac{1}{r_2}\right] .$$

Now, considering a cylindrical tube as shown in Figure 118a, and taking an element at a position x, as shown in Figure 118b, and resolving forces in the axial direction gives:

$$\pi . D . t_0 . \sigma_x - \pi . D . t_0 . (\sigma_x + d\sigma_x) + \mu . N . dx . \pi . D = 0 ,$$

$$- \pi . D . t_0 . d\sigma_x + \mu . N . dx . \pi . D = 0 ,$$

$$- t_0.d\sigma_x + \mu.N.dx = 0 \ ,$$

$$d\sigma_x = \frac{\mu.N.dx}{t_0} \qquad \ldots\ldots (36)$$

Integrating equation (36) with respect to x gives:

$$\sigma_x = \frac{\mu.N.x}{t_0} + C \ .$$

Now if it is assumed that N is equal to P,

$$\sigma_x = \frac{\mu.P.(x)}{t_0} + C \ .$$

Assuming the initial conditions of x=0, Tresca gives:

$$\sigma_y = |(\sigma_x - P)| \text{ or } |(0 - \sigma_x)| \text{ or } |(P - 0)|$$

However, for this case $\sigma_x \gg P$ thus:

$$\sigma_y = \sigma_x \ .$$

Therefore,

$$\sigma_y = \frac{\mu.P.(0)}{t_0} + C \ ,$$

hence, $C = \sigma_y$,

and $$\sigma_x = \frac{\mu.P.x}{t_0} + \sigma_y \qquad \ldots\ldots (37)$$

However, replacing P from equation (35) gives:

$$\sigma_x = \frac{\mu.x.(\sigma_y.t.\left[\frac{1}{r_1} + \frac{1}{r_2}\right]}{t_0} + \sigma_y \ .$$

However, x can be expressed as (X - a) thus:

$$\sigma_x = \sigma_y.(\frac{\mu.(X - a).t.\left[\frac{1}{r_1} + \frac{1}{r_2}\right]}{t_0} + 1) \qquad \ldots\ldots (38)$$

Equating forces in the axial direction gives:

$$F = \pi.D.t_0.\sigma_x + \frac{\pi}{4}.(D - 2.t_0)^2 P \qquad \ldots\ldots (39)$$

Replacing σ_x in equations (38) and (39) gives:

$$F = \pi.D.t_0.\left[\frac{\sigma_y.(\mu.(X - a).t.\left[\frac{1}{r_1} + \frac{1}{r_2}\right] + 1)}{t_0}\right] + \frac{\pi.(D - 2.t_0)^2}{4}.\left[\sigma_y.t.\left[\frac{1}{r_1} + \frac{1}{r_2}\right]\right] \quad \ldots (40)$$

However, for a pure hemisphere, $r_1 = r_2 = a$, thus:

$$F = 2.\pi.a.t_0.\left[\frac{\sigma_y(2.\mu(X - a).t + 1)}{a.t_0}\right] + \pi.(a - t_0)^2.\left[\frac{2.\sigma_y.t}{a}\right]$$

$$F = \pi.\sigma_y.\left[4.\mu.(X - a).t + 2.a.t_0 + \frac{(a - t_0)^2.2.t}{a}\right] \quad \ldots (41)$$

From the geometrical analysis of a tee piece, Case 2 gave the wall thickness t as,

$$t = \frac{t_0}{\left[1 + \frac{H_2 h_2}{a^2}\right]^2}.$$

At the top of the dome, $H_2 = h_2$, therefore,

$$t = \frac{t_0}{\left[1 + \frac{H_2^2}{a^2}\right]^2}.$$

Also, for a hemisphere, $H_2 = a$, thus,

$$t = \frac{t_0}{\left[1 + \frac{a^2}{a^2}\right]^2}.$$

$$t = \frac{t_0}{4} \quad \ldots\ldots (42)$$

Combining equations(41) and (42) gives:

$$F = \pi.\sigma_y.[\mu.(X - a).t_0 + 2.a.t_0 + \frac{(a - t_0)^2.t_0}{2}] \quad \ldots.(43)$$

From compression tests carried out on copper rings (see Chapter 3), it can be shown (Figure 60) that:

$$\sigma_y = [340 + 9350.(X_0 - X)] \times 10^6 \quad \ldots\ldots(44),$$

and thus equation (43) becomes:

$$F = \pi.[(340+9350(X_0-X).10^6)].[\mu(X-a)t_0+2at_0+\frac{(a-t_0)^2t_0}{2}]$$

If it is assumed that the volume of metal lost by the reduction in length in the tube is gained by the side-branch (since the radius of the branch is the same as the tube), it can also be assumed that the area over which friction acts is constant throughout the process. Therefore, equation (43) is modified to:

$$F = \pi.\sigma_y.[\mu.(X_0 - a).t_0 + \frac{(a - t_0)^2.\ t_0}{2}] \quad \ldots\ldots(45)$$

4.3) Comparison of the Theoretical and Experimental Results

4.3.1) Analysis of Wall Thickness Distribution

As has been previously illustrated, the bulge can be formed in three ways - Case 1, 2 or 3. It is possible that each case could produce a branch of the same length, e.g. suppose a branch length of 15 mm is produced. This could be made up of:

Case 1) a cap of height 3 mm, and a tubular branch formed from axial deformation 12 mm long,

Case 2) a cap of height 5 mm, and a tubular branch formed from axial deformation 10 mm long or,

Case 3) a cap of height 5 mm, a tubular branch formed from the cap of length 3 mm, and a tubular branch formed from axial deformation 7 mm long.

In order to decide on how the branch has been formed, the theoretical predictions are based on the amount of axial deformation occurring. Knowing the original and final lengths of the tube blank, the theoretical length of the tubular branch formed from the deformation can be obtained from equation (34). Also, the theoretical height of the spherical cap, H_S, is known (5.00 mm for the tubes with a radius of 12.06 mm). Therefore, subtracting the theoretical branch length from the actual length of the branch will leave the height of the cap or the height of the cap and the tubular branch formed from it. Comparison of this height with the value of H_S will determine which

case the example falls into i.e.,

Case 1) where the height of the cap is less than H_S,

Case 2) where the height of the cap equals H_S or,

Case 3) where the height of the cap is greater than H_S, and in which the length of the tubular branch expanded from the cap, L_0, is the difference between the height of the cap and H_S.

With this informatiom it is possible to predict the wall thickness distribution around the bulge. A computer program was used to plot the experimental results, and also calculate the theoretical distributions (see Appendix 1).

For each component, this program initially evaluates the theory as Case 2, and then compares the heights of the branch as previously mentioned, and evaluates a second time to deduce whether a Case 1 or Case 3 example is also required. However, the theory used in predicting the Case 3 examples tended to predict impractical values when there was a large amount of deformation (over 50% reduction in tube blank length). The theory would predict a bulge height of the correct magnitude, but would give a wall thickness distribution at this point of about 5% to 10%. Therefore, a loop was added to the program so that if this occurred, only the values of wall thickness distribution coinciding with those for Case 2 would be used (i.e. if Case 2 predicted a minimum wall thickness

distribution of 45%, then only the values calculated to that point in Case 3 would be used).

The graphical outputs show a plot of the actual values with solid lines, and the theoretical values with dashed lines. There are three types of theoretical plots (Figure 119):

Case 2) when there is a single dashed line,

Case 1 and Case 2) when there is one dashed line with another two lines coming from it. The Case 2 distributions always predict a larger value of '**Y**' (i.e. the Case 2 line always lies to the right of the Case 1 line),

Case 2 and Case 3) when there is a single straight line with two lines coming from it, and where one of them consists of two stages.

The program was used to give theoretical predictions for four values of branch radius (2 mm, 3 mm, 4 mm and 5 mm). Graphs are presented which depict the theoretical and practical distributions for all of the internal pressures for each of the axial loads. As stated previously, the final lengths of components formed with a given axial load are approximately the same, irrespective of the internal pressure used. Hence, the final lengths of the components formed with each of the axial loads were averaged, and this value used to obtain the theoretical distribution. However, the theory also requires a value for bulge height, in order to determine which case(s) to use. Therefore, the maximum value (for an internal pressure of 62.10 N/mm^2)

was inputted, so that the theoretical line gave a minimum value of the wall thickness ratio. However, although the line predicted the bulge height of a component formed with 62.10 N/mm^2 of pressure, the trend was still correct for the lower pressures, and hence the wall thicknesses were correct for the respective bulge heights.

Each graph has the values inputted to the theoretical equations displayed in the top right-hand corner, and the test numbers of the experimental data and the internal pressures used in forming displayed in the bottom left-hand corner (Figure 119).

4.3.1.1) Tee Piece with a Branch Radius of 2 mm

All of the test numbers used in the branch radius comparisons have a similar structure (i.e. T201 refers to a tee piece [T], with a branch radius of 2 mm [2], and an individual test number of 1 [01]). There are twenty-four sets of results for each of the radii, although not all appear on the graphs, as those which ruptured or buckled were ignored.

With an axial load of 85 kN, and a range of internal pressures from 27.60 N/mm^2 to 62.10 N/mm^2 (Figure 120), there is close agreement at Y=0 and Y=h (the bulge height), although there is a variation in the central section, where the theory predicts a larger value of 'Y' than was infact the case.

An axial load of 106 kN produced tee pieces over a range of internal pressures from 34.50 N/mm^2 to 62.10 N/mm^2 (Figure 121). The values are similar at

Y=h, although at Y=0 the theory predicts a larger value of wall thickness. This variation remains constant for the analysis of the branch (the first stage of the theoretical line), but the lines converge when the theory analyses the dome (the second stage).

An axial load of 128 kN (Figure 122) gave similar results to those of 106 kN, except that for the analysis of the dome, the lines converge and then separate, so that at Y=h, the theory predicts a smaller bulge height than was in fact the case.

With an axial load of 149 kN (Figure 123) there is the least agreement. At Y=0 the theoretical results are about 50% larger than the experimental results, and at the minimum value of the percentage of original wall thickness, the theory predicts a bulge height of half the value of the experimental results.

4.3.1.2) Tee Piece with a Branch Radius of 3 mm

For an axial load of 85 kN and internal pressures from 27.60 N/mm^2 to 62.10 N/mm^2 (Figure 124), the theoretical predictions are similar to those with a 2 mm branch radius, with good agreement at Y=0 and Y=h.

With an increased axial load of 106 kN, and the same pressure range (Figure 125), there is close agreement at Y=h, but discrepancies at Y=0. As in the previous cases, the theory predicts higher values of wall thickness over the length of the branch.

An axial load of 128 kN and the above pressure range (Figure 126) gave the same trends as the 106 kN axial load.

With a 149 kN axial load, and the above pressures (Figure 127), there is a higher degree of inaccuracy, especially for Y=0. As in the case of the 2 mm branch radius, at the higher axial loads the theory predicts smaller bulge heights than was infact the case. With the lower internal pressures, the bulge height prediction at Y=h is not as inaccurate as at the higher values.

4.3.1.3) Tee Piece with a Branch Radius of 4 mm

An axial load of 85 kN and internal pressure range from 27.60 N/mm^2 to 62.10 N/mm^2 (Figure 128) gives a higher degree of accuracy at the lower pressures, and as the pressure increased, the lines converge to give a close agreement at Y=h.

For an axial load of 106 kN and the same internal pressure range as above (Figure 129), the trends are also similar, except that there is a discrepancy at the lower values of 'Y' as is seen for the other radii.

A 128 kN axial load (Figure 130) gives some inaccuracies over the branch length, but there is convergence at the dome.

With an axial load of 149 kN and internal pressure range from 27.60 N/mm^2 to 55.20 N/mm^2 (Figure 131), the theory gives the best predictions for this axial load so far. There is the usual inaccuracy over the branch length, but the lines do converge at the dome. The theory still predicts a smaller value for the bulge height than is infact the case

4.3.1.4) Tee Piece with a Branch Radius of 5 mm

An 85 kN axial load and internal pressure range from 27.60 N/mm^2 to 62.10 N/mm^2 (Figure 132) gives accuracy over the whole range of 'Y' values.

With the 106 kN axial load and the same pressure range as above (Figure 133), there is some degree of inaccuracy in the predictions of the wall thickness over the branch length, but close correlation at the dome, with the exception of the high pressures where there are some discrepancies.

The 128 kN axial load (Figure 134) gives similar results to the above.

With 149 kN axial load and internal pressures from 27.60 N/mm^2 to 55.20 N/mm^2 (Figure 135) there is inaccuracy over the branch length, but convergence at the dome. The bulge height predicted was less than those obtained experimentally, and the difference increased with pressure.

4.3.2) Discrepancies in the Theoretical Predictions

The theory gives similar trends over the four branch radii used, and the inclusion of the branch radius in it has improved the accuracy.

For tee pieces formed from low axial loads, the theory gives reasonable agreement with the experimental results. However, as the load is increased, greater discrepancies occur, especially in the calculation of the final bulge height. This is due to the alterations made in the program when calculating Case 3. Without the alteration, the theory would have

predicted the bulge heights much more accurately, but for values of wall thickness which testing had shown to be impossible (5% to 10% compared to known minimums of around 50%). In the examples where Case 3 is used, the approximations are better than those obtained using Case 1 or Case 2. However, in general, Case 2 gives the best approximations over the full range of axial loads and internal pressures.

At the higher values of axial load, there are greater inaccuracies in the wall thickness predictions. The theory gives a basic straight line representation of the reduction in the wall thickness along the branch, which is not representative at high axial loads, when a large amount of deformation takes place. The theory calculates the wall thickness from the intersection of the branch and the tube to the start of the dome, and does not take into account the metal which has built up along the length of the tube. Therefore, the theory estimates a higher value of wall thickness at Y=0 than is in fact the case. As the distribution along the branch is a straight line, this error affects all of the values (thus, the theoretical prediction runs parallel and above the experimental data for the length of the branch). It is not until the theory is used to calculate the dome thickness distribution that the practical and theoretical lines converge.

Another discrepancy is caused by the high internal pressures bulging the dome of the branch after

the end of the axial deformation. This exaggerates the bulge height and adds to the inaccuracy caused by the above. This high internal pressure also expands the dome so that it is no longer a circular arc (which is an assumption on which the theory is based).

Finally, although the geometrical analysis allows for variations in the branch radius, there is no relationship with the coefficient of friction between the die-blocks and the tube, or the strain-hardening properties of the material (which increases during deformation).

4.3.3) Analysis of the Axial Load Estimations

This theory allows for the effect of friction and strain-hardening in the bulge forming process, and estimates the axial load required to produce a specific reduction in the tube length.

The assumptions made are that:

1) the bulge is a hemispherical thin shell,

2) the stresses in the tube are compressive, and those in the bulge, tensile and,

3) the reduction in length of the tube is equal to the increase in height of the bulge.

A computer program was written to produce a full range of values of the axial loads required to produce given reductions in length of the tube, for a range of coefficients of friction. Two sizes of tubes were selected for comparison:

1) 94.14 mm in length, 16.86 mm outside diameter, and 0.95 mm wall thickness, and,

2) 107.00 mm in length, 24.12 mm outside diameter, and 1.37 mm wall thickness.

The values obtained were depicted graphically and then experimental data was plotted to give a comparison (Figures 136 to 139). For low values of 'X', the theoretical lines gives accurate representations of the actual loads measured, but as the value of 'X' (the reduction in length of one half of the tube) increases, the theoretical predictions of the axial loads are lower than the experimental data. This occurs for both of the sizes of tubes analysed (Figures 136 and 138), and there is approximately 40% difference for a reduction in length of the tube of 50%.

The programme was run again, except that assumption (3) was made. This time the theory predicts higher axial loads for the larger reductions in 'X', but retains the same accuracy for the small reductions. For both types of tube (Figures 137 and 139), the estimations are substantially closer than the initial theory, with an error of between 15% to 20% for a reduction in length of 50%.

4.3.4) Discrepancies in the Axial Load Theory

The initial theory predicts loads which have the same trends as the experimental data. Although accuracy is attained for the lower values of 'X' (up to 25% deformation of the tube), the predictions are highly inaccurate for the higher values, with the practical and theoretical lines diverging (the theoretical values are less than those obtained

experimentally). The theoretical values of axial load calculated using different co efficients of friction agree with those obtained from the lubricant tests, in that the axial loads required to give specific reductions in length reduce with the value of the co-efficient of friction.

The main reason for the discrepancy is that the friction in the branch is overlooked. This will not create a noticeable inaccuracy for small values of bulge height, but will as the value increases. By assuming that the reduction in length of the tube is equal to the increase in height of the bulge (which is approximately correct if the metal required to form the dome is overlooked), the theory can be adjusted to take account of the friction acting between the bulge and the die-branch. The effect of this is to leave the initial values relatively unchanged, but increase the subsequent values proportionally (the lines start from the same point, but have steeper positive gradients). The values obtained from the theory are now closer, and although the lines still diverge (with the theory under-estimating the axial load), there is some form of agreement.

The inaccuracies in the theory stem from the assumptions made in setting up the equations. That is, the bulge does not remain a hemisphere, but becomes a hemisphere on top of a branch. Also, the walls of the cylindrical tube do thicken towards the deformation zone. In addition, although the stresses in the tube

remain in hydrostatic compression, those in the bulge do not remain equal when the bulge shape changes. This affects the determination of σ_x in the final equation. However, the theory still provides a method of judging the required axial load necessary to produce a given reduction in the length of the tube.

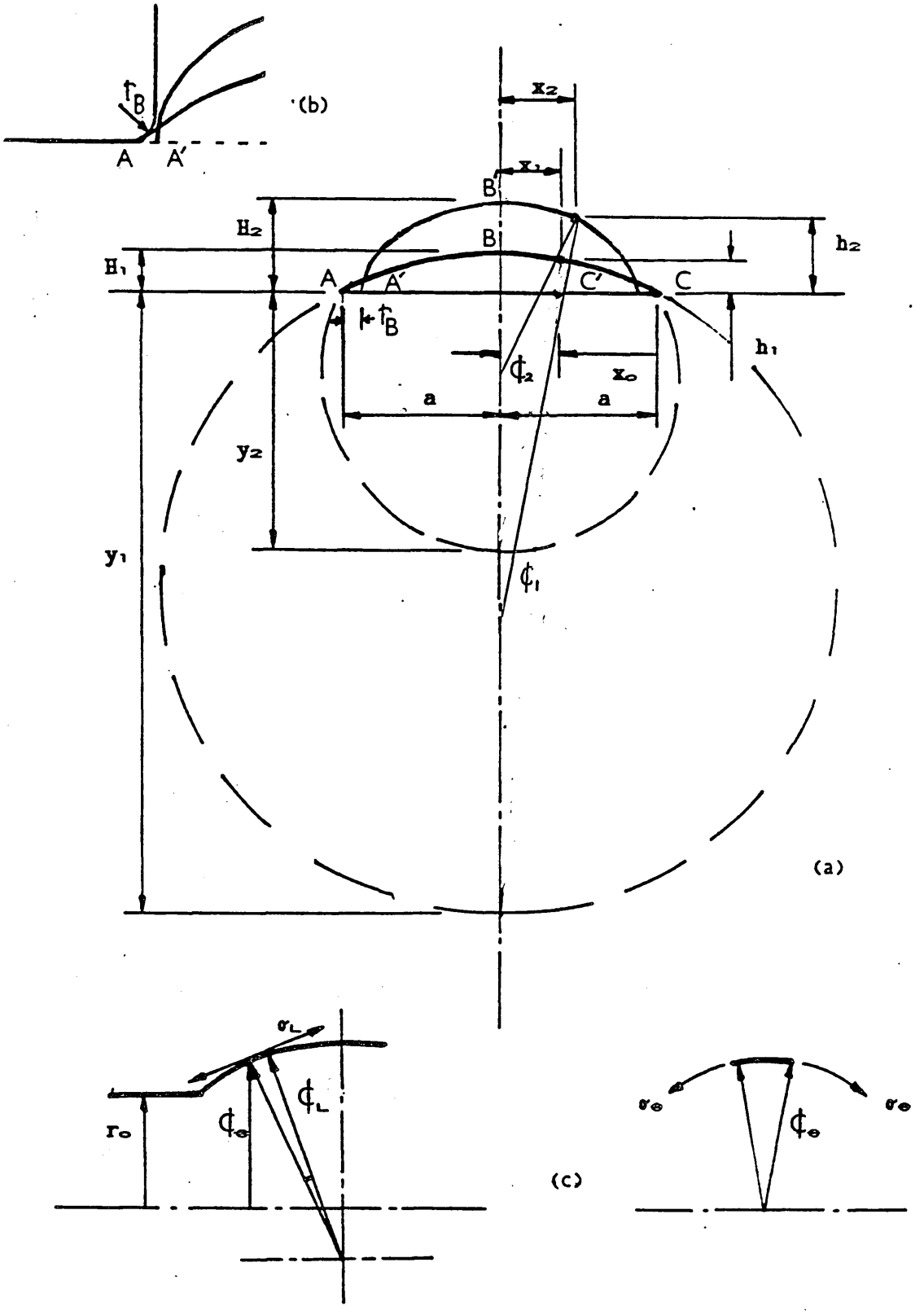

FIGURE 115

(a) The Geometric Expansion Mode Of A Circular Arc.

(b) The Branch Radius.

(c) The Force Equilibrium.

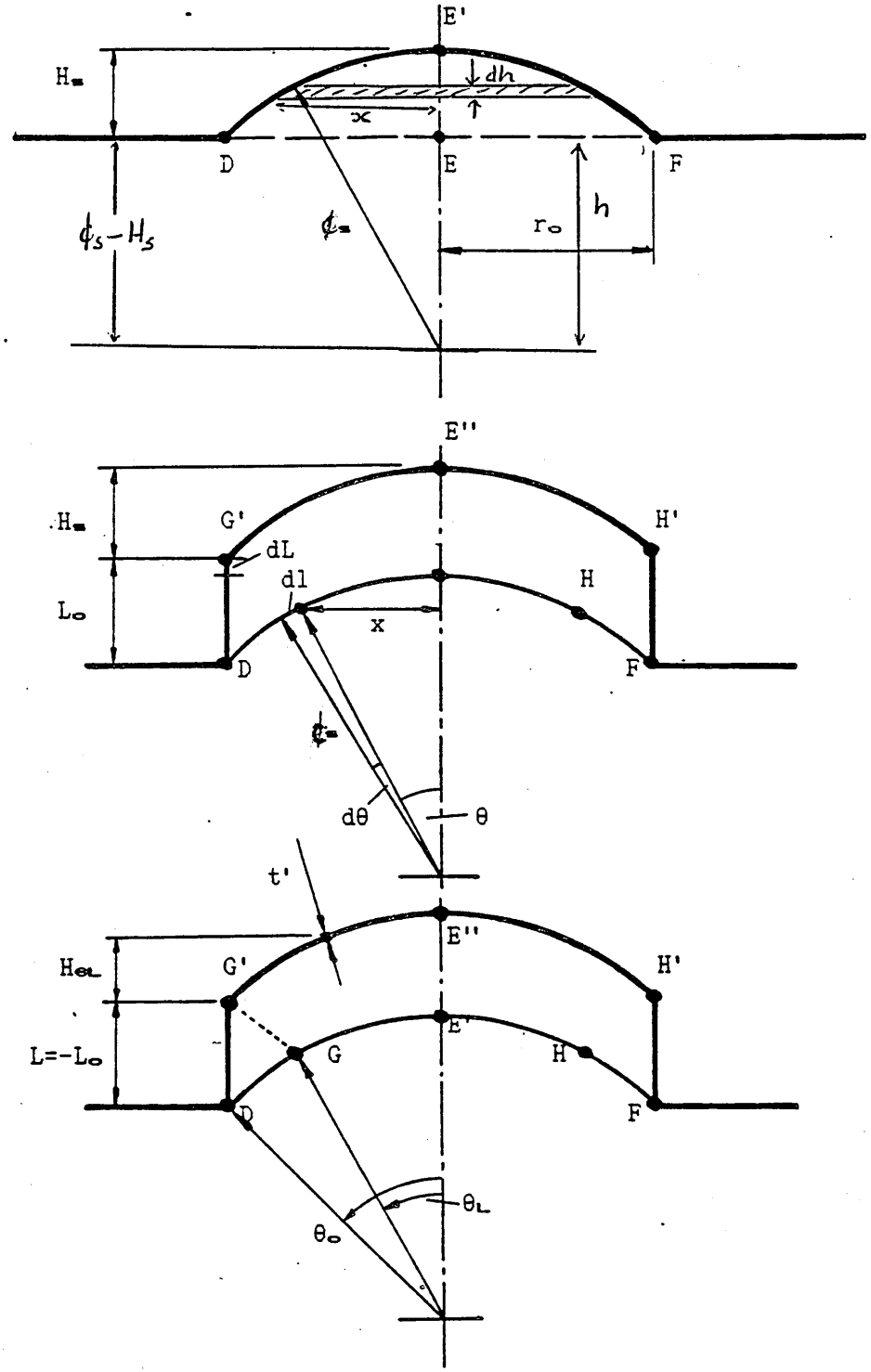

FIGURE 116

The Formation Of A Tubular Branch.

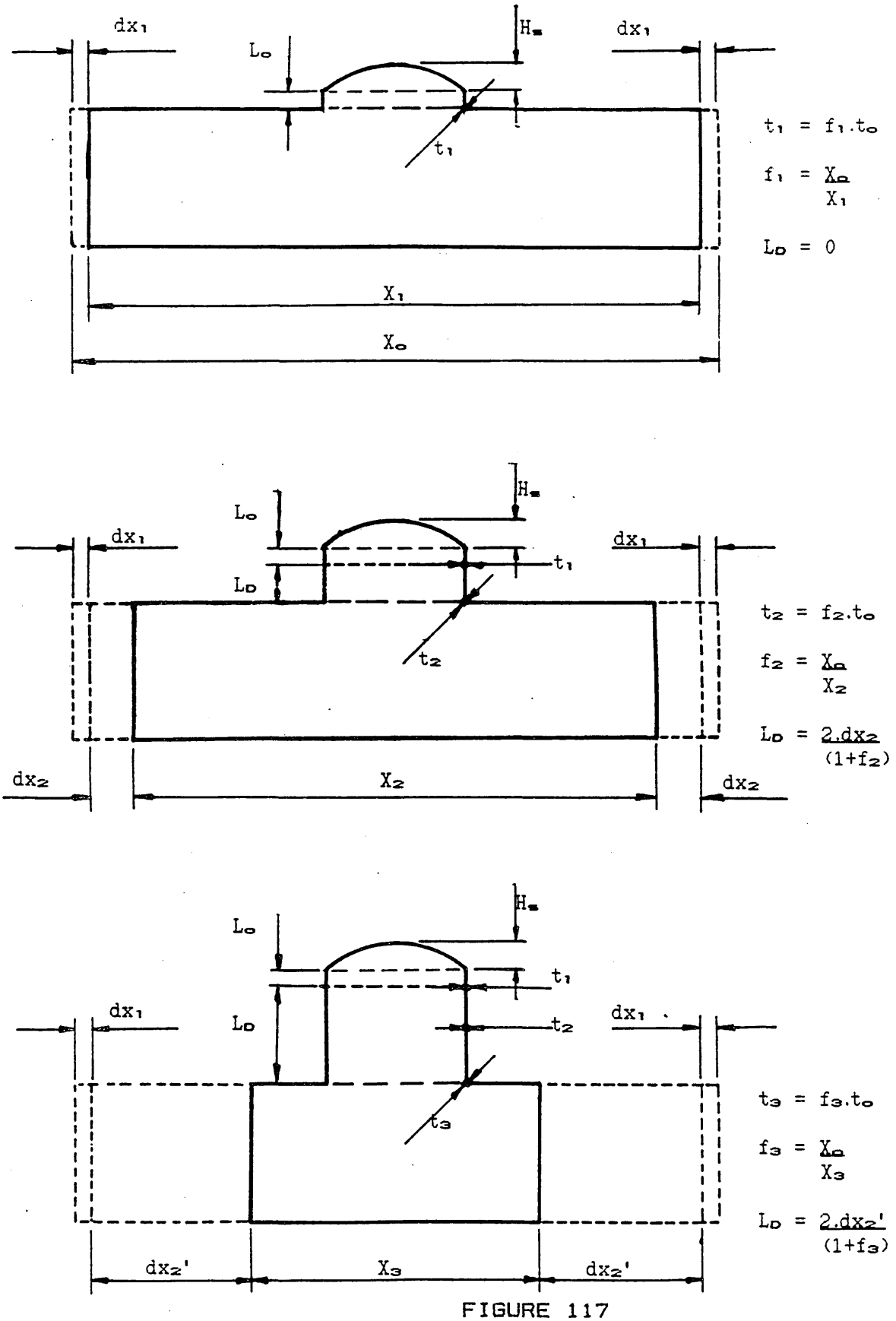

FIGURE 117

The Effect Of Axial Deformation During Forming.

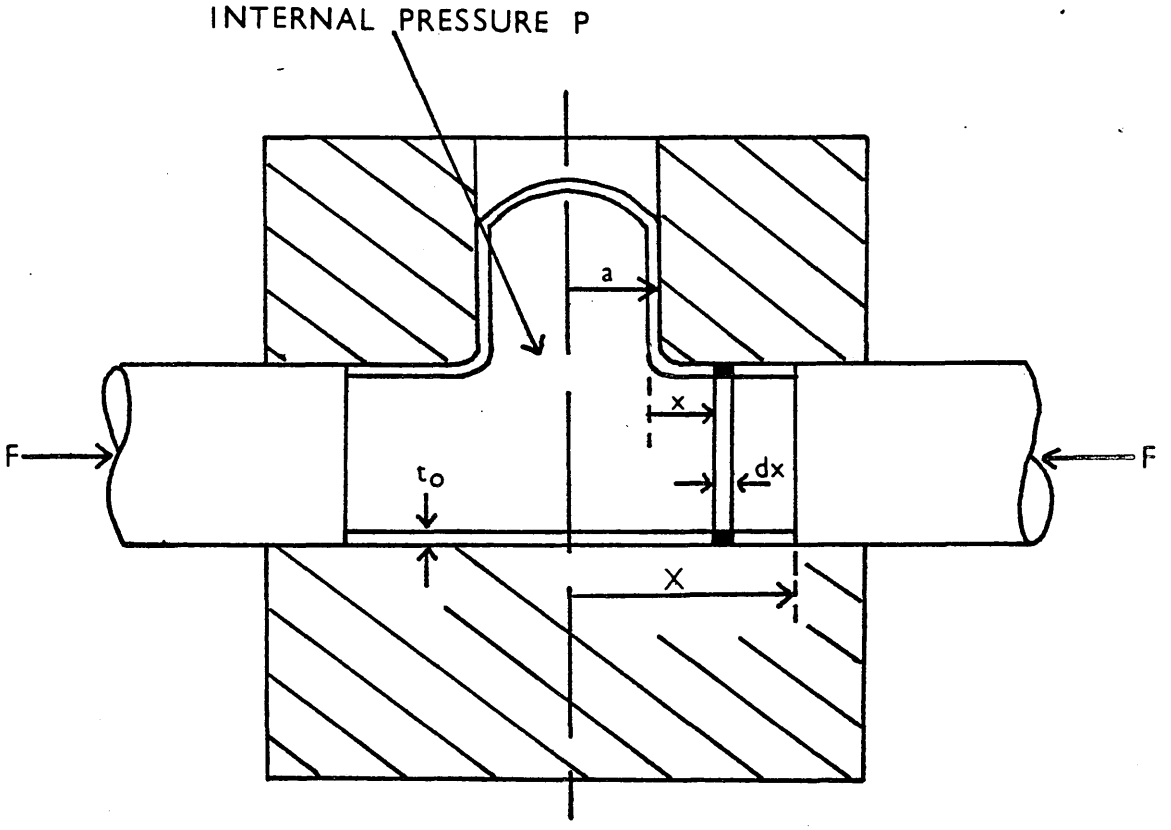

FIGURE 118(a)

A Tee Piece During Forming.

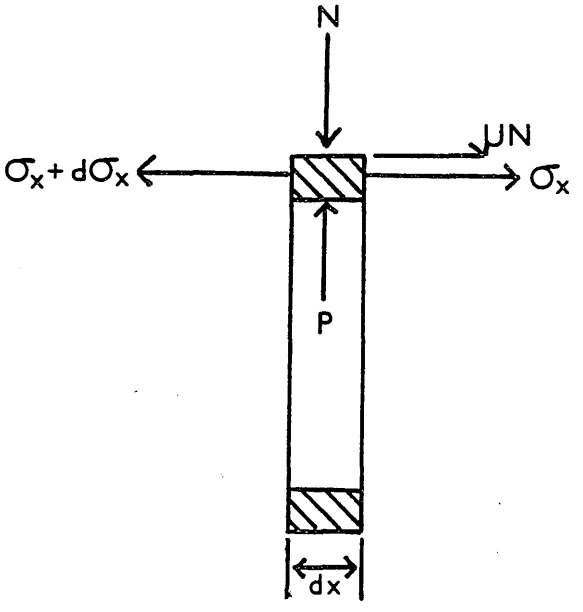

FIGURE 118(b)

Element Of Tee Piece During Forming.

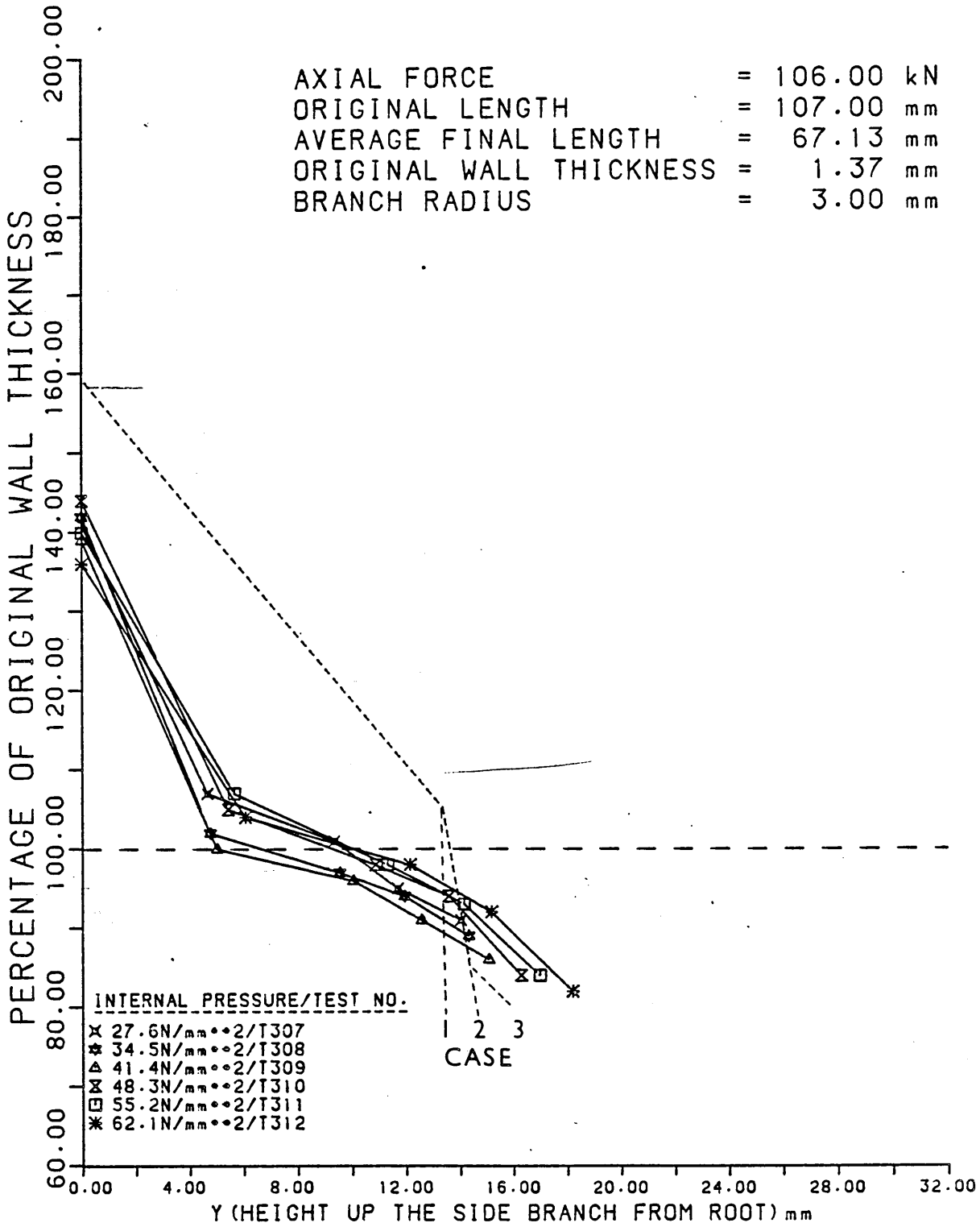

FIGURE 119

The Wall Thickness Distributions Along The Side Branches And Domes Of Tee Pieces Formed At Various Internal Pressures For Experimental And Theoretical Results.

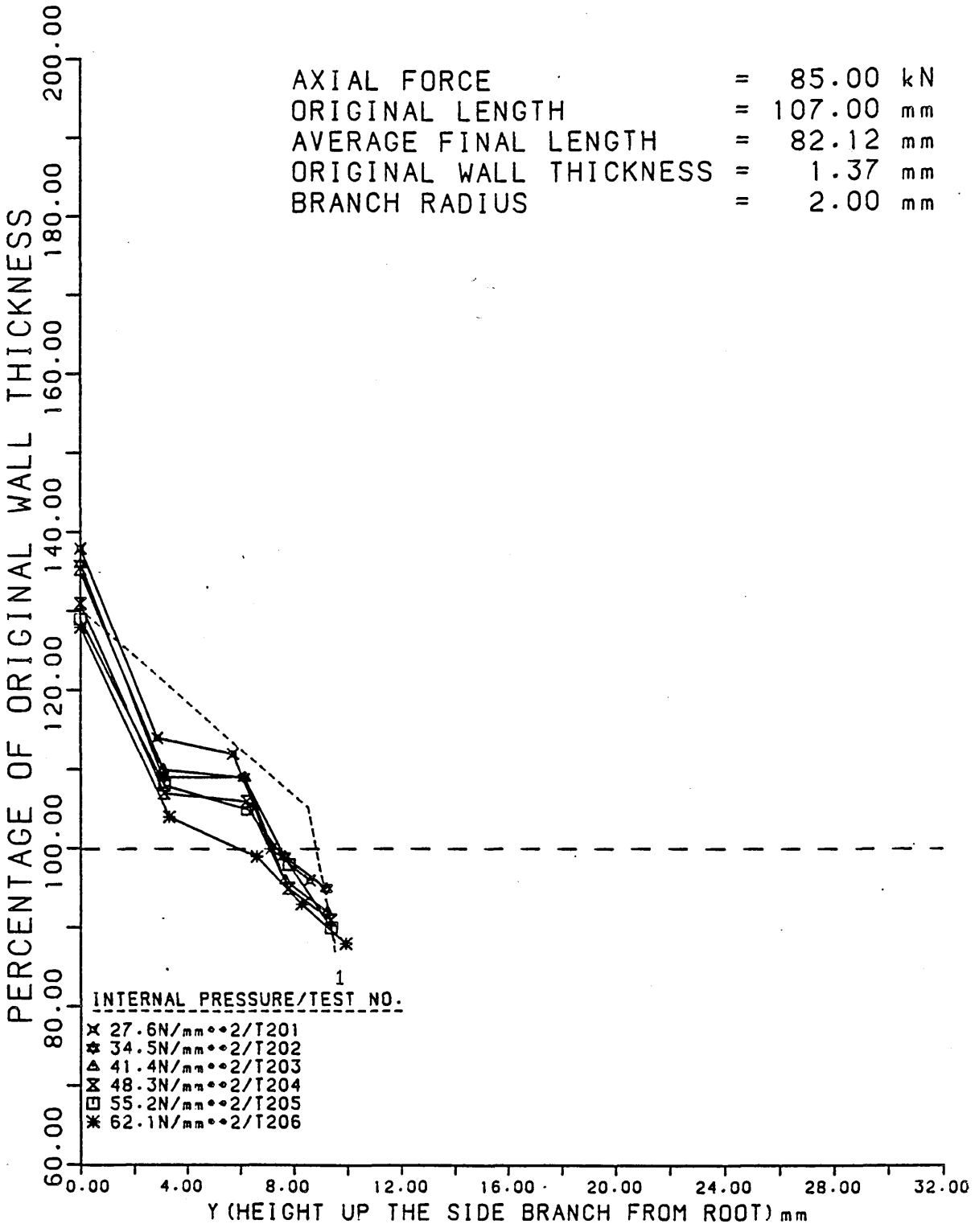

FIGURE 120

The Wall Thickness Distributions Along The Side Branches And Domes Of Tee Pieces Formed At Various Internal Pressures For Experimental And Theoretical Results.

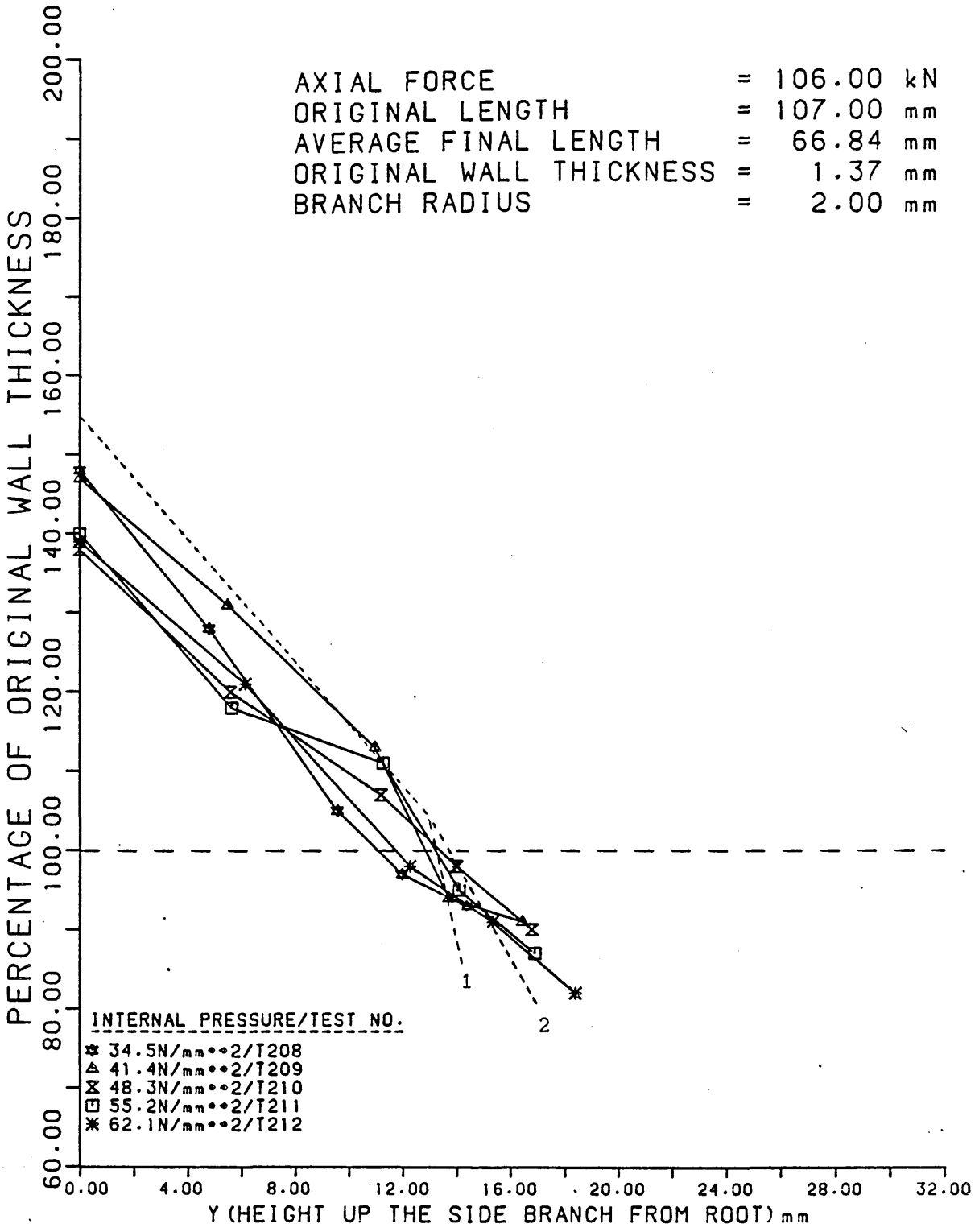

FIGURE 121

The Wall Thickness Distributions Along The Side Branches And Domes Of Tee Pieces Formed At Various Internal Pressures For Experimental And Theoretical Results.

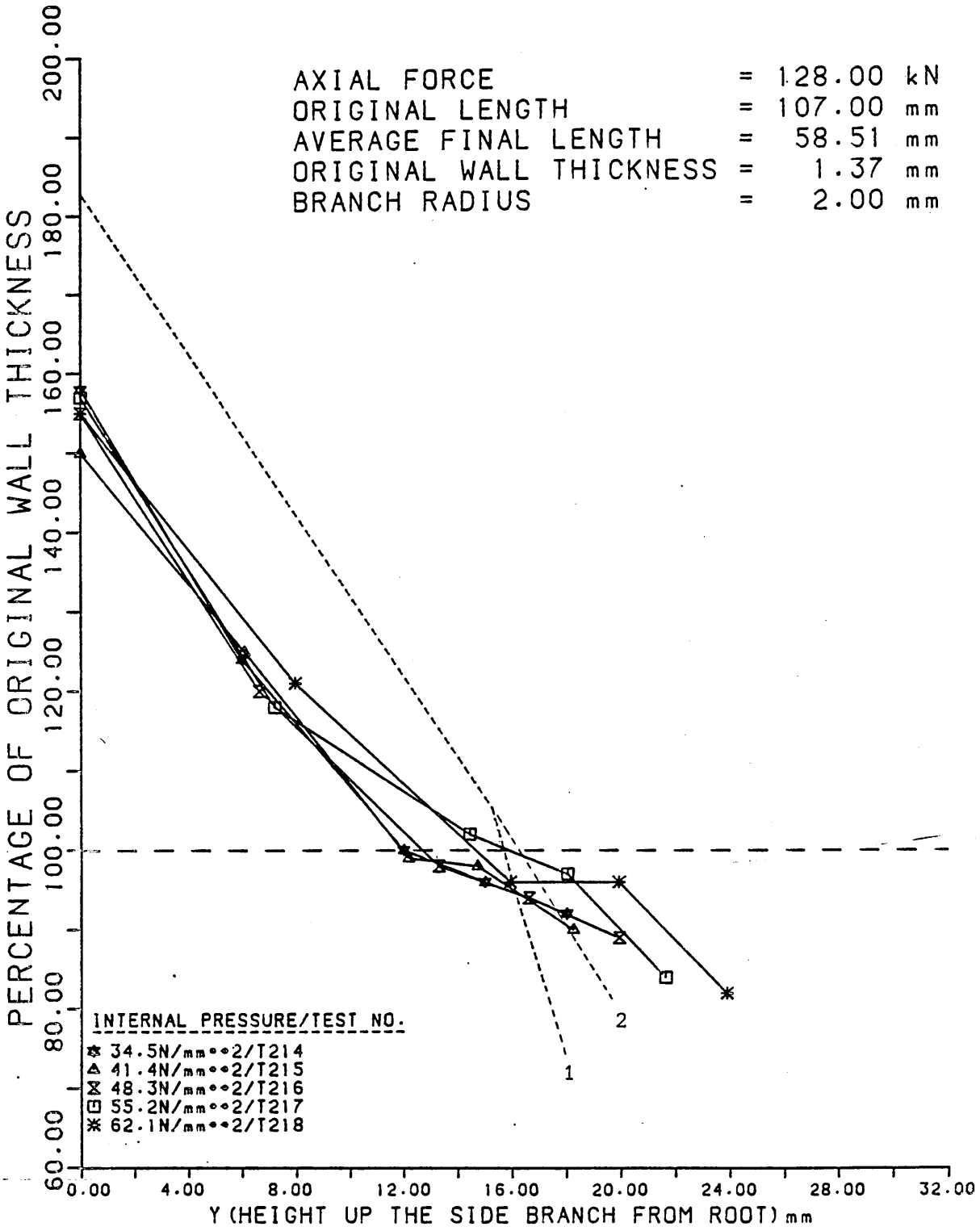

FIGURE 122

The Wall Thickness Distributions Along The Side Branches And Domes Of Tee Pieces Formed At Various Internal Pressures For Experimental And Theoretical Results.

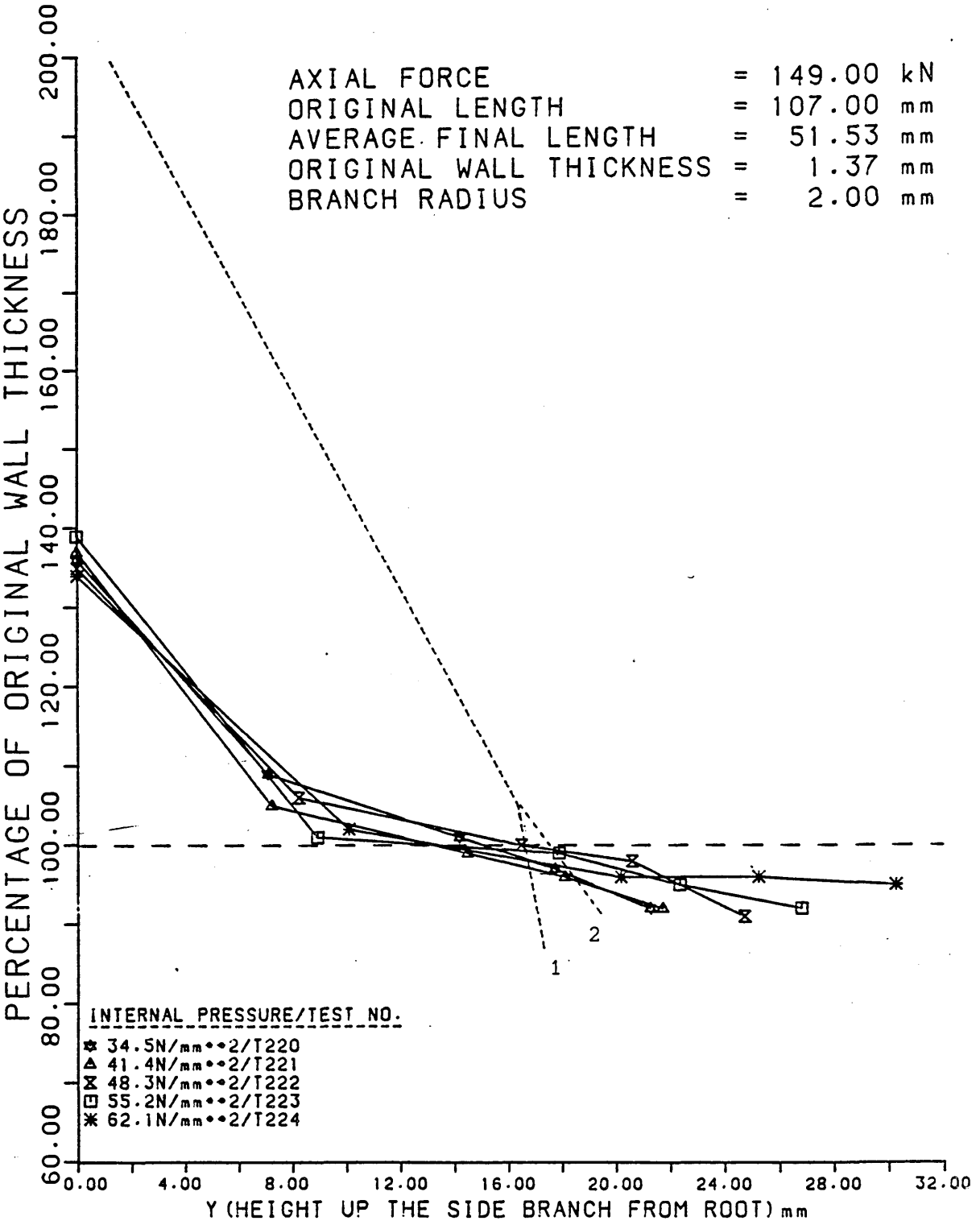

FIGURE 123

The Wall Thickness Distributions Along The Side Branches And Domes Of Tee Pieces Formed At Various Internal Pressures For Experimental And Theoretical Results.

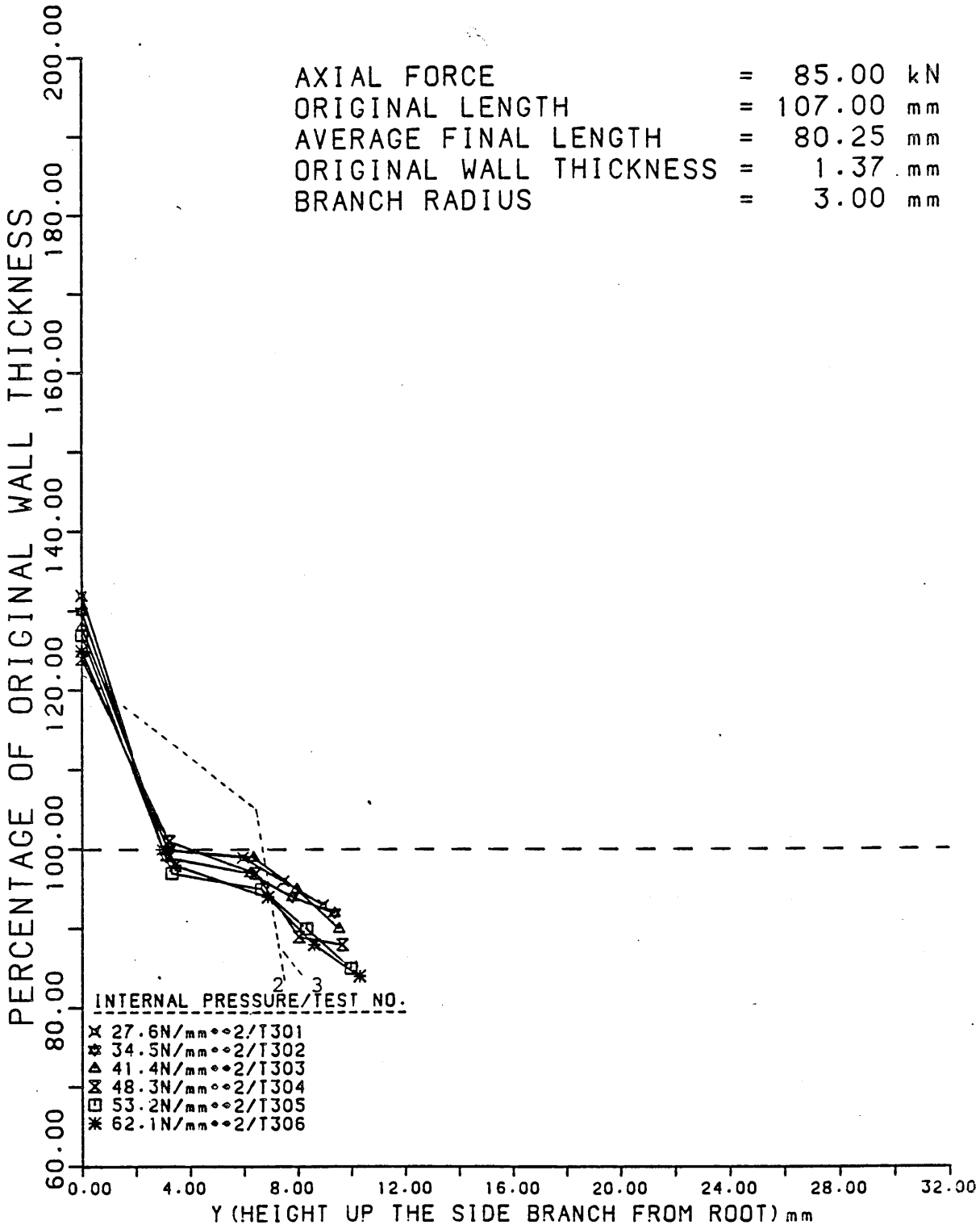

FIGURE 124

The Wall Thickness Distributions Along The Side Branches And Domes Of Tee Pieces Formed At Various Internal Pressures For Experimental And Theoretical Results.

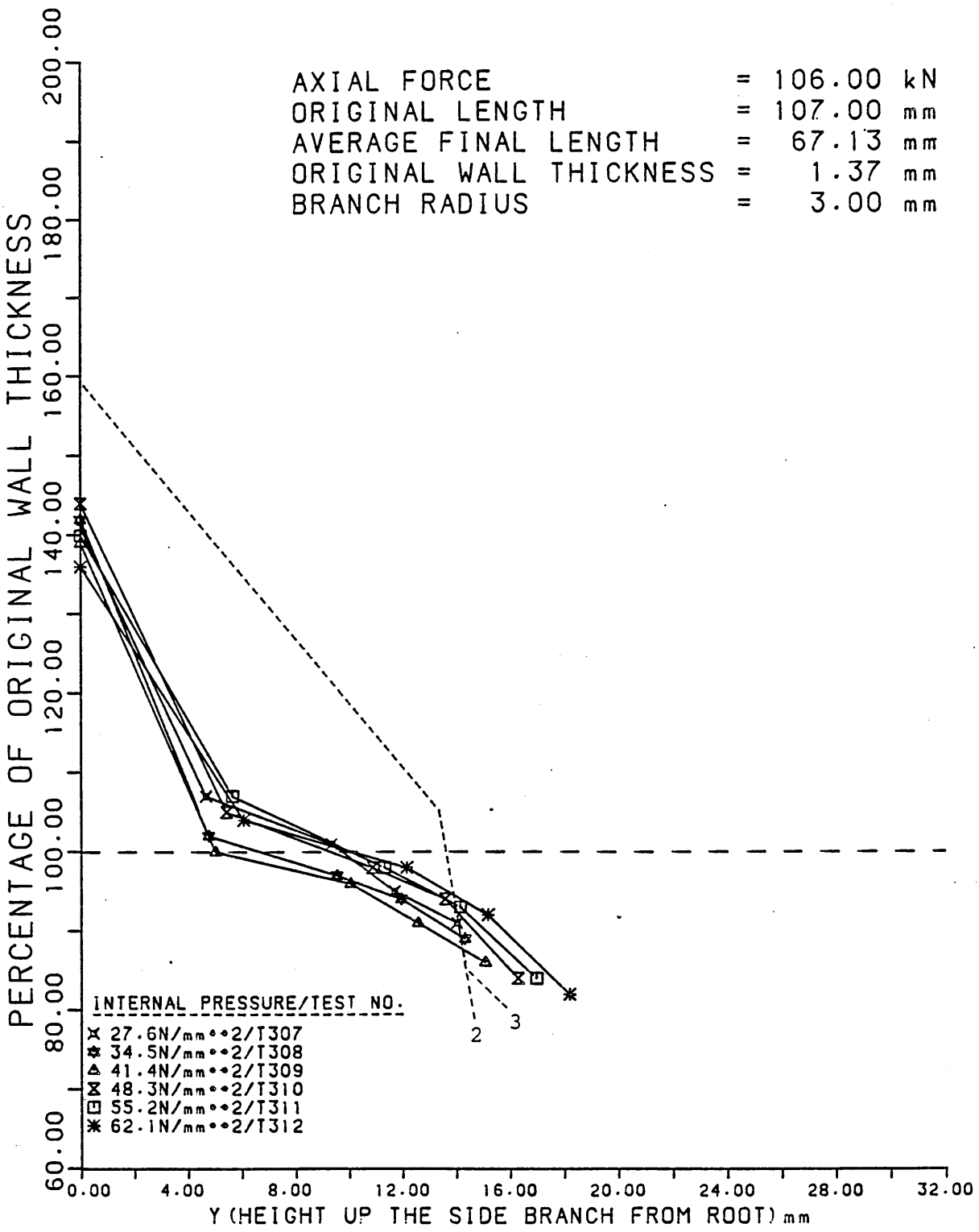

FIGURE 125

The Wall Thickness Distributions Along The Side Branches And Domes Of Tee Pieces Formed At Various Internal Pressures For Experimental And Theoretical Results.

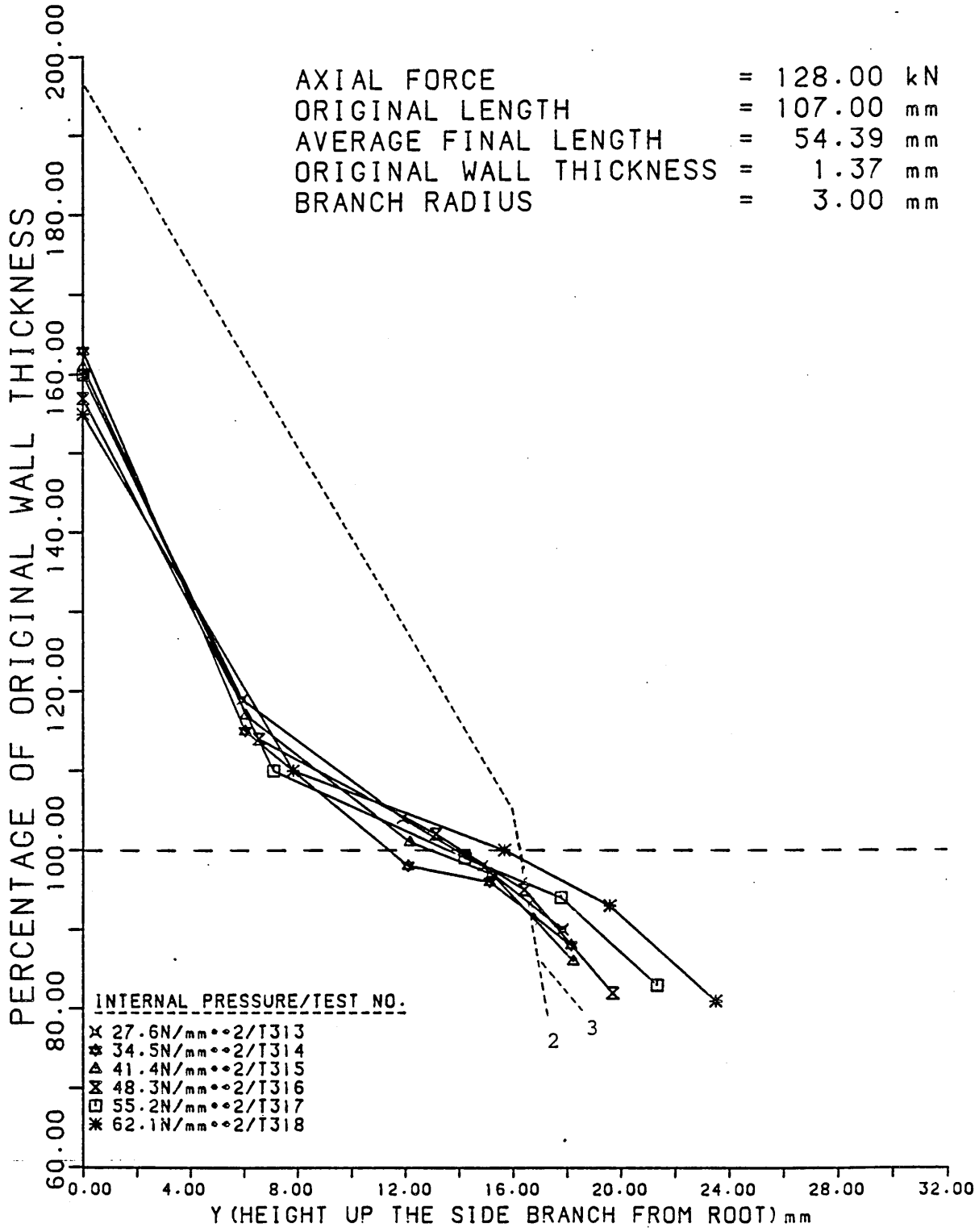

FIGURE 126

The Wall Thickness Distributions Along The Side Branches And Domes Of Tee Pieces Formed At Various Internal Pressures For Experimental And Theoretical Results.

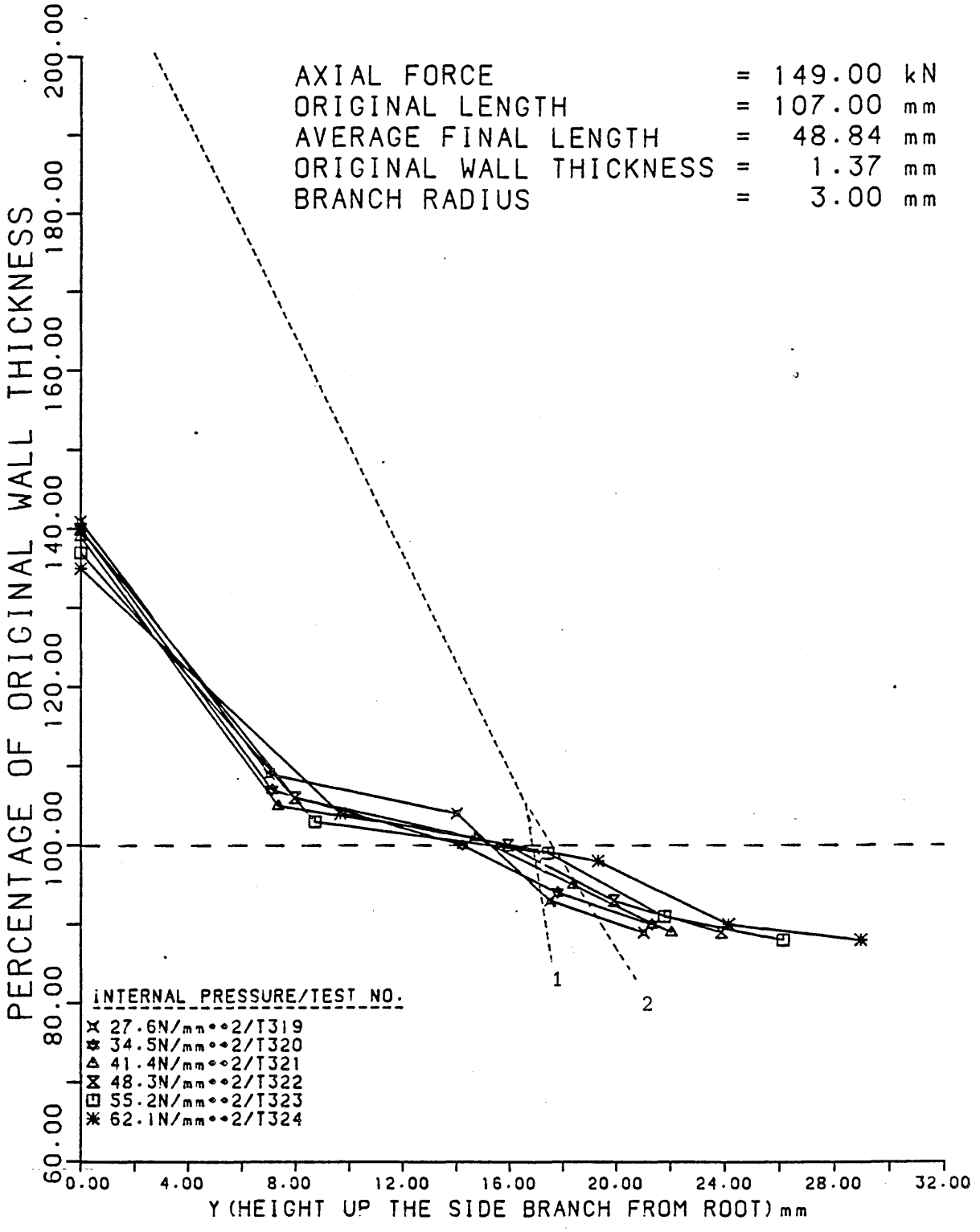

FIGURE 127

The Wall Thickness Distributions Along The Side Branches And Domes Of Tee Pieces Formed At Various Internal Pressures For Experimental And Theoretical Results.

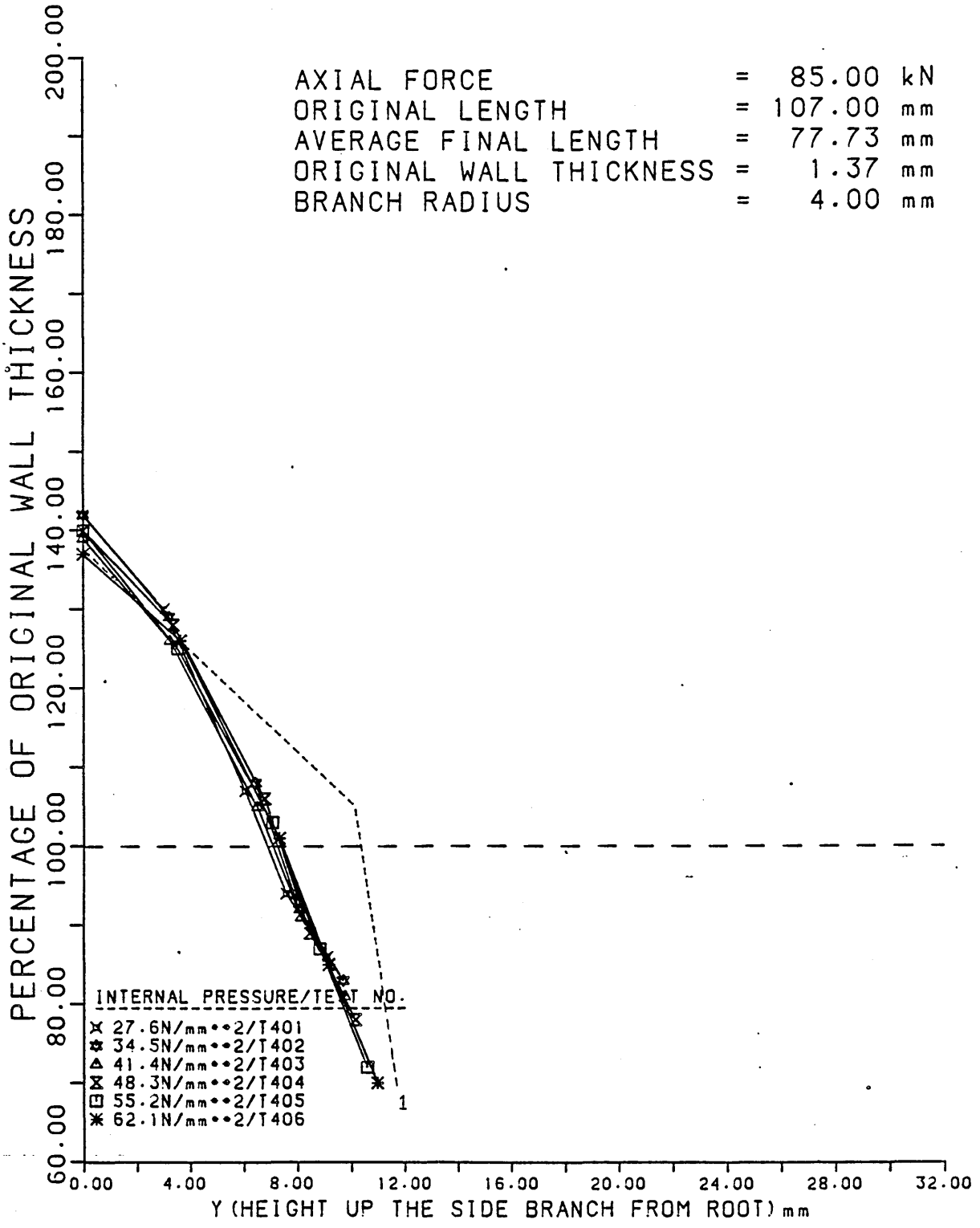

FIGURE 128

The Wall Thickness Distributions Along The Side Branches And Domes Of Tee Pieces Formed At Various Internal Pressures For Experimental And Theoretical Results.

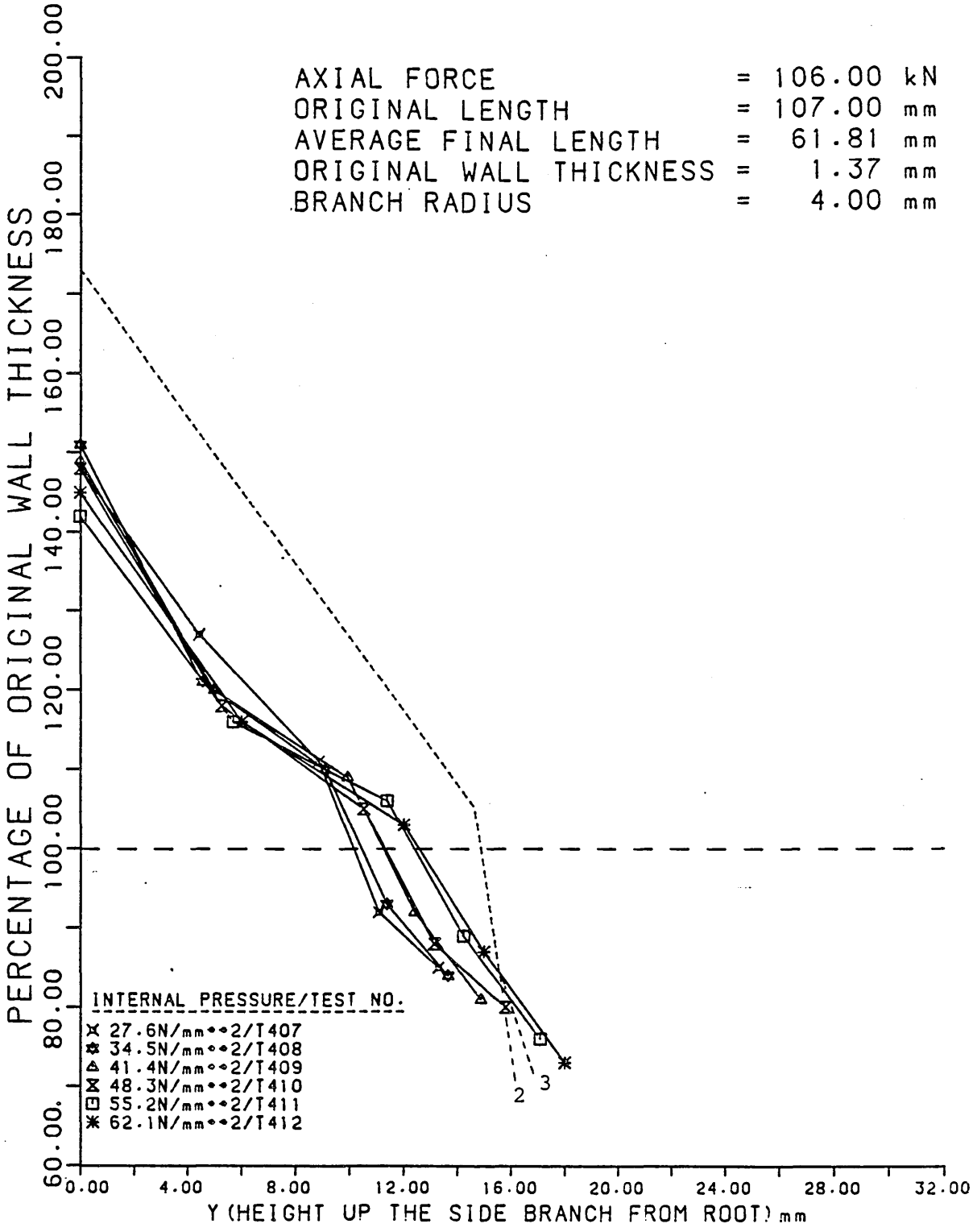

FIGURE 129

The Wall Thickness Distributions Along The Side Branches And Domes Of Tee Pieces Formed At Various Internal Pressures For Experimental And Theoretical Results.

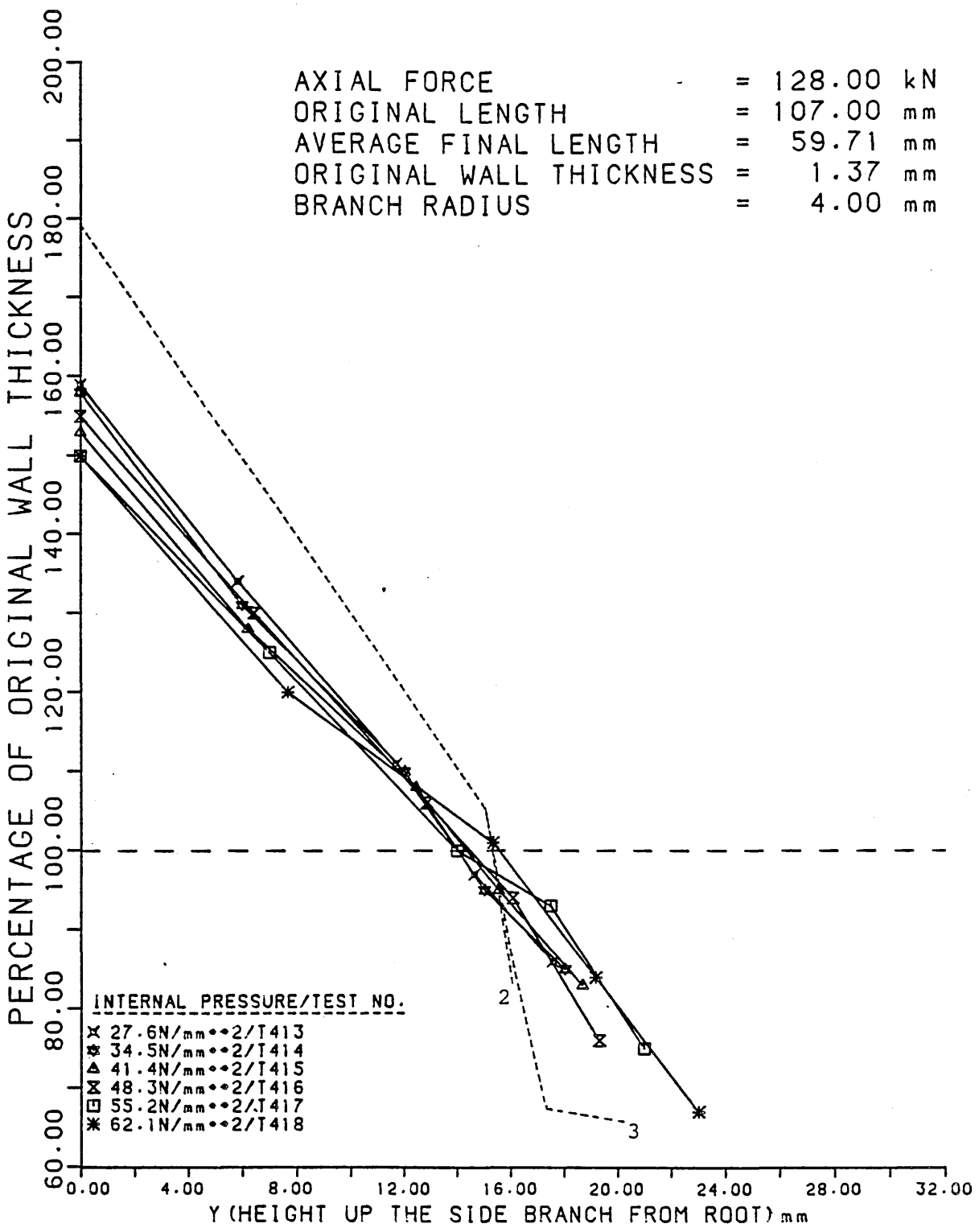

FIGURE 130

The Wall Thickness Distributions Along The Side Branches And Domes Of Tee Pieces Formed At Various Internal Pressures For Experimental And Theoretical Results.

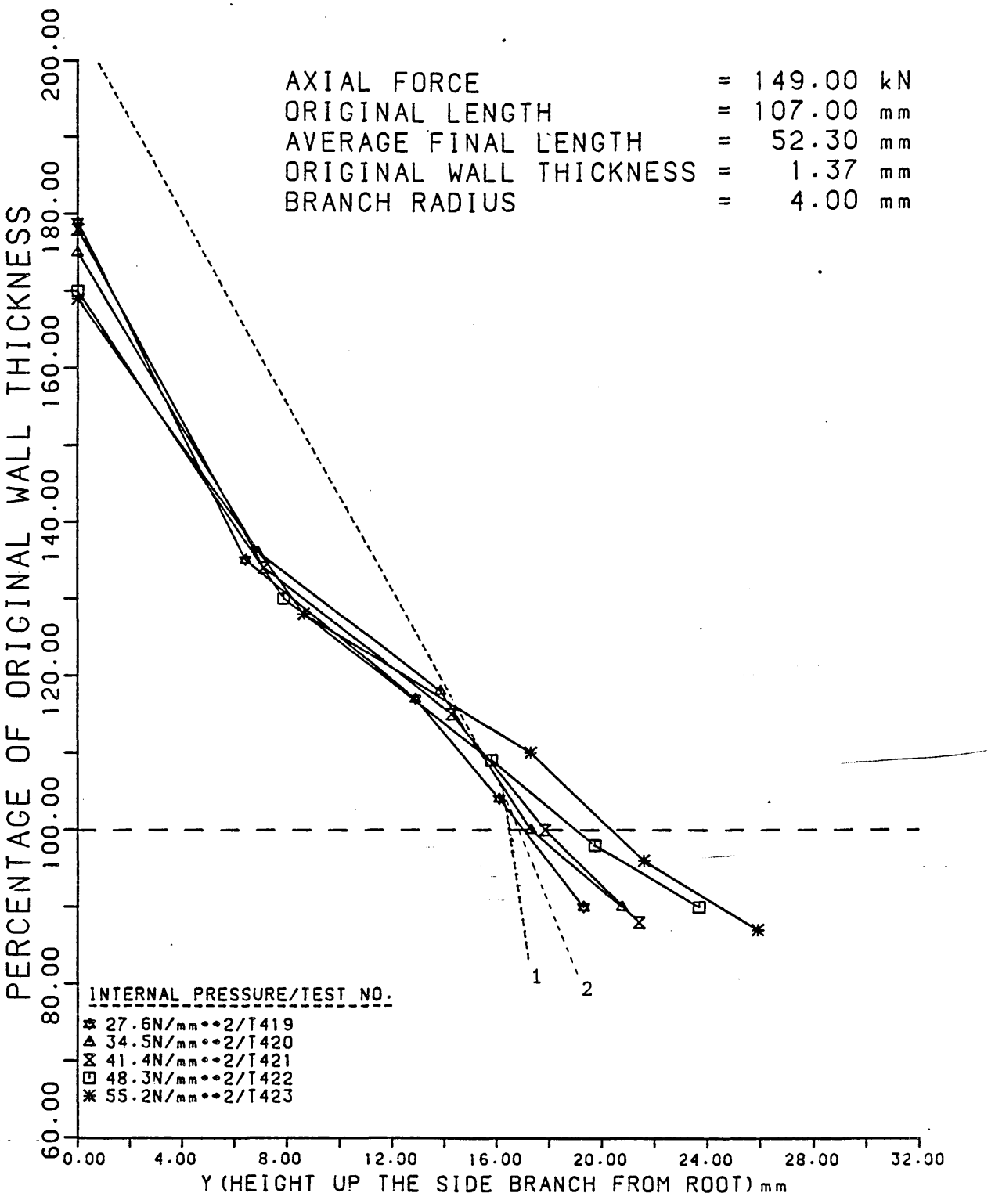

FIGURE 131

The Wall Thickness Distributions Along The Side Branches And Domes Of Tee Pieces Formed At Various Internal Pressures For Experimental And Theoretical Results.

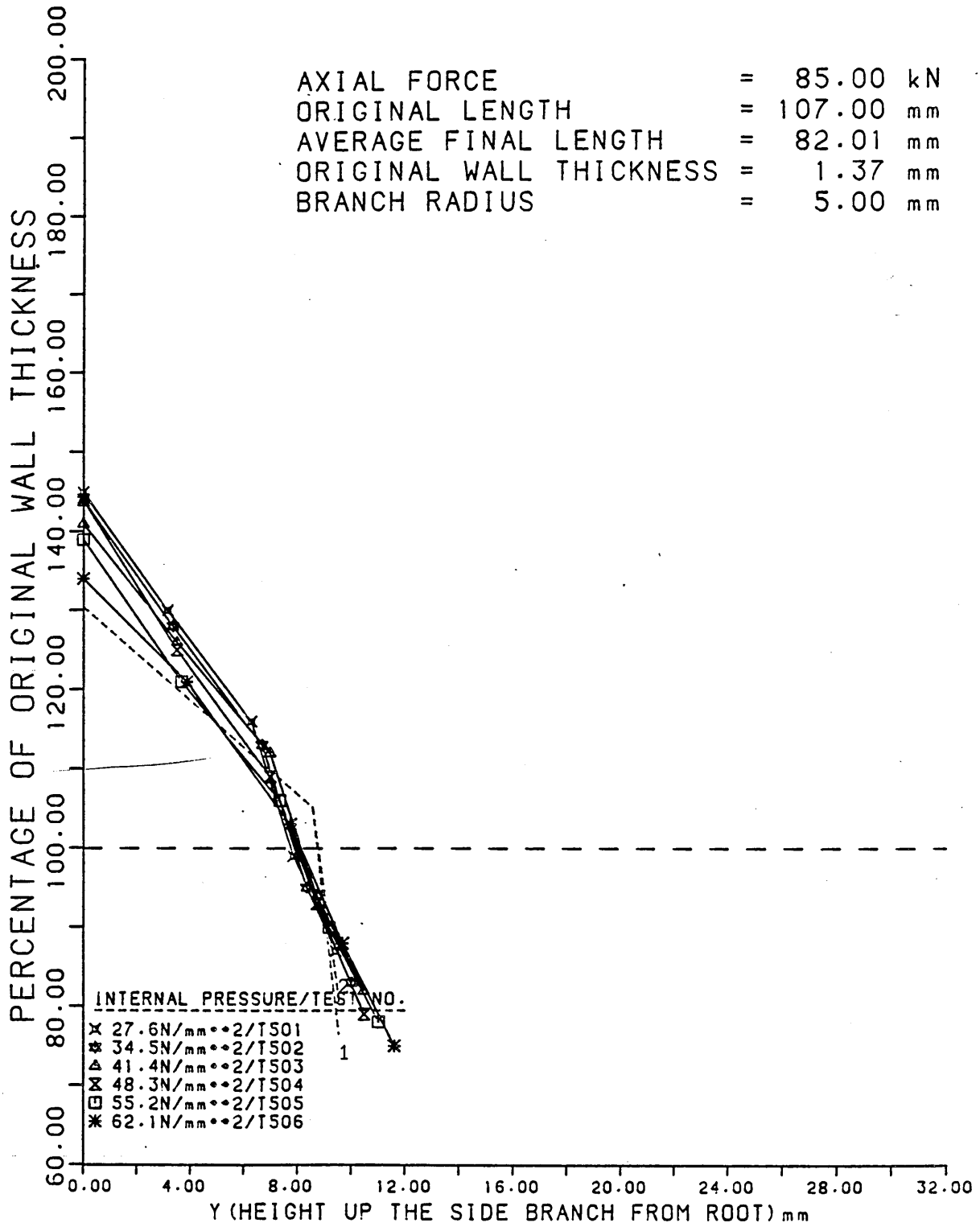

FIGURE 132

The Wall Thickness Distributions Along The Side Branches And Domes Of Tee Pieces Formed At Various Internal Pressures For Experimental And Theoretical Results.

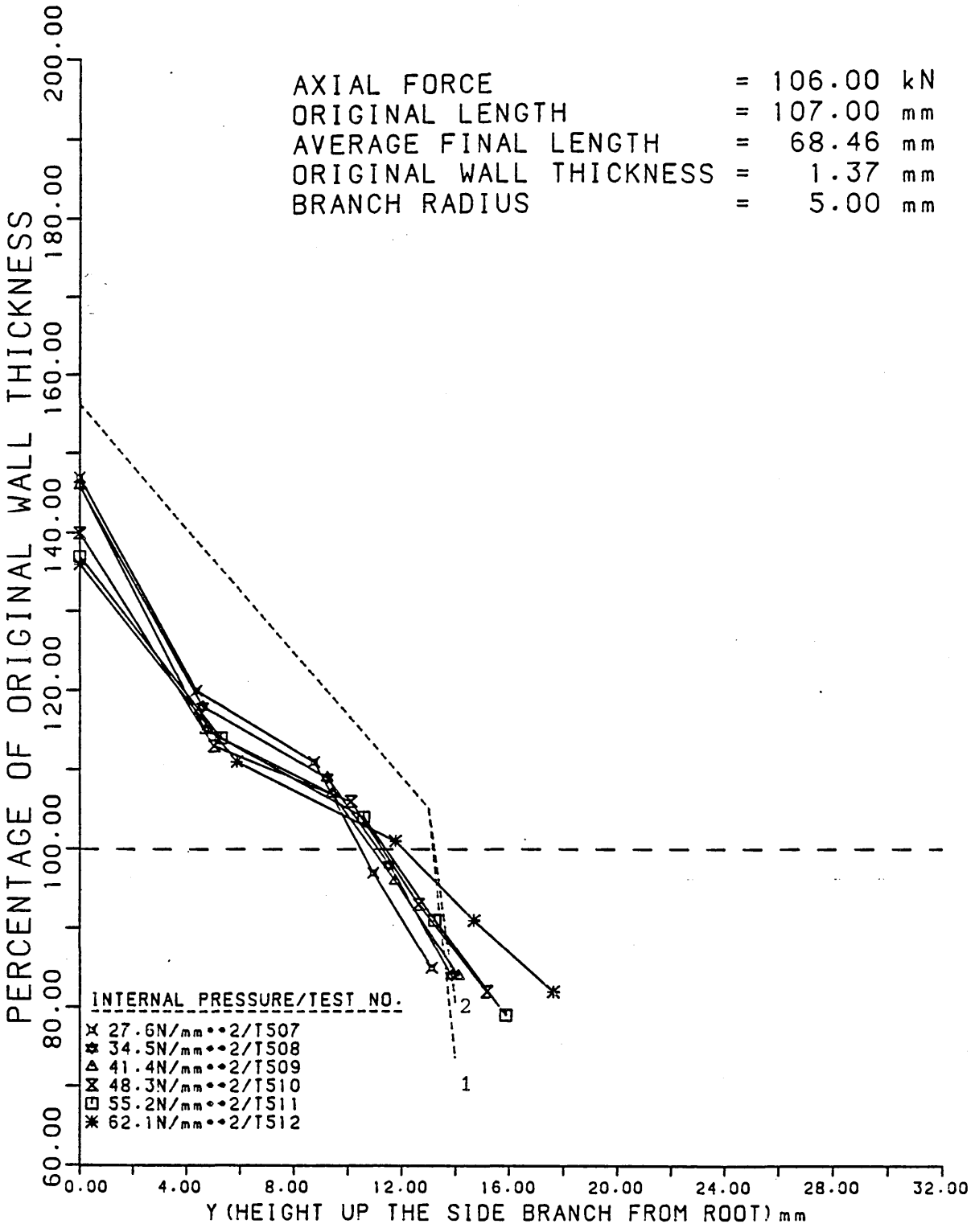

FIGURE 133

The Wall Thickness Distributions Along The Side Branches And Domes Of Tee Pieces Formed At Various Internal Pressures For Experimental And Theoretical Results.

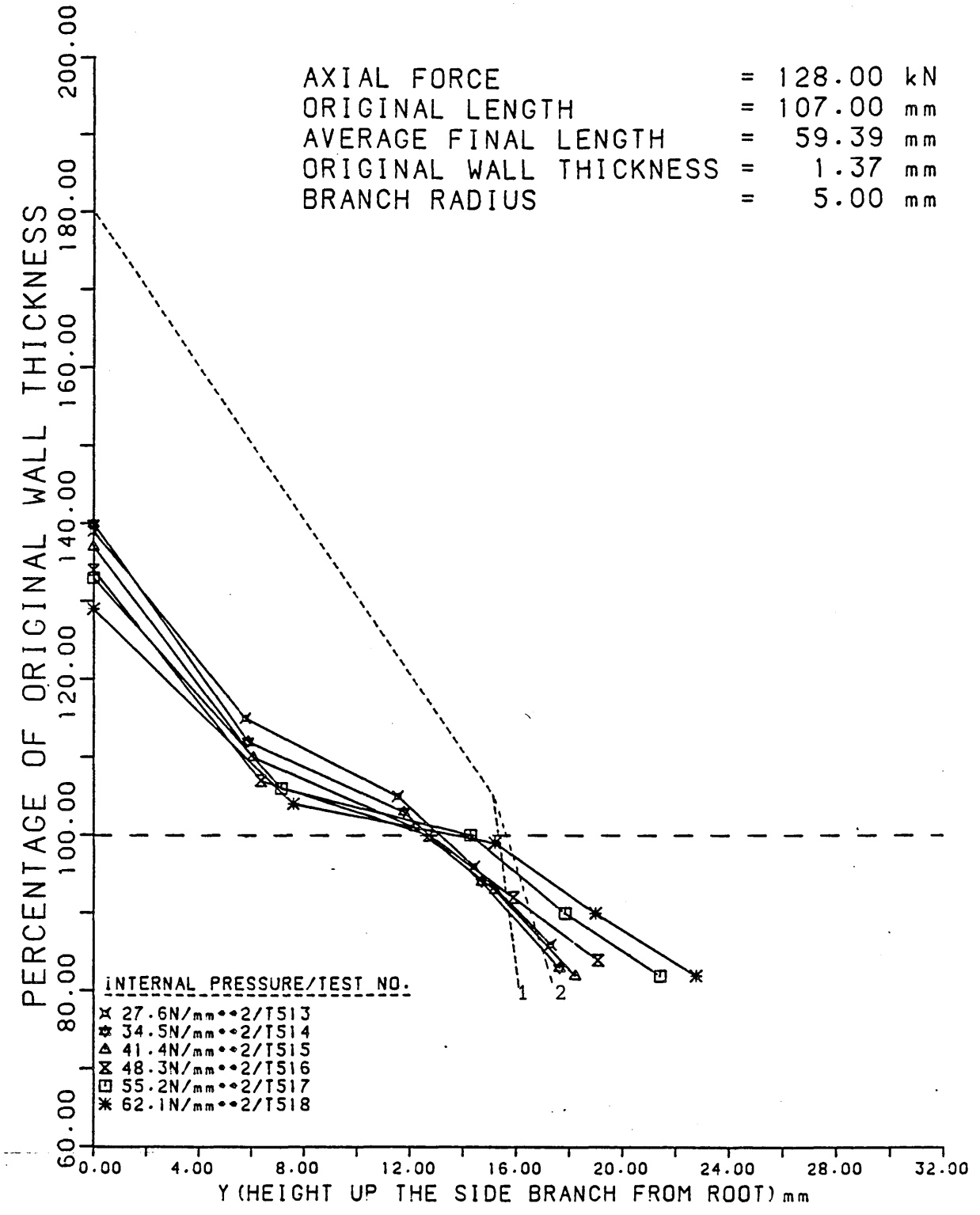

FIGURE 134

The Wall Thickness Distributions Along The Side Branches And Domes Of Tee Pieces Formed At Various Internal Pressures For Experimental And Theoretical Results.

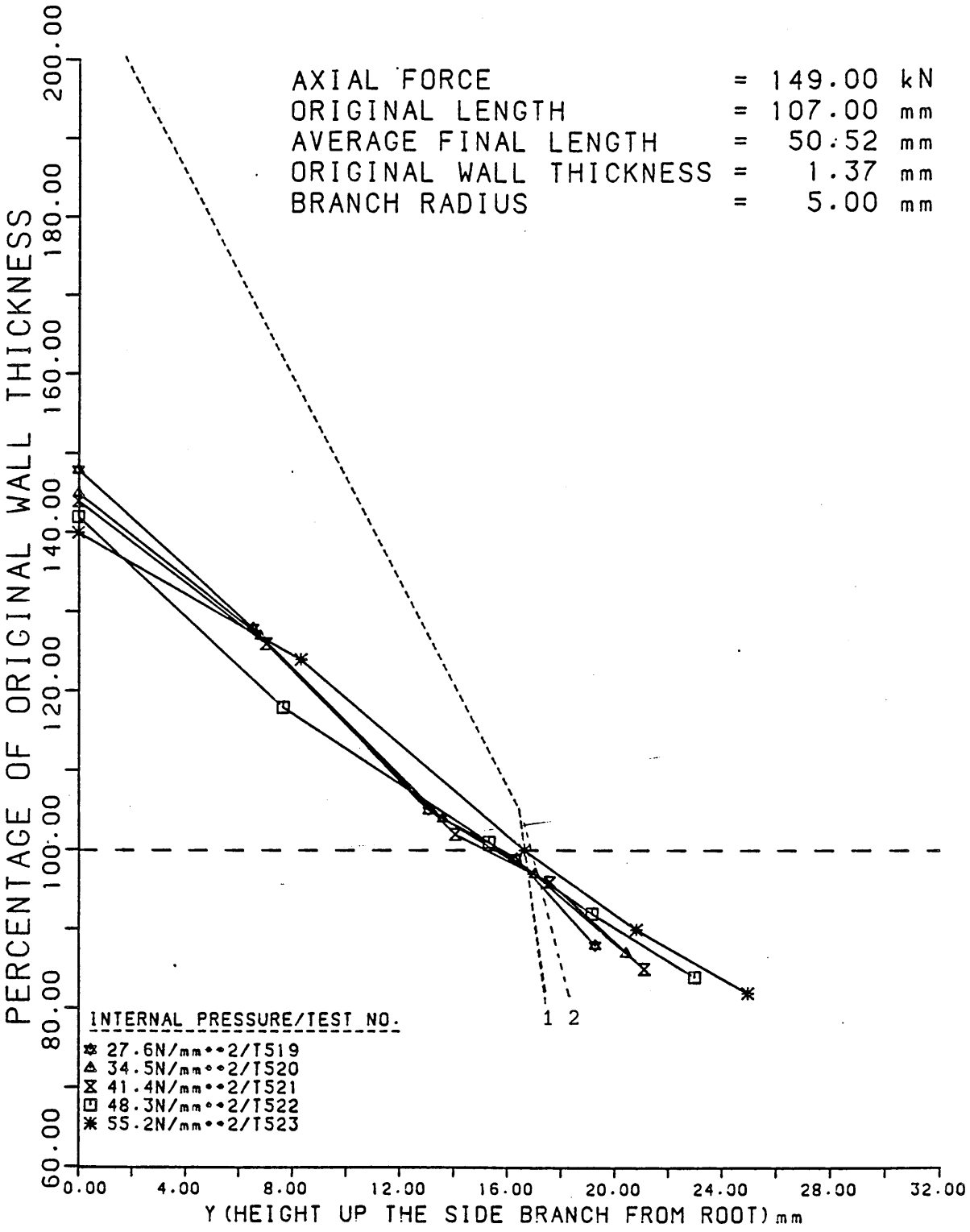

FIGURE 135

The Wall Thickness Distributions Along The Side Branches And Domes Of Tee Pieces Formed At Various Internal Pressures For Experimental And Theoretical Results.

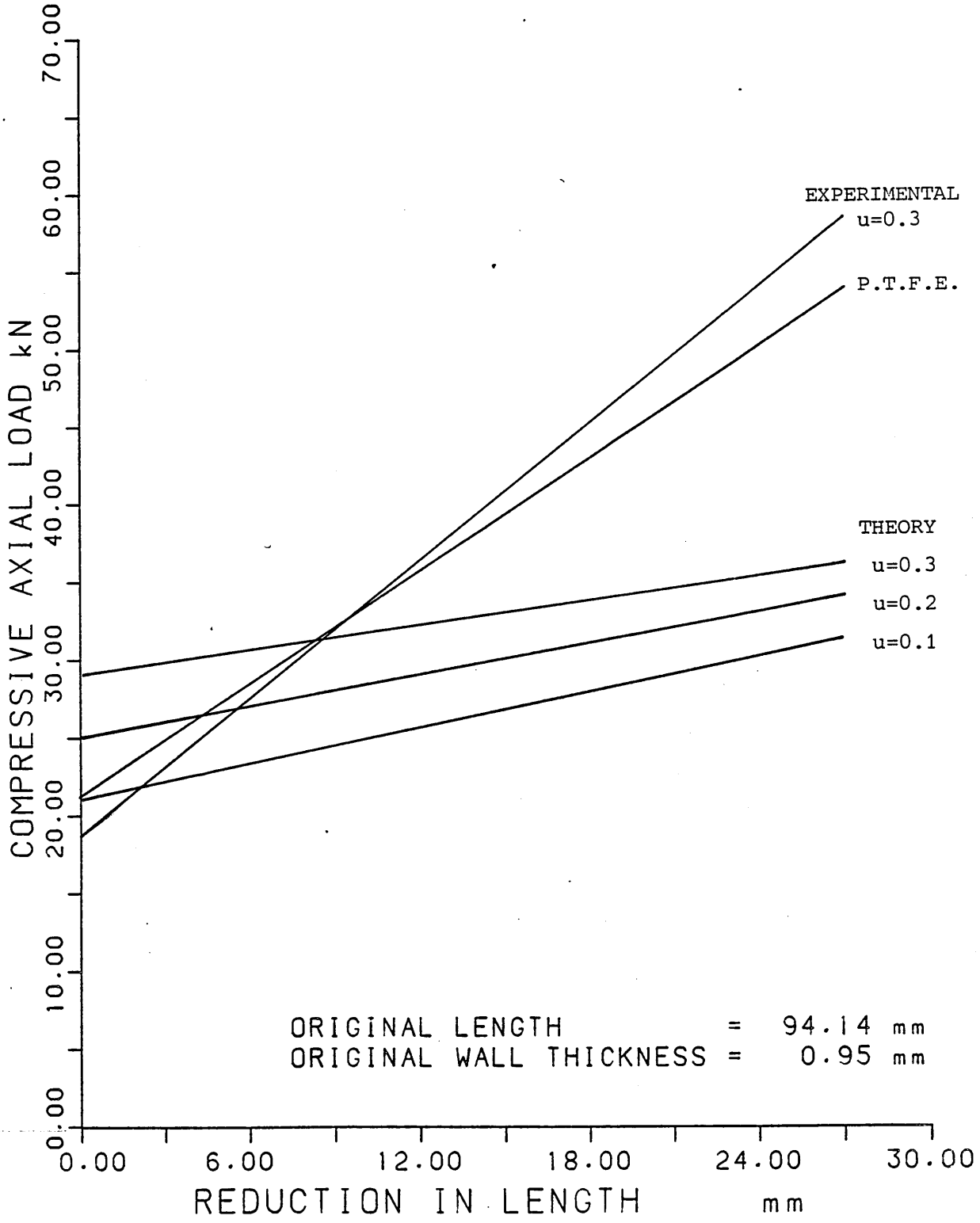

FIGURE 136

The Experimental Results And Theoretical Predictions For Tee Pieces Formed In Die-Blocks Coated With Lubricants Giving Different Co-Efficients Of Friction.

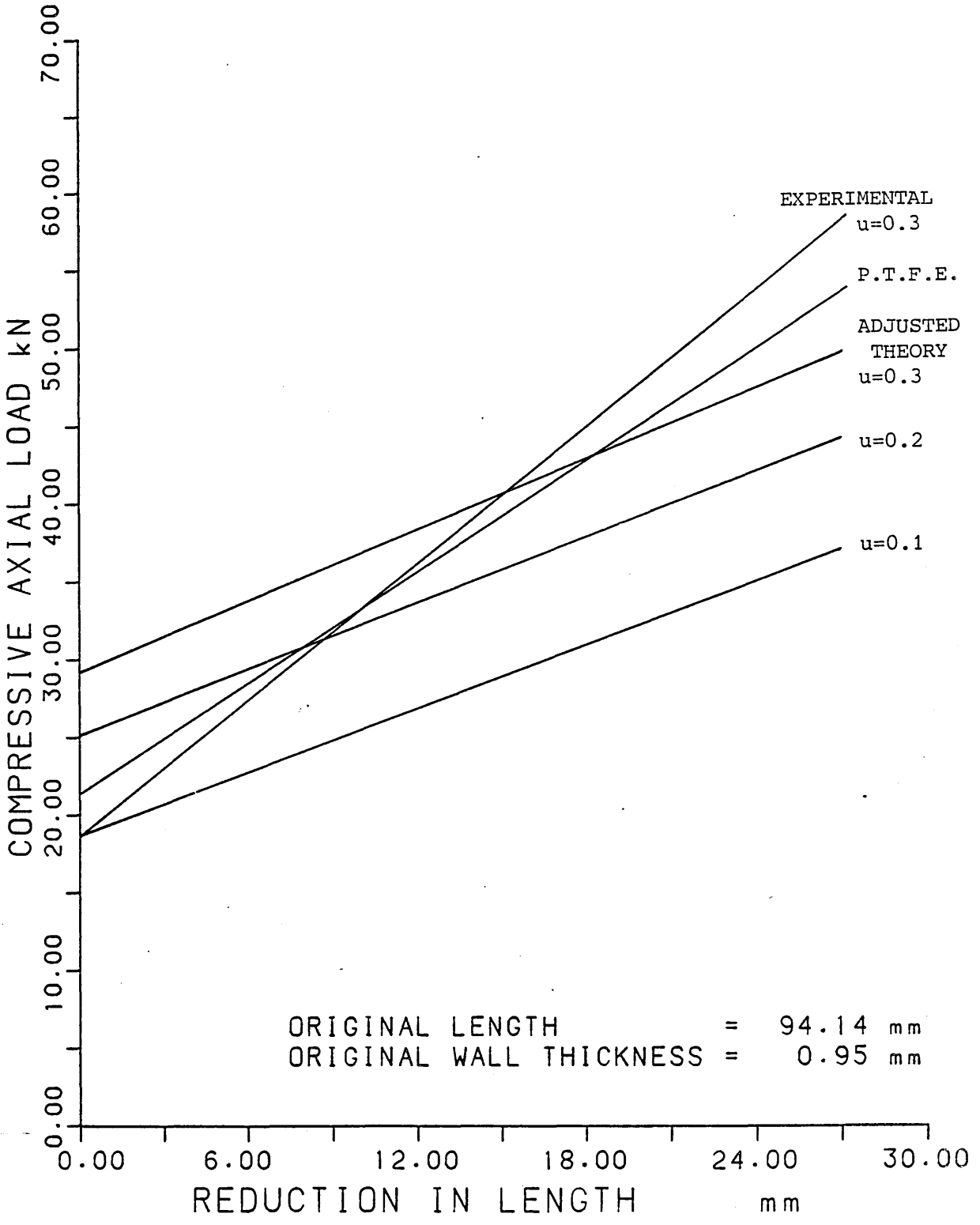

FIGURE 137

The Experimental Results And Theoretical Predictions For Tee Pieces Formed In Die-Blocks Coated With Lubricants Giving Different Co-Efficients Of Friction.

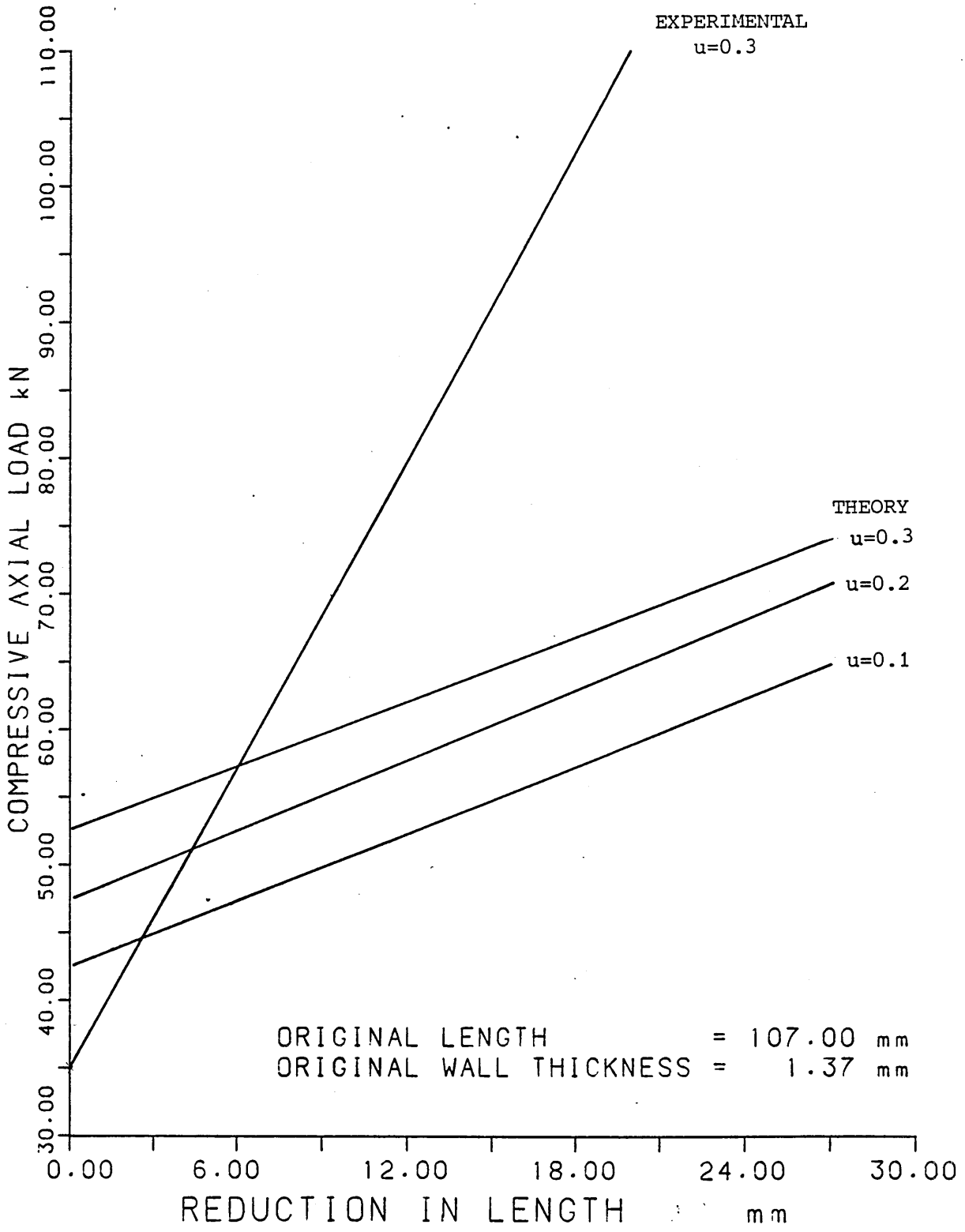

FIGURE 138

The Experimental Results And Theoretical Predictions For Tee Pieces Formed In Die-Blocks Coated With Lubricants Giving Different Co-Efficients Of Friction.

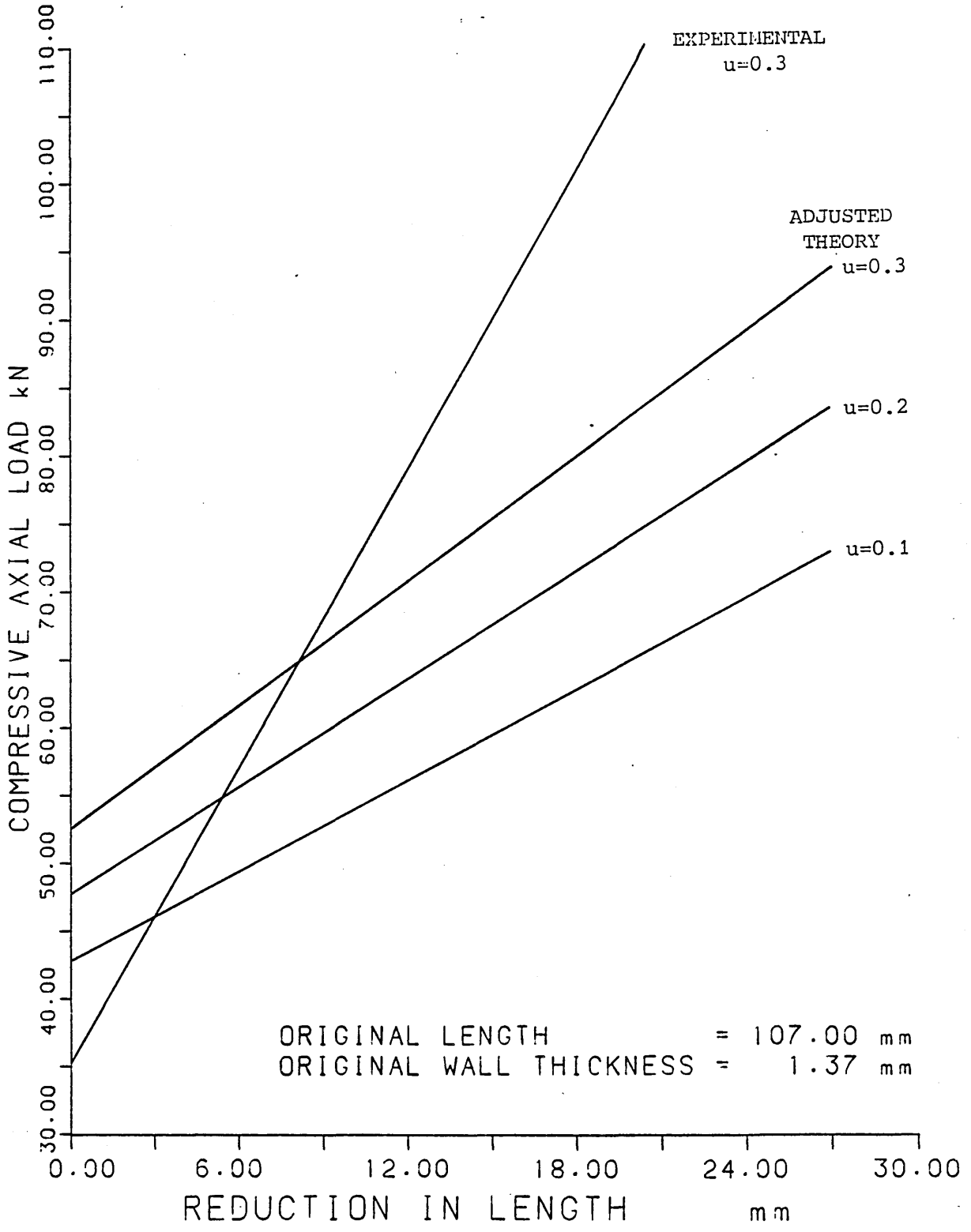

FIGURE 139

The Experimental Results And Theoretical Predictions For Tee Pieces Formed In Die-Blocks Coated With Lubricants Giving Different Co-Efficients Of Friction.

5. DISCUSSION

5.1) Alterations to the Bulge Forming Machine

The bulge forming machine used prior to this investigation was capable of producing tee pieces from two thicknesses of copper tube. However, the valves controlling the compressive axial load and internal pressure could only be used to give approximate values, because the hydraulic circuit was fitted with point-gauges which had inaccuracies of 10%. This limited the use of the machine, because it was impossible to obtain accurate test results, or relate tests carried out on different days. Also, because there was no permanent record made of the deformation process against time, the values of load and pressure at which rupture occurred were hard to calculate, and tended to be a 'hit or miss' affair. Knowing the values which lead to rupture allowed the forming limits to be determined more closely. This was of specific use if a two stage deformation process was used, because the first stage could be allowed to reach a point where the forming values were just below those causing rupture, and hence the secondary forming would allow for the maximum permissible bulge height.

Not only was the instrumentation on the machine limited, but it was felt that certain features of it made the operating process slower than necessary, and in some cases, even created flaws in the finished components. The alterations made to it allowed smooth,

consistent operation and the production of a high quality component.

5.1.1) Instrumentation

On the original machine, there was only one permanent gauge, which recorded the pressure of the hydraulic fluid within the tube. The gauges recording the circuit pressure, and the pressure to the cylinders controlling the plungers, were only temporary ones, and were subject to a 10% error. Although the gauge reading the pressure to the cylinders gave the operating value, the one monitoring the internal pressure gave a value before the effect of the pressure intensifier (6.5:1), and thus when setting a value this had to be taken into account. Therefore, the cumulative error could be in excess of 10%.

In order to reduce the errors, piezo-electric transducers were incorporated into the machine. A load washer was installed between the ram of one cylinder and the plunger, so that the compressive axial load could be recorded (previously, the pressure to the cylinder had to be converted). A pressure transducer was also positioned in the hydraulic piping, just prior to its entry into the plunger. This not only recorded the high pressure circuit, but also the low pressure circuit, so that the process could be monitored from the point where the tubes were first sealed. Finally, a displacement transducer was used to monitor the position of the plungers.

All of the transducers were connected to

scaling amplifiers, and then the outputs fed into an ultra-violet recorder, oscilloscope, and digital voltmeters. The voltmeters allowed the initial pressures and loads to be set more accurately than the temporary gauges, and the u-v recorder produced a hard-copy (on a time scaled grid) of the whole process.

5.1.2) Die-Blocks

5.1.2.1) Alignment

The die-blocks used in the formation of components were designed such that they were easily interchangable, and could be machined independently from the holder in which they were mounted. However, this did not prove to be the case, and it soon became evident that there was some mis-alignment between the plungers, holder and die-blocks. The initial tee piece dies had been manufactured whilst clamped in the holder, and so had worked perfectly well. However, when new sets of die-blocks were made and installed in the holders, not only were they mis-aligned, but quite often they could not be screwed in place, because their holes did not coincide. In order to rectify the situation, one of the inner faces of the holder (which would be in contact with the die-blocks) was re-machined so that it was parallel to the axis of the plungers. It was then possible to manufacture the die-blocks so that all of their dimensions were in respect to this face, and so that they were also aligned with the plungers, and could be screwed in place.

5.1.2.2) **Fluid Entrapment**

The main problem encountered in the formation of components, was that of fluid entrapment. When the machine has been used to produce several components, one after another, there is a quantity of hydraulic fluid left on the die-block surfaces (each time a formed component is unsealed, the fluid inside it runs out onto the die-block). When a tube is placed in the dies, this fluid becomes trapped between the two, and when the clamping load is applied, creates slight indentations on the tube surface. When the tube is then deformed, these indentations 'fold' inwards, and create a buckled component. No matter what combination of internal pressure and axial load are used, once the indentations have been made, they will always cause buckling.

In order to rectify this situation, the die-blocks had to have fluid channels inscribed onto their surfaces. These took the form of a cross-hatching of lines, which originated at the deformation zone, and ended on the face of the dies (Plate 7). When used in the machine, they allowed any excess fluid to be channelled away from the deformation zone, and so prevent buckling. They do, however, leave the cross-hatched pattern on the side of the component opposite the branch.

5.1.2.3) **Branch Radius**

The branch joins the tube at an angle of 90^{o} in the components formed for this work, and hence,

there are two 'corners' formed. Without any blending, these corners would be right-angled bends, and make the formation of components difficult (the tube walls would be incised as soon as deformation took place). It is therefore necessary to put radii on these corners to allow the metal to flow around them. In the original die-blocks, these corners were prepared very roughly, with no specific radius being used (in fact, the radii had different values on the original tee piece - 2.5 mm and 3.5 mm).

The results obtained for the die-blocks with radii of 2 mm, 3 mm, 4 mm and 5 mm showed two distinctive trends when considering the bulge heights obtained. With an axial load of 85 kN, the results showed that the greater the branch radius, the greater the bulge height. However, for the other axial loads (106 kN, 128 kN and 149 kN), the trend was reversed. The die-blocks with the branch radius of 2 mm gave the greatest bulge heights, and then the values decreased as the branch radius was increased.

The analysis of the wall thicknesses shows relatively constant values across the four test samples, although the values at the domes do tend to decrease with an increase in branch radius. However, the results obtained for the 4 mm and 5 mm samples do vary over a greater range (the build-up of material around the branch radius is thicker than for the 2 mm or 3 mm radius, although the values at the dome are less).

When analysing the samples separately, it was noticeable that the minimum wall thickness ratios were obtained with the 106 kN or 128 kN axial loads, and the maximum wall thickness ratios were obtained for the highest axial load, 149 kN.

With regards to the final lengths of the component, it was again observed that the values were constant for any given axial load. There was no apparent trend in the various samples, and no connection between the bulge height and the final length of the component.

The results indicated that, to produce the greatest bulge height, it was preferable to use a set of die-blocks with small radius at the branch and tube intersection. The results obtained with a compressive axial load of 85 kN contradicted this, but it was felt that the reason for this was that because only a small bulge was formed (and not a domed branch), the process was closer to one based on pure internal pressure causing deformation. In the samples with the larger radius, the metal is more easily bulged, as the unrestricted area under the branch is larger (Figure 140a). Also, the amount of bulging that can take place before contact is made with the die-block walls is greater. As stated previously, friction plays a vital role in deciding the height of the bulge.

When considering the cases for the three higher axial loads, the relationship between the bulge heights and wall thicknesses is also important. The

results show that the smaller the radius at the intersection, the greater the bulge height. A reason for this is that to produce a branch, it takes 3.142 mm of material to turn the 90^{o} angle necessary for the components formed with the die-blocks with the 2 mm branch radius, whereas for the 5 mm radius, the value is 7.85 mm (since the circumference of a circle is $2.\pi.r.$, and the turning angle is exactly 90^{o}). In a frictionless case a decrease of one unit in the branch radius would increase the bulge height by one unit. However, although the trend is correct, the values predicted by the above are inaccurate. In the results obtained, the difference in the bulge heights between the four groups increases the higher the axial load.

Therefore, although the material required to travel around the radius is an important factor in the final bulge height, other factors are involved. As the axial load is increased, more material flows into the deformation zone, and thus more material is made available to produce the bulge. Friction causes a resistance to this flow, and will eventually produce a rupture of the dome, because insufficient material will be supplied to withstand the internal pressure. The axial load acts along the length of the tube, and not into the branch. It merely supplies the material to the deformation zone, and it is the internal pressure which bulges the material into the branch. If the internal pressure is too low, with respect to the axial load, the tube buckles, since the material tries to flow

axially. However, components are sometimes formed which have walls which are not in contact with the die-blocks around the branch radius (the axial load pushes the material into the deformation zone, but there is insufficient internal pressure to push the material against the die-block walls - see Figure 140b). The process, therefore, consists of material being pushed into the deformation zone, and then bulged into the branch.

In the case of the 2 mm radius, the amount of contact between the material and the dies at the intersection is a minimum (the metal will flow past the start of the branch and then be bulged upwards), whereas, in the larger radiused die-blocks, the metal will be in constant contact with the dies. Therefore, the resistance created by the friction will be greater than for the 2 mm radius, and the bulge height will be reduced accordingly. This explains the wall thickness distributions obtained for the various samples. In the cases of the smaller radii, the thickness distributions are more even, and do not thin as much at the centre of the domes. The larger values of 4 mm and 5 mm produce wall thicknesses which are larger at the intersection (the metal is not able to flow away as easily), but thinner at the domes (the metal finds it harder to flow into the branch).

The above points are also supported by the forming ranges of the samples. The 2 mm radius produces slightly buckled components with the lowest internal

pressure (27.60 N/mm^2), but did not rupture at 62.10 N/mm^2. The 4 mm and 5 mm radii however, ruptured with the 149 kN axial load and an internal pressure of 62.10 N/mm^2. Only the 3 mm radius formed for all combinations of pressure and load.

From the point of view of manufacturing, the components formed with the die-blocks with 2 mm branch radius are selected. Not only are the components the most pleasing aesthetically, but they are the cheapest to produce (the material saved by keeping the radius a minimum can be 2 to 3 mm per tube - I.M.I. Yorkshire Fittings Ltd. produce 90 million components a year [approximately 250 tonnes of material saved]).

The components formed with the 149 kN axial loads had the highest ratios of wall thickness at the domes, as the ideal combination of pressure and load was used. Enough metal was pushed into the deformation zone for the internal pressure to be able to form a branch which was not excessively thinned at the dome.

5.1.3) Plungers

It is necessary for the plungers to apply axial load to the ends of the tube, to seal it and maintain the internal pressure. In order to facilitate the sealing of the tube, the tip of the plunger is stepped (so that the end of the tube butts-up against it), and also tapered (to allow a greater degree of freedom when it enters the tube). Initially, the plungers used with the machine had a slight taper, which allowed them to enter the tube, but which then

made contact with the inside of the tube walls (the plungers were forced into the tubes so that over most of the length of the taper, there was contact between the plunger and tube). The effect of this was that when the dies were clamped together, the tube was pinched between the dies and the plungers. When the tube was deformed, the resistance caused by this effect meant that higher axial loads were required to produce a component than if this contact had not existed. Also, when the tips of the plungers were in contact with the insides of the tube, when the walls thickened, a stepped build-up of material occurred on the side opposite the branch, which meant that in a manufacturing situation a secondary machining process would be required to remove it.

Three different types of plungers were designed in an attempt to reduce the built-up area. The first type had rounded ends which forced the material away from the lower section of the tube, but the end result was that the stepped area occurred at the sides of the tube. The second type had shearing tips to remove the metal built-up during the process, but the process produced cracks in the tube walls. An amended plunger was then used to remove the build-up after the component was formed, and although successful, still entailed a secondary machining operation. The third type of plungers had tips with an increased angle of taper so that the tube did not come in contact with them until the area where the plungers were stepped.

The effect of this was to enable components to be produced with lower axial loads (or, if the same loads were used, to produce increases in bulge heights in the order of 20% to 30%), and without a stepped build-up of material (the material was more evenly distributed along the length of the tube).

5.2) Variations in the Component Shape

The initial set of die-blocks used with the machine produced tee pieces over a wide range of operating parameters. With regard to the process, the production of unrestrained bulges (for the manufacture of reduction/expansion joints, or gear box casings) and tubes with bends in them (corners and tap spouts) had been going on since 1940. These did not require the same amount of pressure control as the more complex shapes such as tee pieces or cross joints.

Tee pieces were formed from two thicknesses of material over a wide range of compressive axial loads and internal pressures. A two stage deformation process was used to attempt to improve the bulge heights and wall thicknesses. In cases where the tubes burst at a value of, say, 48.30 N/mm^2 with a one stage deformation, it was possible to exceed 58.65 N/mm^2 when a two stage process was used. The process worked because in the first stage of the deformation process the tube underwent work-hardening, and this allowed it to withstand the increased pressure in the second stage. Therefore, the process was operated so that the first stage finished at values of pressure and axial load just less than those which would cause rupture. The use of the process produced an increased bulge height, because the top of the branch became more spherical when the internal pressure was re-applied.

Die-blocks were manufactured to produce cross joints, and these proved even easier to form than tee

pieces. The range of loads and pressures from which components could be formed was greater than with the tees , because the metal flowed evenly between the two branches (there was no build-up of material). The cross joints were less likely to rupture, but the ease at which they could be formed produced the problem of over-developed shapes. This problem was not found with the tee pieces, and that was most likely because the tee's burst before ever reaching that stage. The tests on components formed by a two stage process were similar to those from the tee piece.

After the successful testing of both the tee piece and cross joint, die-blocks were manufactured to produce a component with off-set joints (the bulges were on opposite sides of the tube, similar to the cross joint, but their centres were equi-spaced, and on opposite sides from the centre line of the tube). It proved difficult to form components in this configuration, because when the bulges started to form, they located the tube in the die-blocks, and hence no axial deformation could take place in the centre section of the tube. Axial deformation did take place at the ends of the tube (up to the start of the bulges), which caused the bulges to be lop-sided and ruptured for relatively low values of load and pressure (compared to the tee pieces and cross joints). The initial purpose of producing the component was in an attempt to manufacture two tee pieces from the same blank (using a longer tube blank to produce two tee

pieces of the same dimensions as the individual ones, which could be divided after the process). However, although this proved impossible, the process could still be used to form the component shape, if only small bulges were required. The results from these tests indicated that it would be difficult to produce large bulge heights (equal to half the final tube length) on any component with two branches either side of the centre-line, due to the lack of axial deformation in the central region.

A limitation of the process is that it requires the metal to flow into the deformation zone without requiring such a large axial load that the tube buckles, or the internal pressure ruptures the dome. The components which allow the most deformation are those in which the metal flows the easiest, and does not build up unduly. Hence, a cross joint, unrestrained bulge or circumferential bulge will form easier than a tee piece or other one sided bulge, and those in turn will form easier than ones in which the axial deformation is limited.

5.3) Tube Specifications

In order to determine the versatility of the bulge forming process, four different sizes of copper tube were used. Three of these had the same outside diameter, 24.12 mm. One tube, which was taken as the standard for all of the tests carried out on the machine, was 107 mm in length, and had a wall thickness of 1.37 mm. Another had the same wall thickness, but was 94 mm in length, whilst the third was 147 mm in length and had a wall thickness of 1.03 mm. The other tube used was of completely different dimensions: 94.14 mm in length, 16.86 mm outside diameter, and a wall thickness of 0.95 mm.

When tested, the 'standard' tube produced components over a wide range of values of compressive axial load and internal pressure. There was some buckling of the tube with low internal pressures, and the occasional rupture at high pressures, but in general, fully formed components could be produced consistently.

The tube, 94 mm in length, produced similar results to the 'standard' tube, except that the amount of axial deformation possible was less (owing to the fact that it was necessary to stop the process before the plungers made contact with each other). However, the forming ranges were the same, and it could be assumed that this would apply to any length of tube. The bulge heights produced for any particular range of loads and pressures were not the same for the two

tubes, because the longer the tube, the greater the compressive axial load needed to overcome friction.

The tubes with the wall thicknesses of 1.03 mm did not produce components over the same range as the previous tubes. They were much more susceptible to buckling at low internal pressures, and ruptured for only moderately high internal pressures. They did produce greater bulge heights than the other tubes for the same forming values, but the disadvantage of having a limited forming range made them the least applicable for the process.

The smaller dimensioned tubes produced components over a wide range of values, although axial loads and internal pressures were much lower than for the larger diameter tubes. There were very few examples of buckling or rupture, and the trends could be likened to those of the 'standard' tube.

The important blank dimensions when selecting a tube for the bulge forming process are outside diameter and wall thickness. The ratio of the two determines the forming range over which components can be produced. For example, the standard tube had a ratio of 17.74 and the smaller dimensioned tube 17.50. However, the tube with a wall thickness of 1.03 mm had a ratio of 23.42. Obviously, the smaller the ratio, the greater the forming range (although the axial loads and internal pressures needed to produce a given bulge height will increase as the ratio decreases).

5.4) The Effect of Lubrication

From the results of the tests carried out on the plungers, it was known that the coefficient of friction between the tube and the die-blocks determined the forming load required to give a particular bulge height. The lower the value of friction, the greater the forming range. In order to verify these assumptions and also to check the advantages of various lubricants, a full set of tests was carried out on the formation of a tee piece. Tubes were coated with four types of lubricant, designated 'A', 'B', 'C', and 'D'. Lubricant 'A' was a base oil with a viscosity of 32 with a 2% dispersion of oleic acid, 'B' was the base oil with a 2% dispersion of P.T.F.E., 'C' was the base oil with a 2% dispersion of a friction modifier, and 'D' was P.T.F.E. in an aerosol spray. All of these were tested over a full range of axial loads and internal pressures and the results compared against those obtained for standard set of tests.

All of the lubricants produced results which were improvements on the standard results. Although there was little difference in the wall thickness distributions among the five sets of test results, there was an increase in the bulge heights obtained for the lubricated samples. The increase in the bulge heights varied between 3% and 7% of those obtained with the standard samples. Considering that the wall thicknesses for any given set of forming parameters were approximately the same, then since the lubricated

samples produced greater bulge heights, the ratios of the minimum wall thickness to the bulge height were reduced compared to the standard sample. Therefore, if the compressive axial load and internal pressure were set so that a given bulge height was obtained, the use of a lubricant would improve the wall thickness distribution. Another feature was that the final lengths of components formed with a given axial load were approximately the same. Hence, although additional bulge heights were achieved with the lubricants, it was not as a result of more axial deformation. The effect of the lubricants acting between the die-block and the tube surface enabled the metal in the deformation zone to flow more easily into the branch, without building up around the radius to the same extent. Therefore, if the purpose of the bulge forming process was to produce a tee piece of given bulge height (as is the case in industry), then by using lubricants in the process, the lengths of the tube blanks could be reduced by the same amount that the bulge heights were increased. For example, producing tee pieces from the standard tubes, it was possible to obtain a 3.5 mm increase in the bulge height of a fully-formed component (three equal length branches) without any significant change in the final component length. Hence, a tube blank 3.5 mm shorter could be used to obtain the same amount of bulge height as was achievable with the unlubricated component (saving 3.6×10^{-7} m^3 of material on each component - I.M.I. Fittings Ltd. produce about

90 million components a year, which would be a saving of about 300,000 kg of copper).

As far as the individual lubricants were concerned, the best overall results were obtained with the P.T.F.E. spray which was applied to the tubes and allowed to dry prior to them being placed in the machine. However, when a specific range of operating parameters was analysed (those producing fully formed components), the P.T.F.E. dispersion ('B') produced slightly better results than the spray. This was thought to be because the P.T.F.E. dispersion required 'working-in' to the die-block and tube surfaces, which was only achieved when there was extensive axial deformation (40% to 50%). Prior to this the P.T.F.E. was on the surface of the tube and dies, but had not been forced into the microscopic undulations. Therefore, although it produced some lubrication, its full effect was not achieved. The P.T.F.E. spray, on the other hand, produced constant lubrication throughout, giving the best results for the low axial loads, and only slightly inferior ones to the dispersion at higher loads.

The other lubricants produced slight improvements on the standard tests, with the base oil with the dispersion of oleic acid being superior to the one with the dispersion of a friction modifier.

The main concern when considering the use of the lubricants on the formation of components was their applicability to an industrial process. Although all of

the lubricants produced improved results, not all could readily be used in the industrial mass production of components. The lubricants would have had to be incorporated into the hydraulic oil used as the pressurising medium, which was a base oil with an I.S.O. viscosity of 32. However, of the four lubricants used, two of them (the oleic acid and friction modifier dispersions) did not produce results which would justify the additional cost of their use. The P.T.F.E. dispersion produced satisfactory results, but the major problem was that it would not stay in suspension and separated from the base oil. Therefore, if it was incorporated in the pressurising medium, it would settle at the bottom of the oil reservoir, and clog up the filtration system.

The only applicable lubricant was the P.T.F.E. spray which could be applied to the tubes before they were fed into the machine. This could be achieved by feeding them through the spray on a conveyor belt. Once the spray had dried on the surface of the tubes, it was quite resilient and would not wipe off. The tubes could then be fed into the machine and the effect of the lubricant utilised.

5.5) The Effect of Using Different Tube Materials

To determine the extent to which the bulge forming process could be used to produce components from different materials, tests were carried out on copper, mild steel and commercially pure aluminium tubes. All of the blanks were of the 'standard' dimensions. The copper tubes were supplied in an annealed state by I.M.I. Fittings Ltd., and the steel and aluminium tubes, which had to be machined to give the required dimensions, were annealed prior to testing. All of the tubes had similar surface finishes and appeared flawless.

The testing was carried out over a range of internal pressures and compressive axial loads. The steel and copper components were formed over the same range: 27.60 N/mm^2 to 62.10 N/mm^2 internal pressure, and 85 kN to 149 kN axial load. The aluminium could not be formed properly in these ranges and was therefore tested with internal pressures varying from 6.90 N/mm^2 to 20.70 N/mm^2, and with axial loads varying from 42 kN to 106 kN.

All of the materials deformed in a manner which allowed bulge forming to occur. The copper, which had been tested thoroughly in previous experiments, gave the best results, with an acceptable component being formed over a wide range of values. The aluminium proved difficult to form, because a bulge could only be achieved with a small range of values. If the combination of internal pressure and compressive axial

load was slightly too low, or high, the tubes buckled or burst. For example, the aluminium tubes could produce a bulge with internal pressures which varied by 10 N/mm^2, and compressive axial loads which varied by 60 kN, whereas the copper tubes could be formed with internal pressures varying by 40 N/mm^2 and axial loads varying by 100 kN. The steel could withstand even larger variations.

The components which were formed from aluminium had an acceptable shape, although the surface finish of the tubes was poor. The reason for the limited forming range of the aluminium was that it does not work harden to the same extent as the copper or steel, and thus lacks resilience to the higher pressures and loads.

The steel proved a very satisfactory medium for the process. The forming values of pressure and load were far in ess of those for the copper, and this made it difficult to obtain a large bulge height with the machine, since the maximum system pressure was 69 N/mm^2. The tubes did not buckle at the lower values of internal pressure like the copper, because of the extra strength in the tube walls. The quality of the formed components was good, with a near-polished surface finish.

The tests showed that it was possible to use various materials in the bulge forming process, particularly those which would work-harden extensively. The steel was a suitable material to use in the process, although the machine was unable to produce a

fully-formed component.

The steel followed the same trends as the copper, and as the minimum wall thickness ratio acceptable before rupture in the copper components was 60% to 65%, the value of 95% which was obtained for the steel showed how much more deformation was possible. It was considered that the values of load and pressure up to which steel tubes could be formed were likely to be in the region of twice those tested (300 kN and 120 N/mm^2).

The tests on the aluminium suggested that its use would be limited in its present form. A more suitable suggestion would be to use it within an alloy which could provide some additional work-hardening characteristics.

5.6) Theoretical Predictions

5.6.1) Wall Thickness Distributions

The theory was used with four different values of branch radius (2 mm, 3 mm, 4 mm, and 5 mm). These were compared with sets of data which had been obtained using the standard tubes. Although there were discrepancies between the actual wall thickness distributions and the theoretical predictions, the two did follow the same trends. The inclusion of the branch radius in the theoretical equation tended to improve the accuracy of the predictions, with those obtained with the branch radius of 4 mm and 5 mm giving the best correlations. With low axial loads the predictions were close to the experimental data, especially at the root of the branch and the tip of the dome. However, as the axial load increased, there were some discrepancies at the root of the branch, where the theoretical predictions were giving larger values. This variation increased with the axial load, and produced wall thickness distributions for the branch which were excessive. The predictions of the dome thicknesses were more accurate, and tended to bring the theoretical and experimental lines together. However, when there was a large side-branch formed, the theory tended to underestimate the final branch length. The thickness profile was relatively accurate, but the branch length was sometimes only 50% of its experimental value.

The problem associated with the prediction of the branch length was that it assumed a straight line

relationship for the reduction in wall thickness, and hence only calculated an initial value at the root, and one where the branch joined the dome. Therefore, the inaccuracy of the value at the root created a discrepancy along the entire length of the branch, which in most cases accounted for over 75% of the bulge height. The theory used in the prediction of the values at the root assumed that the axial deformation had forced all of the material into the deformation zone, and that there was no material build-up along the length of the tube. However, material flows both into the deformation zone and along the tube, causing an increase in the wall thickness along the tube. Therefore, when the theory was used to predict the thickness at the root for large axial deformations, the value was too high, and this was reflected along the length of the branch.

The predictions of the wall thickness distributions across the dome were reasonably close, and only became inaccurate with the higher internal pressures. The reason for this was that the theory was based on the expansion of an arc, and with high internal pressures, this was not the case.

The theoretical predictions generally give close approximations of the values obtained experimentally. However, the theory tends to become inaccurate as the forming values reach a maximum, since it does not take into account the friction between the die-block and the tube, the strain-hardening

characteristics of the material, or the increase in wall thickness along the entire length of the tube.

5.6.2) Compressive Axial Load

The above theory predicts the wall thickness distributions of a tee piece given the initial and final lengths of the tube, by assuming that the branch and dome are made up of the material made available by the axial deformation. However, no account is taken of the compressive axial load that is required to produce this reduction in length, and more importantly, the characteristics of the tube material and the friction between the die-blocks and tubes which affect it.

This theory is based upon the axial compression of a tube where a bulge is formed where there is no restraint.

The theory predicted accurate results for the formation of bulges under low axial loads, but tended to become inaccurate as the amount of axial deformation became large. On re-examination of the theory, it became evident that this inaccuracy was created by the fact that no account was taken of the friction between the component branch and the die. An assumption was made that the reduction in length of the tube was equal to the increase in height of the bulge, and hence the frictional factor could be included. The new predictions were much closer to the experimental data, and although the theory still produced values lower than those obtained practically for the larger deformations, the maximum error was limited to 15%.

Comparisons were made with two different size tubes, and the same trends were obtained for both. Also, the effect of increasing the coefficient of friction created the same trends in the theoretical predictions and the experimental data, in that the compressive axial load required to produce a given axial deformation increased.

The theory produced accurate results considering the assumptions that were made in setting up the model. These were that the bulge was a hemisphere, that the cylinder walls did not thicken towards the deformation zone, that the stresses in the bulge were equal, and that the reduction in axial length equalled the increase in bulge height.

Although the two sets of theory had certain variables in common, a combination of the two was not considered feasible, since the assumptions made in them, when combined, would have created a large inaccuracy.

5.7) Further Work

To undertake any further work on the bulge forming process, it will be necessary to make major alterations to the machine. Although at present several shapes can be formed, the process is still based on a one-off principle, with the control of the machine very much a manual operation. The design of the plungers and dies is satisfactory, although if the die-blocks were made in four sections, it would be possible to provide better drainage for the entrapped fluid.

The main area of work should be aimed at the automation of the machine so that the tube blanks and the finished components can be injected and removed without the intervention of the operator, so making the machine more compatible with an industrial process. Also, the valves need to be electronically controlled, and operated by a micro-processor. If a computer was used which was inputted with all of the forming ranges of the various tube sizes, it would be possible to enter in the required bulge height and tube specifications, and then let the micro-processor handle the formation. The use of micro-processor control would also limit the amount of ruptured components, since the internal pressure could be monitored by an electronically controlled relief valve.

Apart from the up-dating of the machine, the areas in which testing needs to be done are those relating to friction. Although lubricants have been tested and shown to reduce friction, their application

to a manufacturing process is still dependent on the way in which they are applied. It will be necessary to test various base oils with additives to find a combination which produces satisfactory results but which does not entail major alterations to the pump and filtration system.

The reduction of friction may be achievable without the use of lubricants by altering the die-block material from a metal, to perhaps, a carbon graphite. The effects of wear and the savings entailed would also have to be considered.

The theories produce reasonable approximations of the wall thickness distributions and compressive axial loads. The purely geometrical approach of the first theory limits its use, because it is difficult to take into account the stresses during the process. However, if better approximations could be achieved with regard to the branch thicknesses, then it may be possible to combine it with the theory predicting axial loads. This would also have to be expanded so that it took into account various bulge heights and shapes, and the effect of axial deformation on the tube wall thickness.

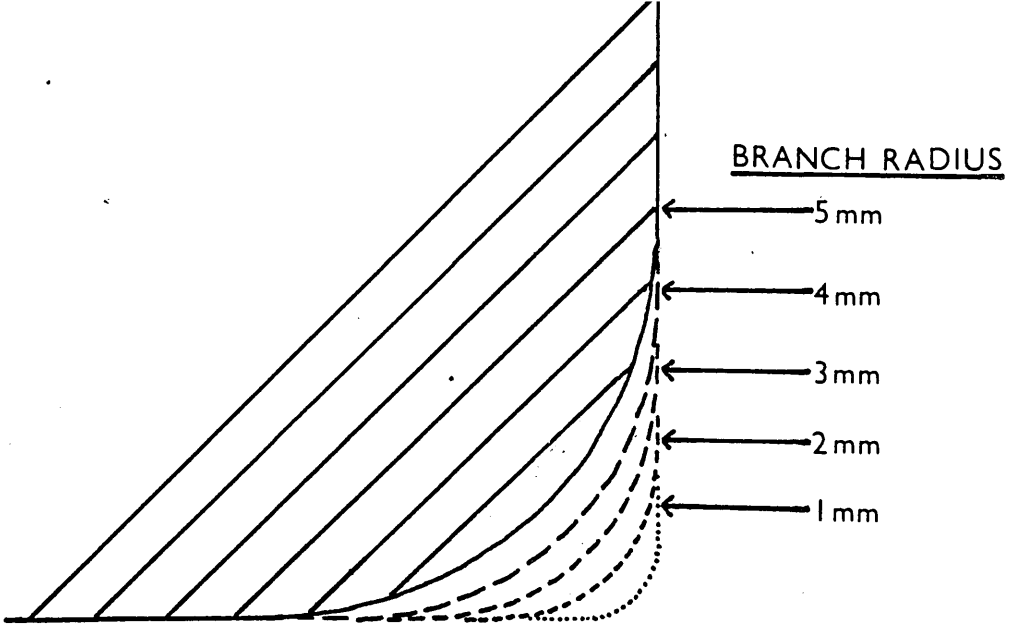

FIGURE 140(a)

The Variation In Branch Radii.

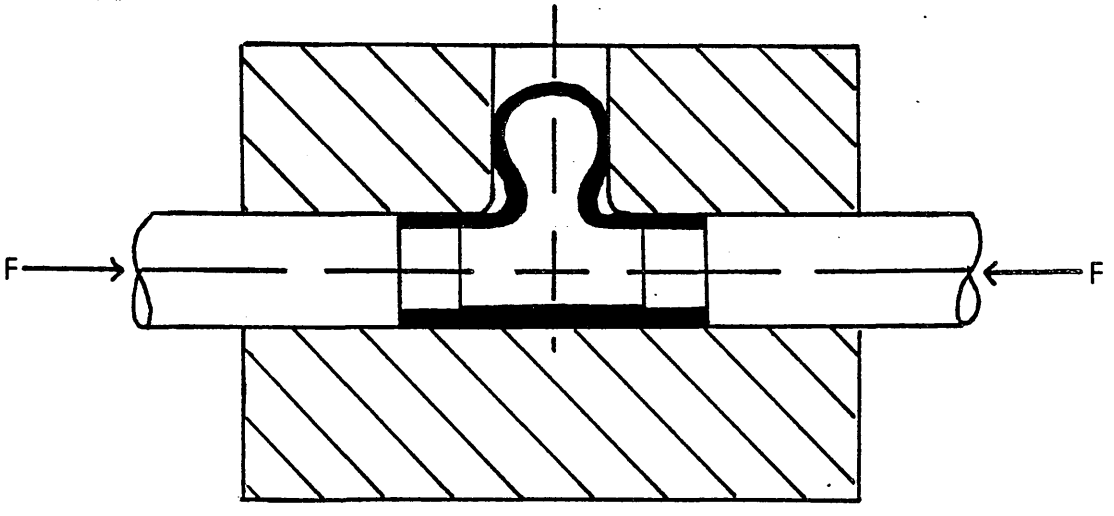

FIGURE 140(b)

Tube Shrinkage.

6. CONCLUSION

The bulge forming process is a useful method of shaping tubular components, by the use of an internal hydrostatic pressure, and a compressive axial load. It can be used to form a variety of components, both axisymmetrical and asymmetrical. However, its use is primarily aimed at components in which there is uniform axial deformation when forming the bulge.

An extensive literature survey indicated the areas in which clarification of the process was required. Alterations were made to the bulge forming machine so that accurate control and recording of the tests could be obtained. This entailed the installation of piezo-electric transducers to monitor internal pressure, compressive axial load and axial displacement.

A series of tests were carried out which indicated the limits of the process. Tee pieces and cross joints were formed successfully from various dimensioned sizes of copper tubes. It was noted that the ratio between the wall thickness and outside diameter gave the extent of the forming range (the lower the ratio, the larger the forming range).

The effect of increasing the branch radius was to reduce the bulge heights and the relative wall thicknesses, whereas the use of lubricants on the tube surface produced increased bulge heights and increased wall thicknesses.

The process was as applicable to steel as it was to copper, although aluminium did tend to form components over a smaller range of values. The important factor seemed to be the strain-hardening characteristics of the material used.

The two sets of theory produced, indicated that it was possible to predict the wall thickness distribution, and compressive axial loads required in the process. The wall thickness distributions did tend to be inaccurate at the roots of the branch, and also in the estimation of bulge heights for high axial loads.

7. REFERENCES

1) **GREY, J.E., DEVEREAUX, A.P. and PARKER, W.M.,** "Apparatus For Making Wrought Metal T's". U.S.A. Patents Office, Filed June 1939, Patent No. 2,203,868.

2) **CRAWFORD, R.E.,** "Solder Fittings". Industrial Progress, May 1948, pp 33-36.

3) **STALTER, J.D.,** "Method Of Forming Complex Tubing Shapes". U.K. Patent Office, Filed March 1968, No. 1,181,611.

4) **HYDROSTATIC COLD FORMING OF TUBULAR COMPONENTS.** Metallurgia, June 1978, pp 293-294.

5) **SMITH, J.A.,** "Hydrostatic Forming Of Tubing Produces Complex Parts". Automation, June 1963, pp 84-89.

6) **"IMPROVEMENTS RELATING TO THE MANUFACTURE OF ELBOW FITTINGS FROM STRAIGHT TUBING".** U.K. Patent Office, Filed May 1963, No. 1,029,892.

7) **"DEVICE AND METHOD FOR MANUFACTURING ELBOW FITTINGS FROM STRAIGHT TUBES".** U.S.A. Patents Office, Filed July 1967, No. 3,328,996.

8) **REMMERSWAAL, J.L. and VERKAIK, L.**, "Use Of Compensating Forces And Stresses In Difficult Metal-Forming Operations". Int. Conf. Manu. Tech., Am. Sc. Tool & Manu. Eng., Michigan, 1967.

9) **BOYD, C. and TRAVIS, F.W.**, "Bending Of Thin Walled Tubes By Combined External Mechanical Forces And Internal Fluid Pressure". Proc. 12th. Int. M.T.D.R. Conf., 1971.

10) **POWELL, G. and AVITZUR, B.**, "Forming Of Tubes By Hydraulic Pressure". 1971.

11) **WOO, D.M.**, " Development Of A Bulge Forming Process". Sheet Metal Industries, May 1978, pp 623-625.

12) **YOSHITOMI, Y., KAMOHARA, H., NOMURA, H. and MAKINO, K.**, "Hydraulic Bulge Forming For Large-Sized Structure Parts". J.H.P.I. Vol. 23 No. 3, 1985, pp 8-13.

13) **AL-QURESHI, H.A.**, "Comparison Between The Bulging Of Thin-Walled Tubes Using Rubber Forming Techniques And A Hydraulic Forming Process". Sheet Metal Industries, July 1970, pp 607-612.

14) **LIMB, M.E., CHAKRABARTY, J. and GARBER, S.**, "The Forming Of Axisymmetric And Asymmetric Components From Tube". Proc. 14th. Int. M.T.D.R. Conf., 1973, pp 799-805.

15) **LIMB, M.E., CHAKRABARTY, J. and GARBER, S.**, "Hydraulic Forming Of Tubes". Sheet Metal Industries, November 1976, pp 418-424.

16) **WOO, D.M.**, "Tube Bulging Under Internal Pressure And Axial Force". Journal Of Engineering Materials And Technology, October 1973, pp 219-223.

17) **WOO, D.M. and LUA, A.C.**, "Plastic Deformation Of Anisotropic Tubes In Hydraulic Bulging". Journal Of Engineering Materials And Technology, October 1978, pp 421-425.

18) **AL-QURESHI, H.A.**, "Forming Cylindrical Corrugations On Metal Tubes By An Internal Elastomer Rod Technique". Metals And Materials, July 1973, pp 317-323.

19) **BANERJEE, J.K.**, "Limiting Deformations In Bulge Forming Of Thin Cylinders Of Fixed Length". Int. Journal Of Mech. Sci., Vol. 17, 1975, pp 650-662.

20) **KANDIL, S.E.A.E.**, "Hydrostatic Metal Tube Bulging As A Basic Process". Metallurgia And Metal Forming, May 1976, pp 152-155.

21) **BADRAN, F.M.F. and EMARA, K.M.**, "Axially Uniform Tube Bulging". Sheet Metal Industries, May 1976, pp 152-155.

22) **SAVER, W.E., GOTERA, A., ROBB, F. and HUANG, P.** "Free Bulge Forming Of Tubes Under Internal Pressure And Axial Compression". Proc. 6$^{th.}$ N. American Metalwork Research Conference, 1978, pp 228-235.

23) **FUCHIZAWA, S. and TAKEYAMA, H.**, "Study On Bulge Forming Of Thin-Walled Cylinder (2nd Report), 1978, pp 70-76.

24) **MANABE, K., MORI, S., SUZUKI, K. and NISHIMURA, H.**, "Bulge Forming Of Thin-Walled Tubes By Micro-Computer Controlled Hydraulic Press". Advanced Technology Of Plasticity, Vol. 1, 1984, pp 279-284.

25) **"AGENCY OF INDUSTRIAL SCIENCE AND TECHNOLOGY".**, "A Liquid Pressure Bulge Forming Apparatus And Process". U.K. Patent Office, Filed September 1964, No. 1,083,354.

26) **OGURA, T., UEDA, T. and TAKAGI, R.**, "The Use Of An Hydraulic Hollowing-out Process". Industrie-Anzeiger, 10th May and 17th June 1966, pp 107-110 and pp 137-140.

27) **OGURA, T. and UEDA, T.**, "Liquid Bulge Forming". Metalworking Production, April 1968, pp 73-81.

28) **LUKANOV, V.L., KLECHILOV, V.V., SHATEEV, V.P. and ORLOV, L.V.**, "Hydromechanical Stamping Of T's With Regulated Liquid Pressure". Forging And Stamping Industry, No. 3, 1980, pp 5-7.

29) **BARLOW, T.J.**, "The Hydraulic Bulge Forming Of Tubular Components". Ph.D. Thesis, December 1986.

30) **HASHMI, M.S.J.**, "Radial Thickness Distribution Around A Hydraulically Bulge Formed Annealed Copper T-Joint: Experimental And Theoretical Predictions". Proc. 22nd Int. M.T.D.R. Conf., 1981, pp 507-516.

31) **HASHMI, M.S.J.**, "Forming Of Tubular Components From Straight Tubing Using Combined Axial Load And Internal Pressure: Theory And Experiment". Proc. Int. Conf. On Developments On Drawing Of Metals, Metals Society, 1983, pp 146-155.

```
      CHARACTER*8 FNAME(10),FTYP/'DATA'/
      CHARACTER*4 DEVICE/'DISK'/
      CHARACTER*2 FMOD/'B'/
      INTEGER IRET,UNIT/3/
      DIMENSION TITL(4),THICK(15),XPLOT(17),YPLOT(17)
     *,MARK(10),YDIS(15)
     *,RATTH(10),DISY(10)
      DATA MARK/11,0,12,2,14,10,1,4,5,3/,Y/0.4/
     *,RADIN/12.06/,PI/3.1415926/
      WRITE(6,10)
10    FORMAT(' NUMBER OF TESTS TO ENTER - ')
      READ(5,*)N
      DO 50 M=1,N
      WRITE(6,20)M
20    FORMAT(' ENTER TEST NUMBER FOR TEST -',I2)
      READ(5,30)FNAME(M)
30    FORMAT(A8)
50    CONTINUE
      XSTART=0.0
      XSCALE=32.0/14.0
      YSTART=60.0
      YSCALE=140.0/18.0
      CALL PLOTS(0,0,1)
      CALL PLOT(1.5,6.0,-3)
      CALL FACTOR(18.0/14.0)
      CALL AXIS(0.0,0.0,'PERCENTAGE OF ORIGINAL WALL THICKNESS',37,14.0
     *,90.0,60.0,10.0)
      CALL FACTOR(14.0/16.0)
      CALL AXIS(0.0,0.0,'Y(HEIGHT UP THE SIDE BRANCH FROM ROOT)',-38
     *,16.0,0.0,0.0,2.0)
      CALL FACTOR(1.0)
      CALL PLOT(0.0,5.14,3)
      CALL DASHP(14.0,5.14,0.3)
      DO 600 I=1,N
      CALL FILEDF(IRET,UNIT,DEVICE,FNAME(I),FTYP,FMOD)
      WRITE(6,60)IRET
60    FORMAT(I6)
      REWIND 3
      WRITE(6,70)FNAME(I)
70    FORMAT(' LOADING TEST - ',A8)
      READ(UNIT,80)ORGTH,TITL
      WRITE(6,80)ORGTH,TITL
80    FORMAT(F6.2,4X,4A4)
      READ(UNIT,90)BULHT,TOPTH,NUM
      WRITE(6,90)BULHT,TOPTH,NUM
90    FORMAT(F6.2,4X,F6.2,4X,I4)
      READ(UNIT,100)(YDIS(M),THICK(M),M=1,NUM)
      WRITE(6,100)(YDIS(M),THICK(M),M=1,NUM)
100   FORMAT(4(F6.2,2X,F6.2,2X))
      DO 150 J=1,NUM
      XPLOT(J)=YDIS(J)
      YPLOT(J)=THICK(J)/0.01
150   CONTINUE
      XPLOT(NUM+1)=BULHT
      YPLOT(NUM+1)=TOPTH/0.01
```

```
      THICK(NUM+1)=TOPTH*ORGTH
      XPLOT(NUM+2)=XSTART
      YPLOT(NUM+2)=YSTART
      XPLOT(NUM+3)=XSCALE
      YPLOT(NUM+3)=YSCALE
      NUM=NUM+1
      WRITE(6,200)(XPLOT(M),THICK(M),YPLOT(M),M=1,NUM)
200   FORMAT(' Y = ',F6.2,2X,'THICKNESS = ',F6.2,2X,'THICKNESS RATIO =
     *',F6.2)
      CALL LINE(XPLOT,YPLOT,NUM,1,1,MARK(I))
      Y=Y+0.3
      CALL SYMBOL(0.2,Y,0.2,MARK(I),0.0,-1)
      CALL SYMBOL(0.5,Y-0.1,0.2,TITL,0.0,16)
600   CONTINUE
C**********************THEORY*****************************************
      WRITE(6,210)
210   FORMAT(' ENTER THE AXIAL FORCE')
      READ(5,*)AXF
      WRITE(6,220)
220   FORMAT(' ENTER THE INITIAL AND FINAL LENGTHS OF THE BLANK')
      READ(5,*)BLENIN,BLNFIN
      F=BLENIN/BLNFIN
      DX1=0.219*RADIN
      DX2=(BLENIN-BLNFIN)/2-DX1
      BRALEN=2*DX2/(F+1.0)
      HS=(2.0**0.5-1.0)*RADIN
      WRITE(6,230)F,DX1,DX2,BRALEN,HS
230   FORMAT(5F10.4)
      RATTH(1)=F*100
      DISY(1)=0.0
      RATTH(2)=100*BLENIN/(BLENIN-2*DX1)
      DISY(2)=BRALEN
C*****************************CASE 2*************************************
      RB=3.0
      SHRAT=HS/(RADIN-RB)
      DO 300 I=1,5
      H=I
      IF(H.GT.HS)THEN H=HS
      DISY(I+2)=BRALEN +H
      RATTH(I+2)=RATTH(2)/((1.0+SHRAT*H/HS)**2.0)
      TOP=TOPTH/0.01
      WRITE(6,280)I,RATTH(I+2),TOP,DISY(I+2)
280   FORMAT(I10,3F6.2)
      IF(RATTH(I+2).LE.TOP)GOTO 305
300   CONTINUE
305   NPTS=I+2
      DISY(NPTS+1)=XSTART
      RATTH(NPTS+1)=YSTART
      DISY(NPTS+2)=XSCALE
      RATTH(NPTS+2)=YSCALE
      CALL DASHS(ARRAY,1)
      CALL LINE(DISY,RATTH,NPTS,1,0,3)
      CALL DASHS(ARRAY,0)
      WRITE(6,320)(DISY(I),RATTH(I),I=1,NPTS)
320   FORMAT('    Y =  ',F10.6,'  THICKNESS RATIO = ',F10.6)
```

```
C*******************************CASE 1***********************************
      RB=3.0
      H2=BULHT-BRALEN
      IF(H2.LT.0.0)GOTO 610
C     IF(H2.GT.HS)GOTO 450
      ROEH=RADIN+H2
      ROEL=(RADIN**2+H2**2)/(2.0*H2)
      ROERAT=ROEH/ROEL
      PM=(3.0-2.0*ROERAT)/ROERAT
      HTRAT=(H2/(RADIN-RB))**2
      WRITE(6,340)ROEH,ROEL,ROERAT,PM,HTRAT
340   FORMAT(5F10.4)
      DO 400 I=1,5
      H=I
      IF(H.GT.H2)H=H2
      DISY(NPTS)=BRALEN +H
      RATTH(NPTS)=RATTH(2)/((1+HTRAT*H/H2)**(PM+1.0))
      IF(RATTH(NPTS).LE.TOP)GOTO 405
400   CONTINUE
405   RATTH(1)=RATTH(2)
      DISY(1)=DISY(2)
      CALL DASHS(ARRAY,1)
      CALL LINE(DISY,RATTH,NPTS,1,0,5)
      CALL DASHS(ARRAY,0)
      WRITE(6,420)(DISY(I),RATTH(I),I=1,NPTS)
420   FORMAT('    Y =  ',F10.6,'  THICKNESS RATIO = ',F10.6)
      GOTO 610
C*******************************CASE 3***********************************
450   WRITE(6,460)
460   FORMAT('***********************************CASE 3*************
     ********')
      RB=3.0
      BL1=BULHT-(BRALEN+HS)
      THEL=2*ATAN(TAN(PI/8)*EXP((0.0-BL1)/RADIN))
      HTHEL=HS-(2**0.5*RADIN*(1-COS(THEL)))
      SHRAT=HS/(RADIN-RB)
      TRAT=1/((1.0+SHRAT*HTHEL/HS)**2)
      RATTH(3)=RATTH(2)*2.0*TRAT*(SIN(THEL)**2)
      DISY(3)=BRALEN+BL1
      DO 530 I=1,5
      H=I
      IF(H.GT.HS)H=HS
      DISY(I+3)=DISY(3)+H
      RATTH(I+3)=RATTH(3)/((1.0+SHRAT*H/HS)**2)
      IF(RATTH(I+3).LE.TOP)GOTO 535
530   CONTINUE
535   NPTS3=I+3
      RATTH(1)=RATTH(2)
      DISY(1)=DISY(2)
      DISY(NPTS3+1)=XSTART
      RATTH(NPTS3+1)=YSTART
      DISY(NPTS3+2)=XSCALE
      RATTH(NPTS3+2)=YSCALE
      CALL DASHS(ARRAY,1)
      CALL LINE(DISY,RATTH,NPTS3,1,0,5)
```

```
      CALL DASHS(ARRAY,0)
      WRITE(6,550)(DISY(I),RATTH(I),I=1,NPTS3)
550   FORMAT('   Y =  ',F10.6,'  THICKNESS RATIO = ',F10.6)
610   WRITE(6,620)
620   FORMAT(' NOW TYPE PLOT IF YOU REQUIRE A COPY ')
      CALL SYMBOL(0.2,Y+0.4,0.2,'INTERNAL PRESSURE/TEST NO.',0.0,26)
      CALL SYMBOL(0.2,Y+0.2,0.2,'--------------------------',0.0,26)
      CALL SYMBOL(3.5,13.5,0.3,'AXIAL FORCE              =        kN'
     *,0.0,35)
      IF(AXF.GE.100.00)GOTO 625
      CALL NUMBER(11.6,13.5,0.3,AXF,0.0,2)
      GOTO 630
625   CALL NUMBER(11.3,13.5,0.3,AXF,0.0,2)
630   CALL SYMBOL(3.5,13.0,0.3,'ORIGINAL LENGTH          = 107.00 mm'
     *,0.0,35)
      CALL SYMBOL(3.5,12.5,0.3,'FINAL LENGTH             =        mm'
     *,0.0,35)
      CALL NUMBER(11.6,12.5,0.3,BLNFIN,0.0,2)
660   CALL SYMBOL(3.5,12.0,0.3,'ORIGINAL WALL THICKNESS =   1.37 mm'
     *,0.0,35)
      CALL SYMBOL(3.5,11.5,0.3,'BRANCH RADIUS           =   3.00 mm'
     *,0.0,35)
      CALL PLOT(10.0,0.0,999)
      CALL EXIT
      STOP
      END
```

BULGE FORMING OF TUBULAR COMPONENTS; THE EFFECTS OF LUBRICATION

M I Hutchinson*, R Crampton*, M S Ali*, M S J Hashmi+

* Department of Mechanical & Production Engineering
Sheffield City Polytechnic, Sheffield, England.
+ School of Mechanical Engineering, N I H E,
Dublin, Ireland.

Abstract

The hydraulic bulge forming process is used to produce seamless components from tubular blanks. A combination of internal hydraulic pressure and axial load are used to deform the cylindrical metal tubes whilst being contained within pre-shaped die blocks.

A dedicated experimental hydraulic bulge forming machine has been designed and built at Sheffield City Polytechnic. The machine allows control of the various forming parameters to be achieved.

This paper deals with investigations conducted on the machine into the effects of coating the tubes with various lubricants prior to the deformation process. In particular, the work examines the required forming pressure and loads and compares bulge heights and wall thickness distributions obtained for the lubricants used.

Introduction

The bulge forming process is a method whereby tubular metal components can be shaped without the use of cutting tools. Instead, internal hydrostatic pressure is transmitted via a medium such as a liquid (eg. hydraulic oil or water), or a soft metal (eg, lead or a lead alloy). This internal pressure is applied to a tubular blank whilst it is contained in a die bearing the shape of the component to be formed. Where the tube wall is unrestrained, expansion occurs until the required shape is formed.

Bulge forming occurring as a result of pure internal pressure has a major limitation of excessive thinning of the tube wall, which leads to rupture of the tube for only moderate expansions. However, if sufficient compressive axial force is applied to the ends of the tube, metal can be fed into the deformation zone during forming and much greater expansions can be obtained with less reduction in tube wall thickness. Throughout the process, the axial force must be great enough to deform the metal and overcome friction between the tubular blank and the die blocks. If the coefficient of friction could be reduced, then greater deformation would take place for a given internal pressure and compressive axial force. To verify this and deduce the possible improvements, tests were conducted using several lubricants.

Previous Studies

Investigations into the effects of lubricants ha been carried out by Limb [1]. Tee pieces were produced from 36mm outside diameter tubes of commercially pure aluminium, aluminium alloy, copper, 70/30 brass and low carbon steel, with wall thicknesses varying from 1.22mm to 2.03mm.

The most satisfactory method of producing components from thin walled tubes was found to be by increasing the internal pressure incrementally during the ram movement. A large increase in the wall thickness occurred in the main branch during the process. The formed tee had a very pronounced dome if there was no lubricant between the tube and die. The best lubricant was found to be PTFE film, followed by colloidal graphite and Rocal. With lubricants, the dome of the tee was much flatter and the length of the branch increased by as much as 20%. The wall thickness of the branch was also found to have increased.

In a later paper by the same authors [2], lubricant tests were again carried out using the same size tubes and materials.

In this paper, the effects of eight different lubricants on the maximum length of branch formed were investigated. The PTFE film was again found to give the largest bulge height, with PTFE spray being the next best. Tellus 27 was found to be the worst.

Present Study.

Tee pieces were formed with a hydraulic bulge forging machine which could supply a maximum internal pressure of 70 N/mm^2 and compressive axial force of 150 kN. The tubular blanks used in the process were of annealed copper; 94.14 mm long, 16.86 mm outside daimeter and 0.95 mm wall thickness.

Normally, the tubes would be formed with the hydraulic oil used as the pressurising medium acting as a lubricant. The hydraulic oil was 'Silkdene Derwent' with an ISO viscosity of 32 and was coded lubricant 'N' and used for the standard test samples.

Four specific lubricants were used initially in the analysis of the effects of lubrication on the formation of tee pieces. Three of these were oil based and the fourth was a PTFE solution in an aerosol form. These lubricants were coded 'A', 'B', 'C' and 'D' and were;
lubricant 'A'; a base oil with an ISO viscosity of 32, containing a 2% oleic acid dispersion,
lubricant 'B'; the same base oil with 2% PTFE dispersion,
lubricant 'C'; the base oil with a 2% friction modifier dispersion (as used in wet brake applications),
lubricant 'D'; the PTFE in an aerosol spray.

Prior to being placed in the machine, the tubes were totally immersed in the lubricant and the excess allowed to drain off (except in the case of PTFE spray when the tubes were evenly coated and allowed to dry). The bulge forming process was then carried out as normal.

The compressive axial loads applied to the tubes were; 26 kN (merely acting to seal the tubes), 43 kN, 64 kN and 85 kN. For each of these axial loads, the internal pressure was increased from 20.7 N/mm^2 up to rupture in 6.9 N/mm^2 increments. After each set of tests, the die blocks were thoroughly cleaned with alcohol to remove any trace of lubricant. Several components would then be formed with the new lubricant, these being discarded. This was to ensure that the die blocks were properly coated with the new lubricant before actual tests began.

Once formed, the components were measured and their final lengths and bulge heights recorded. They were then cut in half and the wall thickness profiles measured.

Table 1 shows the maximum forming ranges of the tests along with the bursting pressures. Although in some cases the standard lubricant gave better results than the others, in general, additional lubrication improved the features of the component formed. For each axial load, the cummulative bulge height differences were tabulated and in all but one of the sixteen cases, positive values were obtained. These values, which are shown in Table 2, were compared and it was found that the PTFE spray gave the most consistent improvement in bulge height (1.1mm), followed by PTFE in suspension (0.625mm), friction modifier (0.57mm) and finally the oleic acid (0.415mm).

When a different approach was used, the trends altered slightly. Instead of comparing the results over the full range of tests, only those combinations of load and pressure which produced fully formed components were considered. The results are shown in Table 3. This table indicates that the PTFE in suspension was marginally better than PTFE spray with the other two lubricants showing the same trends as before.

Table 1. Forming Ranges

Lubricant	Compressive Axial Load (kN)	Maximum Bulge Height (mm)	Minimum Wall Thickness Ratio (%)	Maximum Internal Pressure (N/mm^2)	Bursting Pressure (N/mm^2)	Maximum Buckling Pressure (N/mm^2)
N	26	2.69	75	34.5	41.4	----
A	26	2.90	66	34.5	41.4	----
B	26	3.29	63	34.5	41.4	----
C	26	2.83	71	34.5	41.4	----
D	26	2.81	71	34.5	41.4	----
N	43	10.13	81	41.4	48.3	20.7
A	43	11.65	70	48.3	55.2	20.7
B	43	11.67	91	41.4	48.3	20.7
C	43	12.24	71	48.3	55.2	20.7
D	43	12.93	71	48.3	55.2	20.7
N	64	18.65	79	41.4	48.3	20.7
A	64	18.38	75	48.3	55.2	20.7
B	64	18.99	76	48.3	55.2	20.7
C	64	18.15	78	41.4	48.3	20.7
D	64	19.54	81	41.4	48.3	20.7
N	85	20.5	77	41.4	48.3	20.7
A	85	22.23	71	48.3	55.2	20.7
B	85	23.45	59	48.3	55.2	20.7
C	85	22.72	66	48.3	55.2	20.7
D	85	23.14	68	48.3	55.2	20.7

Table 2. Averaged Bulge Height Variations (mm) from Standard Tests

Compressive Axial Load / Lubricant	26 (kN)	43 (kN)	64 (kN)	85 (kN)	Compressive Axial Loads Averaged
A	+0.09	+0.52	-0.14	+1.19	+0.415
B	+0.41	+0.78	+0.10	+1.26	+0.625
C	+0.37	+0.95	+0.39	+0.57	+0.570
D	+0.22	+1.49	+0.57	+1.38	+1.100

Table 3. Bulge Heights (mm) for Selected Pressures & Loads

Load~Pressure ($kN \sim N/mm^2$) / Lubricant	64 & 41.4	64 & 48.3	85 & 41.4	85 & 48.3
N	18.65	-----	20.5	-----
A	18.06	18.38	21.41	22.23
B	18.36	18.99	22.09	23.45
C	18.15	-----	21.31	22.72
D	19.54	-----	21.60	23.14

The analysis of the wall thickness profile showed no clear trends, (see Fig 1), but the fact that the components could be formed at higher internal pressures when lubricants were used on them, suggested that the wall thicknesses should be greater. In fact, the wall thicknesses were similar for any given combination of compressive axial load and internal pressure across the five sets of tests. Since the components formed with lubricants gave greater bulge heights, for a given bulge height, the use of an effective lubricant would increase wall thickness.

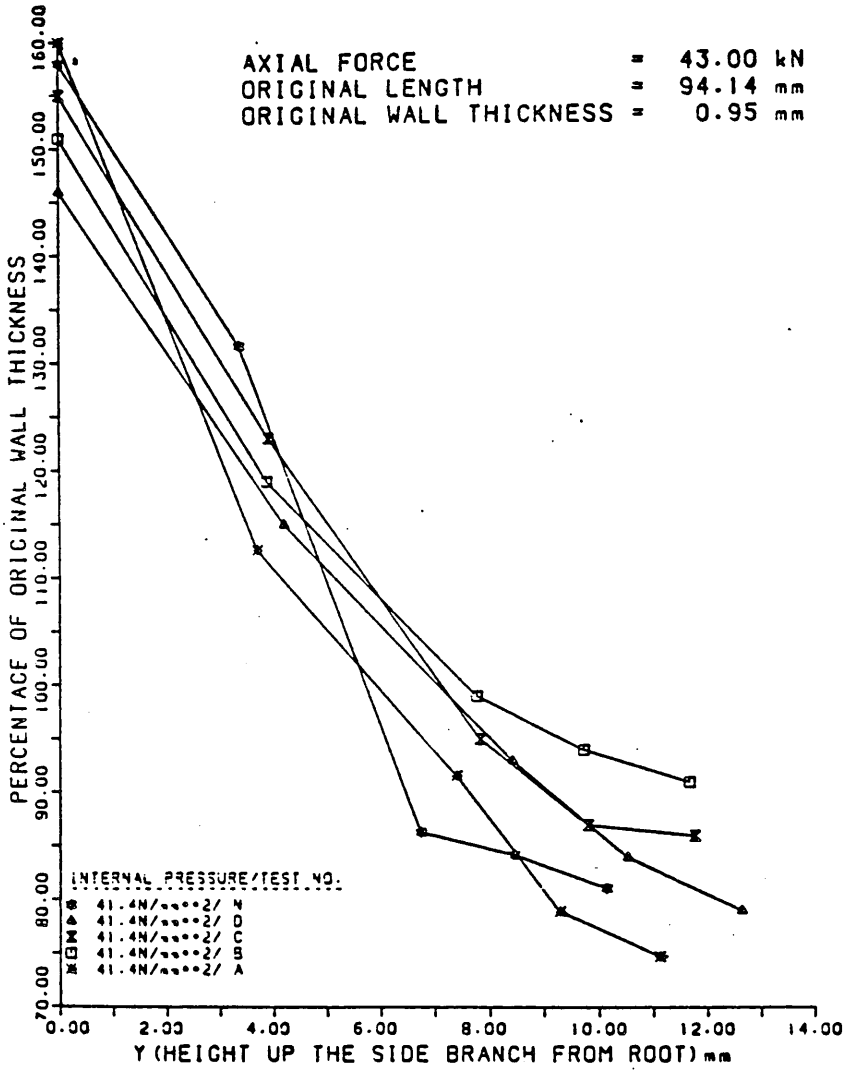

FIGURE 1

The Wall Thickness Distributions Along The Side Branches And Domes Of Tee Pieces Formed Using Various Lubricants.

The final length of the tubes was relatively constant for any given axial load, regardless of the lubricant used.

The results show that an improvement in bulge height is achievable if an effective lubricant is used, but unfortunately, the two cases where a substantial increase was achieved in these tests could not be readily incorporated into a manufacturing process. It had been hoped that the two oil based lubricants which stayed in suspension ('A' and 'C') might produce results similar to the others, because they could have easily been incorporated into the hydraulic fluid used as the pressurising medium. The PTFE in suspension, however, tended to separate from the base oil and settle at the bottom of its container. This would cause problems in the hydraulic system and possibly clog the pump. Further tests were performed in order to verify this and find a possible solution to the problem.

Three more lubricants were investigated; the base oil with 0.5% PTFE dispersion, 4% PTFE dispersion and 5% synthetic fat dispersion.

The tests were conducted with a single combination of load and pressure (128kN, 48.3N/mm^2) to produce fully formed components. The results were related to a standard set of tests and the information processed in the same manner as before. Table 4 shows the results from these tests.

Table 4. Bulge Height for Further Lubricants
Axial Load = 128kN Pressure = 48.3N/mm

Lubricant	Bulge Height (mm) 1	2	3	4	5	Ave	Comparison with N
N	20.12	19.14	19.85	19.34	18.50	19.39	----
Base + 5% Synth fat	19.82	20.20	20.07	19.85	19.00	19.79	+0.40
Base + 0.5% PTFE	18.92	18.53	19.10	18.92	19.22	18.94	-0.45
Base + 4% PTFE	20.26	20.54	20.29	20.36	20.56	20.40	+1.01

The 4% PTFE dispersion gave the best results, followed by the 5% synthetic fat dispersion. The 0.5% PTFE dispersion and the standard lubricant gave similar results. These tests verified that the bulge height obtained was related to the percentage of PTFE in dispersion and in order to obtain a reasonable increase in height, the percentage of PTFE required would result in clogging the pump and filter system in the hydraulic circuit. The 5% dispersion of synthetic fat gave similar results to 2% dispersion of PTFE in the earlier tests, and did not require constant agitation to keep it in suspension.

Conclusions.

Tests performed with additional lubricants produced greater bulge heights that those formed with the hydraulic oil alone. The PTFE spray gave the best results over the full range of forming values, however, when a specific range of operating parameters was analysed (those producing fully formed components), PTFE in dispersion produced slightly better results than the spray. This was possibly because the PTFE in suspension required 'working in' to the die block surfaces, which was only achieved when there was extensive axial deformation (40-50%). The PTFE spray, on the other hand, produced consistent lubrication throughout and was best for the low axial loads and only slightly inferior to the dispersion at the higher loads. In the second set of tests, it was shown that the bulge height obtained was directly related to the percentage of PTFE in dispersion.

The 5% dispersion of synthetic fat produced similar results to the 2% dispersion of PTFE for the higher forming ranges, but 2% dispersion of oleic acid and 2% dispersion of friction modifier yielded only slight improvements on the standard hydraulic oil.

The main concern when considering the use of lubricants is their applicability to the industrial process. Although all of the lubricants produced improved test results, not all could readily be used in the mass production of components. The lubricant would ideally be incorporated into the hydraulic oil used as the pressurising medium. Of the six oil based lubricants used in these tests, only the 5% dispersion of synthetic fat produced an increase in bulge height that would have justified the additional cost of its use in the process, and which would not require major alterations to the pump or filtration system.

References.

1. Limb, M E et al. 'The Forming of Axisymmetrical and Asymmetric Components from Tubes'. Proc 14th Int. MTDR Conference, 1973

2. Limb, M E et al. 'Hydraulic Forming of Tubes'. Sheet Metal Industries, Nov 1976, pp 416-424.

THE HYDRAULIC BULGE FORMING OF TUBULAR COMPONENTS

- THE EFFECT OF CHANGING THE TUBE BLANK MATERIAL

by

M.I.HUTCHINSON *
R.CRAMPTON *
M.S.ALI *
M.S.J.HASHMI +

* Department of Mechanical and Production Engineering,
Sheffield City Polytechnic.
+ School of Mechanical Engineering,
National Institute of Higher Education, Dublin, Eire.

ABSTRACT

The hydraulic bulge forming process is used to produce seamless components from cylindrical metal tubes. A combination of internal hydrostatic pressure and compressive axial load are used to deform the tubes whilst contained within pre-shaped die-blocks.

A dedicated experimental hydraulic bulge forming machine has been designed and built at Sheffield City Polytechnic and allows control of the various forming parameters to be achieved.

This paper deals with tests conducted on the machine into the effects of changing the tube blank material. Aluminium, copper and steel tubes, of the same initial dimensions, were formed into tee pieces. The work investigates the required forming pressure and loads and compares bulge heights and thickness distributions obtained for the materials used.

1. INTRODUCTION

In the hydraulic bulge forming process, cylindrical metal tubes are deformed using hydrostatic internal pressures and compressive axial loads. The tubes are placed in pre-shaped die-blocks which have a side branch into which the metal is forced when a combination of pressure and load are applied. Without the compressive axial load, some bulging occurs, but only small branch heights are attainable without rupture of

the tube. If the axial load is too high, the tubes buckle.

The area around the side branch is called the deformation zone, and when the axial load is applied, the tube is compressed and shortens, and material flows into the zone, which is then used to help form the branch.

This paper deals with the effect of using tubular blanks of different materials and the combinations of internal pressure and compressive axial load needed to produce given heights in them.

2. REVIEW OF PREVIOUS WORKS

The first patent taken out on the bulge forming proces, Grey (1), described how copper tubes could be formed using hydraulic fluid as the pressurising medium, in conjunction with an axially applied load. Since then, the majority of research on the process has been conducted with copper tubes, since the material's ductility and work-hardening characteristics enable components to be formed over a wide range of internal pressures and compressive axial loads. Some investigations have been carried out using different materials, and the following are the relevant publications.

An article which appeared in Metallurgia (2) described a hydrostatic cold forming process which produced tee pieces from steel tubes which had been cut to length. Smith (3), noted the design of a machine that could produce components using a hydrostatic bulge forming technique which allowed for component expansions over 100%. The system was very similar to that patented by Grey (1), except that the pressurising medium was water. The main use for the process was in the manufacture of brass kitchen tap spouts.

An article by Powell (4) detailed a process where aluminium tubes were bent into '90^{o}' joints and 'Z' joints using internal pressure and sliding die-blocks. Woo (5) also used aluminium tubes, along with pewter ones, to form circular vessels. Yoshimoto (6) described how a Japanese company were using bulge forming equipment to produce large structure parts from steel tubes 1.10 metres long and with a diameter of 0.43 metres.

The most extensive work, to date, was carried out by Limb (7 and 8) who produced tee pieces from commercially pure aluminium, aluminium alloy (HV9 - Al/Mag/Si alloy), copper, 70/30 brass and low carbon steel. Each type of tube was formed by the maximum amount, without bursting or buckling, sectioned, and strain measurements taken. In all expanded regions, thinning of the wall occurred, but opposite the branch, the wall thickness was greater than the original tube wall thickness. When failure occurred, brass and steel tended to fail by buckling due to the inability of the machine to provide a sufficiently high internal pressure. In general, the softer materials were formed with less thinning of the branch wall than the stronger materials.

3. EXPERIMENTATION AND RESULTS

The present paper describes tests carried out on three different materials - copper, steel and commercially pure aluminium. All of the tube blanks were of the same e dimensions: 107 mm in length, 24.12 mm outside diameter and 1.37 mm wall thickness. The materials were annealed prior to testing and the tube surfaces were of a similar surface finish.

Testing was performed over a range of internal pressures and compressive axial loads. The steel and copper components were formed over the same range: 27.60 N/mm^2 to 62.10 N/mm^2 internal pressure and 85 kN to 149 kN compressive axial load. The aluminium, however, would not form in these ranges and was tested between 6.90 N/m^2 and 20.70 N/mm^2 internal pressure and 43 kN and 106 kN compressive axial load.

The results were analysed so that a comparison was obtained between the various metals when used to form a tee piece. Bulges of similar heights were selected for each of the materials, and these were plotted graphically with their respective forming ranges. It was thus possible to identify the internal pressures and compressive axial loads required to form a given bulge height with each of the materials. Table 1 shows the maximum forming values for the tests.

Table 1. Forming Ranges for Different Tube Materials

Material	Compressive Axial Load (kN)	Maximum Bulge Height (mm)	Minimum Wall Thickness Ratio (%)	Maximum Internal Pressure (N/mm^2)	Bursting Pressure (N/mm^2)
Aluminium	43	8.14	82	17.25	20.7
Aluminium	64	17.23	78	17.25	20.7
Aluminium	85	22.00	69	17.25	20.7
Copper	85	13.60	67	55.20	62.1
Steel	85	1.88	98	62.10	----
Aluminium	106	26.51	78	17.25	20.7
Copper	106	20.00	65	55.20	62.1
Steel	106	4.88	96	62.10	----
Copper	128	28.51	77	55.20	62.1
Steel	128	12.10	98	62.10	----
Copper	149	27.97	84	55.20	62.1
Steel	149	13.51	95	62.10	----

3.1) Aluminium

The aluminium tubes were formed using four compressive axial loads: 43 kN, 64 kN, 85 kN and 106 kN and internal pressures starting at 6.90 N/mm^2 and incremented by 3.45 N/mm^2 until failure. The components formed had a very poor surface finish with the material flow lines in the deformation zone being very noticable.

3.2) Copper

The copper was tested with compressive axial loads of 85 kN, 106 kN, 128 kN and 149 kN. The internal pressures used varied from 27.60 N/mm^2 to 55.20 N/mm^2. The surface finish of the components was satisfactory, although the flow paths of the material in the deformation zone could be seen.

3.3) Steel

As might have been expected, the steel required the highest values of compressive axial load and internal pressure to produce a formed component. Even at the maximum forming limits of the machine, the steel had not achieved a branch height which could have deemed the component fully-formed (when the three branches are of approximately the same length).

For the full range of internal pressures and axial loads used, there were no cases where the components were buckled or burst. The surface finish of the steel components appeared polished even after major deformations.

Figure 1 shows the forming ranges needed to produce a given bulge height in the materials.

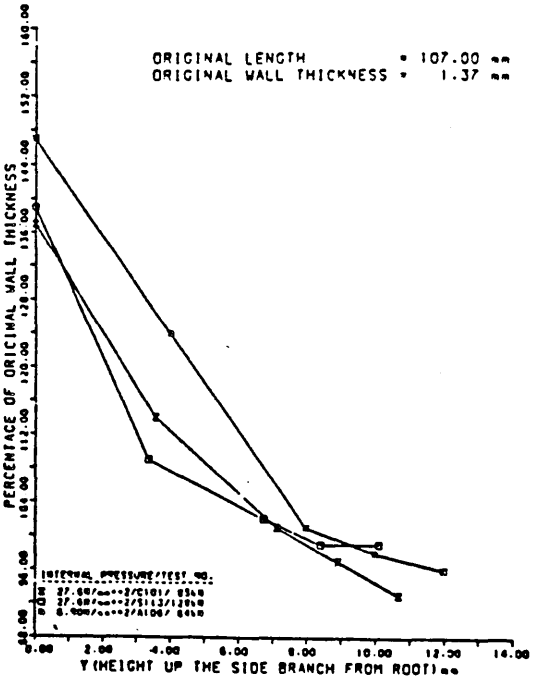

FIGURE 1
The Wall Thickness Distributions Along The Side Branches And Domes Of Tee Pieces Formed From Aluminium, Copper And Steel.

4. DISCUSSION

All of the materials deformed in a manner which allowed bulge forming to occur. The copper, which had been tested thoroughly in previous experiments, gave the best results, with an acceptable component being formed over a wide range of values. The aluminium proved difficult to form, because a bulge could only be achieved between a small range of values. If the combination of internal pressure and compressive axial load was slightly too low, or high, the tubes buckled or burst. For example, the aluminium tubes could produce a bulge with internal pressures which varied by 10 N/mm^2, and compressive axial loads which varied by 60 kN, whereas the copper tubes could be formed with internal pressures varying by 40 N/mm^2 and axial loads varying by 100 kN. The steel could withstand even larger variations.

The components which were formed from aluminium had an acceptable shape, although the surface finish of the tubes was poor. The reason for the limited forming range of the aluminium was that it does not work harden to the same extent as the copper or steel, and thus lacks the strength to resist the higher pressures and loads.

The steel proved a very satisfactory medium for the process, however, the forming requirements were far in excess of those for copper (for which the machine was designed), making it difficult to obtain a large bulge height. Unlike the copper, the tubes did not buckle at the lower values of internal pressure like the copper, because of the extra strength in the tube walls. The quality of the formed components was good, with a near-polished surface finish.

The tests showed that it was possible to form various materials using the bulge forming process, particularly those which would work harden extensively. The steel was a suitable material to use in the process, although the machine used in these tests was unable to produce a fully-formed component.

The steel followed the same trends as the copper, and since the minimum wall thickness ratio acceptable before rupture in the copper components was 60% to 65%, the value of 95% which was obtained for the steel showed that much more deformation was possible. It was considered that the values up to which the steel tubes could be formed was likely to be in the region of twice those tested (300 kN and 120 N/mm^2).

The tests on the pure aluminium suggested that its use would be limited. Aluminium alloy, which could provide additional work hardening characteristics, should prove more suitable.

5. CONCLUSION

All three metals formed components using the bulge forming process. The copper and steel tubes were applicable over a wide range of internal pressures and compressive axial loads. The steel required approximately twice the values of pressure and load to form a component with the same bulge height as the copper. However, the

steel did have the best surface finish, with a polished appearence.

The aluminium would only form components over a small range of values, and these were considerably less than for the copper or steel. The surface finish of the components was poor with noticable flow lines in the deformation zone. It was felt that aluminium would be more suitable if it was part of an alloy which could provide greater strain-hardening characteristics.

6. REFERENCES

1) **GREY, J.E., DEVEREAUX, A.P. and PARKER, W.M.**, "Apparatus For Making Wrought Metal T's". U.S.A. Patents Office, Filed June 1939, Patent N°. 2,203,868.

2) **HYDROSTATIC COLD FORMING OF TUBULAR COMPONENTS.** Metallurgia, June 1978, pp 293-294.

3) **SMITH, J.A.**, "Hydrostatic Forming Complex Tubing Shapes". U.K. Patent Automation, June 1963, pp 84-89.

4) **POWELL, G. and AVITZUR, B.**, "Forming Of Tubes By Hydraulic Pressure". 1971.

5) **WOO, D.M.**, "Developement Of A Bulge Forming Process". Sheet Metal Industries, May 1978, pp 623-625.

6) **YOSHITOMI, Y., KAMOHARA, H., NOMURA, H. and MAKINO, K.**, "Hydraulic Bulge Forming For Large-Sized Structure Parts". J.H.P.I. Vol. 23 N°. 3, 1985, pp 8-13.

7) **LIMB, M.E., CHAKRABARTY, J. and GARBER, S.**, "The Forming Of Axisymmetric And Asymmetric Components From Tube". Proc. 14TH. Int. M.T.D.R. Conf., 1973, pp 799-805.

8) **LIMB, M.E., CHAKREBARTY, J. and GARBER, S.**, "Hydraulic Forming Of Tubes". Sheet Metal Industries, November 1976, pp 418-424.